# Finite - Temperature topological Susceptibility of QCD with heavy Quarks

**Die topologische Suszeptibilität der QCD bei endlichen Temperaturen mit schweren Quarks**
Zur Erlangung des Grades eines Doktors der Naturwissenschaften (Dr. rer. nat.)
Genehmigte Dissertation von Bruno Maria Högl aus München
Tag der Einreichung: 22.04.2025, Tag der Prüfung: 19.05.2025

1. Gutachten: Prof. Ph.D. Guy D. Moore
2. Gutachten: Prof. Dr. rer. nat. Dietrich Bödeker
Darmstadt, Technische Universität Darmstadt

TECHNISCHE
UNIVERSITÄT
DARMSTADT

Fachbereich Physik
Institut für Kernphysik
Theoriezentrum - AG Moore

Finite - Temperature topological Susceptibility of QCD with heavy Quarks
Die topologische Suszeptibilität der QCD bei endlichen Temperaturen mit schweren Quarks

Accepted doctoral thesis by Bruno Maria Högl

Date of submission: 22.04.2025
Date of thesis defense: 19.05.2025

Darmstadt, Technische Universität Darmstadt

Bitte zitieren Sie dieses Dokument als:
URN: urn:nbn:de:tuda-tuprints-300922
DOI: https://doi.org/10.26083/tuprints-00030092
Jahr der Veröffentlichung auf TUprints: 2025

Dieses Dokument wird bereitgestellt von tuprints,
E-Publishing-Service der TU Darmstadt
https://tuprints.ulb.tu-darmstadt.de
tuprints@ulb.tu-darmstadt.de

Die Veröffentlichung steht unter folgender Creative Commons Lizenz:
Namensnennung 4.0 International
https://creativecommons.org/licenses/by/4.0/
This work is licensed under a Creative Commons License:
Attribution 4.0 International
https://creativecommons.org/licenses/by/4.0/

*“I have no idea! You can say that.”*
Guy Moore, 1st March 2023

*“Oh, everyone knows that!”*
Guy Moore, 7th June 2023

*“I don’t understand it, but I can explain it to you.”*
Guy Moore, 10th January 2024

*“In principle, what you’re saying should make sense ...”*
Parikshit Junnarkar, 8th July 2023

*“I’m still confused by the whole process, but it’s fine.*
*[...] That’s orthogonal to my direction of confusion.”*
Nicolas Wink, 28th February 2024

*“If I see that you’re trying, but you made a few mistakes, I’m not going to fail you. Come on, man!”*
Guy Moore, 15th November 2023

*“That’s still crazy to me. But that’s okay.”*
Guy Moore, 8th November 2024

# Erklärungen laut Promotionsordnung

## § 8 Abs. 1 lit. d PromO

Ich versichere hiermit, dass zu einem vorherigen Zeitpunkt noch keine Promotion versucht wurde. In diesem Fall sind nähere Angaben über Zeitpunkt, Hochschule, Dissertationsthema und Ergebnis dieses Versuchs mitzuteilen.

## § 9 Abs. 1 PromO

Ich versichere hiermit, dass die vorliegende Dissertation – abgesehen von den in ihr ausdrücklich genannten Hilfen – selbstständig verfasst wurde und dass die „Grundsätze zur Sicherung guter wissenschaftlicher Praxis an der Technischen Universität Darmstadt" und die „Leitlinien zum Umgang mit digitalen Forschungsdaten an der TU Darmstadt" in den jeweils aktuellen Versionen bei der Verfassung der Dissertation beachtet wurden.

## § 9 Abs. 2 PromO

Die Arbeit hat bisher noch nicht zu Prüfungszwecken gedient.

Darmstadt, 22.04.2025

Bruno Maria Högl

# Abstract

The *axion* is a very interesting hypothetical particle, as it is not only an ideal dark matter candidate, but also dynamically, i.e., “naturally”, solves the *strong* CP *problem* - the discrepancy between the theoretically allowed violation of the combined particle - anti-particle exchange and spatial flip - symmetry in QCD on the one hand and its experimentally observed (nearly perfect) conservation on the other hand.

“Hypothetical particle” means here that, despite significant experimental effort, the axion has until now avoided experimental detection. Therefore, precise theoretical predictions about its properties, especially its mass, are required. Furthermore, the investigation of cosmology with axions has shown that the cosmological history of axions depends critically on the temperature - dependent axion mass in the temperature range between $400$ and $1100\,\mathrm{MeV}$, where very little is known about the axion mass so far.

The axion, and especially its mass, are directly linked to the topological properties of QCD. The QCD vacuum allows for topologically non - trivial, local configurations, which do not play a role in perturbation theory, but have non - perturbative effects on the quarks and gluons. At zero temperature, these configurations are called *instantons* and for finite $T$ they are called *calorons*. The strength of these instanton/caloron effects, i.e., the strength of the quark - gluon system’s response to such a topological background, is determined by the *topological susceptibility* $\chi_{\mathrm{top}}$. In turn, the axion mass is proportional to $\sqrt{\chi_{\mathrm{top}}}$.

Using lattice QCD, the main model for accessing non - perturbative QCD effects, to obtain $\chi_{\mathrm{top}}$ becomes very challenging at high temperatures as $400\,\mathrm{MeV} < T < 1100\,\mathrm{MeV}$, because the topological susceptibility is strongly suppressed at high $T$ and since the bottom quark is not heavy enough to ignore at such temperatures, while so far only $2+1+1$, but no $2+1+1+1$ (including a dynamical bottom quark) lattice simulations exist.

Therefore, we estimate the effect of the bottom quark on $\chi_{\mathrm{top}}$ at high temperatures by computing the ration between the $4$ - quark $\chi_{\mathrm{top}}$ (available from lattice QCD) and the $4+1$ - quark $\chi_{\mathrm{top}}$ in the caloron gas approximation. We do this by computing small - mass and large - mass expansions of the finite - mass and -temperature fermionic fluctuation determinant and connecting them with a Padé approximant. Together with the lattice QCD results, this allows for predictions for $\chi_{\mathrm{top}}$ with a bottom quark at arbitrary temperatures.

# Zusammenfassung

Das *Axion* ist ein sehr interessantes hypothetisches Teilchen, denn es ist nicht nur ein idealer Kandidat für die Dunkle Materie, sondern bietet über seine natürliche Dynamik auch eine Lösung des CP - *Problems der starken Wechselwirkung*, der Diskrepanz zwischen der theoretisch erlaubten Brechung der kombinierten Symmetrie aus Teilchen - Antiteilchen Austausch und räumlicher Spiegelung in der QCD einerseits und der experimentell gemessenen (nahezu perfekten) Symmetrieerhaltung andererseits.

"Hypothetisches Teilchen" bedeutet hierbei, dass das Axion, trotz großen experimentellen Aufwands, bisher nicht detektiert werden konnte, weswegen genaue theoretische Vorhersagen zu seinen Eigenschaften, speziell seiner Masse, von Nöten sind. Des Weiteren hat das Studium der Axionen - Kosmologie gezeigt, dass die kosmologische Entwicklung der Axionen entscheidend von der Entwicklung der temperaturabhängigen Axionenmasse im Temperaturbereich zwischen $400\,\mathrm{MeV}$ und $1100\,\mathrm{Mev}$ abhängt. Bei solchen Temperaturen ist jedoch nur wenig über die Axionenmasse bekannt.

Das Axion, und seine Masse im Besonderen, hängen direkt mit den topologischen Eigenschaften der QCD zusammen. Das Vakuum der QCD erlaubt topologisch nicht - triviale, lokale Zustände, die zwar in der Störungstheorie keine Rolle spielen, aber nicht - perturbativ Einfluss auf Quarks und Gluonen nehmen. Am Temperaturnullpunkt heißen diese Zustände *Instantonen*, bei endlicher Temperatur *Caloronen*. Die Stärke dieser Instanton- bzw. Caloron - Effekte, also des Maßes, in dem Quarks und Gluonen auf solche topologischen Hintergrundzustände reagieren, ist durch die *topologische Suszeptibilität* $\chi_{\text{top}}$ gegeben. Die Axionenmasse wiederum ist proportional zu $\sqrt{\chi_{\text{top}}}$.

Gitter QCD, das erfolgreichste Model zur Beschreibung nicht - perturbativer QCD, stößt bei der Berechnung von $\chi_{\text{top}}$ bei hohen Temperaturen $400\,\mathrm{MeV} < T < 1100\,\mathrm{MeV}$ auf Probleme: nicht nur ist $\chi_{\text{top}}$ bei solchen Temperaturen stark $T$ - gedämpft, es exstieren auch bis jetzt nur $2+1+1$- und keine $2+1+1+1$ - Simulationen, die das bottom Quark, das nicht schwer genug ist, um bei diesen Temperaturen vernachlässigt zu werden, als dynamisches Quark beinhalten.

Aus diesen Gründen bestimmen wir den Effekt des bottom Quarks auf $\chi_{\text{top}}$ bei hohen Temperaturen durch die Berechnung des Verhältnisses der $4$ - Quark Suszeptibilität (bekannt aus der Gitter QCD) und der $4+1$ - Quark Suszeptibilität in der Calorongas -

Näherung. Dafür entwickeln wir die fermionische Fluktuationsdeterminante bei endlichen Temperaturen in kleinen und großen Massen und verbinden diese Entwicklungen mittels einer Padé Approximation. Zusammen mit den Ergenissen aus der Gitter QCD ermöglicht dies Vorhersagen für $\chi_{\text{top}}$ mit inkludiertem bottom Quark bei beliebigen Temperaturen.

# Notation, Naming and Conventions

- We employ a system of natural units with $c = \hbar = k_{\mathrm{B}} = 1$, so that for example Length = Time = Energy$^{-1}$ = Temperature$^{-1}$ = Mass$^{-1}$ and Momentum = 1. Typically one then sets the defining length (or energy) unit to be MeV$^{-1}$ (or MeV).

  In order to convert back to standard SI-units, one plugs in the appropriate combination of [1, 2] $c = 299792458\,\frac{\mathrm{m}}{\mathrm{s}}$, $h = 6.62607015 \cdot 10^{-34}\,\mathrm{Js} = 4.135667697 \cdot 10^{-15}\,\mathrm{eVs}$ and $k_{\mathrm{B}} = 1.380649 \cdot 10^{-23}\,\frac{\mathrm{J}}{\mathrm{K}} = 8.617333262 \cdot 10^{-5}\,\frac{\mathrm{eV}}{\mathrm{K}}$.

- We use the convention $\mathbb{N} = \mathbb{N}_0 = \{0, 1, 2, ...\}$, i.e., we include 0 so that the natural numbers are the non-negative integers. The positive integers we write as $\mathbb{N}^+$. This is used for summation.

- We denote dimensionful physical quantities $Q$ as $Q = \{Q\} \cdot [Q]$, where $[Q]$ is the dimension of the quantity and $\{Q\}$ is the corresponding numerical value. Furthermore, we often rescale physical quantities $Q$ by the inverse temperature $\beta = T^{-1}$, thus obtaining dimensionless quantities. These numbers we assign an artificial "$\beta$-dimension" of their non-rescaled counterparts. As an example, for $[Q] =$ Length$^{a}$ we then have $q = Q\beta^{-a}$ with $\beta$-dimension $[q]_\beta =$ Length$^{a}$.

- Capital $M$'s denote dimensionfull masses $[M] =$ Length$^{-1}$, while small $m$'s denote $\beta$-rescaled, dimensionless masses $[m] = [M\beta] = 1$ with $[m]_\beta =$ Length$^{-1}$. Accordingly, we denote instanton/caloron sizes by $\rho$ and their $\beta$-rescaled counterparts by $\varrho$ with $[\rho] =$ Length $= [\varrho]_\beta = [\rho\beta^{-1}]_\beta$.

- Every pair of indices, equal on both sides of an equation, independent of whether they appear diagonally ($Q^a\, Q'_a$), horizontally ($Q^a Q'^a$ or $Q^{aa}$) or vertically ($Q^a_a$), implies a summation over these indices. We do not state these summations explicitly. If no explicit metric is given, the metric for index contractions is always the Kronecker delta. In the case of Minkowski spacetime the indices are marked with a subscript "M" (cf. (2.1.1)).

- We are limited to (flat) 4-dimensional spacetime (cf. section 2.4.2). In Minkowski space $\mathbb{R}^{1,3}$ we label coordinates as $\chi^{\mu_{\mathrm{M}}}$ with indices $\mu_{\mathrm{M}}, \nu_{\mathrm{M}}$ running from 0 to 3 and Roman indices $i_{\mathrm{M}}, j_{\mathrm{M}}$ from 1 to 3. We chose the "mostly minus" - convention $\eta_{\mu_{\mathrm{M}}\nu_{\mathrm{M}}} = \mathrm{diag}(1, -1, -1, -1)$. Real time is denoted as $\chi^0 = t$ and we write $|\vec{\chi}| = r$.

In Euclidean spacetime $\mathbb{R}^3 \times S^1_{\mathrm{rad.} = \beta/2\pi}$, corresponding to a finite temperature $T = \beta^{-1}$, we have coordinates $X = (\vec{X}, X^4)$, where Greek indices $\mu$, $\nu$ run over $1, ..., 4$ and roman indices $i$, $j$ run over $1, 2, 3$. Imaginary time is denoted as $X^4 = t$. Temporally infinite Euclidean space $\mathbb{R}^4$ (corresponding to the zero temperature limit $T \searrow 0 \Rightarrow \beta \to \infty$) is denoted by coordinates $\overline{X}^\mu$ with $\overline{X}^4 = \bar{t}$. We write $|\vec{X}| = \sqrt{X^i X^i} = R$ and $|\overline{X}| = \sqrt{\overline{X}^\mu \overline{X}^\mu} = \overline{R}$.

In $\beta$ - rescaled Euclidean spacetime $\mathbb{R}^3 \times S^1_{\mathrm{rad.} = 1/2\pi}$ we label the dimensionless coordinates $x = \frac{X}{\beta}$ with $x^4 = \frac{t}{\beta} = \tau$ and keep the indices $\mu, \nu$.[1] Analogously, we denote the coordinates and tensors of infinite, but appropriately dimensionless space $\mathbb{R}^4_{\text{dimensionless}}$ by $\bar{x}^\mu$ and $\bar{q}^{\nu_1 \cdots \nu_n}(\bar{x})$. Like above: $|\vec{x}| = r$ and $|\bar{x}| = \bar{r}$.

The unit vector in the $\mu$ - direction is denoted as $\hat{e}_{\mu_{(\mathrm{M})}}$ - and analogously in the other spacetime settings, including abstract spaces. For the Levi - Civita symbol in Minkowski spacetime we use the convention $\varepsilon^{0_{\mathrm{M}}1_{\mathrm{M}}2_{\mathrm{M}}3_{\mathrm{M}}} = -\varepsilon_{0_{\mathrm{M}}1_{\mathrm{M}}2_{\mathrm{M}}3_{\mathrm{M}}} = 1$.

- A "daggered" derivative operator is to be understood as acting to the left $\partial^\dagger = \overleftarrow{\partial}$.

- Wick rotation is defined as $t = \chi^0 \to it = t = X^4$ and analogously for vectors $v^{\mu_{\mathrm{M}}} \to v^\mu = \begin{cases} v^{i_{\mathrm{M}}} \\ iv^{0_{\mathrm{M}}} \end{cases}$ and covectors $w_{\mu_{\mathrm{M}}} \to w_\mu = \begin{cases} w_{i_{\mathrm{M}}} \\ -iw_{0_{\mathrm{M}}} \end{cases}$. For the metric this means $\eta_{\mu_{\mathrm{M}}\nu_{\mathrm{M}}} \to -\delta_{\mu\nu}$ in the sense that $v^{\mu_{\mathrm{M}}}\eta_{\mu_{\mathrm{M}}\nu_{\mathrm{M}}}v^{\nu_{\mathrm{M}}} \to -v^\mu \delta_{\mu\nu} v^\nu$.

  We choose an analogous transformation for the $\gamma$ - matrices: $\gamma^{\mu_{\mathrm{M}}} \to \gamma^\mu = \begin{cases} \gamma^{i_{\mathrm{M}}} \\ i\gamma^{0_{\mathrm{M}}} \end{cases}$.

  These Euclidean $\gamma$ - matrices are then anti-Hermitian ${\gamma^\mu}^\dagger = -\gamma^\mu$ and satisfy the Clifford algebra $\{\gamma^\mu, \gamma^\nu\} = -2\delta^{\mu\nu}\mathbb{1}$. The fifth Euclidean $\gamma$ - matrix $\gamma^5 = \gamma^1\gamma^2\gamma^3\gamma^4$ is Hermitian ${\gamma^5}^\dagger = \gamma^5$, involutory $(\gamma^5)^2 = \mathbb{1}$ and anti-commuting $\gamma^5\gamma^\mu = -\gamma^\mu\gamma^5$.

  The Dirac operator then Wick rotates as $\partial\!\!\!/_{\mathrm{M}}, D\!\!\!\!/_{\mathrm{M}} \to -\partial\!\!\!/, -D\!\!\!\!/$ which yields the transformation $\int_{\mathbb{R}}^4 \mathrm{d}^4\chi\,(i\partial\!\!\!/_{\mathrm{M}}, iD\!\!\!\!/_{\mathrm{M}}) \to -\int_{\mathbb{R}}^4 \mathrm{d}^4\overline{X}(i\partial\!\!\!/, iD\!\!\!\!/)$ in the action.

- We always suppress indices in Dirac space. For reasons of clarity we sometimes write the Dirac space - spinors and -matrices explicitly.

- We write elements of a general Lie Group $G$ via the exponential with a factor of $-i$, i.e., $G \ni A(\theta) = \exp\big(-i\theta^a T^a\big)$ with parameters $\theta^a$ and generators $T^a$ satisfying

---

[1] Actually, these coordinates are also always going to be chosen as centered around the caloron, cf. (3.1.1).

$[T^a, T^b] = if^{abc}T^c$, where $f^{abc}$ is the completely anti-symmetric structure constant. This also defines the commutator $[Q, Q'] = if^{abc}Q^b Q'^c\, T^a$. When stating the defining commutator relations or structure constants, we give only the non-vanishing ones. All other relations/constants are to be understood as 0.

The $SU(2)$-generators in the defining or fundamental representation are then given by "$\frac{1}{2}$ × Pauli matrices" $T^a_{SU(2),\,\text{def}} = \frac{\sigma^a}{2}$ with $\sigma^1 = \begin{pmatrix} 0 & 1 \\ 1 & 0 \end{pmatrix}$, $\sigma^2 = \begin{pmatrix} 0 & -i \\ i & 0 \end{pmatrix}$, $\sigma^3 = \begin{pmatrix} 1 & 0 \\ 0 & -1 \end{pmatrix}$ and $f^{abc}_{SU(2)} = \varepsilon^{abc}$.

The defining $SU(3)$-generators are the "$\frac{1}{2}$ × Gell-Mann matrices" $T^a_{SU(3),\,\text{def}} = \frac{\lambda^a}{2}$:

$$\lambda^1 = \begin{pmatrix} 0 & 1 & 0 \\ 1 & 0 & 0 \\ 0 & 0 & 0 \end{pmatrix}, \quad \lambda^2 = \begin{pmatrix} 0 & -i & 0 \\ i & 0 & 0 \\ 0 & 0 & 0 \end{pmatrix}, \quad \lambda^3 = \begin{pmatrix} 1 & 0 & 0 \\ 0 & -1 & 0 \\ 0 & 0 & 0 \end{pmatrix}, \quad \lambda^4 = \begin{pmatrix} 0 & 0 & 1 \\ 0 & 0 & 0 \\ 1 & 0 & 0 \end{pmatrix},$$

$$\lambda^5 = \begin{pmatrix} 0 & 0 & -i \\ 0 & 0 & 0 \\ i & 0 & 0 \end{pmatrix}, \lambda^6 = \begin{pmatrix} 0 & 0 & 0 \\ 0 & 0 & 1 \\ 0 & 1 & 0 \end{pmatrix}, \lambda^7 = \begin{pmatrix} 0 & 0 & 0 \\ 0 & 0 & -i \\ 0 & i & 0 \end{pmatrix}, \lambda^8 = \frac{1}{\sqrt{3}} \begin{pmatrix} 1 & 0 & 0 \\ 0 & 1 & 0 \\ 0 & 0 & -2 \end{pmatrix}$$

with $f^{123}_{SU(3)} = 1$, $f^{147}_{SU(3)} = -f^{156}_{SU(3)} = f^{246}_{SU(3)} = f^{257}_{SU(3)} = f^{345}_{SU(3)} = -f^{367}_{SU(3)} = \frac{1}{2}$ and $f^{458}_{SU(3)} = f^{678}_{SU(3)} = \frac{\sqrt{3}}{2}$.

- We use the following integral operator abbreviations: $\int_0^\beta \mathrm{d}t \int_{\mathbb{R}^3} \mathrm{d}^3X = \int^\beta \mathrm{d}^4X$ and $\int_0^1 \mathrm{d}\tau \int_{\mathbb{R}^3} \mathrm{d}^3x = \int^1 \mathrm{d}^4x$.

  We also write the operator trace as $\mathrm{Tr}(\cdot) = \int_{\chi,X,x,\overline{X},\overline{x}} \mathrm{tr}_{\text{Dirac, color, etc.}}(\cdot)$, where the general integral denotes the spacetime integral appropriate for the specific integrand and " tr " performs the trace over all uncontracted index-pairs.

- We choose the "geometrical normalization" of the gauge field $A$. The gauge-covariant derivative is then $D^{\mu_\mathrm{M}} = \partial^{\mu_\mathrm{M}} - iA^{\mu_\mathrm{M}}$ and the Yang-Mills Lagrangian is given by $\mathcal{L}_\mathrm{YM} = -\frac{1}{2g^2}\mathrm{tr}\big(G^{\mu_\mathrm{M}\nu_\mathrm{M}}G_{\mu_\mathrm{M}\nu_\mathrm{M}}\big)$ with the (explicitly $g$-independent) field strength $G^{\mu_\mathrm{M}\nu_\mathrm{M}} = i[D^{\mu_\mathrm{M}}, D^{\nu_\mathrm{M}}] = \partial^{\mu_\mathrm{M}}A^{\nu_\mathrm{M}} - \partial^{\nu_\mathrm{M}}A^{\mu_\mathrm{M}} - i[A^{\mu_\mathrm{M}}, A^{\nu_\mathrm{M}}]$ - and analogously in Euclidean spacetime.[2]

  Occasionally we employ the following short-hand notation for gauge-covariant derivatives: $D^{\mu_\mathrm{M}}Q^{\nu_{\mathrm{M}\,1}\cdots\nu_{\mathrm{M}\,n}} = Q^{\nu_{\mathrm{M}\,1}\cdots\nu_{\mathrm{M}\,n};\mu_\mathrm{M}}$.

---

[2] In comparison to the "physical normalization" of the gauge field where $D^{\mu_\mathrm{M}} - igA^{\mu_\mathrm{M}}_M$ and $\mathcal{L}_\mathrm{YM} = -\frac{1}{2}\mathrm{tr}\big(G^{\mu_\mathrm{M}\nu_\mathrm{M}}G_{\mu_\mathrm{M}\nu_\mathrm{M}}\big)$ this amounts to absorbing the coupling strength into the gauge field.

- We denote the field configuration of the Belavin - Polyakov - Schwarz - Tyupkin instanton ((2.4.24) in regular, (2.4.27) in singular gauge) by $A_{\text{BPST}}$ and the field configuration of the Harrington - Shepard caloron (2.4.37) by $A_{\text{HS}}$. The corresponding field strengths are denoted without the subscripts “BPST” or “HS”.

- In order to avoid confusion with the effective action $\Gamma$, we denote the gamma function by $\widetilde{\Gamma}(x)$. The digamma function is denoted conventionally as $\psi(x) = \widetilde{\Gamma}^{-1}(x)\,\mathrm{d}_x\widetilde{\Gamma}(x)$.

- We use $\mathbb{1}_{n\times n}$ to denote $n \times n$ unit matrices (with the subscript included only if we wish to emphasize the dimensionality) and id for infinite - dimensional operator-, functional-, etc. identities.

- We use the following (standard) abbreviations: “SM“ for Standard Model, “QFT” for Quantum Field Theory, “QCD” for Quantum Chromodynamics, “YM (theory)” for Yang - Mills (theory), “pNG boson” for pseudo - Nambu - Goldstone boson, “DGA” for dilute gas approximation, “VEV” for vacuum expectation value, “IBP” for integration by parts

- Footnote - citations at the end of paragraphs provide sources for the whole paragraph (sometimes even for multiple paragraphs, since the last footnote - citation, which discuss one topic); “in text” - citations provide sources for one piece of information.

- We use passive language or “one [finds/...]” to provide information from the literature; in return, we write “we” when presenting our findings.

# Contents

**Notation, Naming and Conventions** **xi**

**1 Introduction** **1**
- 1.1 Matter Content of the Universe, Quantum Chromodynamics and the Standard Model . . . 1
- 1.2 Topology and the Axion . . . 4
- 1.3 Aim of this Work . . . 7

**2 Quantum Chromodynamics, Topology, Instantons and Axions** **9**
- 2.1 The “naive” Action of Quantum Chromodynamics . . . 9
- 2.2 Path Integral Quantization and Thermal Field Theory . . . 23
  - 2.2.1 Path Integral Quantization and the Effective Action . . . 24
  - 2.2.2 Gauge fixing in the Path Integral Formalism . . . 29
  - 2.2.3 Thermal Field Theory in the Imaginary Time or Matsubara Formalism 30
  - 2.2.4 Symmetry Group of Thermal Field Theory . . . 33
- 2.3 Chiral Symmetry and Chiral Perturbation Theory . . . 34
- 2.4 Topology of $SU(N)$ - Gauge Theories and the Interplay with Particles . . . 40
  - 2.4.1 Instantons in non - relativistic Quantum Mechanics . . . 40
  - 2.4.2 Vacuum Topology, Instantons and Calorons . . . 47
  - 2.4.3 Caloron Density with massive Quarks . . . 64
  - 2.4.4 Dilute Gas Approximation for Calorons . . . 80
  - 2.4.5 Topological Susceptibility . . . 82
- 2.5 Observable Effects of Topology . . . 83
  - 2.5.1 Axial Anomaly and the missing Nambu - Goldstone Boson . . . 84
  - 2.5.2 Strong CP Problem and its Resolution by Axions . . . 87
  - 2.5.3 The Axion and its Relation to Topology . . . 89

**3 Caloron Density for heavy Fermions – Large and Small Mass - Expansion** **97**
- 3.1 Large Mass - Expansion of the Caloron Density . . . 97
  - 3.1.1 Schwinger Proper Time - Representation . . . 97

3.1.2 Heat Kernel Expansion at finite Temperature . . . . . . . . . . . . . 99
3.1.3 Heat Kernel Expansion Order by Order - Numerical Results . . . . . 107
3.2 Small Mass - Expansion of the Caloron Density . . . . . . . . . . . . . . . . 122
3.2.1 Expansion Strategy . . . . . . . . . . . . . . . . . . . . . . . . . . . . 122
3.2.2 Periodic and anti-periodic massless scalar Propagator in a HS Caloron Background . . . . . . . . . . . . . . . . . . . . . . . . . . . . 125
3.2.3 Taylor Expansion . . . . . . . . . . . . . . . . . . . . . . . . . . . . 136
3.3 Interpolation between Mass Regimes and Topological Susceptibility . . . . 139

**Appendices**

A. Partial Differential Equation . . . . . . . . . . . . . . . . . . . . . . . . . 153
B. Heat Kernel Coefficient $\bar{a}_{10}$ . . . . . . . . . . . . . . . . . . . . . . . . . 155
C. Alternative Small - Mass Expansion . . . . . . . . . . . . . . . . . . . . . . 156
D. Numerical Methods . . . . . . . . . . . . . . . . . . . . . . . . . . . . . . 161
D.1 Heat Kernel Coefficients - Obtaining the functional Form . . . . . . . . 161
D.2 Spacetime Integration . . . . . . . . . . . . . . . . . . . . . . . . . . . 162
D.3 Ancillary Files . . . . . . . . . . . . . . . . . . . . . . . . . . . . . . 163

**List of Figures** 167

**Bibliography** 168

**Curriculum Vitae** 186

# 1 Introduction

## 1.1 Matter Content of the Universe, Quantum Chromodynamics and the Standard Model

All visible matter in the universe is made up of atoms, which are in turn composed of electrons, protons and neutrons. The protons and neutrons are hadrons, i.e., particles that consist of *quarks*, which interact via the electromagnetic, weak, *strong* and gravitational *interaction*. On short length scales and for small masses, for example in hadronic bound states such as protons, neutrons or pions, the strong interaction is the dominant force of nature. The electromagnetic and weak interactions still play a role, while gravitational effects are negligible. Just as electromagnetic and weak interactions are mediated by photons and the $W^{\pm}$ - and $Z$ - bosons, respectively, the strong force is associated to bosonic mediators as well, the *gluons*. The theory describing quarks and their strong - force interactions via gluons is called *Quantum Chromodynamics*, QCD for short. It is discussed thoroughly in a plethora of literature, e.g., [3–6], which serve as general references for the introduction (together with explicitly stated sources).

QCD is a confining theory, which means that quarks and gluons are not observed in nature as individual particles, but always only in hadronic bound states [7, 8]. Additionally, these hadrons are neutral with respect to the charge of the strong interaction carried by both quarks and gluons. Gluons being charged and therefore self - interacting results in many of the differences between QCD and Quantum Electrodynamics, as the photons carry no electrical charge. Hadrons are composed of either two quarks, where one is positively and one negatively charged with respect to the strong force, or three quarks which each carry one of three different (positive) charges of the strong interaction. As an analogy to color theory, these three charges are called *color charges* - red, blue and green - and the quark - anti-quark hadrons (mesons) are called black, while the 3 - quark hadrons (baryons) are labeled white. Confinement can for example be seen in terms of the quark - anti-quark potential [9]

$$V(r) = -\frac{g^2}{3\pi r} + \sigma_{\mathrm{QCD}}\, r \,, \tag{1.1.1}$$

where $g$ is the QCD - coupling constant marking the strength of the strong interaction and $\sigma_{\mathrm{QCD}}$ is the quark string - tension. The linear rise in the potential shows that an increasing amount of energy is required the further the bound quarks are to be separated, until the string of binding energy (i.e., virtual particle - anti-particle pairs) eventually creates a new quark - anti-quark pair, forming new bound mesons with the original pair.

Confinement means that there is no asymptotically free quarks (and gluons) for large distances, i.e., small energies. QCD however allows for asymptotic freedom in the large energy/small distance regime, as is shown by the energy dependency of the coupling constant. At first order of quantum corrections (one - loop order), the coupling $g$ at energy scale $\mu$ reads

$$\frac{8\pi^2}{g^2(\mu^2)} = \frac{11N - 2N_f}{3} \ln\left(\frac{\mu}{\Lambda_{\mathrm{QCD}}}\right), \tag{1.1.2}$$

where $\Lambda_{\mathrm{QCD}} = (341 \pm 12)$ MeV [10] is the “typical QCD - energy scale” and the energy scale of confinement, $N$ denotes the general number of colors and $N_f$ is the general number of different quark *flavors* [11, 12]. From the spectroscopy of hadrons six quarks, up $(u)$, down $(d)$, strange $(s)$, charm $(c)$, bottom $(b)$ and top $(t)$, have (so far) been identified. They have (widely) different masses and carry electric charges of either $\frac{2e}{3}$ or $-\frac{e}{3}$, but are otherwise indistinguishable under (strong) interactions. The six quarks, their masses and charges are listed in table 1.1. The quark flavor number $N_f = 6$ shows that $g(\mu)$ (1.1.2) does increase for small $\mu$ and decrease for large energy scales, as is shown in figure 1.1.

| up $(u)$ | down $(d)$ | strange $(s)$ | charm $(c)$ | bottom $(b)$ | top $(t)$ |
|---|---|---|---|---|---|
| $2.16^{+0.49}_{-0.26}$ | $4.67^{+0.48}_{-0.17}$ | $93.4^{+8.6}_{-3.4}$ | $1270 \pm 20$ | $4180^{+30}_{-20}$ | $172760 \pm 300$ |
| $\frac{2e}{3}$ | $-\frac{e}{3}$ | $-\frac{e}{3}$ | $\frac{2e}{3}$ | $-\frac{e}{3}$ | $\frac{2e}{3}$ |

Table 1.1: Masses of the six quark flavors given in MeV and their charges [2]. up-, down- (and strange-) quark are often called the two (three) light quarks.

QCD as the theory of quarks, gluons and their strong - force interactions is only a part of the bigger theory, the *Standard Model of Particle Physics* (SM) which includes also Quantum Electrodynamics (i.e., electromagnetic force) and the electroweak interactions, as well as all related particles: leptons such as electrons, muons or neutrinos, the other gauge bosons and the Higgs boson. The SM thus describes three of the four fundamental forces, lacking a description of gravity. Furthermore, for high enough temperatures $T \gtrsim 160\,\mathrm{GeV}$ [13] a unification of electromagnetic and weak interaction in the Glashow - Salam - Weinberg model of the electroweak interaction was found; however, there are no experimental findings suggesting an analogous unification with the strong interaction. Despite these “aesthetic” shortcomings, the SM is exceptionally successful and excellently verified by

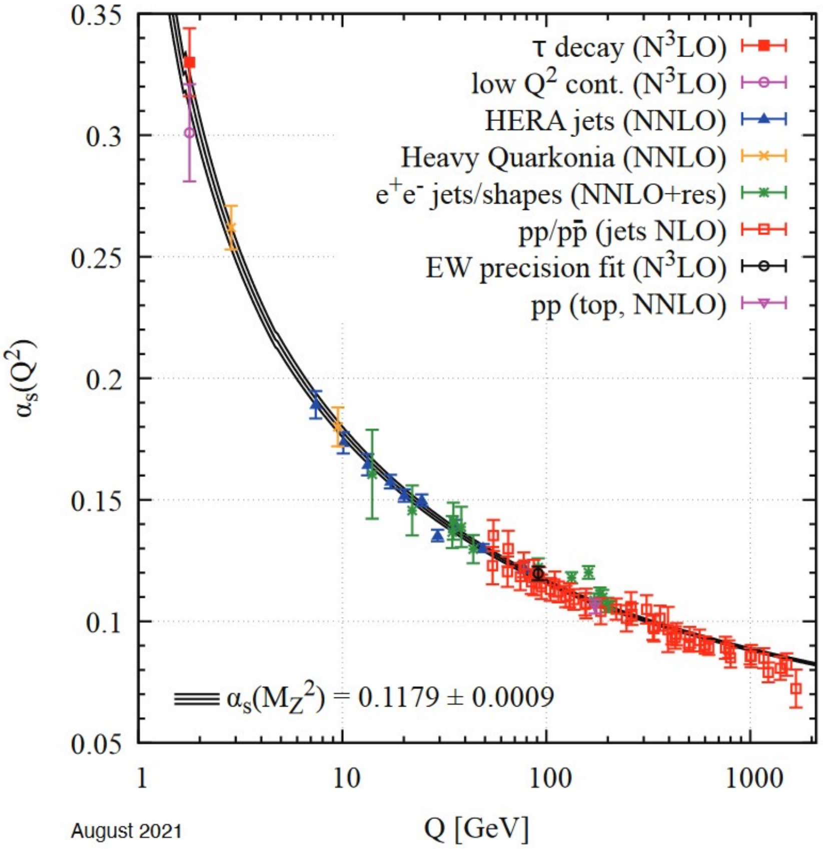

Figure 1.1: Taken from [2]: Energy - dependency of the QCD coupling strength. Comparison of the theoretical predictions for the coupling strength $\alpha_s = \frac{g^2}{4\pi}$ of QCD as a function of the momentum transfer $Q$ (corresponds to the energy scale $\mu$ in (1.1.2)) and experimental values. One sees the divergence of $\alpha$ at small energies/large distances (confinement) and its vanishing for large energies/small distances (asymptotic freedom).

experimental results: the predicted and measured value of the electron magnetic moment agree to over ten significant digits [14], the gluon [15, 16] and the hadron spectrum [17, 18] were discovered as predicted, the Higgs boson was detected [19, 20] over 50 years after its prediction in the predicted mass range, etc.

From astrophysical and cosmological observations like [21–25], it has been determined, however, that about 85% of all matter in the universe is indeed not visible, hadronic matter. It is, in fact, not SM - matter at all. Instead, this so - called *dark matter* interacts only gravitationally, meaning it is either uncharged with respect to the electromagnetic, weak and strong interactions or its coupling is very small. This makes dark matter very difficult to detect. Additionally, dark matter appears to be cold, i.e., of non - relativistic energies, which allows it to “clump together” gravitationally [26]. Beyond that, not much is known about dark matter, but many interesting (SM extending) models and dark matter candidate particles have been put forward, one of which is the *axion* which we are going to introduce in more detail in the following section 1.2 and discuss thoroughly in section 2.5.3. The axion, specifically, its mass, is the main motivation for this work.

## 1.2 Topology and the Axion

From the study of *Yang - Mills theory*, which describes the gluons and their self - interactions, it is known that there is no single, distinct gluon vacuum, but instead there are infinitely many classical gluonic vacuum states which differ only by their topological properties. These otherwise distinct vacua are connected by topologically non - trivial quantum mechanical tunneling processes called *instantons* at zero temperature and *calorons* for finite temperature $T > 0$ [27, 28].

The topological properties of any geometric object or space are determined by its global properties and are independent of any local features. This also means that local, continuous deformations such as stretching, twisting, bending, etc. leave these topological properties invariant, while discontinuous deformations such as cutting, opening and closing of holes, etc. change the topology. The topologically interesting instanton- or caloron - gauge configurations are local vacuum configurations that nevertheless change the global, topological properties of the gluon vacuum, which are found by integrating over all of spacetime. As an intuition, one can imagine a sheet of paper ($\mathbb{R}^2$) in which one pierces a hole at the center ($\mathbb{R}^2 \setminus \{(0,0)\}$). This local change nevertheless has global implications: without the hole the sheet of paper ($\mathbb{R}^2$), understood as a topological space, was simply connected, i.e., every closed path could be continuously contracted to a single point; with the hole this is no longer the case, as simple connectedness now fails for every closed path around $(0,0)$.

The presence of instantons and calorons and the non-trivial topology of the gluon vacuum is indeed reflected in the quark sector. Two import observables linked to the gluonic topology are the *chiral anomaly/the $\eta$-$\eta'$-puzzle* and the *strong* CP *problem*.

At high temperatures, the light $u$-, $d$- and $s$-quarks are (almost) massless and QCD exhibits an $SU(N_{fl})_\mathrm{V} \otimes SU(N_{fl})_\mathrm{A} \otimes U(1)_\mathrm{V} \otimes U(1)_\mathrm{A}$-symmetry in the space of $N_{fl} = 3$ light quarks, with the axial symmetries flipping chirality. The classical $U(1)_\mathrm{A}$-axial symmetry is anomalously broken, however, which is explained by topological effects [29–31]. Therefore, it is no quantum symmetry after all. For temperatures where the thermal energy of the light quarks drops below their binding energy, the classical axial symmetries are spontaneously broken [8, 32]. This is due to the non-zero expectation value for quark-anti-quark condensates $\langle \mathrm{vac} \,|\, \overline{\psi}\psi \,|\, \mathrm{vac} \rangle = \langle \overline{\psi}_\mathrm{L}\psi_\mathrm{R} + \overline{\psi}_\mathrm{R}\psi_\mathrm{L} \rangle = -E_\mathrm{bind}$ allowed by the QCD-vacuum, i.e., the QCD quark vacuum settles into a lower energy state dominated by quark condensates. For $SU(3)_\mathrm{A}$ this results in eight pseudo Nambu-Goldstone bosons: the pions, kaons and the $\eta$-meson. The $\eta$-$\eta'$-puzzle is the large mass gap between the $\eta$ and the related $\eta'$ meson and especially between $\eta'$ and the pions . Since $U(1)_\mathrm{A}$ is no symmetry, however, there is no ninth Nambu-Goldstone bosons and the $\eta'$-mass is thus not protected from being large. Topology consequently solves the $\eta$-$\eta'$-puzzle [8, 33]. More so, the $\eta'$-mass is determined by topology via the Witten-Veneziano mechanism [34, 35].

The strong CP problem is the discrepancy between the CP breaking of topological effects and the experimental exclusion of CP breaking by QCD. In detail, topological terms enter QCD with the angle $\theta$ as a parameter and, from the point of theory, every value $\theta \in [-\pi, \pi)$ is viable. The topological terms then result, for example, in a neutron electric dipole moment of $-1.52(71) \cdot 10^{-18}\, \theta\, e \cdot \mathrm{m}$ [36] with an experimental upper bound on the moment's absolute value of $1.8 \cdot 10^{-28}\, e \cdot \mathrm{m}$ (90% confidence level) [37]. This sets an upper bound of $|\theta| \lesssim 1.2 \cdot 10^{-10}$. Therefore, the strong CP problem is the following fine-tuning problem: given that a priori every value $\theta \in [-\pi, \pi)$ is equally viable and CP is not a fundamental symmetry of nature/QCD, why is $\theta$ fine-tuned to a very small value $|\theta| \lesssim 1.2 \cdot 10^{-10}$, so that CP is conserved and $\theta$ plays no role in (perturbative) particle physics? [38]

A very promising solution of the strong CP problem is the extension of the SM in terms of the aforementioned axion [39, 40]. For this, an additional $U(1)_\text{Peccei Quinn}$-symmetry [41, 42] in the high temperature limit of the early universe is introduced. After the cooling of the universe and spontaneous symmetry breaking of $U(1)_\mathrm{PQ}$ at some very high energy scale $f_a$, the axion $a$ appears as the associated Nambu-Goldstone boson. Astrophysical and cosmological observations set the range $10^8$ GeV $\lesssim f_a \lesssim 10^{17}$ GeV for the PQ-symmetry breaking scale [43–45]. As the temperature decreases further, the axion obtains a coupling to gluons via topological terms and settles into its vacuum expectation value $\langle a \rangle = -\theta f_a$, thus picking up a very small mass $m_a \propto f_a^{-1}$ and turning into a pseudo Nambu-Goldstone boson. Thereby, the axion also modifies $\theta$ as $\theta \rightarrow \theta_{\text{eff}} = \theta + \frac{\langle a \rangle}{f_a} = 0$. This means that by settling in its vacuum expectation value, the axion dynamically ensures CP conservation of QCD and settles the entire system in its lowest energy state described by $\theta_{\text{eff}} = 0$. Additionally, all interactions of the axion with SM - particles are also suppressed as $f_a^{-1}$ (*invisible axion*), which makes the axion an ideal dark matter candidate [46–49]. As of yet, the axion is still a hypothetical particle, i.e., it lacks verification by observation, but many experiments focusing on axion dark matter are ongoing or planned [50].

The axion mass depends not only on the PQ scale $f_a$, but also on the (temperature dependent) topological susceptibility $\chi_{\text{top}}(T)$ via

$$M_a(T) = \frac{\sqrt{\chi_{\text{top}}(T)}}{f_a} \,. \tag{1.2.1}$$

Susceptibilities describe the response of physical systems to some perturbation, often of an external force. As an example, the magnetic susceptibility $\chi_{\text{mag}} \propto \frac{\partial^2 \ln Z(B)}{\partial B^2}$ measures the strength of a system's magnetization given an external magnetic field $B$. We are interested in the topological susceptibility $\chi_{\text{top}}$ of a QCD - system of gluons and quarks, which determines the system's response to the presence of topologically non - trivial instanton or caloron configurations. The strength of the topological background is determined by the fluctuation of $\theta_{(\text{eff})}$ away from the vacuum expectation value $\langle \theta \rangle \approx 0$ (the value predicted by both experiment and theory):

$$\chi_{\text{top}} = -\frac{1}{V} \left. \frac{\partial^2 \ln\big(Z(\theta)\big)}{\partial \theta^2} \right|_{\theta = 0} \,, \tag{1.2.2}$$

where $Z$ is the partition function and $V$ is the volume of spacetime.

At zero temperature and including only the light quarks, $\chi_{\text{top}}$ is determined using chiral perturbation theory[1] and precise results are available: $\sqrt[4]{\chi_{\text{top}}(0)} = (75.44 \pm 0.34)$ MeV [51], which is in good agreement with other recent findings like $\sqrt[4]{\chi_{\text{top}}(0)} = (75.6 \pm 0.6)$ MeV [52], the $SU(2)$ - chiral perturbation theory result $\sqrt[4]{\chi_{\text{top}}(0)} = (75.5 \pm 0.5)$ MeV [44] or the lattice QCD result $\sqrt[4]{\chi_{\text{top}}(0)} = (75.6 \pm 1.8_{\text{statistical}} \pm 0.9_{\text{systematic}})$ MeV [53].For high enough temperatures, where QCD - perturbation theory is applicable, a $T$ - dependency $\chi_{\text{top}} \propto T^{-a-N_f/3}$ was established, where $a \approx 7$ depends on chromoelectric screening effects [44, 49, 54].

Using the well - established value of the topological susceptibility at $T = 0$, the axion mass was determined: $M_a(0) = (5.691 \pm 0.051)\,\mu\text{eV} \left(\frac{10^{12}\,\text{GeV}}{f_a}\right)$ [51]. Together with the range of $f_a$ one finds the zero temperature axion mass range $10^{-11}$ eV $\lesssim m_a(0) \lesssim 10^{-2}$ eV. In fact, assuming that axions constitute all of the dark matter and using the light-quark topological susceptibility results, [55] determines the axion mass and PQ-symmetry breaking scale as $M_a(0) = 26.2 \pm 3.4\,\mu$eV and $f_a = (2.21 \pm 0.29) \cdot 10^{11}$ GeV.

---

[1] The effective theory emerging from QCD at low $T$ where all quarks are subject to confinement.

The topological susceptibility is temperature dependent and its evaluation well above the QCD crossover temperature $T_c \simeq 155$ MeV [56, 57] is more challenging. But axion cosmology requires precise results; ref. [55] shows that the cosmological history of the axion depends critically on $\chi_{\text{top}}(T)$ in the temperature range $400\,$MeV $\lesssim T \lesssim 1.1\,$GeV. In this temperature range, $\chi_{\text{top}}$ is small and dominated by isolated topological objects. Unfortunately, the density of these topological objects cannot reliably be determined perturbatively, requiring a lattice investigation instead. Both existing lattice investigations in this temperature range [53] and any future investigations using topology reweighting techniques [58, 59] will be performed in so-called $2+1+1$ simulations, meaning that the $u$, $d$, $s$, and $c$ quarks are included, but the $b$ quark is not. Indeed, we are not aware of any lattice simulations which include dynamical bottom quarks - and adding them to the existing simulation framework would require very significant additional work. At the highest temperatures mentioned above, however, the bottom quark cannot be considered heavy compared to the thermal scale and may influence the topological susceptibility, i.e., accurate results for $\chi_{\text{top}}$ at high temperatures with heavy quarks are not available.

## 1.3 Aim of this Work

We address the question of how adding a dynamical $b$ quark alters the topological susceptibility of finite temperature $2+1+1+1$ theory compared to the $2+1+1$ case accessible to lattice QCD. We compare the two theories keeping the infrared physics fixed, e.g., at the same mass and decay-constant values for the $(u, d, s, c)$-containing pseudoscalars. We do this by comparing the results of a dilute caloron gas model with a heavy $b$ quark of physical mass and the same model where the $b$ quark is asymptotically heavy and the coupling is matched so the $2+1+1$ theories agree in the infrared (IR)/low energy limit.

For that, we calculate $\chi_{\text{top}}(T)$, once with physical bottom quark mass $M_b$ and once with an asymptotic bottom mass $M_{\text{asy}}$, keeping the 4-flavor effective theories in the IR fixed, i.e., equal for both cases. The physical-mass case is treated by computing the small-mass and large-mass expansions of the finite-temperature fermion fluctuation determinant - which, together with known bosonic results, yields the caloron density in the dilute gas approximation and thus the topological susceptibility - and connecting these expansions with a “Padé-like” approximant to obtain an general-mass result.

We choose this approach of small- and large-mass expansions and an interpolation due to the excellent agreement of analogously obtained results at zero temperature [60] with the general - mass result at $T = 0$ [61] (for a more detailed reference, cf. below (2.4.83)). Alternatively, one would have to solve a complicated 2 - dimensional partial differential equation, which we obtain in appendix A.

Finally, we compute the ratio $\frac{\chi_{\text{top}}(M_b, T)}{\chi_{\text{top}}(M_{\text{asy}}, T)}$ which, together with the 4 - flavor lattice result, gives the full 5 - flavor topological susceptibility at high temperatures. For the impatient reader: this result is plotted and discussed in figure 3.17.

A better understanding of $\chi_{\text{top}}$ at high temperatures and with heavy quarks directly translates to a better understanding of the axion's cosmological history, specifically and especially its mass and cosmological abundance.

# 2 Quantum Chromodynamics, Topology, Instantons and Axions

## 2.1 The “naive” Action of Quantum Chromodynamics

Quantum Chromodynamics, as stated in chapter 1, is the relativistic quantum field theory which, as a part of the Standard Model, describes (fermionic) quarks [62, 63][1] and their interactions with (bosonic) gluons [64]. QCD has proven to be a very successful theory and has thus been thoroughly discussed in a plethora of literature, e.g., [3–6], which serve as general references for this entire section.

### Symmetry in Physics

A guiding principle of physics is that nature is invariant under certain symmetry transformations, which form mathematical groups. This makes symmetry an invaluable tool for physics, not only as, arguably, the most aesthetic and natural basis for theory building, but also for solving concrete physical problems, finding conservation laws for conserved charges and currents [65] or scrutinizing and remodeling one’s theory to satisfy experimental results (two important examples for this are reviewed in section 2.5). [66] provides a more detailed discussion of this topic and [67] presents a comprehensive review of the role of symmetry and geometry in physics (in German); [68] shows, as an example, how symmetries manifest in non - relativistic Quantum Mechanics. In detail, symmetries are realized in a theory by having the physical constituents transform under irreducible (the constituents are fundamental), unitary (transition probabilities between physical states are preserved) representations of the respective symmetry groups and by constructing the Lagrangian to be invariant under these symmetry transformations. We now give an outline on how one constructs the QCD Lagrangian $\mathcal{L}_{\text{QCD}}$ purely based on symmetry.

Excluding gravity and thus general relativity, every fundamental theory (at zero temperature, for finite temperature cf. section 2.2) has to be invariant under global Poincaré transformations of special relativity [69], i.e., the translational and rotational symmetries of flat, empty spacetime have to be respected as well as the equality of all inertial frames of reference and the invariance of the speed of light [70]. The constituents of QCD, i.e., quarks and gluons, therefore have to transform under irreducible, unitary representations of the Poincaré group - the Lie group of Minkowski spacetime isometries. This means that, mathematically, the constituents form vectors spaces such that Poincaré transformations are realized as matrix operations on these vectors with the matrices obeying the structure/rules of Lorentz transformations. These representations were first classified in [71], where it was also shown that they are uniquely classified by the mass $m \geq 0$ and spin $j \in \{0, \frac{1}{2}, 1, \frac{3}{2}, ...\} = \mathbb{N} \cup \mathbb{N} + \frac{1}{2}$ of the particles and that the representations have $2j + 1$ degrees of freedom for every value of momentum with $j$ the spin of the physical constituent. Special relativity is formulated in 4 - dimensional Minkowski spacetime $\mathbb{R}^{1,3}$ with its coordinates $\chi$ and metric $\eta$:

---

[1] In [62] quarks are called “aces”.

$$\chi^{\mu_\mathrm{M}} = (\chi^0 = t, \vec{\chi}) , \quad \eta_{\mu_\mathrm{M}\nu_\mathrm{M}} = \mathrm{diag}(1, -1, -1, -1) . \tag{2.1.1}$$

We choose the mostly minus - convention for the Minkowski metric and emphasize the underlying spacetime (in contrast to Euclidean spacetime which is later going to be used almost exclusively) by the subscript “M”.

Furthermore, QCD is invariant under internal, local rotations, so called gauge rotations, in 3 - dimensional color space, i.e., “exchanging colors” of the quarks. The quarks thus also need to transform under an irreducible representation of the color rotation Lie group $SU(3)$ and the gluons, via their interactions with the quarks based on color charge, ensure the invariance of the Lagrangian despite the local, i.e., $\chi$ - dependent nature of these gauge rotations [64].

In [72] it was shown that the two above types of symmetries, spacetime and internal symmetries, can never mix their transformations and only combine trivially. They can therefore be discussed separately.

### Representation Theory of the Poincaré Group, Quarks and Gluons

Describing $\mathbb{R}^{1,3}$ - isometries, the Poincaré group $ISO(1, 3)$ contains translations and Lorentz transformations. For the latter, one chooses the subgroup of proper, orthochronous Lorentz transformations $SO^+(1, 3)$ which excludes spatial flips and preserves the temporal direction by excluding time reversals. As a Lie group, the Poincaré group is then described by the Lie algebra $\mathfrak{iso}(1, 3)$ with generators $\{P^0, P^i\}_{i=1,...,3}$ for translations, $\{J^i\}_{i=1,...,3}$ for rotations and $\{K^i\}_{i=1,...,3}$ for boosts together with the Lie algebra structure

$$\begin{aligned} &[P^0, K^i] = iP^i\,, &&[P^i, K^j] = i\delta^{ij} P^0\,,\\ &[P^i, J^j] = i\varepsilon^{ijk} P^k\,, &&[J^i, J^j] = i\varepsilon^{ijk} J^k\,,\\ &[J^i, K^j] = i\varepsilon^{ijk} K^k\,, &&[K^i, K^j] = -i\varepsilon^{ijk} J^k\,, \end{aligned} \tag{2.1.2}$$

where the $J^i$ and $K^i$ span the Lorentz subalgebra $\mathfrak{so}(1,3)$ (a good review of this and the following is also given in [73, 74], while [66, 75] provide more mathematical rigor). A general Poincaré transformation is then of the form $\exp\big(-ia^{\mu_\mathrm{M}} P_{\mu_\mathrm{M}}\big) \exp\big(i\theta^i J^i + i\zeta^i K^i\big)$ with translation vector $a^{\mu_\mathrm{M}}$, rotational angles $\theta^i \in [0, 2\pi)$ and rapidities $\vec{\zeta} = \mathrm{artanh}(|\vec{v}|)\hat{e}_{\vec{v}} \in \mathbb{R}^3$ for given spatial boost velocities $\vec{v} = \frac{\vec{v}}{c}$, $|\vec{v}| \in [0, 1)$, which can be understood as hyperbolic angles. A change of basis to generators

$$\begin{aligned} &J^i_\pm = \frac{1}{2}(J^i \pm iK^i) &&\text{yields}\\ &[J^i_\pm, J^j_\pm] = i\varepsilon^{ijk} J^j_\pm\,, &&[J^i_+, J^j_-] = 0\\ &[P^0, J^i_\pm] = \mp P^i\,, &&[P^i, J^j_\pm] = i\varepsilon^{ijk} P^k \mp \delta^{ij} P^0 \end{aligned} \tag{2.1.3}$$

and shows the mixing of rotations and boosts in this basis. The Lorentz algebra is thus isomorphic to the Kronecker sum of two separate 3 - dimensional rotation algebras [75, proposition 4.18],

$$\mathfrak{so}(1,3) \cong \mathfrak{su}(2) \otimes \mathbb{1} + \mathbb{1} \otimes \mathfrak{su}(2)\,, \tag{2.1.4}$$

which are spanned by the $J_\pm$, respectively. The fundamental or defining representation of $\mathfrak{su}(2)$ is given by generators $T^i_{SU(2),\,\mathrm{def}} = \frac{\sigma^i}{2}$ with the Hermitian, traceless Pauli matrices $\sigma^1 = \begin{pmatrix} 0 & 1 \\ 1 & 0 \end{pmatrix}$, $\sigma^2 = \begin{pmatrix} 0 & -i \\ i & 0 \end{pmatrix}$, $\sigma^3 = \begin{pmatrix} 1 & 0 \\ 0 & -1 \end{pmatrix}$ and $\left[\frac{\sigma^i}{2}, \frac{\sigma^j}{2}\right] = i\varepsilon^{ijk}\frac{\sigma^k}{2}$.[2] Since the $J^i_\pm$ are thus Hermitian, the $K^i$ need to be anti-Hermitian and the $J^i_\pm$ - parameters are then complex $\theta^i_\pm = \theta^i \mp i\zeta^i$ such that $i\theta^i_\pm J^i_\pm = i\theta^i J_i + i\zeta^i K^i$. All of this has profound consequences and requires all particles to be infinite - dimensional field representations of the Poincaré group, as we are going to discuss below. With yet another change of basis to anti-symmetric generators

$$\begin{aligned} &J^{\mu\nu} = \begin{cases} J^{0i} &= K^i \\ J^{ij} &= \varepsilon^{ijk} J^k \end{cases} \qquad \text{with}\\ &\big[J^{\mu_\mathrm{M}\nu_\mathrm{M}}, J^{\rho_\mathrm{M}\sigma_\mathrm{M}}\big] = i\Big(\eta^{\mu_\mathrm{M}\sigma_\mathrm{M}} J^{\nu_\mathrm{M}\rho_\mathrm{M}} - (\mu_\mathrm{M} \leftrightarrow \nu_\mathrm{M})\Big) - \Big(\rho_\mathrm{M} \leftrightarrow \sigma_\mathrm{M}\Big)\,,\\ &\big[P^{\mu_\mathrm{M}}, J^{\rho_\mathrm{M}\sigma_\mathrm{M}}\big] = i\Big(\eta^{\mu_\mathrm{M}\sigma_\mathrm{M}} P^{\rho_\mathrm{M}} - \eta^{\mu_\mathrm{M}\rho_\mathrm{M}} P^{\sigma_\mathrm{M}}\Big) \end{aligned} \tag{2.1.5}$$

---

[2] The Dynkin index [66, 75] of this representation is $I(\mathrm{def}) = \frac{1}{2}$, as $\mathrm{tr}\big(\frac{\sigma^i}{2}\frac{\sigma^j}{2}\big) = I(\mathrm{def})\,\delta^{ij} = \frac{1}{2}\delta^{ij}$.

one makes the relation to Minkowski spacetime obvious, since the Lorentz transformations themselves are then explicitly Lorentz - covariant: $\exp\big(-ia^{\mu_\mathrm{M}}P_{\mu_\mathrm{M}}\big)\exp\big(\frac{i}{2}\omega_{\mu_\mathrm{M}\nu_\mathrm{M}}J^{\mu_\mathrm{M}\nu_\mathrm{M}}\big)$ with anti-symmetric 2 - tensors $\omega$ containing the (hyperbolic) angles $\omega_{0i}=\zeta_i$, $\omega_{ij}=\varepsilon_{ijk}\theta_k$.

As we stated above, one looks for irreducible, unitary representation of the Poincaré group, denoted as $\Pi\big(ISO(1,3)\big)$, to describe quarks and gluons. Excluding translations, the representations of the Lorentz group $\Pi\big(SO^+(1,3)\big)$ can be constructed from those of the $J_\pm$ - $\mathfrak{su}(2)$ algebras, denoted as $\pi_{j_\pm}\big(\mathfrak{su}(2)\big)$, following (2.1.4) and are labeled $(j_+,j_-)$ by the spins/eigenvalues $j_\pm(j_\pm+1)$ of the Casimir operators $J_\pm^2=(J_\pm^i)^2$. In fact, exponentiation shows that $\pi_{j_+}\big(\mathfrak{su}(2)\big)\otimes\mathbb{1}_{(2j_-+1)\times(2j_-+1)}+\mathbb{1}_{(2j_++1)\times(2j_++1)}\otimes\pi_{j_-}\big(\mathfrak{su}(2)\big)$ is the Lie algebra for the tensor product of matrix representations $\Pi_{j_+}\big(SU(2)\big)\otimes\Pi_{j_-}\big(SU(2)\big)$. The corresponding vector space of physical constituents is $(2j_++1)(2j_-+1)$ - dimensional, as there are $2j_\pm+1$ polarizations for each spin $j_\pm$.

One now adds the $j_\pm$ - spins according to the Clebsch - Gordan coefficients (see [66, 75] or [68] for a physicist's review), which corresponds to the change of basis from (2.1.3) to (2.1.5), i.e., one obtains irreducible representations of the full Lorentz group. The total spins $j$ of the particles described by the vector space corresponding to said representations are in the range $|j_+-j_-|\leq j\leq j_++j_-$, each with $2j+1$ polarizations. This again describes a $\sum_{j\,=\,|j_+-j_-|}^{j_++j_-}(2j+1)=(2j_++1)(2j_-+1)$ - dimensional vector space. From the point of view of Lie algebras this addition of spins is given by the isomorphism $\pi_{j_+}\big(\mathfrak{su}(2)\big)\otimes\mathbb{1}_{j_-}+\mathbb{1}_{j_+}\otimes\pi_{j_-}\big(\mathfrak{su}(2)\big)\cong\bigoplus_j\pi_j\big(\mathfrak{so}(1,3)\big)=\bigoplus_j j$.[3] The direct sum of Lie algebras describes, by use of the exponential map, the direct product of the associated Lie groups $\mathfrak{g}\oplus\mathfrak{h}\overset{\exp}{\to}G\times H$.

### Spin $0$:

The simplest, trivial representation is the $(0,0)$ - representation of spin 0 - scalars, which are Lorentz singlets, i.e, $J_\pm^i=0$ and $SO^+(1,3)$ is represented by $1=\mathbb{1}_{1\times1}$. Fundamentally, QCD does not contain scalars.

### Spin $\frac{1}{2}$:

The next simplest irreducible representations, $\big(\frac{1}{2},0\big)$ and $\big(0,\frac{1}{2}\big)$, correspond to one of the sets being in the fundamental representation, $J_+^i=\frac{\sigma^i}{2}$ or $J_-^i=\frac{\sigma^i}{2}$, respectively. The fundamental representations for $J_\pm^i$ are realized by $J^i=\frac{\sigma^i}{2}$ and $K^i=\mp i\frac{\sigma^i}{2}$, where the two cases are related by parity transformation. All in all, $\big(\frac{1}{2},0\big)$ and $\big(0,\frac{1}{2}\big)$ describe right- and left - chiral (depending on the handedness of the Lorentz representation) two component - spinors $\psi_{\mathrm{R,L}}$ of spin $\frac{1}{2}$. These fermionic spinors are parity partners, i.e., by a flip in the spatial coordinates $\vec{x} \to -\vec{x}$ the left - chiral $\psi_\mathrm{L}$ transforms as $\psi_\mathrm{R}$ and vice versa. Since QCD does not violate parity, one has to combine them as $\left(0, \frac{1}{2}\right) \oplus \left(\frac{1}{2}, 0\right)$ to obtain the spin $\frac{1}{2}$ four component - Dirac spinor $\psi = \begin{pmatrix} \psi_\mathrm{L} \\ \psi_\mathrm{R} \end{pmatrix}$.

---

[3] The final shorthand notation is of common use.

Lorentz transformations are then represented by $\psi \to \begin{pmatrix} \exp(i\theta_-^i J_-^i) & 0 \\ 0 & \exp(i\theta_+^i J_+^i) \end{pmatrix} \psi$. The Dirac spinor is thus an irreducible representation of the Lorentz group extended by parity and can be used to describe quarks. The above Lorentz group - representation can be written covariantly as $\exp\left(\frac{i}{2}\omega_{\mu_\mathrm{M}\nu_\mathrm{M}} S^{\mu_\mathrm{M}\nu_\mathrm{M}}\right)$, where $S^{\mu_\mathrm{M}\nu_\mathrm{M}} = \frac{i}{4}[\gamma^{\mu_\mathrm{M}}, \gamma^{\nu_\mathrm{M}}]$ is a representation of the Lorentz algebra given by the $4 \times 4$ $\gamma$ - matrices in the Weyl/chiral representation

$$\gamma^{0_\mathrm{M}}_\text{Weyl} = \begin{pmatrix} 0 & \mathbb{1}_{2\times 2} \\ \mathbb{1}_{2\times 2} & 0 \end{pmatrix} , \quad \gamma^{i_\mathrm{M}}_\text{Weyl} = \begin{pmatrix} 0 & \sigma^i \\ -\sigma^i & 0 \end{pmatrix} . \tag{2.1.6}$$

In fact, $S^{\mu_\mathrm{M}\nu_\mathrm{M}}$ is a Lorentz algebra - representation for all choices of $\gamma$ - matrices satisfying the Clifford algebra

$$\{\gamma^{\mu_\mathrm{M}}, \gamma^{\nu_\mathrm{M}}\} = \mathbb{1}_{4\times 4} \cdot 2\eta^{\mu_\mathrm{M}\nu_\mathrm{M}} . \tag{2.1.7}$$

One also chooses to impose the Hermiticity condition $\gamma^{\mu_\mathrm{M}\,\dagger} = \gamma^{0_\mathrm{M}}\gamma^{\mu_\mathrm{M}}\gamma^{0_\mathrm{M}} = \begin{cases} \gamma^{0_\mathrm{M}} \\ -\gamma^{i_\mathrm{M}} \end{cases}$, which is satisfied by (2.1.6).

An anti-quark is described by the Dirac adjoint row spinor $\overline{\psi} = \psi^\dagger \gamma^{0_\mathrm{M}}$, which in Weyl representation means $\overline{\psi} = (\psi_\mathrm{R}^\dagger \ \psi_\mathrm{L}^\dagger)$. It transforms inversely as $\overline{\psi} \to \overline{\psi} \exp\left(-\frac{i}{2}\omega_{\mu_\mathrm{M}\nu_\mathrm{M}} S^{\mu_\mathrm{M}\nu_\mathrm{M}}\right)$.

The 2 - spinors can be retrieved from $\psi$ by the Poincaré - invariant chiral projectors

$$\mathrm{P}_\mathrm{R,L} = \mathrm{P}_\pm = \frac{1}{2}\left(\mathbb{1} \pm \gamma^{5_\mathrm{M}}\right) , \tag{2.1.8}$$

where $\gamma^{5_\mathrm{M}} = i\gamma^{0_\mathrm{M}}\gamma^{1_\mathrm{M}}\gamma^{2_\mathrm{M}}\gamma^{3_\mathrm{M}}$ is the fifth $\gamma$ - matrix. It is Hermitian $\gamma^{5_\mathrm{M}\,\dagger} = \gamma^{5_\mathrm{M}}$, involutory $(\gamma^{5_\mathrm{M}})^2 = \mathbb{1}_{4\times 4}$ and anti-commuting $\{\gamma^{5_\mathrm{M}}, \gamma^{\mu_\mathrm{M}}\} = 0$. In the Weyl basis $\gamma^{5_\mathrm{M}}$ and the chiral projectors read

$$\gamma^{5_\mathrm{M}}_\text{Weyl} = \begin{pmatrix} -\mathbb{1}_{2\times 2} & 0 \\ 0 & \mathbb{1}_{2\times 2} \end{pmatrix} , \quad \mathrm{P}_\text{L, Weyl} = \begin{pmatrix} \mathbb{1} & 0 \\ 0 & 0 \end{pmatrix} , \quad \mathrm{P}_\text{R, Weyl} = \begin{pmatrix} 0 & 0 \\ 0 & \mathbb{1} \end{pmatrix} . \tag{2.1.9}$$

Thus, $\gamma^{5_\mathrm{M}}$ then also measures the chirality of the 2 - spinors since $\gamma^{5_\mathrm{M}}\mathrm{P}_\mathrm{R,L} = \gamma^{5_\mathrm{M}}\mathrm{P}_\pm = \pm\,\mathrm{P}_\pm$.

Note that since chirality is determined by the type of Lorentz representation, it is a Poincaré - invariant. After a spatial flip $\psi_\mathrm{R,L}$ might transform as their partner, but their type of representation remains unchanged and the projectors $\mathrm{P}_\mathrm{R,L}$ give the same result. Helicity, on the other hand, measures the (anti-)parallelism of momentum and spin and can be changed via boosts (boosting from a frame slower than the particle to a faster one) or parity flips. Often, a particle's helicity is also called its parity. For Dirac spinors, the parity transformation P is realized by

$$\mathrm{P}\psi(\chi)\mathrm{P}^{-1} = \gamma^{0_\mathrm{M}}\psi(t,-\vec{\chi})\,. \tag{2.1.10}$$

For massless particles, which travel at maximum velocity, the speed of light, no such helicity-flipping boost is possible, since the speed of light is invariant of the reference frame and one cannot "overtake" the particle. Therefore, for massless particles chirality and helicity are the same and the chiral projectors (2.1.8) are also the helical projectors.

**Spin** $1$**:**

The representation $\left(\frac{1}{2},\frac{1}{2}\right)$ with both the $J^i_+$ and $J^i_-$ in the fundamental representation describes 4-vectors. To see this, one first notes that the vector space acted upon is 4-dimensional: the available total spins are $\in\{0,1\}$, i.e., one has a spin 1-particle with three polarizations and a spin 0-singlet adding one more degree of freedom. In terms of Lie algebras: $\left(\frac{1}{2},\frac{1}{2}\right) = \pi_{1/2}\big(\mathfrak{su}(2)\big)\otimes\mathbb{1}_{2\times 2} + \mathbb{1}_{2\times}\otimes\pi_{1/2}\big(\mathfrak{su}(2)\big)\cong 1\oplus 0$. We are going to outline below how to reduce these four degrees of freedom down to the two known polarizations of massless vector particles like photons or gluons.

The straightforwardly constructed representation $\frac{\sigma^i}{2}\otimes\mathbb{1}+\mathbb{1}\otimes\frac{\sigma^i}{2}$ satisfies (2.1.3), but for the case of 4-vectors it is better to reverse engineer using the known form of Lorentz transformations for 4-vectors. Rotations are generated by $\begin{pmatrix}1 & 0\\ 0 & R(\vec{\theta})\end{pmatrix}$, with $R$ the 3-dimensional rotation matrix, and boosts in the $\chi^{i_\mathrm{M}}$-direction are of the form $\begin{pmatrix}\gamma(v^1) & v^1\gamma(v^1) & & \\ v^1\gamma(v^1) & \gamma(v^1) & & \\ & & 1 & \\ & & & 1\end{pmatrix}$, $\begin{pmatrix}\gamma(v^2) & & v^2\gamma(v^2) & \\ & 1 & & \\ v^2\gamma(v^2) & & \gamma(v^2) & \\ & & & 1\end{pmatrix}$, $\begin{pmatrix}\gamma(v^3) & & & v^3\gamma(v^3)\\ & 1 & & \\ & & 1 & \\ v^3\gamma(v^3) & & & \gamma(v^3)\end{pmatrix}$ with the Lorentz factor $\gamma(v) = \left(1-v^2\right)^{-1/2}$. Taking the infinitesimal limits of a general Lorentz transformation $\Lambda(\vec{\theta},\vec{v})$, one finds the generators for rotations $J^i = -i\partial_{\theta^i}\Lambda|_{\vec{\theta}=\vec{v}=0}$ and boosts $K^i = -i\partial_{v^i}\Lambda|_{\vec{\theta}=\vec{v}=0}$:

$$J^1 = -i\begin{pmatrix}0 & 0 & 0 & 0\\ 0 & 0 & 0 & 0\\ 0 & 0 & 0 & 1\\ 0 & 0 & -1 & 0\end{pmatrix},\quad J^2 = -i\begin{pmatrix}0 & 0 & 0 & 0\\ 0 & 0 & 0 & -1\\ 0 & 0 & 0 & 0\\ 0 & 1 & 0 & 0\end{pmatrix},\quad J^3 = -i\begin{pmatrix}0 & 0 & 0 & 0\\ 0 & 0 & 1 & 0\\ 0 & -1 & 0 & 0\\ 0 & 0 & 0 & 0\end{pmatrix},$$

$$K^1 = -i \begin{pmatrix} 0 & 1 & 0 & 0 \\ 1 & 0 & 0 & 0 \\ 0 & 0 & 0 & 0 \\ 0 & 0 & 0 & 0 \end{pmatrix}, \; K^2 = -i \begin{pmatrix} 0 & 0 & 1 & 0 \\ 0 & 0 & 0 & 0 \\ 1 & 0 & 0 & 0 \\ 0 & 0 & 0 & 0 \end{pmatrix}, \; K^3 = -i \begin{pmatrix} 0 & 0 & 0 & 1 \\ 0 & 0 & 0 & 0 \\ 0 & 0 & 0 & 0 \\ 1 & 0 & 0 & 0 \end{pmatrix}. \tag{2.1.11}$$

These satisfy (2.1.2) and one can construct from them $J_\pm$ - matrices as well as $J^{\mu\nu}$ according to (2.1.3) and (2.1.5). Like the photon, the gluon carries spin 1 and is thus a vector particle described by a Lorentz 4 - vector $A^{\mu_\mathrm{M}}$.

**Higher spins:**
Representations with $j_+ > \frac{1}{2}$ and/or $j_- > \frac{1}{2}$ describe higher spins, i.e., Lorentz tensors, and are not fundamentally realized in QCD.

As we stated above, the boost generators $K^i$ are anti-Hermitian. This results in anti-unitary boost transformations, i.e., none of the above representations of the Lorentz group are unitary and they cannot describe particles. Roughly speaking, this is because the Lorentz groups is non - compact as the velocities and rapidities take values on open intervals $(-1, 1)$ and $(-\infty, \infty)$ unlike the rotation angles $\theta^i \in [0, 2\pi)$, i.e., the Lorentz group has an infinite group space. Finite - dimensional representations of non - compact groups (as all of the above) are always non - unitary, whereas infinite - dimensional field representations of such groups are indeed unitary. Infinite - dimensional representations of the Lorentz group can be constructed by considering momentum - dependent basis vectors for the quark spinors and gluon vector fields. For fixed momenta $p^{\mu_\mathrm{M}}$ the Lorentz group $SO^+(1, 3)$ then reduces to the stabilizer group of momentum, the rotation group $SO(3)$ which is unitary and of the same form for all moments. Having $p^{\mu_\mathrm{M}}$ - dependent basis vectors is the Fourier transformed analogue to having the particles be $\chi$ - dependent fields $\psi(\chi)$ and $A^{\mu_\mathrm{M}}(\chi)$ characterized by their spins. Now one also reintroduces the translation operator $P^{\mu_\mathrm{M}}$. The field representation of the Poincaré group is given by the generators

$$P^{\mu_\mathrm{M}} = -i\partial^{\mu_\mathrm{M}}\,, \qquad J^{\mu_\mathrm{M}\nu_\mathrm{M}} = -i(\chi^{\mu_\mathrm{M}}\partial^{\nu_\mathrm{M}} - \chi^{\nu_\mathrm{M}}\partial^{\mu_\mathrm{M}}) = \chi^{\mu_\mathrm{M}}P^{\nu_\mathrm{M}} - \chi^{\nu_\mathrm{M}}P^{\mu_\mathrm{M}}\,, \tag{2.1.12}$$

which perform translations and rotations of the particle fields by Taylor expansion.

Since $P^2$ commutes with all other Poincaré group generators, one has (Schur's Lemma) $P^2 = \text{const.} \cdot \mathbb{1}$ and can use this Lorentz scalar constant to characterize particles. By Fourier transformation, the $\chi$ - dependency of the fields can be written via exponentials $e^{\pm i p_{\mu_\mathrm{M}} \chi^{\mu_\mathrm{M}}}$, so that the constant is fixed by the energy - momentum - relation $P^2 = p^2 = m^2$. The proper orthochronous Lorentz transformations contain no time reversals, therefore $\mathrm{sign}(p^{0_\mathrm{M}})$ is invariant. All in all, [71] thus identifies six categories of representations:

1a) $p^2 = m^2$, $p^{0_\mathrm{M}} > 0$: massive, timelike particle,

1b) $p^2 = m^2$, $p^{0_\mathrm{M}} < 0$: massive, timelike particle, traveling backwards in time $\Rightarrow$ unphysical,

2a) $p^2 = 0$, $p^{0_\mathrm{M}} > 0$: massless, timelike particle,

2b) $p^2 = 0$, $p^{0_\mathrm{M}} < 0$: massless, timelike particle, traveling backwards in time $\Rightarrow$ unphysical,

3) $p^{\mu_\mathrm{M}} = 0$: vacuum,

4) $p^2 < 0$: virtual particles.

Particle spin is the second characterizing quantity, but it is actually not associated to the total spin operator $J^2 = (J^i_+ \otimes \mathbb{1} + \mathbb{1} \otimes J^i_-)^2 = J^2_+ \otimes \mathbb{1} + \mathbb{1} \otimes J^2_- + 2J^i_+ \otimes J^i_-$, as $J^2$ is not a Casimir invariant $[J^2, J^i_\pm] \neq 0$ (compare (2.1.3)). Alternatively, the total spin operator can be defined as $J^2 = (J^i)^2$, which again is not a Casimir operator as $[J^2, K^i] \neq 0$ (compare (2.1.2)). The actual Casimir invariant corresponding to spin is $W^2 = m^2 j(j+1)\mathbb{1}$, where $W^{\mu_\mathrm{M}} = -\frac{1}{2}\varepsilon^{\mu_\mathrm{M}}{}_{\nu_\mathrm{M}\rho_\mathrm{M}\sigma_\mathrm{M}} J^{\nu_\mathrm{M}\rho_\mathrm{M}} P^{\sigma_\mathrm{M}}$ is the Pauli - Lubanski pseudovector.[4] $W^{\mu_\mathrm{M}}$ is orthogonal to the momentum $W^{\mu_\mathrm{M}} P_{\mu_\mathrm{M}} = 0$. In the particle's rest frame $p^{\mu_\mathrm{M}} = (m, \vec{0}\,)$ this Casimir operator reduces to the total spin operator, $W^{i_\mathrm{M}} W_{i_\mathrm{M}} = m^2 (J^i)^2$, but this is not a Lorentz invariant relation.

The QCD - particles therefore categorize as follows: quarks are 1a) - type particles with spin $\frac{1}{2}$ and gluons are 2a) - type particles of spin 1.

### Constructing the Lagrangian of free Quarks

Using the above, one constructs the Lagrangian for free quarks $\mathcal{L}_\text{quark}$. Since the action

$$S = \int_{\mathbb{R}^{1,3}} \mathrm{d}^4\chi \; \mathcal{L} \tag{2.1.13}$$

for any Lagrangian has to be dimensionless, $\mathcal{L}_\text{quark}$ has to be a Lorentz scalar of dimension $[\mathcal{L}_\text{quark}] = \text{Length}^{-4}$ containing Dirac spinors $\psi$ and their derivatives. Note that since physics is described in terms of fields, Lagrangians are only Poincaré - covariant, i.e., $\chi$ - dependent Lorentz scalars, not Poincaré - invariant. The action is Poincaré - invariant, however.

---

[4] $W^{\mu_\mathrm{M}}$ satisfies the commutation relations $[P^{\mu_\mathrm{M}}, W^{\nu_\mathrm{M}}] = 0$, $[J^{\mu_\mathrm{M}\nu_\mathrm{M}}, W^{\rho_\mathrm{M}}] = -i\eta^{\rho_\mathrm{M}\mu_\mathrm{M}} W^{\nu_\mathrm{M}} - (\mu_\mathrm{M} \leftrightarrow \nu_\mathrm{M})$, $[W^{\mu_\mathrm{M}}, W^{\nu_\mathrm{M}}] = -i\varepsilon^{\mu_\mathrm{M}\nu_\mathrm{M}}{}_{\rho_\mathrm{M}\sigma_\mathrm{M}} W^{\rho_\mathrm{M}} P^{\sigma_\mathrm{M}}$

For the quarks one can construct, from the Dirac and adjoint spinors, quantities which transform as Lorentz - scalars, -vectors, -pseudoscalars, -pseudovectors or general Lorentz - tensors:

$$\begin{aligned}&\text{scalar: } \overline{\psi}\psi\,, \quad \text{pseudoscalar: } \overline{\psi}\gamma^{5_\mathrm{M}}\psi\,, \quad \text{vector: } \overline{\psi}\gamma^{\mu_\mathrm{M}}\psi\,,\\ &\text{pseudovector: } \overline{\psi}\gamma^{\mu_\mathrm{M}}\gamma^{5_\mathrm{M}}\psi\,, \quad \begin{pmatrix}\text{symmetric}\\ \text{anti-symmetric}\end{pmatrix} \text{ 2 - tensor: } \overline{\psi}\begin{pmatrix}\{\gamma^{\mu_\mathrm{M}},\gamma^{\nu_\mathrm{M}}\}\\ [\gamma^{\mu_\mathrm{M}},\gamma^{\nu_\mathrm{M}}]\end{pmatrix}\psi\,,\dots\,.\end{aligned} \tag{2.1.14}$$

The prefix “pseudo” means that these objects gain an additional factor $-1$ under parity transformations (2.1.10).

Using the Feynman slash notation $a^{\mu_\mathrm{M}}\gamma_{\mu_\mathrm{M}} = \not{a}$, the possible $\mathcal{L}_\mathrm{QCD}$ - terms are then $\overline{\psi}\psi$, $\overline{\psi}\not\partial\psi$ and $\overline{\psi}\{\not\partial,\not\partial\}\psi$. “Pseudo” - terms are excluded, since QCD preserves parity, i.e., it is invariant under (2.1.10), and parity - invariant terms built from $\overline{\psi}\gamma^{5_\mathrm{M}}\psi$ and $\overline{\psi}\gamma^{\mu_\mathrm{M}}\gamma^{5_\mathrm{M}}\psi$ would be at least of order $\mathcal{O}(\psi^4)$, i.e., interaction terms. Furthermore, terms containing higher order symmetric combinations of $\not\partial$’s are excluded as well, since they produce pathological effects like negative energy states, non - unitarity, etc. Employing the Clifford algebra, the third possible term reduces to $\overline{\psi}\not\partial\not\partial\psi = \overline{\psi}\frac{1}{2}\partial^2\psi$, which is just the theory of four scalar fields $\psi^{1,2}_{\mathrm{R,L}}$, so it is insufficient to describe fermions. The remaining terms thus give the Lagrangian for, in general, $N_f$ flavors of free quark fields (in QCD $N_f = 6$, cf. table 1.1):

$$\mathcal{L}_\text{quark} = \sum_{f=1}^{N_f} \overline{\psi}_f i\not\partial\psi_f - M_f\overline{\psi}_f\psi_f\,. \tag{2.1.15}$$

Dirac spinors are thus of dimension $[\psi] = \text{Length}^{-3/2}$. The factor $i$ in (2.1.15) ensures that the differential operator $i\not\partial - M_f$ be self - adjoint with respect to the fermion inner product, i.e., $(\psi(x),\psi'(x)) = \int_{\mathbb{R}^{1,3}}\mathrm{d}^4x\,\overline{\psi}(x)\psi'(x) = \int_{\mathbb{R}^{1,3}}\mathrm{d}^4x\,\psi^\dagger(x)\gamma^{0_\mathrm{M}}\psi'(x)$,

$$\begin{aligned}(i\not\partial\psi,\psi') &= \int_{\mathbb{R}^{1,3}}\mathrm{d}^4x\,(\overline{i\not\partial\psi})\psi' = -\int_{\mathbb{R}^{1,3}}\mathrm{d}^4x\,i\psi^\dagger\partial^\dagger_{\mu_\mathrm{M}}\gamma^{\mu_\mathrm{M}\,\dagger}\gamma^{0_\mathrm{M}}\psi' =\\ &= \int_{\mathbb{R}^{1,3}}\mathrm{d}^4x\,i\psi^\dagger\partial_{\mu_\mathrm{M}}\gamma^{0_\mathrm{M}}\gamma^{\mu_\mathrm{M}}\psi' = \int_{\mathbb{R}^{1,3}}\mathrm{d}^4x\,\overline{\psi}i\not\partial\psi' = (\psi,i\not\partial\psi')\,,\end{aligned} \tag{2.1.16}$$

where one uses $\gamma^{\mu_\mathrm{M}\,\dagger} = \gamma^{0_\mathrm{M}}\gamma^{\mu_\mathrm{M}}\gamma^{0_\mathrm{M}}$. Therefore, $i\not\partial - M$ has real eigenvalues. The fermionic equation of motion then reads

$$(i\not\partial - M_f)\psi_f = 0 \quad \Leftrightarrow \quad \overline{\psi}_f(i\overleftarrow{\not\partial} + M_f) = 0\,. \tag{2.1.17}$$

### Gauge Invariance, the Yang - Mills Lagrangian and the QCD Lagrangian

The quarks are not only spinors to be acted upon by representations of the Lorentz group, but also carry color charge and thus transform under irreducible, unitary representations of the color group $SU(3)$. Specifically, quarks are vectors in color space $\mathbb{C}^3 = \text{span}\left(\hat{e}_{\text{red}} = \begin{pmatrix}1\\0\\0\end{pmatrix}, \hat{e}_{\text{blue}} = \begin{pmatrix}0\\1\\0\end{pmatrix}, \hat{e}_{\text{green}} = \begin{pmatrix}0\\0\\1\end{pmatrix}\right)$, transforming under the fundamental representation of $SU(3)$ given by generators $T^a_{SU(3),\,\text{def}} = \frac{\lambda^a}{2}$, with the Hermitian, traceless Gell-Mann matrices $\lambda^1 = \begin{pmatrix}0&1&0\\1&0&0\\0&0&0\end{pmatrix}$, $\lambda^2 = \begin{pmatrix}0&-i&0\\i&0&0\\0&0&0\end{pmatrix}$, $\lambda^3 = \begin{pmatrix}1&0&0\\0&-1&0\\0&0&0\end{pmatrix}$, $\lambda^4 = \begin{pmatrix}0&0&1\\0&0&0\\1&0&0\end{pmatrix}$, $\lambda^5 = \begin{pmatrix}0&0&-i\\0&0&0\\i&0&0\end{pmatrix}$, $\lambda^6 = \begin{pmatrix}0&0&0\\0&0&1\\0&1&0\end{pmatrix}$, $\lambda^7 = \begin{pmatrix}0&0&0\\0&0&-i\\0&i&0\end{pmatrix}$ and $\lambda^8 = \frac{1}{\sqrt{3}}\begin{pmatrix}1&0&0\\0&1&0\\0&0&-2\end{pmatrix}$. These satisfy commutation relations $\left[\frac{\lambda^a}{2}, \frac{\lambda^b}{2}\right] = i f^{abc}\frac{\lambda^c}{2}$ with $f^{123} = 1$, $f^{147} = -f^{156} = f^{246} = f^{257} = f^{345} = -f^{367} = \frac{1}{2}$ and $f^{458} = f^{678} = \frac{\sqrt{3}}{2}$.[5]

The Dirac adjoint $\overline{\psi}$ describing an anti-quark is then also a row vector in dual color space, transforming under the anti-fundamental representation, i.e., the inverse/Hermitian-conjugate of the fundamental representation.

The defining property of gauge symmetries is their locality, i.e., they correspond to $x$-dependent transformations. Therefore one considers gauge rotations $\psi \to U(x)\psi$, $U(x) = \exp\left(i\theta^a(x)\frac{\lambda^a}{2}\right) \in SU(3)$. The Lagrangian (2.1.15) is not invariant (not even covariant) under such transformations, however, and thus has to be modified by replacing $\partial^{\mu_\text{M}}$ with a gauge-covariant derivative

$$D^{\mu_\text{M}} = \partial^{\mu_\text{M}} - iA^{\mu_\text{M}}(x) \tag{2.1.18}$$

given in terms of the gluon vector field $A^{\mu_\text{M}}$; the coupling strength $g$ is here absorbed into the gluon field. This is called the “geometrical normalization” of $A$. Alternatively, the “physical normalization” of the gauge field which makes the coupling strength $g$ explicit, $D^{\mu_\text{M}} - igA^{\mu_\text{M}}$, is also often used. The gluon field is of dimension $[A] = [\partial] = \text{Length}^{-1}$. The structure of the gauge-covariant derivative also fixes the coupling of gluons to quarks

---

[5] As for the fundamental $\mathfrak{su}(2)$-representation, the Dynkin index of the fundamental $\mathfrak{su}(3)$-representation is also $\frac{1}{2}$.

- the gluon is an $\mathfrak{su}(3)$ - matrix $A^{\mu_\mathrm{M}}(x) = A^{a\,\mu_\mathrm{M}}(x)\frac{\lambda^a}{2}$ and couples to quarks via matrix multiplication - and the gluon's transformation properties under gauge rotations:

$$A^{\mu_\mathrm{M}}(x) \to A'^{\,\mu_\mathrm{M}}(x) = U(x)A^{\mu_\mathrm{M}}(x)U^{-1}(x) + iU(x)\partial^{\mu_\mathrm{M}}U^{-1}(x)\,. \tag{2.1.19}$$

This transformation property ensures that $D^{\mu_\mathrm{M}}\psi$ transform under gauge rotations as $\psi$,

$$D^{\mu_\mathrm{M}}\psi \;\to\; U(x)D^{\mu_\mathrm{M}}\psi\,, \tag{2.1.20}$$

and therefore that the combination $\overline{\psi}i\not{D}\psi$ be gauge - invariant. The gauge - covariant derivative $D$ is analogous in design to the (geometrically) covariant derivative $\nabla$ of general relativity. Furthermore, just as the Christoffel symbol of general relativity, which ensures the proper tensor transformation properties of covariant derivatives $\nabla_\mu T^{\alpha\beta\cdots}$, is not and cannot be a tensor itself, the gluon gauge field does not transform under any representation of the gauge group. Only for constant transformations $U \neq U(x)$ does it transform by the $SU(3)$ - adjoint representation. Finally, the fermion equation of motion (2.1.17) also gets modified: $\not{\partial}$ is replaced by $\not{D}$.

One has to construct the Lagrangian of free gluons, the Lagrangian of Yang - Mills theory [76], from terms which are both Lorentz scalars and gauge - invariant. General relativity serves as a guide: the fundamental building block of the Einstein - Hilbert action [77] of curved spacetime and gravity is the Riemann curvature tensor $R^\alpha{}_{\beta\gamma\delta}v^\beta = [\nabla_\gamma, \nabla_\delta]v^\alpha$, which is given by the commutator of said covariant derivatives. Analogously, one constructs the gauge gluonic field strength tensor

$$\begin{aligned} G^{\mu_\mathrm{M}\nu_\mathrm{M}} &= i[D^{\mu_\mathrm{M}}, D^{\nu_\mathrm{M}}] = \partial^{\mu_\mathrm{M}}A^{\nu_\mathrm{M}} - \partial^{\nu_\mathrm{M}}A^{\mu_\mathrm{M}} - i[A^{\mu_\mathrm{M}}, A^{\nu_\mathrm{M}}] = \\ &= \left(\partial^{\mu_\mathrm{M}}A^{a\,\nu_\mathrm{M}} - \partial^{\nu_\mathrm{M}}A^{a\,\mu_\mathrm{M}} + f^{abc}A^{b\,\mu_\mathrm{M}}A^{c\,\nu_\mathrm{M}}\right)\frac{\lambda^a}{2} \end{aligned} \tag{2.1.21}$$

which is anti-symmetric $G^{\mu_\mathrm{M}\nu_\mathrm{M}} = -G^{\nu_\mathrm{M}\mu_\mathrm{M}}$ and transforms under the adjoint representation of the gauge group $G^{\mu_\mathrm{M}\nu_\mathrm{M}} \to U(x)G^{\mu_\mathrm{M}\nu_\mathrm{M}}U^{-1}(x)$. To construct a Lorentz scalar, one can contract the unpaired $G^{\mu_\mathrm{M}\nu_\mathrm{M}}$ - Lorentz indices with either another field strength, the gluon field or derivatives. The only unique, non - vanishing and gauge - invariant field combinations are then found to be $\mathrm{tr}\big(G^{\mu_\mathrm{M}\nu_\mathrm{M}}G_{\mu_\mathrm{M}\nu_\mathrm{M}}\big)$ and $\mathrm{tr}\big(\widetilde{G}^{\mu_\mathrm{M}\nu_\mathrm{M}}G_{\mu_\mathrm{M}\nu_\mathrm{M}}\big)$ with the dual field strength tensor $\widetilde{G}^{\mu_\mathrm{M}\nu_\mathrm{M}} = \frac{1}{2}\varepsilon^{\mu_\mathrm{M}\nu_\mathrm{M}}{}_{\rho_\mathrm{M}\sigma_\mathrm{M}}G^{\rho_\mathrm{M}\sigma_\mathrm{M}}$. The second term is a total derivative, however, and with the usual arguments of fields vanishing at large distances it should not contribute to the action. Furthermore it does not alter the equations motion and thus does not contribute at any order of perturbation theory. Thus it is discarded for the usual gluon Lagrangian. This is, as we are going to discuss in section 2.4, too "naive" an approach, however, as there exist gluon configurations such that boundary terms do in fact contribute non - perturbatively. Therefore, one actually should include the dual field strength - term. Neglecting it for now, however, the Yang - Mills (YM) Lagrangian for gluons (in geometrical gauge field normalization) reads

$$\mathcal{L}_{\text{YM}} = -\frac{1}{2g^2}\mathrm{tr}\big(G^{\mu_{\text{M}}\nu_{\text{M}}}G_{\mu_{\text{M}}\nu_{\text{M}}}\big) = -\frac{1}{4g^2}G^{a\,\mu_{\text{M}}\nu_{\text{M}}}G^{a}_{\mu_{\text{M}}\nu_{\text{M}}} \,. \tag{2.1.22}$$

Note that all the above and the Lagrangian (2.1.22) are straightforwardly generalized to $SU(N)$ - gauge theory. The YM equation of motion for free gluons is

$$D_{\mu_{\text{M}}}G^{\mu_{\text{M}}\nu_{\text{M}}} = 0\,. \tag{2.1.23}$$

All in all, the QCD Lagrangian of quarks, gluons and their interactions is given by

$$\mathcal{L}_{\text{QCD}} = \mathcal{L}_{\text{quark}} + \mathcal{L}_{\text{YM}} = \sum_{f=1}^{N_f}\overline{\psi}_f\big(i\not{D} - M_f\big)\psi_f - \frac{1}{2g^2}\mathrm{tr}\big(G^{\mu_{\text{M}}\nu_{\text{M}}}G_{\mu_{\text{M}}\nu_{\text{M}}}\big)\,, \tag{2.1.24}$$

where $M_f = \mathrm{diag}(M_1, ..., M_{N_f})$ is the quark mass matrix generating scalar mass terms.

Quarks are thus described by $\psi(\chi) = \psi_{\text{flavor vector}} \otimes \psi_{\text{Dirac spinor}}(\chi) \otimes \psi_{\text{color vector}}(\chi)$, while anti-quarks are given by $\overline{\psi}(\chi) = \psi^{\mathrm{T}}_{\text{flavor vector}} \otimes \overline{\psi}_{\text{Dirac spinor}}(\chi) \otimes \psi^{\dagger}_{\text{color vector}}(\chi)$. The flavor vector $\psi_{\text{flavor vector}} \in \mathbb{R}^{N_f}$ describes the distinct flavor the quark; in the SM one has $N_f = 6$, cf. table 1.1, and thus $\hat{e}_{u,d,s,c,b,t} = \hat{e}_{1,\,...,\,6}$. This split of the (flavor and) Dirac spinor from the color vector is a result of [72], which was discussed at the beginning of this section. The $SU(N)$ - matrix - valued gluons are given by $A(\chi) = A_{\text{vector}}(\chi) \otimes A_{\text{color matrix}}(\chi)$, with $N = 3$ in the SM. The quark - gluon interaction is described by the covariant derivative $D^{\mu_{\text{M}}} = \partial^{\mu_{\text{M}}} - iA^{\mu_{\text{M}}}$. Note that the coupling strength $g$, which is absorbed into the gluon field as explained below (2.1.18), is universal for all quark flavors.[6]

### Wilson Lines and Loops

To motivate and construct *Wilson lines* and *loops*, one again goes back to the guideline of general relativity (even though general relativity is not a gauge theory) and to drawing analogues:

- Riemann curvature tensor $R^{\alpha}{}_{\beta\gamma\delta} \longleftrightarrow$ field strength $G^{\mu_{\text{M}}\nu_{\text{M}}}$
- covariant derivative $\nabla \longleftrightarrow$ gauge covariant derivative $D$
- Christoffel symbol $\Gamma^{\alpha}{}_{\beta\gamma} \longleftrightarrow$ gauge field $A^{\mu_{\text{M}}}$.

---

[6] In the full SM quarks also carry weak isospin and weak charge, by which they couple to the $W^{\pm}$ - bosons and $Z^0$ - boson, respectively, as well as electric charges so that they couple to photons.

Just like one cannot compare two observables at different points in a curved spacetime without taking into account the effects of translation between the points, one cannot compare quarks at different points while neglecting the influence of the gauge field. In detail, one cannot translate $\psi_{\text{Dirac spinor}}$ without also translating the $x$-dependent orientation $\psi_{\text{color vector}}$ in color space.

In general relativity such a connection between neighboring tangent spaces, i.e., between the velocity vectors determining trajectories, is given by $\nabla$ and the associated parallel transport. In gauge theory, the comparator is the Wilson line $W(x, y)$. One demands that gauge transformations change it as

$$W(x, y)) \;\rightarrow\; U(x)W(x, y)U^{-1}(y)\,, \tag{2.1.25}$$

where $U(x) = \exp\big(i\theta^a(x)\frac{\lambda^a}{2}\big) \in SU(3)$ is also the transformation matrix for quarks, so that

$$W(x, y))\psi(y) - \psi(x) \;\rightarrow\; U(x)\big(W(x, y))\psi(y) - \psi(x)\big) \quad \text{and} \tag{2.1.26}$$

$$D^{\mu_{\mathrm{M}}}\psi(x) = \lim_{\delta x^{\mu_{\mathrm{M}}} \to 0} \frac{W(x, x + \delta x)\psi(x + \delta x) - \psi(x)}{\delta x_{\mu_{\mathrm{M}}}}\,. \tag{2.1.27}$$

Indeed, this completely fixes the structure of the Wilson line and one has

$$W_{\mathrm{C}}(x, y) = \mathrm{P}\,\exp\left(-i\int_{\mathrm{C}} \mathrm{d}z_{\mu_{\mathrm{M}}}\, A^{\mu_{\mathrm{M}}}(z)\right), \tag{2.1.28}$$

where C is a curve linking $y$ and $x$ and P is the path ordering operator for the non-commuting gauge field matrices along that curve. Closing the curve C and taking the trace therefore yields a gauge-invariant object, the Wilson loop

$$W_{\mathrm{C}}[A] = \mathrm{tr}\left(\mathrm{P}\,\exp\left(-i\oint_{\mathrm{C}} \mathrm{d}z_{\mu_{\mathrm{M}}}\, A^{\mu_{\mathrm{M}}}(z)\right)\right) = \mathrm{tr}\left(\exp\left(-\frac{i}{2}\int_{\Sigma} \mathrm{d}\sigma_{\mu_{\mathrm{M}}\nu_{\mathrm{M}}}\, G^{\mu_{\mathrm{M}}\nu_{\mathrm{M}}}\right)\right), \tag{2.1.29}$$

where C encloses the surface $\Sigma$, i.e., $\partial\Sigma = \mathrm{C}$. Obviously, the Wilson line and also the Wilson loop depend on the specific curve C.

### Gauge Fixing

The Lorentz vector field $A^{\mu_{\mathrm{M}}}$ has four degrees of freedom, but from photons one knows that massless vector fields only have two polarizations. The YM Lagrangian is invariant and the resulting equations of motion are covariant under the gauge transformations (2.1.19). This means that one can choose appropriate $U(x)$ to “fix the gauge”, i.e., have

$A'^{\mu_{\mathrm{M}}}$ satisfy some (set of) condition(s) $\mathcal{G}(A') = \mathcal{C}_{\mu_{\mathrm{M}}} A'^{\mu_{\mathrm{M}}} = 0$, with $\mathcal{C}_{\mu_{\mathrm{M}}}$ some vectorial quantity/operator, that reduce the degrees of freedom. These gauge conditions, or gauges for short, are

- Lorenz gauge: $\mathcal{G}_{\text{Lorenz}}(A') = \partial_{\mu_{\mathrm{M}}} A'^{\mu_{\mathrm{M}}} = 0$,
- axial gauge: $\mathcal{G}_{\text{axial}}(A') = n_{\mu_{\mathrm{M}}} A'^{\mu_{\mathrm{M}}} = 0$,
- Fock-Schwinger gauge [78–80]: $\mathcal{G}_{\text{Fock-Schwinger}}(A') = x_{\mu_{\mathrm{M}}} A'^{\mu_{\mathrm{M}}} = 0$,
- Dirac gauge [81]: $\mathcal{G}_{\text{Dirac}}(A') = A'_{\mu_{\mathrm{M}}} A'^{\mu_{\mathrm{M}}} = \text{const.}$,
- Coulomb gauge: $\mathcal{G}_{\text{Coulomb}}(A') = \partial_{i_{\mathrm{M}}} A'^{i_{\mathrm{M}}} = 0$,
- Weyl/temporal gauge: $\mathcal{G}_{\text{Weyl}}(A') = A'^{0_{\mathrm{M}}} = 0$ (special case of the axial gauge),
- "longitudinal axial gauge": $\mathcal{G}_{\text{“long. axial”}}(A') = \hat{e}_{\text{long}} \cdot \vec{A}' = 0$ (special case of the axial gauge).

In ordinary QCD this exhausts all possible unique $\mathcal{C}_{\mu_{\mathrm{M}}}$'s. The advantage of Lorenz gauge is its full Poincaré-invariance, while the axial, Fock-Schwinger and Dirac gauge are Poincaré-covariant. Coulomb, Weyl and "longitudinal axial gauge" break Lorentz covariance (Coulomb and Weyl gauge at least preserve rotational covariance). The "longitudinal axial gauge" is used to eliminate the longitudinal component of $\vec{A}'$ in some Lorentz frame, e.g., $A'^{z_{\mathrm{M}}} = 0$ for a beam in $z$-direction in the lab frame.

Gauges which preserve Lorentz covariance are incomplete gauges, removing only one degree of freedom, while complete gauges which reduce the $A'^{\mu_{\mathrm{M}}}$-degrees of freedom by two break Lorenz invariance. This corresponds to choosing a preferred Lorentz frame in which the complete gauge condition is true, which does however not translate to other frames [82, 83]. For example, transversality and longitudinality as used in the "longitudinal axial gauge" are not conserved under Lorentz boosts. An example of a complete gauge is Coulomb gauge combined with Weyl gauge. This is a prominent example, because the residual gauge freedom left from Coulomb gauge allows one to freely impose Weyl gauge. Complete gauges require caution when boosting to different Lorentz frames, as the physical results in the preferred "gauge frame" are specific to this frame and have to be translated to any other frame. Incomplete gauges do not suffer from this problem, but, in turn, an unphysical degree of freedom, a so-called ghost field, is allowed to remain in the theory. These ghosts have vanishing/negative norms, negative energies, violate the spin-statistics theorem or show other unphysical properties. Depending on the quantization scheme, these ghost fields either only occur as internal states of quantum interactions, but not as external, observable states, or, if that is not the case, they have to be removed from the spectrum of all external states explicitly by enforcing the gauge condition. Axial and Fock - Schwinger gauge in fact have the advantage that their ghosts decouple completely from other QCD fields, so that their contributions can safely be neglected [80]. Gauge symmetry is thus not so much a symmetry transformation between physical states, but rather makes obvious a redundancy in describing one and the same state. Therefore, there are also no conserved charges of currents associated to gauge symmetry, making it unobservable as a whole. This corresponds to the statement in the introduction that all observable states are colorless, i.e., color - singlets, and is also why one constructs the Lagrangians to be gauge - invariant, but only Poincaré - covariant.

Having made a big effort to construct a Poincaré - covariant formulation of QCD, one usually employs Poincaré - covariant gauge conditions $\mathcal{G}_{\text{Poincaré - cov.}}(A')$ like the Lorenz, axial or Dirac gauge (another example for such a gauge, which is essential for this work, is given in (2.4.42)).

Given the Lagrangian (2.1.24), gauge fixing still has to be enforced manually. This is because the theory has not been quantized yet. In the following section 2.2 we are going to show how gauge fixing can be automatically ensured in quantized QCD.

## 2.2 Path Integral Quantization and Thermal Field Theory

The Lagrangian $\mathcal{L}_{\text{QCD}}$ (2.1.24) and the resulting action $S_{\text{QCD}} = \int_{\mathbb{R}^{1,3}} \mathrm{d}^4 x \, \mathcal{L}_{\text{QCD}}$ still describe the physics of classical fields. In order to describe quantum physics, a multitude of quantization schemes are available and described in standard literature such as [3–6], which again serve as general references for this section. The most common quantization schemes are the *canonical quantization* scheme, where classical observables and fields are replaced by operators with adequate (anti-)commutation relations, and the *path integral* formalism, which we employ for our discussions. This has several reasons [6, 84, 85]:

1. The path integral is inherently Poincaré - covariant and allows for a natural inclusion of constraints such as gauge conditions.

2. Observables and fields remain numbers (although possibly Graßmannian, to include anti-commutation relations), quantum mechanical phenomena follow from the structure of the fields, the Lagrangian and the fundamental principles of Quantum Mechanics. No additional quantization prescriptions as in the operator formalism are required.

3. Other quantization schemes can be derived from the path integral.

4. The path integral allows for the calculation of perturbative and non - perturbative results; this is going to prove especially useful in this work.
5. Renormalization is comparably easy to express using path integrals.
6. The path integral can easily be modified to describe equilibrium quantum processes in a thermal medium; this is also going to be used extensively in this work.

For the derivation of the path integral we follow again [3–6], the modification to thermal QFT is nicely described in [84–87]. The derivation is performed for the simple case of a real scalar field, but the generalization to vectors or spinors is discussed at length in the literature.

### 2.2.1 Path Integral Quantization and the Effective Action

We introduce the path integral in non - relativistic "standard" quantum mechanics in three dimensions, as the results are straightforwardly extended to QFT.

For a physical system in standard mechanics defined by the degrees of freedom "position $\vec{x}$" and "canonical momentum $\vec{p}$" with a Hamiltonian $\mathcal{H}(\vec{p}, \vec{x}, t) = \vec{p}^{\mathrm{T}}\vec{x} - \mathcal{L}(t)$, the path integral aims at calculating the *generating functional* $Z$:[7]

$$\begin{aligned} Z &= \left\langle \vec{x}_{\text{final}} \middle| e^{-i\mathcal{H}(t_{\mathrm{f}}-t_{\mathrm{i}})} \middle| \vec{x}_{\text{initial}} \right\rangle = N \int_{\text{all possible paths } \vec{x}(t) \text{ from } \vec{x}_{\mathrm{i}} \text{ to } \vec{x}_{\mathrm{f}}} e^{iS[\vec{x}]} \,, \\ S[\vec{x}(t)] &= \int_{t_{\mathrm{i}}}^{t_{\mathrm{f}}} \mathrm{d}t \; \mathcal{L}(\vec{x}, \mathrm{d}_t\vec{x}) = \int_{t_{\mathrm{i}}}^{t_{\mathrm{f}}} \mathrm{d}t \left( \frac{1}{2} \left(\mathrm{d}_t\vec{x}\right)^{\mathrm{T}} \mathcal{M} \, \mathrm{d}_t\vec{x} - V(\vec{x}, t) \right) , \end{aligned} \tag{2.2.1}$$

where $N$ is a normalization constant, the constant mass matrix $\mathcal{M}$ determines the kinetic energy and $V$ is a (potentially time - dependent) potential.

The intuition behind $Z$ is the following: inserting a double slit screen between $\vec{x}_{\mathrm{i}}$ and $\vec{x}_{\mathrm{f}}$ allows for two separate paths to combine, i.e., the final probability at $\vec{x}_{\mathrm{f}}$ is obtained by squaring the sum of the two amplitudes. Adding more screens with more slits produces, in the limit of continuously many screens with continuously many slits, an integral over all possible paths. One of those paths corresponds to the classical path $\vec{x}_{\mathrm{cl}}(t)$, the remaining paths are quantum corrections. This is illustrated in figure 2.1a. In the *semi - classical limit*, where quantum effects are accompanied by a factor $\{\hbar\} \ll 1$, the *stationary phase approximation* holds and the main contribution to $Z$ is due to those paths $\vec{x}(t)$ which are

---

[7] To emphasize the relation of the non - relativistic quantum mechanical processes to real time, i.e., Minkowski time, we use here the same time symbols as for Minkowski spacetime (2.1.1), despite the symmetry group of non - relativistic quantum mechanics being the Galilean group (see, for example, [67, p. 53]).

“close” to the classical solution of $-\frac{\delta S}{\delta \vec{\chi}}\Big|_{\vec{\chi}_{\mathrm{cl}}} = \left(\mathcal{M}\,\mathrm{d}_t^2\vec{\chi} + \vec{\partial}V\right)\Big|_{\vec{\chi}_{\mathrm{cl}}} = 0$. “Close” means here that the phase difference between the classical path and the quantum perturbation around the classical path does not exceed $\pi$ and no cancellations occur: $S[\vec{\chi}_{\mathrm{cl}}] - S[\vec{\chi}] \lesssim \pi\hbar$. The region of such quantum paths close to the classical solution is called the *coherence region*.

To obtain the relation between the propagator $\langle\vec{\chi}_{\mathrm{f}}|e^{-i\mathcal{H}\Delta t}|\vec{\chi}_{\mathrm{i}}\rangle$, i.e, the matrix element of the time evolution operator, and the integral over all paths, one splits the translation along $\vec{\chi}(t)$ into infinitesimal steps using Trotter’s Lie product formula [88] $e^{\mathcal{M}+\mathcal{N}} = \lim_{n\to\infty}\left(e^{\mathcal{M}/n}e^{\mathcal{N}/n}\right)^n$ (for arbitrary square matrices $\mathcal{M},\mathcal{N}$) and by inserting identities $\mathrm{id} = \int_{\mathbb{R}^3}\mathrm{d}^3\chi\ |\vec{\chi}\rangle\langle\vec{\chi}|$:

$$\begin{aligned}&\left\langle\vec{\chi}_{\mathrm{f}}\,\middle|\,e^{-i\mathcal{H}\Delta t}\,\middle|\,\vec{\chi}_{\mathrm{i}}\right\rangle = \\ &= \int_{\mathbb{R}^3}\mathrm{d}^3\chi_n\cdots\mathrm{d}^3\chi_1\,\langle\vec{\chi}_{\mathrm{f}}|e^{-i\mathcal{H}(t_n)\delta t}|\vec{\chi}_n\rangle\,\langle\vec{\chi}_n|e^{-i\mathcal{H}(t_n)\delta t}|\vec{\chi}_{n-1}\rangle\cdots\langle\vec{\chi}_1|e^{-i\mathcal{H}(t_{N-1})\delta t}|\vec{\chi}_{\mathrm{i}}\rangle\ ,\end{aligned} \tag{2.2.2}$$

where $\frac{\Delta t}{n} = \delta t,\ t_j = t_0 + j\delta t$ and $\vec{\chi}_j = \vec{\chi}(t_j)$. Using $\vec{p} = \mathcal{M}\,\mathrm{d}_t\vec{\chi}$ and $\langle\vec{p}\,|\vec{\chi}\rangle = e^{-i\vec{p}^{\mathrm{T}}\vec{\chi}}$, each of the matrix elements for infinitesimal translations can be evaluated by performing a Gaussian integration:

$$\begin{aligned}\left\langle\vec{\chi}_{j+1}\,\middle|\,e^{-i\mathcal{H}(t_j)\delta t}\,\middle|\,\vec{\chi}_j\right\rangle &= \int_{\mathbb{R}^3}\frac{\mathrm{d}^3p}{(2\pi)^3}\,\langle\vec{\chi}_{j+1}|\vec{p}\,\rangle\,\langle\vec{p}\,|e^{-i\left(\frac{1}{2}\vec{p}^{\mathrm{T}}\mathcal{M}^{-1}\vec{p}+V(\vec{\chi},t_j)\right)\delta t}|\vec{\chi}_j\rangle = \\ &= e^{-iV(\vec{x}_j,t_j)\delta t}\int_{\mathbb{R}^3}\frac{\mathrm{d}^3p}{(2\pi)^3}\,\exp\!\left(-\frac{i\delta t}{2}\vec{p}^{\mathrm{T}}\mathcal{M}^{-1}\vec{p} + i\vec{p}^{\mathrm{T}}(\vec{\chi}_{j+1}-\vec{\chi}_j)\right) = \\ &= \underbrace{\left(\frac{-i}{\delta t}\right)^{\frac{3}{2}}\sqrt{\det(\mathcal{M})}}_{\sqrt[n]{N}}\ e^{-iV(\vec{x}_j,t_j)\delta t+\frac{i\delta t}{2}\frac{(\vec{\chi}_{j+1}-\vec{\chi}_j)^{\mathrm{T}}}{\delta t}\mathcal{M}\,\frac{\vec{\chi}_{j+1}-\vec{\chi}_j}{\delta t}} = \sqrt[n]{N}e^{i\delta t\ \mathcal{L}(\vec{\chi},\mathrm{d}_t\vec{\chi},t)}\ .\end{aligned} \tag{2.2.3}$$

One then plugs (2.2.3) into (2.2.2) for every $n$ and takes the limit $n\to\infty\ \Rightarrow\ \delta t\searrow 0$. This means the exponents add up to a time - integral and the integration measures combine to form an infinite - dimensional measure:

$$\lim_{n\to\infty}\sum_{j=0}^{n+1}\mathcal{L}\left(\vec{\chi}(t_j),\,\mathrm{d}_t\vec{\chi}|_{t_j},\,t_j\right)\delta t = \int_{t_{\mathrm{i}}}^{t_{\mathrm{f}}}\mathrm{d}t\,\mathcal{L}\left(\vec{\chi}(t_j),\mathrm{d}_t\vec{\chi},\,t\right), \tag{2.2.4}$$

$$\lim_{n\to\infty}\prod_{j=0}^{n+1}\mathrm{d}^3\chi(t_j) = \mathscr{D}^3\chi(t)\,. \tag{2.2.5}$$

This measure $\mathscr{D}^3\chi$ yields integration over all possible $\vec{\chi}_j$ - values in infinitesimally small separations, i.e., over all paths connecting $\vec{\chi}(t_0) = \vec{\chi}_{\mathrm{i}}$ and $\vec{\chi}(t_{n+1}) = \vec{\chi}_{\mathrm{f}}$. The classical path

$\vec{x}_{\mathrm{cl}}(t)$ is special, as it gives the main contribution and determines the coherence region. The above is illustrated in figure 2.1b.

The path integral (2.2.1) in standard quantum mechanics therefore reads:

$$Z = \left\langle \vec{x}_{\mathrm{f}} \middle| e^{-i\mathcal{H}(t_{\mathrm{f}}-t_{\mathrm{i}})} \middle| \vec{x}_{\mathrm{i}} \right\rangle = N \int_{\vec{x}(t_{\mathrm{i}})=\vec{x}_{\mathrm{i}}}^{\vec{x}(t_{\mathrm{f}})=\vec{x}_{\mathrm{f}}} \mathscr{D}^3 x(t)\, e^{iS[\vec{x}]} \,. \tag{2.2.6}$$

The standard result (2.2.6) can be straightforwardly translated to a relativistic QFT for a real scalar field $\phi(x)$ with $\mathcal{L}(\phi, \partial\phi) = \frac{1}{2}\partial_{\mu_{\mathrm{M}}}\phi\,\partial^{\mu_{\mathrm{M}}}\phi - V(\phi)$. The field contains not three, but infinitely many degrees of freedom, so that the integration measure (2.2.5) is infinite - dimensional as well, facilitating integration over possible all $\phi$ - values everywhere in spacetime:

$$\mathscr{D}\phi(x) = \prod_{\text{“}x\,\in\,\mathbb{R}^{1,3}\text{”}} \mathrm{d}\phi(x)\,. \tag{2.2.7}$$

The action in (2.2.6) is simply replaced by $S[\phi]$, as the above derivation of (2.2.6) can be performed almost analogously for the Hamiltonian $\mathcal{H}\left(\pi(x), \phi(x)\right) = \frac{1}{2}\pi^2 + V'(\phi, \vec{\partial}\phi)$ of field $\phi$ and conjugate momentum $\pi = \partial_t\phi$ and with the potential $V' = \frac{1}{2}\left(\vec{\partial}\phi\right)^2 + V(\phi)$. The normalization $N$ can be absorbed into the path integral measure via a field rescaling. This is possible, since $N$ drops out of all physical observables which can only measure relative effects (of states w.r.t. each other, the vacuum, etc.). The generating functional of QFT again describes the transition of the system, now from vacuum at “$-$ infinity” (both temporal and spatial”) to “$+$ infinity”. Since all physical fields vanish at asymptotic distances or times, the generating functional is therefore a vacuum transition function:

$$\begin{aligned} Z[\phi] = \langle -\infty, -\vec{\infty} | \infty, \vec{\infty} \rangle &= \int \mathscr{D}\phi\, \mathscr{D}\pi\, \exp\left(-i\int \mathrm{d}^4x\, \mathcal{H}\right) = \\ &= \int \mathscr{D}\phi \exp\left(i\int_{\mathbb{R}^{1,3}} \mathrm{d}^4x\; \mathcal{L}(\phi, \partial\phi)\right) . \end{aligned} \tag{2.2.8}$$

It is important to note that the vacuum $|0\rangle$ of a free theory with $V(\phi) = M^2\phi^2$ is not the same as that that of an interacting theory with higher order terms $V \supset \sum_{\mathbb{N}\,\ni\,k\,>\,2} \lambda_k\phi^k$. We denote the vacuum of the (full) interacting theory by $|\Omega\rangle$.

The QFT path integral (2.2.8) works not only for real scalar fields, but also for complex ones as well as vector fields and spinors like the gauge fields $A$ and fermion fields $\psi$ in the QCD Lagrangian (2.1.24). The integral measures are then to be read as (for $SU(N)$ gauge theory):

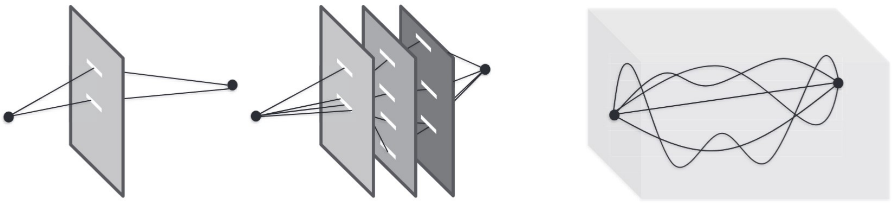

(a). Taken from [4]: The path integral of standard quantum mechanics as the limit of continuously many screens with continuously many slits. The straight line in the right sketch is the classical path and the curved lines depict quantum fluctuations around it.

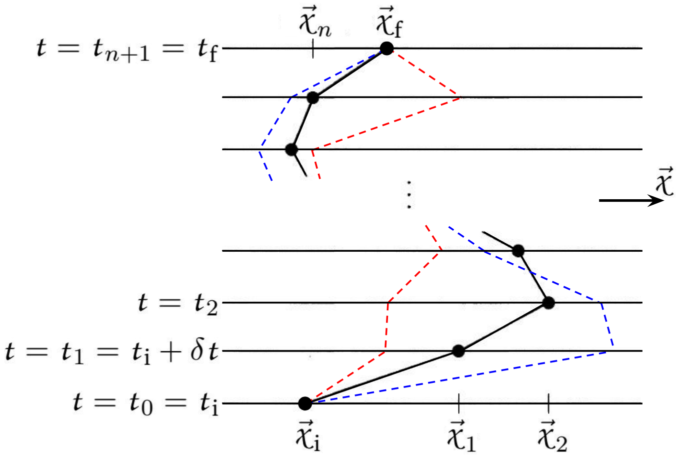
$\vec{x}_n$
$\vec{x}_\mathrm{f}$
$t = t_{n+1} = t_\mathrm{f}$
$\vec{x}$
$t = t_2$
$t = t_1 = t_\mathrm{i} + \delta t$
$t = t_0 = t_\mathrm{i}$
$\vec{x}_\mathrm{i}$
$\vec{x}_1$
$\vec{x}_2$

(b). Taken from [3] and modified: Illustration of the space separation in the non-relativistic path integral. By integrating over all $\vec{x}(t_j)$, all possible paths are covered. The solid line (——) shows the classical path $\vec{x}_\mathrm{cl}$, the dashed lines (- - - -) depict two possible quantum paths (in the coherence region). It is important to note that the quantum fluctuations around $\vec{x}_\mathrm{cl}$ vanish at the start and end point.

Figure 2.1

$$\mathscr{D}A^{\mu_\mathrm{M}} = \prod_{a=1}^{N^2-1} \prod_{\mu_\mathrm{M}=0}^{3} \prod_{\chi \in \mathbb{R}^{1,3}} \mathrm{d}A^{a\,\mu_\mathrm{M}}(x)\,, \quad \mathscr{D}\psi_f = \prod_{f=1}^{N_f} \prod_{\alpha_\mathrm{Dirac}=1}^{4} \prod_{c_\mathrm{color}=1}^{N} \prod_{\chi \in \mathbb{R}^{1,3}} \mathrm{d}\psi_f^{\alpha_\mathrm{Dirac}\,c_\mathrm{color}}(\chi) \tag{2.2.9}$$

and analogously for $\mathscr{D}\overline{\psi}_f$. Importantly, since fermion operators satisfy anti-commutation relations in canonical quantization in order to reproduce Fermi - Dirac statistics and the Pauli exclusion principle, the fermion fields $\psi_f$ and $\overline{\psi}_f$ in the path integral have to be anti-commuting as well. Therefore they need to be anti-commuting *Graßmann numbers* [89] path integral is performed as a *Berezin integral* [90]. The path integral for QCD without gauge fixing then reads

$$Z[\psi_f, A^{\mu_\mathrm{M}}] = \int \mathscr{D}\overline{\psi}_f\, \mathscr{D}\psi_f\, \mathscr{D}A^{\mu_\mathrm{M}} \exp\left( i \int_{\mathbb{R}^{1,4}} \mathrm{d}^4\chi\, \overline{\psi}_f (i\not{D} - M_f)\psi_f - \frac{1}{2g^2}\mathrm{tr}\left(G^{\mu_\mathrm{M}\nu_\mathrm{M}} G_{\mu_\mathrm{M}\nu_\mathrm{M}}\right)\right) \tag{2.2.10}$$

In order to introduce the effective action $\Gamma$ and the effective potential $V_\mathrm{eff}$, two concepts of great importance for this work, one usually considers the real scalar field and adds an external source term $J(\chi)\phi(\chi)$ to the Lagrangian $\mathcal{L} = \frac{1}{2}\partial_{\mu_\mathrm{M}}\phi\, \partial^{\mu_\mathrm{M}}\phi - V(\phi)$ in (2.2.8). The generating functional is then written as

$$Z[J] = e^{iW[J]} = \langle -\infty, -\vec{\infty} | \infty, \vec{\infty} \rangle_J = \int \mathscr{D}\phi \, \exp\left( i \int_{\mathbb{R}^{1,3}} \mathrm{d}^4\chi\, (\mathcal{L} + J\phi) \right). \tag{2.2.11}$$

A “functional Legendre transform” $W[J] = -i\ln(Z[J]) \to \Gamma[\phi_\mathrm{cl}]$ yields the 1 - particle - irreducible effective action

$$\Gamma[\phi_\mathrm{cl}] = W[J] - \int_{\mathbb{R}^{1,3}} \mathrm{d}^4\chi\, J(\chi)\phi_\mathrm{cl}(\chi) \tag{2.2.12}$$

given in terms of the classical field $\phi_\mathrm{cl}(\chi) = -\frac{\delta W[J]}{\delta J(\chi)} = \frac{\langle\Omega|\phi|\Omega\rangle_J}{\langle\Omega|\Omega\rangle_J} = \langle\phi(\chi)\rangle_J$, where $|\Omega\rangle_J$ is the vacuum of the interacting theory in the presence of the source $J$. This means $\phi_\mathrm{cl}$ is the normalized vacuum expectation value (VEV) of $\phi$ in presence of the source $J$. In turn, one also has $J(\chi) = -\frac{\delta\Gamma[\phi_\mathrm{cl}]}{\delta\phi_\mathrm{cl}(\chi)}$. Setting the external source to zero $J = 0$, the effective action $\Gamma$ and $W$ agree, $\Gamma[\phi_\mathrm{cl}]|_{J=0} = -i\ln(Z[J = 0])$, and the classical field vanishes $\phi_\mathrm{cl}|_{J=0} = 0$.

An expansion of the effective action (with $J \neq 0$) in $\phi_\mathrm{cl}$ yields

$$\begin{aligned} \Gamma[\phi_\mathrm{cl}(\chi)] &= \int_{\mathbb{R}^{1,3}} \mathrm{d}^4\chi\, \left(V_\mathrm{eff}(\phi_\mathrm{cl}) + X(\phi_\mathrm{cl})\, \partial_{\mu_\mathrm{M}}\phi_\mathrm{cl}\, \partial^{\mu_\mathrm{M}}\phi_\mathrm{cl} + \mathcal{O}\left((\partial\phi_\mathrm{cl})^4\right)\right), \\ V_\mathrm{eff}(\phi_\mathrm{cl}) &= V(\phi_\mathrm{cl}) + \mathcal{O}(\text{quantum corrections}) \end{aligned} \tag{2.2.13}$$

with $V_\mathrm{eff}$ the *Coleman - Weinberg effective potential* [91, 92]. The effective potential can also be understood as the sum over all $\phi_\mathrm{cl}$ - vacuum diagrams. In case of a translationally invariant, i.e., constant, classical field $\phi_{\text{cl}} \neq \phi_{\text{cl}}(\chi)$, the effective action takes the form

$$\Gamma[\phi_{\text{cl}} = \text{const.}] = \text{vol}\big(\mathbb{R}^{1,3}\big)\ V_{\text{eff}}(\phi_{\text{cl}})\,. \tag{2.2.14}$$

Just as the path integral, all of this also generalizes to QCD.

### 2.2.2 Gauge fixing in the Path Integral Formalism

The QCD - path integral in (2.2.10) shows that a homogeneous and (usually) Poincaré - covariant gauge fixing condition $\mathcal{G}(A) = \mathcal{C}_{\mu_{\text{M}}} A^{\mu_{\text{M}}} = 0$ (homogeneity implies linearity and thus excludes the Dirac gauge)) can be inserted into the path integral as [93, 94]

$$\text{id} = \left(\int_{SU(N)} \mathscr{D}U\right)\ \delta\big(\mathcal{G}(A)\big)\ \det{}_{\text{FP}}\,. \tag{2.2.15}$$

Here $\mathscr{D}U$ is the gauge - invariant group measure and this integral therefore yields an unphysical, diverging constant that drops out via the vacuum - normalization of any physical observable. The equally gauge - invariant *Faddeev - Popov determinant*

$$\det{}_{\text{FP}} = \det\left(\frac{\delta\mathcal{G}(A'(\chi))}{\delta U(\chi')}\right), \tag{2.2.16}$$

with $A'$ as given in (2.1.19), is needed analogously to $\text{id} = \int_{\mathbb{R}^n} \mathrm{d}^n x\, \delta^{(n)}\big(\vec{f}(\vec{x})\big)\ \det\left(\frac{\partial \vec{f}}{\partial \vec{x}}\right)$ for functions $\vec{f} : \mathbb{R}^n \to \mathbb{R}^n$. One can rewrite $\det{}_{\text{FP}}$ as an additional functional integral

$$\det{}_{\text{FP}} = \int \mathscr{D}\bar{c}\, \mathscr{D}c\ \exp\left(-i\int_{\mathbb{R}^{1,3}} \mathrm{d}^4\chi\ \bar{c}^a (\mathcal{C}_{\mu_{\text{M}}} D^{\mu_{\text{M}}} c)^a\right) = \int \mathscr{D}\bar{c}\, \mathscr{D}c\ \exp\left(-i\int_{\mathbb{R}^{1,3}} \mathrm{d}^4\chi\ \mathcal{L}_{\text{ghost}}\right) \tag{2.2.17}$$

over Graßmannian Lorentz - scalar (spin 0), gauge - adjoint fields $c, \bar{c}$. The fact that these fields are bosons yet anti-commute like fermions and thus satisfy Fermi - Dirac statistics describes their unphysical nature. They are called Faddeev - Popov ghosts and are the ghost fields related to the incompleteness of Poincaré - covariant gauges discussed in section 2.1. Finally, the gauge condition $\delta\big(\mathcal{G}(A)\big)$ can be turned into an additional $\mathcal{L}$ - term

$$\mathcal{L}_{\text{gauge}} = -\frac{1}{2\xi}\mathcal{G}^a(A)\,\mathcal{G}^a(A) = -\frac{1}{\xi}\text{tr}\big(\mathcal{G}(A)\,\mathcal{G}(A)\big)\,, \tag{2.2.18}$$

where $\xi \geq 0$ acts as a Lagrange multiplier. The Lagrange multiplier can appear in objects like propagators, but finally drops out when physical observables are calculated.

Setting $\xi$ equal to some number, which has to be done only after quantization, i.e., after expectation values have been calculated, can reproduce gauges discussed in the previous section 2.1. For example, for $\mathcal{C}_{\mu_\mathrm{M}} = \partial_\mu$, taking $\xi \searrow 0$ is called the Landau gauge and is equivalent to the Lorenz gauge. Setting instead $\xi = 1$ is called the Feynman - 't Hooft gauge and $\xi = 3$ is the lesser known Yennie gauge [95].

The full generating functional and Lagrangian to be used for path integral quantization of QCD is therefore given by (2.2.10) together with (2.2.17) and (2.2.18):

$$Z[\psi_f, A^{\mu_\mathrm{M}}] = \int \mathscr{D}\overline{\psi}_f \, \mathscr{D}\psi_f \, \mathscr{D}A^{\mu_\mathrm{M}} \exp\left( i \int_{\mathbb{R}^{1,4}} \mathrm{d}^4\chi \; \mathcal{L}(\psi_f, A^{\mu_\mathrm{M}}, c) \right) \quad \text{with} \tag{2.2.19}$$

$$\begin{aligned} \mathcal{L}(\psi_f, A^{\mu_\mathrm{M}}, c) &= \mathcal{L}_\text{QCD} + \mathcal{L}_\text{gauge} + \mathcal{L}_\text{ghost} = \\ &= \sum_{f=1}^{N_f} \overline{\psi}_f \big(i\not{D} - M_f\big)\psi_f - \frac{1}{2g^2}\mathrm{tr}\big(G^{\mu_\mathrm{M}\nu_\mathrm{M}} G_{\mu_\mathrm{M}\nu_\mathrm{M}}\big) - \frac{1}{\xi}\mathrm{tr}\big(\mathcal{G}(A)\,\mathcal{G}(A)\big) - \frac{1}{N}\mathrm{tr}\big(\bar{c}\,\mathcal{C}_{\mu_\mathrm{M}} D^{\mu_\mathrm{M}} c\big)\,, \end{aligned} \tag{2.2.20}$$

where it was used that the Dynkin index of $SU(N)$ in the adjoint representation is $N$.

### 2.2.3 Thermal Field Theory in the Imaginary Time or Matsubara Formalism

In order to describe quantum processes in a thermal medium, i.e., taking place at finite temperature $T > 0$, three main formalisms have been developed. [84, 86, 87] present detailed reviews of these three formalisms and serve as general references for all of the following.

The *imaginary time* or *Matsubara formalism* based on [96, 97] is computationally easiest and can be obtained from the usual path integral by a simple change of coordinates from real/Minkowski time $\chi^0 = t$ to imaginary time $\mathfrak{t} = it$ which serves as an “inverse temperature” - variable $\mathfrak{t} \in [0, \beta = T^{-1}]$, together with $\beta$ - (anti-)periodicity conditions for (fermionic) bosonic fields. Its downside, however, is that the imaginary time formalism is limited to describing fluctuations around equilibrium configurations.[8] Good reviews of this formalism are for example presented in [85, 98] and since we are going to employ this formalism for our work, these also serve as general references for this section.

The *real time* or *Schwinger - Keldysh formalism* based on [99–103] is both conceptually and computationally more elaborated, but can in turn describe systems evolving in real time $t$ far away from any equilibrium. One finds a good overview of this formalism in [104], for example.

---

[8] Time evolution could be described by analytic continuation back to real time, but both the general validity and specific application of this procedure are non - trivial [84].

*Thermofield Dynamics*, also called the *Umezawa formalism*, is based on [105, 106] and mainly works as an operator formalism complementary to real time formalism, as it can answer questions outside the scope of the latter. Thermofield Dynamics can, however, also be rewritten as a path integral. It describes real time evolution at finite temperatures (close to equilibrium). As an example, [107] reviews this formalism in more detail.

The aforementioned change of coordinates from real time to imaginary time is called *Wick rotation* [108]. At **zero temperature** it is defined as

$$\begin{aligned} \mathbb{R}^{1,3} \to \mathbb{R}^4 \quad \Rightarrow \quad & \chi = (t, \vec{\chi}) \to \overline{X} = (\vec{\overline{X}} = \vec{\chi}, \overline{X}^4 = \bar{t} = it)\,, \\ & \eta_{\mu_\mathrm{M}\nu_\mathrm{M}} = \mathrm{diag}(1,-1,-1,-1) \to -\delta_{\mu\nu} = -\mathrm{diag}(1,1,1,1)\,. \end{aligned} \tag{2.2.21}$$

This gives $v^{\mu_\mathrm{M}} \to v^\mu = \begin{cases} v^{i_\mathrm{M}} \\ iv^{0_\mathrm{M}} \end{cases}$ for vectors, $w_{\mu_\mathrm{M}} \to w_\mu = \begin{cases} w_{i_\mathrm{M}} \\ -\,iw_{0_\mathrm{M}} \end{cases}$ for covectors and $v^{\mu_\mathrm{M}}\eta_{\mu_\mathrm{M}\nu_\mathrm{M}}w^{\nu_\mathrm{M}} = v^{0_\mathrm{M}}w^{0_\mathrm{M}} - v^{i_\mathrm{M}}w^{i_\mathrm{M}} \to -v^0w^0 - v^iw^i = -v^\mu\delta^{\mu\nu}w^\nu$ for scalar products. We define the Euclidean "4 - radius" for $T = 0$ as $|\overline{X}| = \sqrt{\overline{X}^\mu\overline{X}^\mu} = \overline{R}$. Under the Wick rotation, the action of a real scalar field behaves as

$$\left.\begin{aligned} &\mathrm{d}^4\chi = \mathrm{d}t\mathrm{d}^3\chi = -i\,\mathrm{d}\bar{t}\mathrm{d}^3\overline{X} = -i\,\mathrm{d}^4\overline{X} \\ &(\partial_{\mu_\mathrm{M}}\phi)^2 = -(\partial_\mu\phi)^2\,,\ V_\mathrm{M}(\phi) = V(\phi) \end{aligned}\right\} \quad \Rightarrow$$

$$\Rightarrow \quad iS_\mathrm{M} = i\int_{\mathbb{R}^{1,3}} \mathrm{d}^4\chi\ \mathcal{L}_\mathrm{M} \ \to\ -i\int_{\mathbb{R}^4}(-i)\mathrm{d}\overline{X}^4\,\underbrace{\left(\frac{1}{2}(\partial^\mu\phi)^2 + V(\phi\right)}_{\mathcal{L}\,=\,E_\mathrm{M}} = -S \tag{2.2.22}$$

The Euclidean Lagrangian equals the real time - energy of the system and the formerly oscillatory action now acts as an exponential damping in the imaginary - time generating functional $Z[\phi] = \int \mathscr{D}\phi e^{-S[\phi]}$ (cf. (2.2.8)), which is called *partition function* due the resemblance to statistical physics.

To describe **finite temperatures**, one restricts the spacetime $\mathbb{R}^4$ in the temporal direction and introduces a periodicity in this direction by identifying $t = \beta \mathrel{\widehat{=}} 0$. Topologically, this closes the temporal spacetime dimension to a circle of radius $\frac{\beta}{2\pi}$:

$$\mathbb{R}^4 \to \mathbb{R}^3 \times S^1_{\text{rad.}={}^\beta/_{2\pi}} \quad \Rightarrow \quad \overline{X} = (\vec{\overline{X}}, \bar{t}) \to X = (\vec{X} = \vec{\overline{X}}, X^4 = t = \bar{t} \in [0,\beta))\,. \tag{2.2.23}$$

In this spacetime we define the Euclidean, spatial "3 - radius" $|\vec{X}| = \sqrt{X^iX^i} = R$. Due to the $t$ - periodicity $\phi(X + \beta\hat{e}_4) = \phi(X)$, the scalar field can be expanded in a Fourier series

$$\phi(\vec{X}, t) = \frac{1}{\sqrt{\beta}}\sum_{\alpha\,\in\,\mathbb{Z}} \widetilde{\phi}(\vec{X}, i\omega^\text{bos}_\alpha)\, e^{-i\omega^\text{bos}_\alpha t}\,, \qquad \omega^\text{bos}_\alpha = \frac{2\pi\alpha}{\beta}\,, \tag{2.2.24}$$

where $\omega_\alpha^{\text{bos}}$ are called the *bosonic Matsubara frequencies* [96, 97].

For the Euclidean $\gamma$ - matrices we choose a analogous transformation to the vectors, $\gamma^{\mu_\text{M}} \to \gamma^\mu = \begin{cases} \gamma^{i_\text{M}} \\ i\gamma^{0_\text{M}} \end{cases}$, so that they are anti-Hermitian $\gamma^{\mu\dagger} = -\gamma^\mu$ and satisfy the Clifford algebra $\{\gamma^\mu, \gamma^\nu\} = -2\delta^{\mu\nu}\mathbb{1}$. The fifth Euclidean $\gamma$ - matrix $\gamma^5 = \gamma^1\gamma^2\gamma^3\gamma^4$ is Hermitian $\gamma^{5\dagger} = \gamma^5$, involutory $(\gamma^5)^2 = \mathbb{1}$ and anti-commuting $\gamma^5\gamma^\mu = -\gamma^\mu\gamma^5$. The Dirac operator Wick rotates as $\not{\partial}_\text{M}, \not{D}_\text{M} \to -\not{\partial}, -\not{D}$, where we explicitly marked the real time - derivatives with the subscripts “M”.

One Wick rotates (2.2.19) together with (2.2.20) analogously to (2.2.22), using now $\int_{\mathbb{R}^{1,3}} \mathrm{d}^4\chi\, (i\not{\partial}_\text{M}, i\not{D}_\text{M}) \to -\int_{\mathbb{R}^4} \mathrm{d}^4\overline{X}(i\not{\partial}, i\not{D})$ as well as $G^{\mu_\text{M}\nu_\text{M}} G_{\mu_\text{M}\nu_\text{M}} \to G^{\mu\nu}G^{\mu\nu}$, and finds the QCD partition function at $T > 0$:

$$Z[\psi_f, A^\mu] = \int \mathscr{D}\overline{\psi}_f\, \mathscr{D}\psi_f\, \mathscr{D}A^\mu \exp\left( -\int_{\mathbb{R}^3 \times S^1_{\text{rad.} = \beta/2\pi}} \mathrm{d}^4X\ \mathcal{L}(\psi_f, A^\mu, c) \right) \quad \text{with} \quad (2.2.25)$$

$$\mathcal{L} = \sum_{f=1}^{N_f} \overline{\psi}_f \big(i\not{D} + M_f\big)\psi_f + \frac{1}{2g^2}\mathrm{tr}\big(G^{\mu\nu}G^{\mu\nu}\big) \pm \frac{1}{\xi}\mathrm{tr}\big(\mathcal{G}^\mathrm{T}(A)\,\mathcal{G}(A)\big) + \frac{1}{N}\mathrm{tr}\big(\bar{c}\,\mathcal{C}^\mu D^\mu c\big)\,. \tag{2.2.26}$$

Here the sign of the gauge term depends on the Wick rotation of the chosen gauge condition. It is also important to note the Graßmannian fermion (and ghost fields) have to satisfy anti-periodicity conditions $\psi(X + \beta\hat{e}_4) = -\psi(X)$ and are therefore expanded in terms of *fermionic Matsubara frequencies* [96, 97]

$$\psi(\vec{X}, t) = \frac{1}{\sqrt{\beta}} \sum_{\alpha \in \mathbb{Z}} \widetilde{\psi}(\vec{X}, i\omega_\alpha^{\text{ferm}})\, e^{-i\omega_\alpha t}\,, \quad \omega_\alpha^{\text{ferm}} = \frac{2\pi\big(\alpha + \frac{1}{2}\big)}{\beta}\,. \tag{2.2.27}$$

Analogously to (2.2.12), (2.2.13) and (2.2.14) one defines the effective action and potential in the imaginary time - formalism by $\Gamma = -\ln(Z)$ and, for a real scalar field,

$$\Gamma_\text{E}[\phi_\text{cl} = \text{const.}] = \mathrm{vol}\Big(\mathbb{R}^3 \times S^1_{\text{rad.} = \beta/2\pi}\Big)\ V_\text{eff}(\phi_\text{cl}) = \beta V\, V_\text{eff}(\phi_\text{cl})\,, \tag{2.2.28}$$

where $\beta V = \mathrm{vol}\Big(\mathbb{R}^3 \times S^1_{\text{rad.} = \beta/2\pi}\Big) = \beta\, \mathrm{vol}\big(\mathbb{R}^3\big)$ is the volume of spacetime. This can be applied to QCD as well.

Finally, the temporal periodicity of $\mathbb{R}^3 \times S^1_{\text{rad.} = \beta/2\pi}$ allows for the definition of a special Wilson loop (cf. (2.1.29)): the *Polyakov loop* [109] is a Wilson loop with the path C characterized by a constant and purely temporal velocity so that C and closes by periodicity

$$P(\vec{X}) = W_{C\,=\{\vec{X}+t\hat{e}_4\,,\,0\le t\le\beta\}} = \mathrm{tr}\Big(\mathrm{T}\,\exp\Big(-i\int_0^\beta \mathrm{d}t\,A^4(X)\Big)\Big) = \mathrm{tr}\big(\Omega(\vec{X})\big). \tag{2.2.29}$$

T denotes the *time ordering* of $A^4$ along C, which is a special case of path ordering. $\Omega$ denotes the untraced Polyakov loop, which is going to be important for the short discussion on gluon field - topology at finite temperatures in section 2.4.2 and for the finite - temperature effects in sections 3.1.2 and 3.1.3. [9]

### 2.2.4 Symmetry Group of Thermal Field Theory

As we discussed above, finite temperature field theory in the imaginary time formalism takes place in the Wick rotated and temporally bounded spacetime $\mathbb{R}^3 \times S^1_{\text{rad.}={}^{\beta}/_{2\pi}}$ equipped with a Euclidean metric. Wick rotating $\mathbb{R}^{1,3} \to \mathbb{R}^4$ to Euclidean spacetime at zero temperature maps the group of Lorentz transformations $SO^+(1,3)$ of Minkowski spacetime to the group $SO(4)$ of 4 - dimensional rotations in $\mathbb{R}^4$. This group $SO(4)$ is constructed by Lie algebra exponentiation using the Wick rotated versions of the Lorentz group generators $J^{\mu_\mathrm{M}\nu_\mathrm{M}}$ (cf. (2.1.5)).

At finite temperature $T = \beta^{-1}$, the corresponding spacetime $\mathbb{R}^3 \times S^1_{\text{rad.}={}^{\beta}/_{2\pi}}$ has a distinct time direction in which it is bounded, as opposed to the open space directions. This breaks the 4 - dimensional rotation symmetry group $SO(4)$ down to the 3 - dimensional one $SO(3)$ [87, 98]. From the physical point of view, the presence of the external heat bath implies a preferred Lorentz frame, the heat bath's rest frame, which breaks Lorentz invariance. Rotations (and translations) are still symmetries of the system allowed by the heat bath, but Lorentz boosts are not [87]. Thus, the Lorentz group $SO^+(1,3)$ is broken - as [110] proves in detail - down to $SO(3)$ and the loss of boost symmetry corresponds to the breaking of $SO(4)$ in Euclidean spacetime. Nevertheless, [86] argues that one can still formulate thermal field theory in a manifestly $SO(4)$ - invariant way (translations are not impacted by this and are treated as in Minkowski spacetime) - a result one obtains "by accident" and "without justification" by simply employing the change of coordinates (2.2.21) in the path integral and enforcing the (anti-)periodicity conditions. It must therefore always be remembered that this is merely notational elegance and does not reflect an actual underlying symmetry, as is the case for $T = 0$ (compare the construction of the QCD Lagrangian in section 2.1).

---

[9] [54, 85]

## 2.3 Chiral Symmetry and Chiral Perturbation Theory

### Chiral Symmetry and the Eightfold Way

Take the QCD - Lagrangian (2.1.24) or its gauge fixed version appearing in the path integral (2.2.20) and consider the simplified version of massless quarks $M_f = 0\ \forall f$.[10] Note that in this theory the left- and right - chiral 2 - spinors forming the Dirac spinor decouple. Classically, this simplified Lagrangian is invariant under the chiral symmetry group we also mentioned in the introductory section 1.2:

$$\begin{gathered}SU(N_f)_\mathrm{V} \otimes SU(N_f)_\mathrm{A} \otimes U(1)_\mathrm{V} \otimes U(1)_\mathrm{A}\,, \\ \begin{aligned} \psi_f &\overset{SU(N_f)_\mathrm{V}}{\to} \exp(i\theta^a T^a)_{ff'}\,\psi_{f'} \qquad & \psi_f &\overset{SU(N_f)_\mathrm{A}}{\to} \exp\big(i\vartheta^a T^a \gamma^{5_\mathrm{M}}\big)_{ff'}\,\psi_{f'} \\ \psi_f &\overset{U(1)_\mathrm{V}}{\to} e^{i\alpha}\psi_f & \psi_f &\overset{U(1)_\mathrm{A}}{\to} e^{i\beta\gamma^{5_\mathrm{M}}}\psi_f\,, \end{aligned}\end{gathered} \tag{2.3.1}$$

where $T^a$ with $[T^a, T^b] = if^{abc}T^c$, $a, b, c = 1, ..., N_f^2 - 1$ are the generators of $SU(N_f)_\mathrm{V}$ and $T^a\gamma^{5_\mathrm{M}}$ with $[T^a\gamma^{5_\mathrm{M}}, T^b\gamma^{5_\mathrm{M}}] = if^{abc}T^c$ ($T^a$ and $\gamma^{5_\mathrm{M}}$ act on different spaces and thus commute) are the generators of $SU(N_f)_\mathrm{A}$. Note also $[T^a, T^b\gamma^{5_\mathrm{M}}] = if^{abc}T^c\gamma^{5_\mathrm{M}}$. One forms two separate algebras $T^a_\pm = \frac{1}{2}(T^a \pm T^a\gamma^{5_\mathrm{M}})$ with $[T^a_\pm, T^b_\pm] = if^{abc}T^c_\pm$, $[T^a_\pm, T^b_\mp] = 0$, which describe the separate rotations of the $N_f$ right- and left - chiral 2 - spinors. The chiral group is therefore isomorphic to the symmetry group $SU(N_f)_\mathrm{L} \otimes SU(N_f)_\mathrm{R} \otimes U(1)_\mathrm{V} \otimes U(1)_\mathrm{A}$. These are two sets of $SU(N_f)$ isospin symmetries, one for the left- and one for the right - chiral 2 - spinors, with $N_f$ polarizations each, one global phase multiplication for all flavors and one such phase multiplication that differentiates by chirality and multiplies left- and right - chiral spinors by opposite phases (as $\gamma^{5_\mathrm{M}}\mathrm{P}_\mathrm{R,L} = \pm\,\mathrm{P}_\mathrm{R,L}$, cf. (2.1.8)). The conserved currents $j$ and charges $Q$ according to [65] then are

- $SU(N_f)_\mathrm{V}$ : $\quad j^{a\,\mu_\mathrm{M}}_\mathrm{V} = \overline{\psi}_f\gamma^{\mu_\mathrm{M}}(T^a)_{ff'}\,\psi_{f'} \qquad Q^a_\mathrm{V} = \int_{\mathbb{R}^3} \mathrm{d}^3\chi\, j^{a\,0_\mathrm{M}}_\mathrm{V}$ (2.3.2)
- $SU(N_f)_\mathrm{A}$ : $\quad j^{a\,\mu_\mathrm{M}}_\mathrm{A} = \overline{\psi}_f\gamma^{\mu_\mathrm{M}}\gamma^{5_\mathrm{M}}(T^a)_{ff'}\,\psi_{f'} \qquad Q^a_\mathrm{A} = \int_{\mathbb{R}^3} \mathrm{d}^3\chi\, j^{a\,0_\mathrm{M}}_\mathrm{A}$ (2.3.3)

  $\Longrightarrow \quad j^{a\,\mu_\mathrm{M}}_\mathrm{R,L} = \overline{\psi}_f\gamma^{\mu_\mathrm{M}}\mathrm{P}_\mathrm{R,L}(T^a)_{ff'}\,\psi_{f'} \qquad Q^a_\mathrm{R,L} = \int_{\mathbb{R}^3} \mathrm{d}^3\chi\, j^{a\,0_\mathrm{M}}_\mathrm{R,L}$ (2.3.4)
- $U(1)_\mathrm{V}$ : $\quad j^{\mu_\mathrm{M}}_\mathrm{V} = \overline{\psi}_f\gamma^{\mu_\mathrm{M}}\psi_f \qquad Q_\mathrm{V} = \int_{\mathbb{R}^3} \mathrm{d}^3\chi\, j^{0_\mathrm{M}}_\mathrm{V} = n_\mathrm{R} + n_\mathrm{L}$ (2.3.5)
- $U(1)_\mathrm{A}$ : $\quad j^{\mu_\mathrm{M}}_\mathrm{A} = \overline{\psi}_f\gamma^{\mu_\mathrm{M}}\gamma^{5_\mathrm{M}}\psi_f \qquad Q_\mathrm{A} = \int_{\mathbb{R}^3} \mathrm{d}^3\chi\, j^{0_\mathrm{M}}_\mathrm{A} = n_\mathrm{R} - n_\mathrm{L}\,,$ (2.3.6)

---

[10] All of the following holds analogously after Wick rotation to Euclidean spacetime.

where the $Q^a_{\mathrm{R,L}}$ are $N_f^2 - 1$ isospin components for the left- and right - chiral 2 - spinors each, $Q_V = n_\mathrm{R} + n_\mathrm{L}$ is the total number of 2 - spinor fermions ($n_{\mathrm{R/L}}$ is the number of right-/left - chiral fermions) and $Q_A = n_\mathrm{R} - n_\mathrm{L}$ is the net chirality.[11]

The massless limit is a good approximation for QCD at very high temperatures where $M_f \ll T \; \forall f$. For temperatures where the thermal energy of the quarks drops below their binding energy, however, the axial part of the symmetry is spontaneously broken in quantized QCD [32], which is due to the non - zero expectation value for quark - anti-quark condensates $\langle \mathrm{vac} \,|\, \overline{\psi}\psi \,|\, \mathrm{vac} \rangle = \langle \overline{\psi}_\mathrm{L}\psi_\mathrm{R} + \overline{\psi}_\mathrm{R}\psi_\mathrm{L} \rangle$, as we discussed in section 1.2. QCD is then described by an effective field theory called *chiral perturbation theory* which we briefly discuss below. The quark condensate is conserved under $SU(N_f)_\mathrm{V}$ and $U(1)_\mathrm{V}$, but neither under $SU(N_f)_\mathrm{A}$ nor under $U(1)_\mathrm{A}$. According to the Goldstone theorem [113–115], one thus expects the existence of $N_f^2 - 1 + 1 = N_f^2$ massless pseudoscalar Nambu - Goldstone bosons to reflect the spontaneously broken symmetry degrees of freedom.[12]

The real $N_f = 6$ quarks carry masses $M_f$ (cf. table 1.1), which explicitly breaks all but the $U(1)_\mathrm{V}$ - symmetry, even at $T = 0$:

- $SU(N_f)_\mathrm{V}$ : $$\partial_{\mu_\mathrm{M}} j_\mathrm{V}^{a\,\mu_\mathrm{M}} = -i(M_f - M_{f'})\overline{\psi}_f (T^a)_{ff'}\, \psi_{f'} \neq 0 \tag{2.3.7}$$
- $SU(N_f)_\mathrm{A}$ : $$\partial_{\mu_\mathrm{M}} j_\mathrm{A}^{a\,\mu_\mathrm{M}} = i\overline{\psi}_f \{T^a, M_q\}_{ff'}\, \gamma^{5_\mathrm{M}} \psi_{f'} \neq 0 \tag{2.3.8}$$
- $U(1)_\mathrm{A}$ : $$\partial_{\mu_\mathrm{M}} j_\mathrm{A}^{\mu_\mathrm{M}} = 2i \sum_f M_f \overline{\psi}_f \gamma^{5_\mathrm{M}} \psi_f \neq 0\,, \tag{2.3.9}$$

with the quark mass matrix $M_q = \mathrm{diag}(M_1, ..., M_{N_f})$.

One notes, however, that for quarks with “similar masses” the vectorial isospin rotations are still good approximate symmetry transformations. For light quarks $\psi_l$ even the axial isospin rotations and $U(1)_\mathrm{A}$ would still be good approximate symmetries, were it not for the spontaneous breaking. The chiral symmetry breaking scale $\Lambda_\chi$, which we discuss below, and the QCD scale $\Lambda_\mathrm{QCD} \sim -\langle \overline{\psi}_l \psi_l \rangle$ thus separate the quarks into three heavy quarks $M_{f_\mathrm{h}} > \Lambda_{\chi,\,\mathrm{QCD}}$, i.e., $c$ -, $b$ - and $t$ - quark, which break chiral symmetry explicitly, and three light quarks $M_{f_l} \ll \Lambda_{\chi,\,\mathrm{QCD}}$, i.e., $u$ -, $d$ - and $s$ - quark, where the spontaneous symmetry breaking of the axial symmetries dominates. The light quarks have mass differences $M_d - M_u \sim 2.5\,\mathrm{MeV}$ and $M_s - M_{u,d} \sim 100\,\mathrm{MeV}$ smaller than the interaction scale $\Lambda_\mathrm{QCD} \approx 340\,\mathrm{MeV}$ and much smaller than the chiral symmetry breaking scale $\Lambda_\chi$. Therefore, $SU(3)_\mathrm{V}$ remains as an approximate symmetry for the subspace of the three light quarks, while $SU(3)_\mathrm{A} \otimes U(1)_\mathrm{A}$ are spontaneously broken.[13]

---

[11] [3, 4, 38, 46, 111, 112]

[12] [3, 4, 46, 112, 116]

[13] [4, 111, 112]

From the $SU(3)_{\text{V}}$ - symmetry for the three light quarks and with (anti-)quarks transforming under the (anti-)fundamental representation (cf. $\psi_{\text{flavor vector}}$ below (2.1.24)), one deduces from spin addition (equivalent to the discussion about the Lorentz group in section 2.1) that mesons built from $u$-, $d$- and $s$ - quarks are described by the product representation $3 \otimes \bar{3} = 8 \oplus 1$ and that baryons are described by $3 \otimes 3 \otimes 3 = 10 \oplus 8 \oplus 8 \oplus 1$ (for the representation theory of $SU(3)$ see also [75]). This means that light quark - mesons should exist as meson nonets, i.e., meson octets accompanied by a singlet, all of equal mass, and that baryons should come as decuplets together with an octet and a singlet. Furthermore, there should be an octet together with a singlet state of almost massless/very light pseudoscalar pseudo - Nambu - Goldstone bosons (pNG bosons), where the small mass is a result of the light explicit symmetry breaking. This grouping of mesons and baryons is called the eightfold way [117, 118].[14]

In fact, baryons and mesons are measured to be grouped exactly as described above. However, their masses are only roughly equal, as $M_s \approx 27 \frac{M_u + M_d}{2}$ and other quantum effects such as excitations, spin - alignment, fine structure effects, etc. contribute. Also some states like the lightest baryon singlet state $\Lambda_1$ are excluded by Fermi - Dirac statistics at ground level. The lightest meson octet consists of (unless the temperature dependency is explicitly denoted, all particle masses are to be understood at $T = 0$)

- three pions $M_{\pi^\pm} \approx 140\,\text{MeV}$, $M_{\pi^0} \approx 135\,\text{MeV}$
- four kaons $M_{K^\pm} \approx 494\,\text{MeV}$, $M_{K^0} = M_{\overline{K}^0} \approx 498\,\text{MeV}$
- $\eta$ - meson $M_\eta \approx 548\,\text{MeV}$.

The kaons and $\eta$ are comparably heavier, because they contain the $s$ - quark. If one had excluded the $s$ - quark from the light quarks and considered only the even better approximate symmetry $SU(2)_{\text{V}}$ of $u$ and $d$, one would have found the product representation $2 \otimes \bar{2} = 3 \oplus 1$ containing the triplet of almost equal mass pions. This octet of lightest mesons serves as the octet of pseudoscalar pNG bosons for the $SU(3)_{\text{A}}$ - symmetry: eight pNG bosons for the 8 - dimensional $SU(3)_{\text{A}}$. However, both the above octet and the pion triplet lack an accompanying singlet and the only possible candidate is the $\eta'$ - meson, which is too heavy to both be part of the same nonet and a pNG boson for $U(1)_{\text{A}}$: $M_{\eta'} \approx 958\,\text{MeV}$. This is the $\eta$ - $\eta'$ - puzzle we mentioned in the introduction 1.2. It is resolved by topological effects as we are going to discuss in section 2.5.1.[15]

---

[14] [4, 33, 38, 111]

[15] [2–4, 33, 38, 111, 119]

The next heavier meson group is formed by the octet consisting of

- three $\rho$ - mesons $M_{\rho^{\pm,0}} \approx 775\,\text{MeV}$
- four $K^*(892)$ - mesons $M_{K^{*\pm}} \approx 892\,\text{MeV}$, $M_{K^{*0}} = M_{\overline{K}^{*0}} \approx 896\,\text{MeV}$
- $\omega$ - meson $M_\omega \approx 783\,\text{MeV}$

and the accompanying the singlet $\phi$ - meson $M_\phi \approx 1019\,\text{MeV}$. The lightest baryon group consists of the decuplet containing

- four $\Delta$ - baryons $M_{\Delta^{++,\pm,0}} \approx 1.23\,\text{GeV}$
- three $\Sigma^*$ - baryons $M_{\Sigma^{*+,0}} \approx 1.38\,\text{GeV}$, $M_{\Sigma^{*-}} \approx 1.39\,\text{GeV}$
- two $\Xi^*$ - baryons $M_{\Xi^{*0}} \approx 1.53\,\text{GeV}$, $M_{\Xi^{*-}} \approx 1.54\,\text{GeV}$
- $\Omega$ - baryon $M_{\Omega^-} \approx 1.67\,\text{GeV}$,

the octet containing

- proton and neutron $M_p \approx M_n \approx 0.94\,\text{GeV}$
- $\Lambda^0$ - baryon $M_{\Lambda^0} \approx 1.12\,\text{GeV}$
- three $\Sigma$ - baryons $M_{\Sigma^{+,0}} \approx 1.19\,\text{GeV}$, $M_{\Sigma^-} \approx 1.20\,\text{GeV}$
- two $\Xi$ - baryons $M_{\Xi^0} \approx 1.31\,\text{GeV}$, $M_{\Xi^-} \approx 1.32\,\text{GeV}$,

an additional octet given in [119, Table 5.3] and the singlet given in [119, eq. (5.62)], which is forbidden by the Pauli exclusion principle. One way of setting the chiral symmetry breaking scale is given by the mass scale of these lightest hadrons made up of the light quarks (excluding the lightest meson octet of pNG bosons) and one usually chooses $\Lambda_\chi \sim M_\rho \approx 775\,\text{MeV}$.[16]

Note also that in low energy QCD, which describes most of our current universe, the mass of hadrons is much larger than the mass sum of their constituent quarks (compare the masses of the mesons and baryons in this section with the quark masses in table 1.1). In fact, most of the hadron mass is due to the quark binding energies. Therefore, one can define so - called constituent quark masses, i.e., the "effective" masses of quarks when making up matter. For the light quarks these constituent masses are $M_{u,d\,\text{constituent}} \approx 336\,\text{MeV}$ and $M_{s\,\text{constituent}} \approx 509\,\text{MeV}$. This makes $SU(3)_\text{V}$ for the light quarks a good approximate symmetry - and it is a basis for chiral perturbation theory which we discuss next.[17]

---

[16] [2, 4, 111, 119]

[17] [2, 6]

### Chiral Perturbation Theory

The following is only a short summary of chiral perturbation theory, as this effective theory describing QCD at low or zero temperatures is not the focus of this work. Nevertheless we mention it here, both for the sake of completeness and since chiral perturbation theory is required to determine the mass of the axion (cf. section 2.5.3) at low or zero temperatures - complemented by our efforts to provide a better understanding of the axion mass at high temperatures. Extensive reviews of chiral perturbation theory can be found in [112] and [120], for example.

At low temperatures/energies, where the QCD coupling strength becomes large, the perturbative model of quarks and gluons (i.e., QCD as discussed in sections 2.1 and 2.2) is no longer a suitable theory. Instead, quark confinement shows that in this temperature regime nature is described by an effective theory in which the degrees of freedom are the light hadrons given above. This theory is called chiral perturbation theory [121–124].[18] According to the (approximate) $SU(3)_{\mathrm{V}}$ - symmetry, the light hadrons are grouped in $SU(3)$ - matrices. For the pNG bosons this matrix is given by

$$U = \exp\left(\frac{i}{f_\pi}\pi^a T^a_{SU(3),\,\mathrm{def}}\right) = \exp\left(\frac{i}{f_\pi}\begin{pmatrix} \pi^0 + \frac{\eta}{\sqrt{3}} & \sqrt{2}\pi^+ & \sqrt{2}K^+ \\ \sqrt{2}\pi^- & -\pi^0 + \frac{\eta}{\sqrt{3}} & \sqrt{2}K^0 \\ \sqrt{2}K^- & \sqrt{2}\,\overline{K}^0 & -\frac{2}{\sqrt{3}}\eta \end{pmatrix}\right) \tag{2.3.10}$$

with the pion decay constant $f_\pi(T \searrow 0) = (92.32 \pm 0.13)\,\mathrm{MeV}$ [2], i.e., the strength of the matrix element of the axial - vector current operator between a 1 - pion state and the vacuum. To construct the massless Lagrangian, one again follows the guiding principle of symmetry and an intuitive “theorem” from [112] - “ one writes down the most general possible Lagrangian, including all terms consistent with assumed symmetry principles, and then calculates matrix elements [...] to any given order of perturbation theory, the result will simply be the most general possible $S$ - matrix consistent with analyticity, perturbative unitarity, cluster decomposition and the assumed symmetry principles”[19]: $\mathcal{L}_{\mathrm{chPT}} \supset \frac{f_\pi^2}{4}\mathrm{tr}(\partial^\mu U \partial^\mu U^\dagger) + \sum_{i+j\,\geq\,2} c_{i,j}\Big(\big(\mathrm{tr}(\partial U \partial U^\dagger)\big)^i \cdot \mathrm{tr}\big((\partial U \partial U^\dagger)^j\big)\Big)$, where the traces contain all unique index contractions. This massless Lagrangian yields standard kinetic terms for the mesons as well as all interactions terms and is invariant under $SU(3)_{\mathrm{L}} \otimes SU(3)_{\mathrm{R}}$ - transformations $U \to g_{\mathrm{L}} U g_{\mathrm{R}}^\dagger$. In order to break the $SU(3)_{\mathrm{A}}$ - symmetry as in QCD of massive quarks (cf. (2.3.8)) - and thus break $SU(3)_{\mathrm{L}} \otimes SU(3)_{\mathrm{R}}$ down to $SU(3)_{\mathrm{V}}$ -, one adds a mass term $\mathcal{L}_{\mathrm{chPT}} \supset -\frac{\langle \bar{q}_l q_l \rangle}{3}\mathrm{tr}(M_{q_l} U^\dagger + U M_{q_l}^\dagger)$ to the purely kinetic chiral Lagrangian.

---

[18] Note that chiral perturbation theory is not required because QCD “fails” below $T_{\mathrm{c}}$, but because it fails as a perturbation theory. Non - perturbative QCD models like lattice QCD still work at low temperatures.

[19] The “theorem” is reiterated in [125] and its implications were proven in [126].

The mass matrix for the three light quarks $M_{q_l}$ (cf. (2.1.24) is taken to be complex for convenience (cf. section 2.5.3). At leading order, the Lagrangian of chiral perturbation theory for the pNG bosons reads

$$\mathcal{L}_{\text{chPT}} \supset \frac{f_\pi^2}{4}\text{tr}(\partial_{\mu_\text{M}} U \partial^{\mu_\text{M}} U^\dagger) - \frac{\langle \bar{q}_l q_l \rangle}{3}\text{tr}(M_{q_l} U^\dagger + U M_{q_l}^\dagger)\,. \tag{2.3.11}$$

Chiral perturbation theory also describes baryons and one constructs that part of the theory based on baryonic matrices like the octet matrix

$$\begin{pmatrix} \frac{\Sigma^0}{\sqrt{2}} + \frac{\Lambda^0}{\sqrt{6}} & \Sigma^+ & p \\ \Sigma^- & -\frac{\Sigma^0}{\sqrt{2}} + \frac{\Lambda^0}{\sqrt{6}} & n \\ \Xi^- & \Xi^0 & -\sqrt{\frac{2}{3}}\Lambda \end{pmatrix}\,, \tag{2.3.12}$$

but baryonic chiral perturbation theory is outside of the interest if this work.[20]

The pion decay constant is related to the $u$ - and $d$ - quark condensates $\langle \bar{u}u \rangle \approx \langle \bar{d}d \rangle$ (neglecting the $s$ - quark) by the Gell-Mann - Oakes - Renner relation

$$M_\pi^2 f_\pi^2 = -\langle \bar{u}u \rangle (M_u + M_d) \tag{2.3.13}$$

(for a detailed discussion of this relation at finite temperature see [127]), which gives another way of setting the chiral symmetry breaking scale as $\Lambda_\chi \sim 4\pi f_\pi \approx 1.2$ GeV. Regardless of the definition chosen for $\Lambda_\chi$, it marks an internal momentum/energy scale at which chiral perturbation theory breaks down. This return to regular QCD is an analytic, gradual transition, so assigning a concrete value to $\Lambda_\chi$ always depends on convention. Furthermore, $M_\rho$ and $4\pi f_\pi$ differ by a factor of approximately $1.5$, i.e., an $\mathcal{O}(1)$ - number. To make the nature of $\Lambda_\chi$ as a momentum cut - off scale more obvious, one can re - scale the Lagrangian coefficients of full chiral perturbation theory as $\frac{c_{i,j}}{\Lambda_\chi^{i+j}}$. This is also the origin of the factor $4\pi$ in the pion decay constant - definition of $\Lambda_\chi$, as this factor results from a geometrical factor in 4 - dimensional loop diagrams corresponding to the interactions described by the higher order terms. All in all, $f_\pi \neq 0$ is a necessary and sufficient criterion for spontaneous chiral symmetry breaking, while $\langle \bar{q}_l q_l \rangle \neq 0$ is a sufficient, but not a necessary condition.[21]

The temperature of chiral perturbation theory breakdown, called the critical temperature $T_\text{c} \approx 156$ MeV [128] is (much) smaller than $\Lambda_\text{QCD}$ ($\Lambda_\chi$), however. This is because, just as, for example, in black body radiation, the thermal meson/baryon - medium contains a significant ratio of states with energies $\sim 3T$ ($6T$ for fermions). This does not mean that at $T_c$ the average center of mass energies of the particles already extend the quark condensate binding energy $\Lambda_{\mathrm{QCD}}$, but that a large enough number of mesons reach energy scales high enough to dissolve light quark condensates and close to $\Lambda_\chi$, meaning that it is no longer sensible to use chiral perturbation theory for $T \gtrsim T_{\mathrm{c}}$.[22]

---

[20] [4, 112, 120]

[21] [4, 112, 120]

## 2.4 Topology of $SU(N)$ - Gauge Theories and the Interplay with Particles

After having discussed QCD, its symmetries and its quantization - all based on the Lagrangian (2.1.24) we introduced in section 2.1 -, we are now going to elaborate why we called this Lagrangian "naive" in the corresponding section title. The reason is that it misses the topological effects of QCD; in detail, it does not take into account the non-trivial topology of $SU(N)$ Yang-Mills (YM) theory describing gluons, the importance of which (in the IR limit) was first recognized in [109]. In order to provide an intuitive picture, we are going to first discuss topology in a simplified toy model of non-relativistic quantum mechanics. Following this, the topology of QCD is going to be discussed.

### 2.4.1 Instantons in non-relativistic Quantum Mechanics

The key concepts required to discuss the topology of $SU(N)$ gauge groups can be introduced using the simple quantum mechanics systems of the double well potential and the periodic potential of infinitely many wells as depicted in figure 2.4. These topics are presented more extensively in, for example, [8, 33, 38, 130–132], which therefore all serve as general references for this section 2.4.1.

The amplitude for a quantum mechanical system to transition from $(\vec{\chi}_{\mathrm{i}}, t_{\mathrm{i}})$ to $(\vec{\chi}_{\mathrm{f}}, t_{\mathrm{f}})$ in real time[23] is given by the Schrödinger propagator $Z$, i.e., the matrix element of the time evolution operator, which equals the partition function (2.2.6)

$$\begin{aligned}
&Z(\vec{\chi}_{\mathrm{f}}, t_{\mathrm{f}}; \vec{\chi}_{\mathrm{f}}, t_{\mathrm{i}}) = \langle \vec{\chi}_{\mathrm{f}}, t_{\mathrm{f}} \,|\, \vec{\chi}_{\mathrm{f}}, t_{\mathrm{i}} \rangle = \left\langle \vec{\chi}_{\mathrm{f}} \,\middle|\, e^{-iH\Delta t} \,\middle|\, \vec{\chi}_{\mathrm{i}} \right\rangle = N \int_{\vec{\chi}(t_{\mathrm{i}}) = \vec{\chi}_i}^{\vec{\chi}(t_{\mathrm{f}}) = \vec{\chi}_f} \mathscr{D}^3 \chi \, \exp\bigl(iS[\vec{\chi}(t)]\bigr) \,, \\
&S[\vec{\chi}(t)] = \int_{t_{\mathrm{i}}}^{t_{\mathrm{f}}} \mathrm{d}t \left( -\frac{1}{2} \vec{\chi}^{\mathrm{T}} \mathfrak{T} \, \vec{\chi} - V(\vec{\chi}) \right) = \int_{t_{\mathrm{i}}}^{t_{\mathrm{f}}} \mathrm{d}t \left( -\frac{1}{2} \vec{\chi}^{\mathrm{T}} \mathcal{M} \, \mathrm{d}_t^2 \vec{\chi} - V(\vec{\chi}) \right) \,,
\end{aligned} \tag{2.4.1}$$

---

[22] [98, 129]

[23] Like in section 2.2.1, specifically from (2.2.1) to (2.2.6), we again emphasize real (Minkowski) and imaginary (Euclidean) time by using the same spacetime time as in (2.1.1) and (2.2.21), respectively.

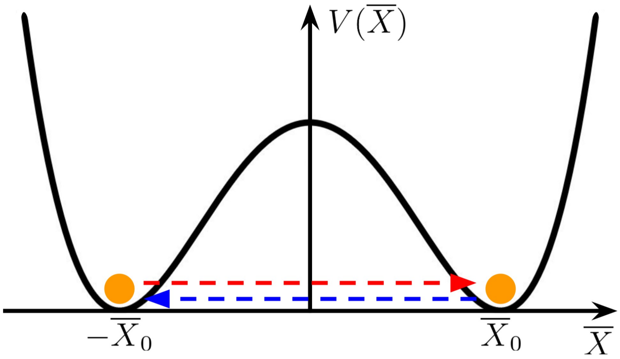
$V(\overline{X})$
$-\overline{X}_0$
$\overline{X}_0$
$\overline{X}$

(a). Double well potential for a quantum particle ●. Even for vanishing kinetic energy, purely quantum mechanical tunneling processes from $-\overline{X}_0$ to $-\overline{X}_0$ (- - - instanton) and vice versa (- - - anti-instanton) are possible. These processes cannot be quantized using the path integral method (cf. section 2.2.1), as there is no classical solution for the quantum processes.

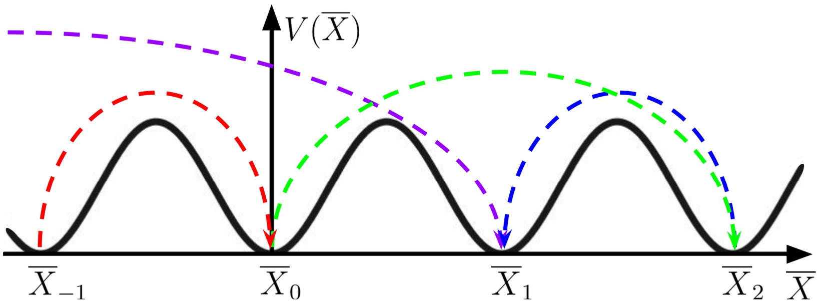
$V(\overline{X})$
$\overline{X}_{-1}$
$\overline{X}_0$
$\overline{X}_1$
$\overline{X}_2$
$\overline{X}$

(b). Periodic potential for a quantum particle, general $n$ - instanton solutions which tunnel from $\overline{X}_\nu$ to $\overline{X}_{\nu+n}$ exist (e.g.: - - - and - - - ). In the dilute instanton gas approximation (DGA), $n$ - instantons are described as $n_\pm$ consecutive instantons $(+)$ and anti-instantons $(-)$ in any order such that $n_+ - n_- = n$, e.g., - - - $= 2\times$ - - - or - - - $= 2\times$ - - - $+$ - - - $+$ - - - .

Figure 2.2

where we chose the form of the kinetic energy in (2.4.1) to match the discussion in section 2.4.3. This form is not linked to the "standard" form in (2.2.6) by IBP for the general case $\vec{\chi}_\mathrm{i} \neq \vec{\chi}_\mathrm{f}$ and/or $(\mathrm{d}_t\vec{\chi})|_{t_\mathrm{i}} \neq (\mathrm{d}_t\vec{\chi})|_{t_\mathrm{f}}$. Nevertheless, the two forms obey the same symmetries and yield the same equations of motion $-\frac{\delta S}{\delta \vec{\chi}}\Big|_{\vec{\chi}_\mathrm{cl}} = \big(\mathfrak{T}\,\vec{\chi} + \vec{\partial} V\big)\Big|_{\vec{\chi}_\mathrm{cl}} = 0$ and thus the resulting instanton solutions (2.4.6) are also identical. The path integral (2.4.1) can be calculated in the stationary phase approximation discussed below (2.2.1) by employing Laplace's method (which is often also called saddle point approximation) [133, 134]: The paths $\vec{\chi}(t)$ are treated as quantum fluctuations $\vec{\eta}$ around the classical solution $\vec{\chi}(t) = \vec{\chi}_\mathrm{cl}(t) + \vec{\eta}(t)$ and the action functional $S$ is expanded up the first non-vanishing order in quantum fluctuations $\mathcal{O}\big(\vec{\eta}^{\,2}\big)$.

However, there exist quantum mechanical processes which have no corresponding classical solution, so that the stationary phase approximation fails. An example are tunneling processes in the double well potential shown in figure 2.2a. Such processes cannot be described by the propagator as given in (2.4.1). This problem can be solved, however, by performing a Wick rotation $t \to \bar{t} = it$ analogous to (2.2.21) - since $\bar{t} \in \mathbb{R}$ the barred notation is used here in accordance to the notation for temporally infinite Euclidean spacetime. This Wick rotation changes the path integral as

$$\begin{aligned} S = \int_{t_\mathrm{i}}^{t_\mathrm{f}} \mathrm{d}t \,\Big( -\frac{1}{2}\vec{\chi}^\mathrm{T}\mathfrak{T}\,\vec{\chi} - V(\vec{\chi})\Big) \;&\to\; iS_\mathrm{E} = i\int_{\bar{t}_\mathrm{i}}^{\bar{t}_\mathrm{f}} \mathrm{d}\bar{t}\,\Big( -\frac{1}{2}\vec{\overline{X}}^{\,\mathrm{T}}\mathfrak{T}_\mathrm{E}\vec{\overline{X}} + V(\vec{\overline{X}})\Big) \\ \Rightarrow \quad \int_{\vec{\chi}(t_\mathrm{i}) = \vec{\chi}_\mathrm{i}}^{\vec{\chi}(t_\mathrm{f}) = \vec{\chi}_\mathrm{f}} \mathscr{D}^3\chi\, e^{iS[\vec{\chi}]} \;&\to\; \int_{\vec{\overline{X}}(t_i) = \overline{X}_\mathrm{i}}^{\vec{\overline{X}}(t_\mathrm{f}) = \overline{X}_\mathrm{f}} \mathscr{D}^3\overline{X}\, e^{-S_\mathrm{E}[\vec{\overline{X}}]}\,, \end{aligned} \tag{2.4.2}$$

where we also used the notation $\overline{X} = \chi$ in accordance with (2.2.21) and the subscript "E" denotes the action in imaginary/Euclidean time. The kinetic energy-differential operator now reads $\mathfrak{T}_\mathrm{E} = \mathcal{M}\,\mathrm{d}^2_{\bar{t}}$. The important differences between the path integral and action in real and imaginary time are the change of the action from a complex phase to an exponential decay factor and the inversion in the potential $V(\chi) \to -V(\overline{X})$.[24] Due to the former, imaginary time-physics structurally resembles thermodynamics, the latter means that physics is now described by the potential $-V(\overline{X}) = -V(\chi)$, while the actual, "physical" potential is $V(\overline{X})$. Therefore, processes like quantum tunneling through a potential barrier which formerly lacked a classical solution in real time are now described by regular, classical propagation paths in imaginary time, $\vec{\overline{X}}_\mathrm{cl}(\bar{t})$, through the well of the inverted potential. These paths are solutions to $-\frac{\delta S_E}{\delta \vec{\overline{X}}}\Big|_{\vec{\overline{X}}_\mathrm{cl}} = \big(\mathfrak{T}_\mathrm{E}\vec{\overline{X}} - \vec{\partial}V\big)\Big|_{\vec{\overline{X}}_\mathrm{cl}} = 0$ as

---

[24] If the "standard" form of the kinetic energy had been chosen, one would have found the Euclidean Lagrangian $\mathcal{L}_\mathrm{E} = \frac{1}{2}(\mathrm{d}_{\bar{t}}\vec{\overline{X}})^\mathrm{T}\mathcal{M}(\mathrm{d}_{\bar{t}}\vec{\overline{X}}) + V(\vec{\overline{X}}) = E_\mathrm{M}$ given by the real time-energy of the system.

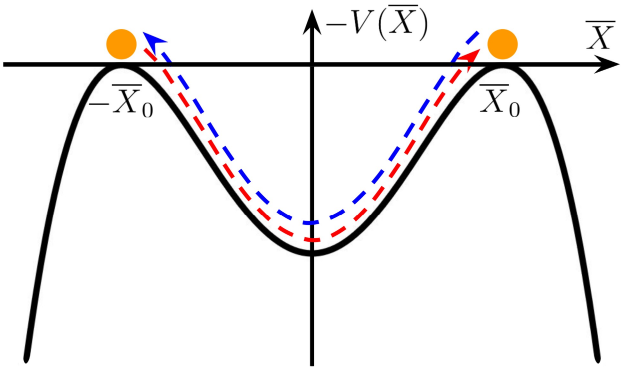

Figure 2.3: Potential in Euclidean time. After a Wick rotation $t \to \bar{t} = it$ the physically relevant, i.e., descriptive, potential is the flipped, negative version $-V(\overline{X})$. Formerly purely quantum processes like – – – instanton and – – – anti-instanton tunneling through a potential barrier (cf. figure 2.2a) now correspond to classical motions through the potential well. The existence of classical paths $\overline{X}_{\text{cl}}$ then ensures the applicability of path integral quantization (cf. section 2.2.1).

illustrated in figure 2.3.

Now the stationary phase approximation can be employed again. Up to $\mathcal{O}(\vec{\eta}^2)$ the path integral is determined by the classical action $S_{\text{E}}[\vec{\overline{X}}_{\text{cl}}]$ and the (elliptic) differential operator $\mathfrak{M}$ defined by $\left.\frac{\delta^2 S_{\text{E}}[\vec{\overline{X}}]}{\delta\vec{\overline{X}}(\bar{t})\delta\vec{\overline{X}}(\bar{t}')}\right|_{\vec{\overline{X}}_{\text{cl}}} = \mathfrak{M}(\vec{\overline{X}}_{\text{cl}})\,\delta(\bar{t}-\bar{t}') = \big(-\mathfrak{T}_{\text{E}} + (\partial_i\partial_j V)|_{\vec{\overline{X}}_{\text{cl}}}\big)\,\delta(\bar{t}-\bar{t}')$, where $(\partial_i\partial_j V)$ is the Hessian matrix:

$$Z = N\,e^{-S_{\text{E}}[\vec{\overline{X}}_{\text{cl}}]} \int_{\vec{\eta}(\bar{t}_{\text{i}})=0}^{\vec{\eta}(\bar{t}_{\text{f}})=0} \mathscr{D}^3\eta\, \exp\left(-\frac{1}{2}\int_{\bar{t}_{\text{i}}}^{\bar{t}_{\text{f}}} \mathrm{d}\bar{t}\,\vec{\eta}^{\mathrm{T}}\mathfrak{M}\,\vec{\eta}\right). \tag{2.4.3}$$

An expansion of the quantum fluctuations in eigenmodes $\vec{s}_n(\bar{t})$ of $\mathfrak{M}$ with eigenvalues $\lambda_n$, $\vec{\eta} = \sum_{n\,\in\,\mathbb{N}} c_n\vec{s}_n$, so that $\int\mathscr{D}^3\eta = \prod_n\int_{\mathbb{R}}\frac{\mathrm{d}c_n}{\sqrt{2\pi}}$ as well as $\vec{\eta}^{\mathrm{T}}\mathfrak{M}\,\vec{\eta} = \sum_n \lambda_n c_n^2$, and a Gaussian integration yield $(\sqrt{\det{}'(\mathfrak{M})})^{-1/2}$, where $\det{}'$ denotes that zero eigenvalues are excluded. In fact, zero modes $\vec{s}_{0,k}$ with vanishing eigenvalues $\lambda_{0,k} = 0$ do not contribute to the Gaussian integration and contribute separately. They correspond to symmetries of the system and have associated collective coordinates which parametrize these symmetries. As an example, the classical velocity $\mathrm{d}_{\bar{t}}\vec{\overline{X}}_{\text{cl}}$ is always a zero mode of $\mathfrak{M}$, since $\mathfrak{M}(\mathrm{d}_{\bar{t}}\vec{\overline{X}}_{\text{cl}}) = -\big(\mathcal{M}(\mathrm{d}_{\bar{t}}^3\vec{\overline{X}}_{\text{cl}}) - (\partial_i\partial_j V)^i{}_j|_{\vec{\overline{X}}_{\text{cl}}}\,\mathrm{d}_{\bar{t}}\overline{X}^j_{\text{cl}}\hat{e}_i\big) = -\mathrm{d}_{\bar{t}}\big(\mathfrak{T}_{\text{E}}\vec{\overline{X}}_{\text{cl}} - \vec{\partial}V|_{\vec{\overline{X}}_{\text{cl}}}\big) = 0$. The underlying symmetry is a time translation symmetry; despite $S_{\text{E}}$ being time - independent, the solution $\vec{\overline{X}}_{\mathrm{cl}}$ depends on a free time parameter $\bar{t}_0$ denoting "when" in the time interval $[\bar{t}_{\mathrm{i}}, \bar{t}_{\mathrm{f}}]$ the classical process takes place. This time parameter $\bar{t}_0$ is the collective coordinate associated with the time translation symmetry and one can replace the integration $\int_{\mathbb{R}} \mathrm{d}c_0$ by $\int_{\bar{t}_{\mathrm{i}}}^{\bar{t}_{\mathrm{f}}} \mathrm{d}\bar{t}_0$ (and a modification of the normalization $N$). Assuming that the velocity is the only $\mathfrak{M}$ - zero mode, one finds the propagator or partition function

$$Z = N'\, e^{-S_{\mathrm{E}}[\vec{\overline{X}}_{\mathrm{cl}}]} \int_{\bar{t}_{\mathrm{i}}}^{\bar{t}_{\mathrm{f}}} \mathrm{d}\bar{t}_0 \, \frac{1}{\sqrt{\det{}'(\mathfrak{M})}} = \int_{\bar{t}_{\mathrm{i}}}^{\bar{t}_{\mathrm{f}}} \mathrm{d}\bar{t}_0 \, đ(\bar{t}_0)\,, \tag{2.4.4}$$

where one can interpret $đ(\bar{t}_0)$ as a temporal density/probability of the classical process.

As a first toy model we present the above analysis employed on tunneling processes for a mass $M$ - particle in the 1 - dimensional double well potential (figure 2.2a), i.e.,

$$V(\overline{X}) = \frac{a^2 M}{2\overline{X}_0^2}\left(\overline{X}^2 - \overline{X}_0^2\right)^2\,, \quad \mathcal{M} = M \tag{2.4.5}$$

with some scale $[a] = \text{Length}^{-1}$. This potential yields three classical solutions of finite (or in this case vanishing) Euclidean energy $E_{\mathrm{E}} = \frac{M}{2}(\mathrm{d}_{\bar{t}}\overline{X})^2 - V(\overline{X})$ that explore one or both of the maxima of $-V$: two trivial solutions $\overline{X}_{1,2} = \pm\overline{X}_0$ and a tunneling solution. The tunneling solution's vanishing energy $E_{\mathrm{E}}(\overline{X}_{\mathrm{tun}}) = 0$ corresponds to a particle with vanishing initial and final velocity taking an infinite time $\bar{t}_{\mathrm{i,f}} \to \mp\infty$ to propagate from $\pm\overline{X}_0$ to $\mp\overline{X}_0$. This is the analogue to the QFT tunneling processes we are going to present below. One finds the tunneling solution by solving $E_{\mathrm{E}} = 0$ for $\mathrm{d}_{\bar{t}}\overline{X}$ and integrating using the separation of variables

$$\overline{X}_{\mathrm{tun}} = \pm\overline{X}_0 \tanh\big(a(\bar{t} - \bar{t}_0)\big)\,. \tag{2.4.6}$$

A plot of these two tunneling solutions in figure 2.4a shows that the actual transitions happen almost "instantaneously" within the timescale $\bar{t}_{\mathrm{inst}} \sim 4a$, compared to the infinite time duration of the complete process. Therefore, one calls such tunneling solutions in imaginary time *instantons* - here the "$+$" - solution describes a tunneling from $-\overline{X}_0$ to $\overline{X}_0$ and is called an instanton, while the inverse "$-$" - solution is called an anti-instanton. The suffix "-on", invoking a particle nature of such tunneling transitions, is due to the Euclidean Lagrangian $\mathcal{L}_{\mathrm{E}} = \frac{M}{2}(\mathrm{d}_{\bar{t}}\overline{X})^2 + V(\overline{X}) = E_{\mathrm{M}}$ or real time - energy having a pronounced peak in time (cf. figure 2.4b) - or in spacetime in the case of QFT - instantons. The instanton time scale, also the width of the $\mathcal{L}_{\mathrm{E}}$ - peak, can be understood as the (anti-)instanton size.

The differential operator used in (2.4.4) is $\mathfrak{M} = -M\mathrm{d}_{\bar{t}}^2 + V''\big(\overline{X}_{\mathrm{tun}}(\bar{t} - \bar{t}_0)\big)$ and the free parameter $\bar{t}_0$ in (2.4.6), which controls when in the time interval $]\bar{t}_{\mathrm{i}}, \bar{t}_{\mathrm{f}}[ = (-\infty, \infty)$

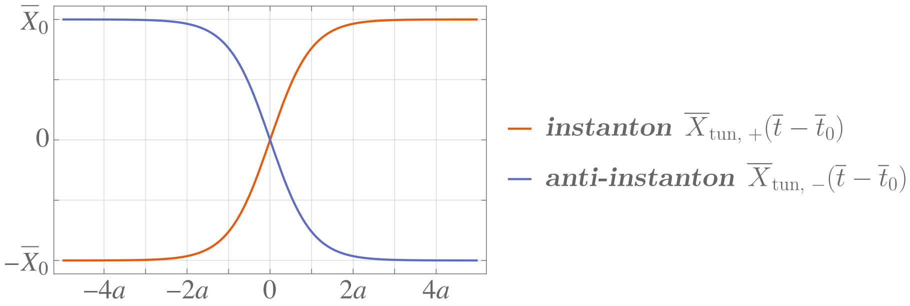

(a). The quantum mechanical instanton and anti-instanton processes (2.4.6) in the double well potential (2.4.5). The (anti-)instanton tunneling process effectively happens within a (Euclidean time frame of $\bar{t}_{\text{inst}} \sim 4a$.

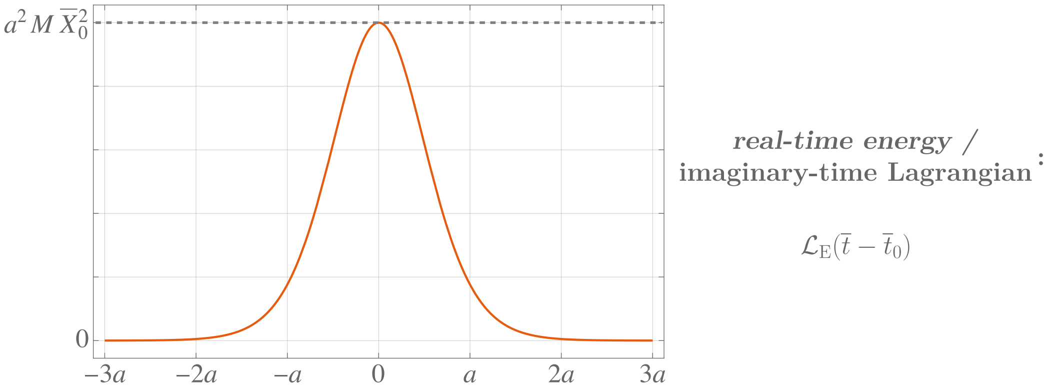

(b). The imaginary - time Lagrangian $\mathcal{L}_E\left(\overline{X}_{\text{tun}}(\bar{t}-\bar{t}_0)\right)$, which equals the real - time energy $E_{\text{M}}$ of the (anti-)instanton. The sharp, localized peak of temporal extent $\bar{t}_{\text{inst}}$ shows why instantons are intuitively understood as particles.

The real - time energy is non - conserved, opposed to the constant, i.e., conserved, imaginary - time energy $E_{\text{E}}(\overline{X}_{\text{tun}}) = 0$. This is unproblematic, however, because the (anti-)instanton tunneling is not a real - time process and $E_{\text{M}}$ is therefore not a meaningful property.

Figure 2.4

the actual “instantaneous tunneling transition” occurs, is the aforementioned collective coordinate. Up to second order in quantum fluctuations, one thus finds the tunneling propagator in the potential (2.4.5):

$$Z = N' \int_{\mathbb{R}} \mathrm{d}\bar{t}_0 \, \frac{e^{-\frac{4}{3}aMX_0^2}}{\sqrt{\det'\left(-M\mathrm{d}_{\bar{t}}^2 + V''\big(\overline{X}_{\text{tun}}(\bar{t}-\bar{t}_0)\big)\right)}} = \int_{\mathbb{R}} \mathrm{d}\bar{t}_0 \, \mathscr{d}_{\text{instanton}}(\bar{t}_0) \, . \tag{2.4.7}$$

The temporal density $\mathscr{d}_{\text{instanton}}$ is then called the *instanton density*. It is equal for instantons and anti-instantons, as $S_{\text{E}}$ is equal for the two due to the spatial symmetry of the potential and the resulting temporal symmetry of the tunneling solutions (2.4.6).

The presence of instantons, i.e., tunneling processes, also means that the ground state of the system cannot be described by the system sitting in either of the two minima, as they become degenerate due to tunneling. The real quantum mechanical ground state is then a linear superposition $|0\rangle = \frac{1}{\sqrt{2}}(|\overline{X}_0\rangle + |-\overline{X}_0\rangle)$ (up to a global phase).

The second important quantum mechanics toy model is the extension of the double well to a periodic potential of infinitely many wells as sketched in figure 2.2b. Here, (anti-)instantons describe tunneling processes from $\overline{X}_\nu$ to $\overline{X}_{\nu+1}$ ($\overline{X}_{\nu-1}$). This again causes a degeneracy in the ground states $|\overline{X}_\nu\rangle$, so that the physical ground state is again given by a linear superposition in the form of a Fourier series

$$|\theta\rangle = \sum_{\nu\,\in\,\mathbb{Z}} e^{-i\nu\theta} \, |\overline{X}_\nu\rangle \tag{2.4.8}$$

defined by a phase parameter $\theta$. In this periodic potential arbitrary $n$ - instanton solutions connecting $\overline{X}_\nu$ to $\overline{X}_{\nu+n}$ are possible as well. Given that instanton transitions occur within short timescales $\bar{t}_{\text{inst}}$, a reasonable assumption is to describe an $n$ - instanton as a combination of $n_+$ instantons and $n_-$ anti-instantons with $n = n_+ - n_-$ which are well - separated in time $|\bar{t}_{0,i} - \bar{t}_{0,j}| \gg \bar{t}_{\text{inst}}$ and thus understood as occurring consecutively. This is called the dilute instanton gas approximation (DGA)[25] and was first established in [8] for $SU(N)$ - instantons (cf. sections 2.4.2 and 2.4.4). Given the propagator/partition function for a (anti-)single instanton $Z_{\text{inst}} = Z_{\overline{\text{inst}}} = \langle \nu \pm 1 | e^{-H\bar{t}_{\text{inst}}} | \nu \rangle$ and the DGA, one constructs the full instanton partition function incorporating all $n$ - instantons in the periodic potential's $\theta$ - ground state in two steps. Firstly, the instanton partition function

---

[25] Usually, the dilute instanton gas approximation is abbreviated as DIGA, but since in section 2.4.4 we employ this approximation to QCD - instantons at finite temperature, which are called calorons, we leave out the “I” in DIGA.

$Z_{\text{inst}}$ is modified in the physical ground state (2.4.8)

$$\begin{aligned} \langle\theta'|e^{-H\bar{t}_{\text{inst}}}|\theta\rangle &= \sum_{\nu',\,\nu\,\in\,\mathbb{Z}} e^{i\nu'\theta'-i\nu\theta}\,\langle X_{\nu'}|e^{-H\bar{t}_{\text{inst}}}|X_{\nu}\rangle = \\ = \sum_{\nu',\,\nu\,\in\,\mathbb{Z}} e^{i\nu'(\theta'-\theta)}e^{i(\nu'-\nu)\theta}\delta_{\nu'-\nu,\pm1}Z_{\text{inst}} &= 2\pi\delta(\theta'-\theta)\ \underbrace{Z_{\text{inst}}e^{\pm i\theta}}_{Z_{\text{inst.}/\overline{\text{inst}}}(\theta)}\ . \end{aligned} \tag{2.4.9}$$

The overall factor $\sum_{\nu'\,\in\,\mathbb{Z}} e^{i\nu'(\theta'-\theta)} = 2\pi\delta(\theta'-\theta)$ shows that instantons transitions cannot connect physical ground states of different phases $\theta'\neq\theta$, i.e., different $\theta$ - values describe entirely different systems (different universes in the case of QCD). Furthermore, in the case of $\theta'=\theta$, the diverging factor $\delta(0)$ (or $\sum_{\nu'}\to\infty$) reflects the fact that there is an infinite number of equal “starting points” $X_{\nu}$ for instanton transitions. This prefactor cancels after appropriate normalization. Secondly, for well - separated instantons and anti-instantons the action exponentials commute and the $n$ - instanton partition function thus factorizes. The full DGA - partition function is then given by a linear superposition of $n$ - instanton partition functions analogously to (2.4.8):

$$\begin{aligned} &\langle\theta|\sum_{n\,\in\,\mathbb{Z}} e^{-H_{n\text{ - inst}}\bar{t}_{n\text{ - inst}}}|\theta\rangle = \sum_{n\,\in\,\mathbb{Z}} Z_{n\text{ - inst}}(\theta) = \\ &= (2\pi)^{n_++n_-}\delta(0) \sum_{n,\,n_+,\,n_-\,\in\,\mathbb{Z}} \frac{\delta_{n,n_+-n_-}}{n_+!\,n_-!}\big(Z_{\text{inst}}(\theta)\big)^{n_+}\big(Z_{\overline{\text{inst}}}(\theta)\big)^{n_-} = \\ &= (2\pi)^{n_++n_-}\delta(0)\exp\!\big(Z_{\text{inst}}\,e^{i\theta}\big)\ \exp\!\big(Z_{\overline{\text{inst}}}\,e^{-i\theta}\big) = (2\pi)^{n_++n_-}\delta(0)\underbrace{\exp\!\big(2Z_{\text{inst}}\cos(\theta)\big)}_{Z_{\text{DGA}}(\theta)}\ . \end{aligned} \tag{2.4.10}$$

One notes that the full DGA partition function $Z_{\text{DGA}}(\theta)$ is completely determined by the parameter $\theta$ and the single - instanton partition function.

### 2.4.2 Vacuum Topology, Instantons and Calorons

Having discussed instantons in simpler toy models in section 2.4.1, we now introduce them in $SU(N)$ - gauge theory relevant for QCD. At first, the zero temperature instanton is going to be discussed and then its finite temperature generalization, the *caloron*.

#### Topologically non - trivial QCD Vacuum Structure

As in the toy models, $SU(N)$ - instantons describe tunneling effects in imaginary time. The potential landscape in which these tunneling processes take place is now given by the topologically non-trivial vacuum structure of $SU(N)$ gauge theories. As we stated at the beginning of the introduction 1.2, the mathematical discipline of topology studies the global properties of geometric objects/spaces and maps from one space to another which are preserved under local continuous deformations. This also means that topological invariants are necessarily global properties independent of any local features. Two geometrical objects or spaces are called topologically equivalent if they are linked by a homeomorphism, a topological isomorphism that describes such a continuous deformation of the one object into the other and vice versa. Any homeomorphic spaces also agree in their topological invariants. Homotopy of maps between topological spaces is another important topological property. In detail, two maps $f, g : M \to N$ between topological spaces $M$ and $N$ are said to be homotopic if there exists a continuous family of maps $h_s : M \to N$ with $s \in [0,1]$ and $h_0 = f$, $h_1 = g$. For the spaces under consideration in this work, namely $n$ - spheres $S^n$, two maps $f, g : S^{n_1} \to S^{n_2}$ are homotopic if their images are homeomorphic. An extensive introduction to topology and its applications as used (implicitly) in this work is presented in various works, e.g., [135–137].

To establish the connection between gluonic $SU(N)$ - vacua and topology [138], first note that these states minimize the Euclidean YM action $S_{\text{YM}} = \frac{1}{2g^2} \int_{\mathbb{R}^4} \mathrm{d}^4\overline{X}\, \mathrm{tr}\big(G^{\mu\nu} G^{\mu\nu}\big)$ (cf. (2.2.26)): they are pure gauge configurations

$$\mathfrak{su}(N) \ni A^{\mu}_{\text{vac}}(\overline{X}) = i\Omega(\overline{X})\partial^{\mu}\Omega^{-1}(\overline{X})\,, \quad \Omega \in SU(N) \tag{2.4.11}$$

for which the Euclidean field strength (cf. (2.1.21)) and therefore $S_{\text{YM}}$ vanish. These vacuum states are gauge transformations (2.1.19) of the trivial vacuum $A^{\mu}_{\text{vac}} = 0$. It turns out that the defining maps $\Omega$ fall into homotopy equivalence classes of maps $\mathbb{R}^4 \to SU(N)$ labeled by integer *winding numbers/topological charges* $n \in \mathbb{Z}$.[26]

As a toy model one considers closed homotopic maps $\vartheta_n : S^1 \to S^1$ with $\vartheta_n(0) = \vartheta_n(2\pi)$ and $n \in \mathbb{Z}$ as depicted in figure 2.5. The most important such maps are $\underline{\vartheta}_n(\varphi) = e^{in\varphi}$. The winding number $n = \frac{i}{2\pi} \int_0^{2\pi} \mathrm{d}\varphi\, \vartheta_n \partial_{\varphi} \vartheta_n^{-1}$ now counts how often the straight line - circle is wound around the dashed line - one. This integral is invariant under continuous (closed) deformations $\vartheta_n = \vartheta_n + i\delta_n(\varphi)\vartheta_n$ and thus a topological invariant. With neither cuts nor reversals (passing through itself completely) of the mapped lines being allowed continuous deformations, the $\vartheta_n$ form distinct equivalence classes. Two equivalent maps $\vartheta_n$ and $\vartheta'_n$ of the same $n$ are homotopic and the equivalence classes are labeled by the winding number. Indeed, every map $\vartheta_n$ is homotopic to the $\underline{\vartheta}_n$ of the same $n$ and thus falls into the corresponding equivalence class. One also notes that combining two maps $\vartheta_n$ and $\vartheta_{n'}$

---

[26] [8, 33, 116, 130, 131, 138]

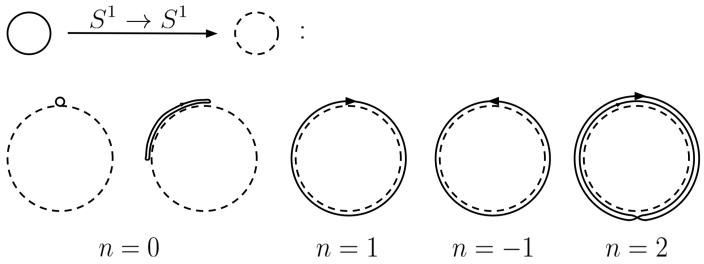

Figure 2.5: The maps $\vartheta_n : S^1 \to S^1$ mapping the solid circle onto the dashed circle. The paradigmatic map with winding number $n = 0$ is the trivial map $\underline{\vartheta}_0(\varphi) = e^{in\varphi}|_{n=0} = 1$ which maps the solid circle onto a single point. Any other path $\vartheta_0(\varphi)$ that does not fully wind around the dashed circle can be contracted to a single point, meaning that $\vartheta_0$ is homeomorphic to $\underline{\vartheta}_0$ and also has winding number 0. If the path winds around the dashed circle $n$ times, where negative $n$ describe a winding in the opposite direction, the winding number is $n$. An addition of a partial winding (like for $n = 0$) to a full winding can again be “contracted away” and thus has no topological impact, leaving $n$ unchanged (cf. (2.4.12)).

by concatenation, the resulting map

$$\vartheta_n * \vartheta_{n'}(\varphi) = \begin{cases} \vartheta_n(2\varphi) & : 0 \leq \varphi \leq \pi \\ \vartheta_{n'}(2\varphi - 2\pi) & : \pi \leq \varphi \leq 2\pi \end{cases} \tag{2.4.12}$$

falls into the equivalence class with winding number $n + n'$. Treating this concatenation as a group operation, the homotopy equivalence classes form the homotopy group $\pi_1(S^1) \cong \mathbb{Z}$ of maps $S^1 \to S^1$.[27]

To translate the above toy model to gluon vacua, i.e., maps $A^\mu_{\text{vac}} : \mathbb{R}^4 \to \mathfrak{su}(N)$ defined by (2.4.11), one considers both “sides” of the map separately. Firstly, one requires $\lim_{\overline{R} \to \infty} A_{\text{vac}} = 0$, i.e., $\lim_{\overline{R} \to \infty} \Omega = \mathbb{1} \cdot \text{const.}$, and up to a trivial rescaling this allows one to restrict the vacua with $\lim_{\overline{R} \to \infty} \Omega = \mathbb{1}$. As a consequence, all points at infinity become indistinguishable from the point of view of the gauge field and can thus be identified; infinite Euclidean spacetime $\mathbb{R}^4$ is thus compactified to a 3 - sphere $S^3_{\text{space}}$. This is analogous to how the stereographic projection $S^2 \to \mathbb{R}^2$ maps the north pole of the sphere to all points at radial infinity (cf. figure 2.6). Secondly, according to Bott’s theorem [139], for any map $S^3 \to G$ with $G$ a simple Lie group like $SU(N)$, only an $SU(2)$ - subgroup of

---

[27] [33, 130]

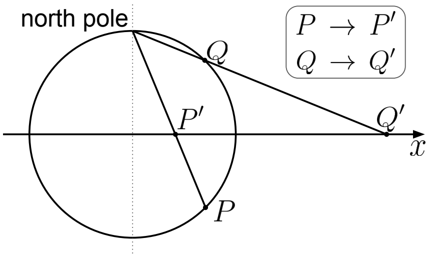

Figure 2.6: The stereographic projection $S^2 \to \mathbb{R}^2$ in the $y = 0$ plane/axis. The points $P, Q \in S^2$ get mapped to the points $P', Q' \in \mathbb{R}^2$. From this construction one sees that the north pole gets mapped to all points $||(x, y)|| \to \infty$, independent of the direction. An inverse map thus compactifies the infinite $\mathbb{R}^2$ to the finite $S^2$ and identifies all of infinity with the single point at the $S^2$ - north pole.

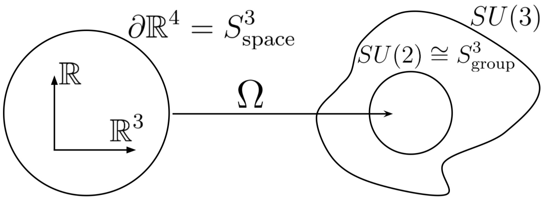
$\partial\mathbb{R}^4 = S^3_{\text{space}}$
$SU(3)$
$SU(2) \cong S^3_{\text{group}}$
$\mathbb{R}$
$\Omega$
$\mathbb{R}^3$

Figure 2.7: The maps $\Omega$ describing gluonic vacua as introduced in (2.4.11). Due to the vanishing of $A_{\text{vac}}$ at spatial infinity independent of the direction and Bott's theorem in [139], only a compactified spatial 3 - sphere gets mapped onto a group 3 - sphere.

$G$ is "topologically active" and relevant for the maps. In other words, any map $S^3 \to G$ can be continuously deformed into map $S^3 \to SU(2) \subset G$. Therefore, one only has to consider $\Omega : S^3_{\text{space}} \to SU(2)$ and, using the fact that $SU(2) \cong S^3_{\text{group}}$, one finds that the vacuum configurations are topologically determined by maps $\Omega : S^3_{\text{space}} \to S^3_{\text{group}}$ according to (2.4.11). This is shown in figure 2.7. The gluon vacuum states can thus be written as

$$A_{\text{vac., }\mathfrak{su}(N)} = \left(\begin{array}{c|c} A_{\text{vac., }\mathfrak{su}(2)} & 0_{2\times(N-2)} \\ \hline 0_{(N-2)\times 2} & 0_{(N-2)\times(N-2)} \end{array}\right) \tag{2.4.13}$$

up to residual gauge transformations, which do not alter the $\mathfrak{su}(2)$ - vacuum topologically or only change the embedding of the $\mathfrak{su}(2)$ - object in the $\mathfrak{su}(N)$ - matrix.[28]

---

[28] [33, 38, 130, 131, 140]

Analogously to the $S^1 \to S^1$ - toy model, one can define a winding number $\nu$ for the gluon vacuum. On the level of the maps $\Omega_\nu : S^3_{\text{space}} \to S^3_{\text{group}}$ it is given by the *Pontryagin index*. Using the angles $\varphi_i$, $i \in \{1,2,3\}$ to parametrize the spatial 3 - sphere, the Pontryagin index reads

$$\mathbb{Z} \ni \nu[\Omega_\nu] = \frac{1}{24\pi^2} \int_{S^3_{\text{space}}} \mathrm{d}^3\varphi\, \varepsilon^{ijk}\, \mathrm{tr}\big(\Omega_\nu \partial_{\varphi_i} \Omega_\nu^{-1}\, \Omega_\nu \partial_{\varphi_j} \Omega_\nu^{-1}\, \Omega_\nu \partial_{\varphi_k} \Omega_\nu^{-1}\big) = \tag{2.4.14}$$

$$= -\frac{i}{12\pi^2} \int_{\partial\mathbb{R}^4} \mathrm{d}^3\varphi\, n^\mu \varepsilon^{\mu\alpha\beta\gamma}\, \mathrm{tr}\big(A^\alpha_{(\nu)} A^\beta_{(\nu)} A^\gamma_{(\nu)}\big)\,, \tag{2.4.15}$$

with $n^\mu$ the unit normal vector of the infinite 3 - sphere $S^3_\infty = \partial\mathbb{R}^4$ and $A_{(\nu)}$ a vacuum state with winding number $\nu$. The integrand in (2.4.14) can be viewed as a suitable measure for integration in group space, since it is invariant under local deformations, i.e., small gauge transformations. As in the toy model, there exist paradigmatic maps

$$\underline{\Omega}_1 = \frac{i(\sigma^\dagger)^\mu \overline{X}^\mu}{\overline{R}}\,,\ \underline{\Omega}_\nu = (\underline{\Omega}_1)^\nu \quad \text{with} \quad \sigma^\mu = (\vec{\sigma}, \mathbb{1}\cdot i) \Leftrightarrow (\sigma^\dagger)^\mu = (\vec{\sigma}, -\mathbb{1}\cdot i) \tag{2.4.16}$$

which “define” homotopy classes labeled by the Pontryagin index as in the toy model. Note especially: $\underline{\Omega}_{-1} = \frac{i\sigma^\mu \overline{X}^\mu}{\overline{R}}$.

Here it is important to differentiate small and large gauge configurations. Small gauge configurations defined by $\Omega_{\text{small}} = \Omega_0 = e^{i\omega^a_{\text{small}} T^a}$, $T^a \in \mathfrak{su}(N)$ the Lie group generators, are those gauge configurations that can be built up from infinitesimal gauge configurations via exponentiation, i.e., the $\Omega_{\text{small}}$ are continuously connected to $\mathbb{1}$ at all $\overline{X}$ and the $A_{\text{small gauge}}$ can be continuously deformed to $0$ everywhere. This is not the case for large gauge configurations defined by $\Omega_{\text{large}} = \Omega_{\nu \neq 0} = e^{i\omega^a_{\text{large}} T^a}$, however, instead they are discontinuous at least at one point, where $A_{\text{large gauge}}$ is then singular. Obviously, small gauge transformations leave the homotopy class or winding number of a gauge configuration intact, while large ones change it. In terms of the $\omega$, the difference between small and large gauge configurations is that $\lim_{\overline{R}\to\infty} \Omega_{\text{small}} = 1$ and $\lim_{\overline{R}\to\infty} \omega_{\text{small}} = 0$, while only the first is true for large gauge configurations. Defining a concatenation analogously to (2.4.12) as a group operation for the maps $\Omega_\nu$, the vacua again form a homotopy group $\pi_3(S^3) \cong \mathbb{Z}$.[29]

As stated above, gluonic vacua of different winding numbers fall into different homotopy equivalence classes and cannot be connected via regular (i.e., small) gauge transformations. Therefore, these gluon vacua must be separated by an energy barrier $E_{\text{M}} = \mathcal{L}_{\text{YM, E}} > 0$ given by the gluon states separating the vacua. The resulting periodic energy landscape is sketched in figure 2.8 and is analogous to the periodic potential in figure 2.2b.[30]

---

[29] [8, 33, 38, 130, 131, 138]

[30] [38, 130]

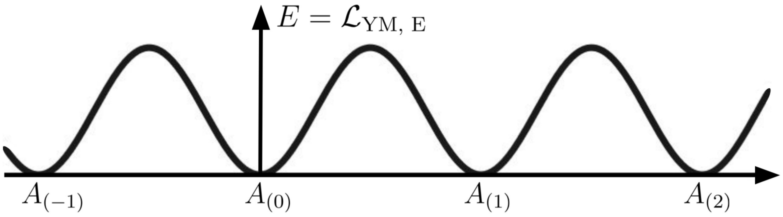

Figure 2.8: Potential landscape for gluon vacua. The gluon vacuum configurations $A_{(\nu)}$ minimize $S_{\text{YM, E}} \geq 0$, any other gluon configuration therefore carries larger action/energy which defines a periodic potential landscape analogous to figure 2.2b.

### Instantons, Vacuum - Tunneling and the $\theta$ - Vacuum

Like in section 2.4.1, the distinct $\nu$ - vacua can again be connected by instantons, i.e., tunneling procedures “through” the energy barriers depicted in figure 2.9. These instantons can then either be understood as “starting out” in one $A_{(\nu)}$ for $\bar{t} \to -\infty$ and “ending up” in another $A_{(\nu')}$ for $\bar{t} \to \infty$ or, in a more topological approach, as local, yet topologically non - trivial, gauge field configurations that change the global, topological properties of the gluon vacuum. These properties are found by integrating over all of $\mathbb{R}^4$. An intuition for this is the hole pierced in a sheet of paper discussed in the introductory section 1.2.[31]

The instantons serve as classical solutions in the stationary phase approximation for tunneling processes from one vacuum homotopy class to another. Therefore, they have to be of finite YM action $S_{\text{YM}} = \frac{1}{2g^2} \int_{\mathbb{R}^4} \mathrm{d}^4\overline{X} \, \mathrm{tr}\big(G^{\mu\nu} G^{\mu\nu}\big)$ and approach pure gauge configurations fast enough as $\overline{R} \to \infty$. In detail, the field strength has to fall off as $\mathcal{O}(\overline{R}^{-a})$, $a > 2$ for $\overline{R} \to \infty$ and therefore the instanton field configuration approaches pure gauge form as $\overline{R} \to \infty$ [141, 142]:

$$\lim_{\overline{R} \to \infty} A^{\mu}_{\text{inst}} = i\Omega\partial^{\mu}\Omega^{-1} + \mathcal{O}(\overline{R}^{-b}) \,, \quad b > 1 \,. \tag{2.4.17}$$

Also, the instantons share the symmetries of the spacetime $\mathbb{R}^4$: they are covariant under rotations, translations and dilatations, i.e., the changing of scales. Plugging this form (2.4.17) into the Pontryagin index (2.4.14) yields a result similar to (2.4.15) with an additional term since the instanton field strength does not vanish identically as for vacuum configurations:[32]

---

[31] [8, 33, 38, 130, 131]

[32] Here and in the following we drop the subscript “inst.” and similar ones in instanton/... field strengths.

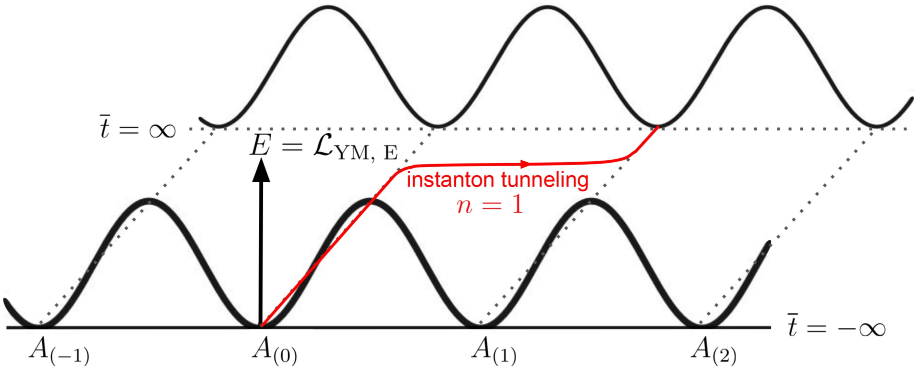

Figure 2.9: Instanton tunneling in the gluon potential between topologically distinct vacuum configurations. As in section 2.4.1 (cf. (2.4.6) and figure 2.4a)), the instanton approaches the vacua asymptotically as $\bar{t} \to \pm\infty$, whereas the actual transition happens “almost instantaneously”.

$$\mathbb{Z} \ni n[A_{\text{inst}}] = \int_{\partial\mathbb{R}^4} \mathrm{d}^3\varphi\, n^\mu\, \underbrace{\varepsilon^{\mu\alpha\beta\gamma}\,\mathrm{tr}\left(\frac{i}{24\pi^2} A^\alpha_{\text{inst}} A^\beta_{\text{inst}} A^\gamma_{\text{inst}} + \frac{1}{16\pi^2} A^\alpha_{\text{inst}} G^{\beta\gamma}\right)}_{K^\mu} . \tag{2.4.18}$$

This surface integral can be rewritten as a volume integral of the total divergence $\partial^\mu K^\mu$, which can in turn be rewritten as a simple expression of field strengths only

$$\mathbb{Z} \ni n[A_{\text{inst}}] = \int_{\mathbb{R}^4} \mathrm{d}^4\overline{X}\, \partial^\mu K^\mu = \frac{1}{16\pi^2} \int_{\mathbb{R}^4} \mathrm{d}^4\overline{X}\, \mathrm{tr}\big(\widetilde{G}^{\mu\nu} G^{\mu\nu}\big) = \int_{\mathbb{R}^4} \mathrm{d}^4\overline{X}\, q_n(\overline{X}) \,, \tag{2.4.19}$$

where $\widetilde{G}^{\mu\nu} = \frac{1}{2}\varepsilon^{\mu\nu\alpha\beta} G^{\alpha\beta}$ is the dual instanton field strength. Note that $\frac{1}{2}\varepsilon^{\mu\nu\alpha\beta}\widetilde{G}^{\alpha\beta} = G^{\mu\nu}$, while $\frac{1}{2}\varepsilon^{\mu_{\mathrm{M}}\nu_{\mathrm{M}}\alpha_{\mathrm{M}}\beta_{\mathrm{M}}}\widetilde{G}_{\alpha_{\mathrm{M}}\beta_{\mathrm{M}}} = -G^{\mu_{\mathrm{M}}\nu_{\mathrm{M}}}$. This integer $n$ is called the *instanton winding number* or *topological charge* and the integrand $q_n$ is called the instanton’s *topological charge density*. Commonly, one speaks of instantons for $n > 0$ and anti-instantons for $n < 0$.[33]

The link to tunneling between different $\nu$ - vacua is most obvious in temporal gauge $A^4 = 0$. One can always enforce this gauge condition by performing a gauge transformation (2.1.19) with $U = \mathrm{T}\,\exp\big( - i \int_0^{\bar{t}} \mathrm{d}\bar{t}' A^4_{\text{inst}}(\overline{X})\big)$, where T is the time ordering operator as in (2.2.29). Then one deforms $S^3_\infty = \partial\mathbb{R}^4$ into a hypercylinder as depicted in figure 2.10. The top and bottom sides stand for the 3 - dimensional space at infinite time $\mathrm{I}, \mathrm{III} = \mathbb{R}^4\big|_{\bar{t} \to \pm\infty} = S^3_{\bar{t} = \pm\infty}$ and the surface II, corresponding to $|\vec{\overline{X}}| \to \infty$ and finite

---

[33] [33, 38, 131, 132]

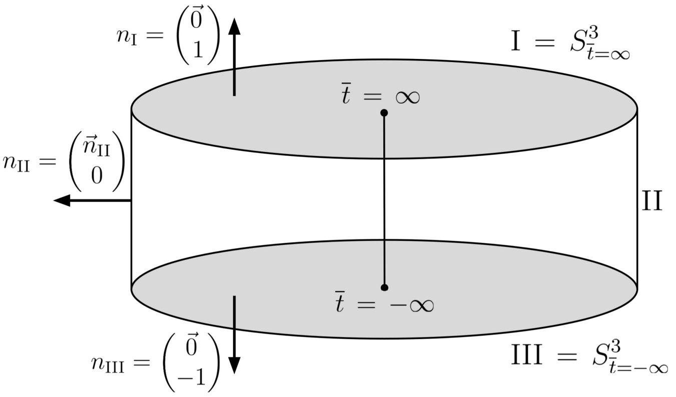
$n_{\mathrm{I}} = \begin{pmatrix} \vec{0} \\ 1 \end{pmatrix}$
$\mathrm{I} = S^3_{\bar{t}=\infty}$
$\bar{t} = \infty$
$n_{\mathrm{II}} = \begin{pmatrix} \vec{n}_{\mathrm{II}} \\ 0 \end{pmatrix}$
II
$\bar{t} = -\infty$
$n_{\mathrm{III}} = \begin{pmatrix} \vec{0} \\ -1 \end{pmatrix}$
$\mathrm{III} = S^3_{\bar{t}=-\infty}$

Figure 2.10: The boundary $\partial\mathbb{R}^4$ of infinite Euclidean spacetime deformed into a hypercylinder: I and III describe the infinite 3 - space at positive and negative temporal infinity $\bar{t} \to \pm\infty$ (here compactified to 3 - spheres $S^3_{\bar{t}=\pm\infty}$), respectively, II is the connecting surface at spatial infinity $|\vec{\overline{X}}| \to \infty$.

times, joins them. Then, the instanton winding number can be directly related to the difference of vacuum winding numbers for $\bar{t} \to \infty$ and $\bar{t} \to -\infty$ using (2.4.18):

$$n = \int_{S^3_\infty} \mathrm{d}^3\varphi\, n^\mu K^\mu = \int_{\mathrm{I}} \mathrm{d}^3\varphi\, n^\mu_{\mathrm{I}} K^\mu - \int_{\mathrm{III}} \mathrm{d}^3\varphi\, n^\mu_{\mathrm{III}} K^\mu + \int_{-\infty}^{\infty} \mathrm{d}\bar{t} \int_{\mathrm{II}} \mathrm{d}^2(\text{cylinder})\, n^\mu_{\mathrm{II}} K^\mu = \\ = \nu(\bar{t} \to \infty) - \nu(\bar{t} \to -\infty)\,. \tag{2.4.20}$$

The second line in (2.4.20) is obtained as follows: the field strength falls off as $\overline{R} \to \infty$ and thus the second term in $K^\mu$ (cf. (2.4.18)) vanishes on all surfaces I, II and III. Since $n_{\mathrm{I,III}} = \pm\hat{e}_4$, the integrands in $\int_{\mathrm{I,III}}$ get reduced to those of the Pontryagin index (2.4.15) in temporal gauge $-\frac{i}{12}\varepsilon^{ijk}\,\mathrm{tr}\big(A^i_{(\nu)}A^j_{(\nu)}A^k_{(\nu)}\big)$ and the integrals $\int_{\mathrm{I,III}}$ yield the winding numbers of the vacuum configurations the instanton reaches as $\bar{t} \to \pm\infty$. The integrand of $\int_{\mathrm{II}}$ vanishes, as $n_{\mathrm{II}}$ is purely spatial (i.e., $n^4_{\mathrm{II}} = 0$). This means that the integrand has to contain one field component $A^4_{\text{inst}} = 0$ due to the Levi - Civita symbol. All in all, an instanton of topological charge $n$ indeed describes a tunneling process from winding number $\nu$ to winding number $\nu + n$.[34]

In order to find explicit instanton configurations, one can solve the Euclidean YM equation of motion $D^\mu G^{\mu\nu} = 0$ (cf. (2.1.23)) in temporal gauge given the boundary conditions $\lim_{\bar{t}\to\pm\infty} A_{\text{inst}} = A_{(\nu+n),(\nu)}$. An easier approach, however, is to employ the fact that $\widetilde{G}^{\mu\nu}\widetilde{G}^{\mu\nu} = G^{\mu\nu}G^{\mu\nu}$ and expand the YM action as

---

[34] [131, 140]

$$\begin{aligned} S_{\text{YM}}[A_{\text{(anti-)inst}}] &= \frac{1}{2g^2}\text{Tr}(G^{\mu\nu}G^{\mu\nu}) = \\ &= \underbrace{\frac{1}{4g^2}\text{Tr}\big((G^{\mu\nu} \mp \widetilde{G}^{\mu\nu})^2\big)}_{\geq 0} \pm \frac{1}{2g^2}\text{Tr}(\widetilde{G}^{\mu\nu}G^{\mu\nu}) \geq \frac{8\pi^2}{g^2}\,|n|\,, \end{aligned} \tag{2.4.21}$$

where we used the notation $\text{Tr}(\cdot) = \int_{\mathbb{R}^4}\text{d}^4\overline{X}\,\text{tr}(\cdot)$ for the full operator trace. In general, the Tr-integration is to be thought of as taken over the appropriate spacetime and the trace in the integrand is over all uncontracted index pairs. Also, $\pm n = |n|$ with $n > 0$ for instantons $(-, +)$ and $n < 0$ for anti-instantons $(+, -)$ was used. This is called the *Bogomol'nyi inequality* [143]. Instantons and anti-instantons minimize $S_{\text{YM}}$ and thus have to satisfy (2.4.21) as an equality, which in turn means that the instanton field strength and YM action $S_{\text{YM}}[A_{\text{(anti-)inst}}]$ satisfy

$$G^{\mu\nu}_{\text{inst}} = \widetilde{G}^{\mu\nu}_{\text{inst}}\,, \quad G^{\mu\nu}_{\text{anti-inst}} = -\widetilde{G}^{\mu\nu}_{\text{anti-inst}} \tag{2.4.22}$$

$$\Rightarrow \quad S_{\text{YM}}[A_{\text{(anti-)inst}}] = \frac{8\pi^2}{g^2}\,|n|\,. \tag{2.4.23}$$

Instantons (and anti-instantons) that satisfy (2.4.22) are called self-dual (anti-self-dual). A straightforward calculation shows that (2.4.22) is a sufficient condition for the equation of motion to be satisfied. However, it is not a necessary condition, i.e., other instanton solutions which do not satisfy (2.4.22) are possible, but usually not considered. A general mechanism for finding solutions to (2.4.22) is provided by the *Atiyah-Drinfeld-Hitchin-Manin* (ADHM) *construction* [144]; for the purposes of this work, instanton solutions with $n = \pm 1$, so-called *Belavin-Polyakov-Schwartz-Tyupkin* (BPST) *instantons* [27] are sufficient. Both the ADHM construction and the BPST solution are limited to $\mathbb{R}^4$, however. This means that dimensional regularization, for example, is not available in a theory with a classical instanton background, as there is no known expression for instantons in $4 - 2\varepsilon$-dimensional spacetime.[35]

The BPST instanton is found using the ansatz $A^{\mu}_{\text{BPST}} = f(\overline{R}) \cdot i\Omega_1\partial^{\mu}\Omega^{-1}$. Plugging this into (2.4.22) yields $f(\overline{R}) = \frac{\overline{R}^2}{\overline{R}^2+\rho^2}$, where $\rho$ is a constant of integration and can be interpreted as the size of the instanton comparable to $\overline{t}_{\text{inst}} \sim 4a$ of the tunneling solution (2.4.6) in the double well potential (2.4.5) in section 2.4.1. With the explicit forms of $\Omega_1$

---

[35] [33, 38, 131, 132]

and $\Omega_{-1}$ (2.4.16) for the instanton and anti-instanton, respectively, one obtains

$$A^{\mu}_{\text{BPST}} = 2\,\eta^{a\mu\nu}\,\frac{(\overline{X}-\overline{C})^{\nu}}{(\overline{X}-\overline{C})^{2}+\rho^{2}}\,\frac{\sigma^{a}}{2} \tag{2.4.24}$$

$$A^{\mu}_{\text{anti-BPST}} = 2\,\overline{\eta}^{a\mu\nu}\,\frac{(\overline{X}-\overline{C})^{\nu}}{(\overline{X}-\overline{C})^{2}+\rho^{2}}\,\frac{\sigma^{a}}{2}\,, \tag{2.4.25}$$

where the additional free translation parameter $\overline{C}^{\mu}$ was introduced, which denotes the center of the instanton analogously to $\bar{t}_0$ in (2.4.6). The BPST instanton and anti-instanton are given in terms of the 't Hooft and anti-'t Hooft symbols $\eta^{a\mu\nu} = \varepsilon^{a\mu\nu4} + \delta^{a\mu}\delta^{\nu4} - \delta^{a\nu}\delta^{\mu4}$ and $\overline{\eta}^{a\mu\nu} = \varepsilon^{a\mu\nu4} - \delta^{a\mu}\delta^{\nu4} + \delta^{a\nu}\delta^{\mu4}$, respectively; in matrix form they read:

$$\eta^{1\mu\nu} = \begin{pmatrix} 0 & 0 & 0 & 1 \\ 0 & 0 & 1 & 0 \\ 0 & -1 & 0 & 0 \\ -1 & 0 & 0 & 0 \end{pmatrix}, \quad \eta^{2\mu\nu} = \begin{pmatrix} 0 & 0 & -1 & 0 \\ 0 & 0 & 0 & 1 \\ 1 & 0 & 0 & 0 \\ 0 & -1 & 0 & 0 \end{pmatrix}, \quad \eta^{3\mu\nu} = \begin{pmatrix} 0 & 1 & 0 & 0 \\ -1 & 0 & 0 & 0 \\ 0 & 0 & 0 & 1 \\ 0 & 0 & -1 & 0 \end{pmatrix},$$
$$\overline{\eta}^{1\mu\nu} = \begin{pmatrix} 0 & 0 & 0 & -1 \\ 0 & 0 & 1 & 0 \\ 0 & -1 & 0 & 0 \\ 1 & 0 & 0 & 0 \end{pmatrix}, \quad \overline{\eta}^{2\mu\nu} = \begin{pmatrix} 0 & 0 & -1 & 0 \\ 0 & 0 & 0 & -1 \\ 1 & 0 & 0 & 0 \\ 0 & 1 & 0 & 0 \end{pmatrix}, \quad \overline{\eta}^{3\mu\nu} = \begin{pmatrix} 0 & 1 & 0 & 0 \\ -1 & 0 & 0 & 0 \\ 0 & 0 & 0 & -1 \\ 0 & 0 & 1 & 0 \end{pmatrix}. \tag{2.4.26}$$

They are self-dual and anti-self-dual, respectively, satisfying $\eta^{a\mu\nu} = \frac{1}{2}\varepsilon^{\mu\nu\kappa\lambda}\eta^{a\kappa\lambda}$ and $\overline{\eta}^{a\mu\nu} = -\frac{1}{2}\varepsilon^{\mu\nu\kappa\lambda}\overline{\eta}^{a\kappa\lambda}$ [141]. The 't Hooft symbols link the group space generators $\frac{\sigma^a}{2}$ and the $SO(4)$ generators of rotations in $\mathbb{R}^4$ (the Wick rotated Lorentz group generators, cf. section 2.2.4) in the sense that $-i\eta^{a\mu\nu}\sigma^a$ and $-i\overline{\eta}^{a\mu\nu}\sigma^a$ are both generators of $SO(4)$. This also shows the implicit rotational symmetry of the instanton: the generators $-i\,\overset{(-)}{\eta}{}^{a\mu\nu}\sigma^a$ transform under the adjoint representation of $SO(4)$-rotations $S^{\alpha\beta}$, i.e., $-i\,\overset{(-)}{\eta}{}^{a\mu\nu}\sigma^a \to S^{\mu\alpha} - i\,\overset{(-)}{\eta}{}^{a\alpha\beta}\sigma^a S^{-1\,\beta\nu}$, while the coordinate vector transforms as $\overline{X}^{\nu} \to S^{\nu\gamma}\overline{X}^{\gamma}$. Together, this means that the instanton is covariant under spatial rotations, it transforms like a constant vector. The BPST instanton Lagrangian $\mathcal{L}_{\text{BPST}} \propto G^{a\,\mu\nu}G^{a\,\mu\nu} = \frac{192\rho^4}{\left((\overline{X}-\overline{C})^2+\rho^2\right)^2}$ also shows the expected rotational invariance.[36]

The instanton size $\rho$ and its center $\overline{C}^{\mu}$ are collective coordinates as $\bar{t}_0$ in section 2.4.1. Since the BPST instanton as an $\mathfrak{su}(2)$-object is embedded into a larger $N \times N$ matrix analogously to (2.4.13), there are additional collective coordinates that either leave the instanton unchanged or simply change its embedding. They are discussed in more detail in section 2.4.3 and it is shown that there are $4N-5$ of them. In total one thus has $4N$ collective coordinates for an instanton in $SU(N)$ gauge theory.

---

[36] [8, 38, 130, 132, 140]

The BPST (anti-)instantons (2.4.24) and (2.4.25) are given in regular gauge. This means that all of their topological charge is “stored” at spatial infinity where they approach pure gauge form. Since the (anti-)self-duality condition (2.4.22) and the equation of motion (2.1.23) are gauge-covariant, the BPST (anti-)instantons can be gauge transformed with the singular gauge transformation (cf. (2.1.19)) $U = \frac{i\sigma^\mu(\overline{X}-\overline{C})^\mu}{\sqrt{(X-C)^2}}$ into their singular gauge-expressions

$$A^\mu_{\text{BPST, sing.}} = U A^\mu_{\text{BPST}} U^{-1} + iU\partial^\mu U^{-1} = 2\,\overline{\eta}^{a\mu\nu} \frac{\rho^2(\overline{X}-\overline{C})^\nu}{(\overline{X}-\overline{C})^2\big((\overline{X}-\overline{C})^2+\rho^2\big)} \frac{\sigma^a}{2}, \tag{2.4.27}$$

$$A^\mu_{\text{anti-BPST, sing}} = U A^\mu_{\text{anti-BPST}} U^{-1} + iU\partial^\mu U^{-1} = 2\,\eta^{a\mu\nu} \frac{\rho^2(\overline{X}-\overline{C})^\nu}{(\overline{X}-\overline{C})^2\big((\overline{X}-\overline{C})^2+\rho^2\big)} \frac{\sigma^a}{2}. \tag{2.4.28}$$

Note that in this gauge ’t Hooft symbol in the instanton is replaced by the anti-’t Hooft symbol and vice versa for the anti-instanton. More importantly, however, in the singular gauge all topological information is moved to the singularity at the instanton center $C$ and “the winding about this singular point corresponds to the winding at infinity of the regular instanton” [145, p. 52]. The singularity in $A_{\text{sing}}$ is just a gauge artifact and not physical, however, since $A$ itself is not physical either - in the sense that it is not an observable. In all physical quantities, like the field strength $G$, for example, the singularity is removed. Nevertheless, even in physical quantities a discontinuity may remain at the instanton center $\overline{C}$, so that they are “only defined on the punctured euclidean space” [145, p. 52]. This is important for our numerical calculations in section 3.1.2. In singular gauge the BPST instanton can also be written as

$$A^\mu_{\text{BPST, sing}} = -\overline{\eta}^{a\mu\nu}\partial^\nu \ln\left(1+\frac{\rho^2}{(\overline{X}-\overline{C})^2}\right) \tag{2.4.29}$$

and analogously for the BPST anti-instanton. This form allows for the generalization to a configuration of $N$ BPST instantons with sizes $\rho_j$ and locations $C_j$

$$A^\mu_{N\times\text{ BPST, sing}} = -\overline{\eta}^{a\mu\nu}\partial^\nu \ln\left(1+\sum_{j=1}^{N}\frac{\rho_j^2}{(\overline{X}-\overline{C}_j)^2}\right); \tag{2.4.30}$$

an $N$-BPST anti-instanton solution is constructed analogously. This form and the singular gauge choice in general is often beneficial in explicit calculations and is indeed required for the construction of finite temperature instantons, as we are are going to elaborate below. In the following, instantons are always thought to be in singular gauge and the subscript “sing” is dropped.[37]

A theory with instantons is quantized using the background field method: the gauge field is set to be $A^\mu = A^\mu_{\text{inst.},\,\mathfrak{su}(N)} + A^\mu_{\text{qm}}$, where the instanton is taken as embedded in an $N \times N$ matrix and $A^\mu_{\text{qm}}$ describes a quantum perturbation around the classical instanton; all other fields $\{\phi_{\text{qm}}\}$ have no classical background and are thus purely quantum. Then one determines the full partition function up to some desired order in quantum fields and integrates out said quantum fluctuations order by order, obtaining a (1-particle-irreducible) effective action $\Gamma[A_{\text{inst}}]$. In this work, the quantum fluctuations are considered and consequentially integrated out up to second order $\mathcal{O}(\{\phi_{\text{qm}}\}, A_{\text{qm}})^2$ (analogously to (2.4.3) and (2.4.4)). An advantage of this approach over, for example, perturbation theory is that only the quantum fields propagate, the classical background is assumed as stationary. Therefore, one has to perform gauge fixing only for $A_{\text{qm}}$ and can choose a gauge condition that respects the background field and its separate choice of gauge. In this background gauge, the effective action $\Gamma$ then turns out to be automatically gauge invariant. This background field quantization is performed in detail in section 2.4.3.[38]

As a consequence of the presence of instantons, the physical gluon vacuum can again not be any of the now degenerate $\nu$-vacua $A_{(\nu)}$, but again has to be a Fourier series-linear superposition (cf. (2.4.8) for the periodic potential in section 2.4.1)

$$|\theta\rangle = \sum_{\nu \in \mathbb{Z}} e^{-i\nu\theta} \left|A_{(\nu)}\right\rangle = \sum_{\nu \in \mathbb{Z}} e^{-i\nu\theta} \left|\nu\right\rangle \ . \tag{2.4.31}$$

The BPST instantons and general instanton configurations with topological charge $n$ then leave this $\theta$-vacuum invariant up to multiplication with a phase factor $e^{in\theta}$. Mathematically speaking, one can define “translation operators” $\mathrm{T}_\pm$ and $\mathrm{T}_n$ in $\nu$-space corresponding to the BPST (anti-)instanton and general instantons, respectively:

$$\begin{aligned} &\mathrm{T}_\pm \left|\nu\right\rangle = \left|\nu \pm 1\right\rangle \ , \quad \mathrm{T}_n \left|\nu\right\rangle = \left|\nu + n\right\rangle \\ \Rightarrow \quad &\mathrm{T}_\pm \left|\theta\right\rangle = e^{\pm i\theta} \left|\theta\right\rangle \ , \ \mathrm{T}_n \left|\theta\right\rangle = e^{in\theta} \left|\theta\right\rangle \ . \end{aligned} \tag{2.4.32}$$

Since instantons are gauge field configurations, these operators define unitary transformations, which again fixes the structure of the $\theta$-vacuum: $|\theta\rangle$ has to be an eigenstate of the $T_n$ and the corresponding eigenvalues have to be complex phases, therefore $|\theta\rangle$ is given as a Fourier series. The instanton operators also satisfy $\mathrm{T}_n^\dagger = \mathrm{T}_n^{-1} = \mathrm{T}_{-n}$ (unitarity) and $[\mathrm{T}_n, \mathrm{T}_{n'}] \neq 0$ ($SU(N)$-instantons do not commute).[39]

---

[37] [38, 131, 132, 140, 141]

[38] [38, 141], [4, p. 734]

[39] [38, 138, 140, 146]

Using the operators (2.4.32), one determines the the partition function for an $n$-instanton in the background field method $A^\mu = A^\mu_{n\text{-inst}} + A^\mu_{\text{qm}}$ describing tunneling from $|\nu\rangle$ to $|\nu'\rangle$ analogously to the tunneling propagator in a periodic potential discussed in section 2.4.1 ([33, 38, 140], for example):

$$\begin{aligned}\lim_{\Delta\bar t\to\infty}\Big\langle \nu' \Big| e^{-H(A_{n\text{-inst}})\Delta\bar t} \Big| \nu\Big\rangle &= \big\langle \nu' \,\big|\, \mathrm{T}_n \,\big|\, \nu\big\rangle = \langle 0 \,|\, \mathrm{T}_{-\nu'}\mathrm{T}_n\mathrm{T}_\nu \,|\, 0\rangle = \\ &= \delta_{\nu'-\nu,n}\underbrace{\int \mathscr{D}A^\mu_{\text{qm}}\, e^{-\frac{8\pi^2|n|}{g^2}} \exp\Big(-\int \mathrm{d}^4\overline{X}\,\big(\mathcal{L}_{\text{int}}(A_{n\text{-inst}}, A_{\text{qm}}) + \mathcal{L}_{\text{gauge}} + \mathcal{L}_{\text{ghost}}\big)\Big)}_{=\,Z_{n\text{-inst}}}\ .\end{aligned} \tag{2.4.33}$$

Here the YM action of the background instanton can be calculated explicitly (2.4.23). The introduction of the T-operators is important, as it generalizes the action of an instanton and makes it independent of the explicit tunneling picture conveyed by $\langle\nu'|e^{-H(A_{n\text{-inst}})\Delta\bar t}|\nu\rangle$. The tunneling picture only holds in the temporal gauge, as was shown in (2.4.20), and is incompatible with finite temperature instantons, as we are going to show in section 2.4.4. The result (2.4.33) also determines the $n$-instanton partition function in the physical $\theta$-vacuum, which is calculated analogously to (2.4.9):

$$\begin{aligned}\big\langle \theta' \,\big|\, \mathrm{T}_n \,\big|\, \theta\big\rangle &= \sum_{\nu',\,\nu\,\in\,\mathbb{Z}} e^{i\nu'\theta'-i\nu\theta}\,\big\langle \nu' \,\big|\, \mathrm{T}_n \,\big|\, \nu\big\rangle = \\ &= \sum_{\nu',\,\nu\,\in\,\mathbb{Z}} e^{i\nu'(\theta'-\theta)}e^{i(\nu'-\nu)\theta}\,\big\langle \nu' \,\big|\, \mathrm{T}_n \,\big|\, \nu\big\rangle = \sum_{\nu'\,\in\,\mathbb{Z}} e^{i\nu'(\theta'-\theta)}e^{in\theta}\,Z_{n\text{-inst}} = \\ &= 2\pi\delta(\theta'-\theta)\underbrace{\int \mathscr{D}A^\mu_{\text{qm}}\,\exp\Big(-\int \mathrm{d}^4\overline{X}\Big(\mathcal{L}_{\text{int}} + \mathcal{L}_{\text{gauge}} + \mathcal{L}_{\text{ghost}} - i\theta q_n(\overline{X})\Big)\Big)}_{=\,Z_{n\text{-inst}}(\theta)}\end{aligned} \tag{2.4.34}$$

The factor $2\pi\delta(\theta'-\theta)$ again shows that instantons cannot connect different $\theta$-vacua and for $\theta' = \theta$ there are infinitely many "starting points" $A_{(\nu)}$ for the instanton transition reflected by $\delta(0)$. Most importantly, however, the phase factor $\sum_{\nu\,\in\,\mathbb{Z}} e^{i(\nu'-\nu)\theta}\delta_{\nu'-\nu,n} = e^{in\theta}$ was absorbed into the action by adding the $\theta$-term $-i\theta q = -\frac{i\theta}{16\pi^2}\mathrm{tr}\big(\widetilde{G}^{\mu\nu}_{n\text{-inst}}G^{\mu\nu}_{n\text{-inst}}\big)$ (2.4.19) to the Lagrangian. Therefore, the non-trivial QCD vacuum structure described by the $\theta$-vacuum enforces the addition of the $\theta$-term to Lagrangian. This is the reason why it was called "naive" to discard the $\theta$-term in section 2.1: it does not contribute perturbatively or in the equation of motion, but instantons are non-perturbative effects which necessitate the addition of this term to the action.[40]

---

[40] [8, 38]

It is also important to note that while the “naive” QCD action is shifted from acting as a phase factor in real time $t$ to an exponential damping factor in Euclidean spacetime with imaginary time $\bar{t}$, the $\theta$ - term is covariant under the Wick rotation and thus remains oscillatory. The reason for this is the Levi - Civita symbol in the dual field strength. In Minkowski spacetime, the corresponding term is $\int_{\mathbb{R}^{1,3}} \mathrm{d}^4\chi \, \frac{1}{2} \varepsilon_{\mu_\mathrm{M}\nu_\mathrm{M}\rho_\mathrm{M}\sigma_\mathrm{M}} G^{\rho_\mathrm{M}\sigma_\mathrm{M}} G^{\mu_\mathrm{M}\nu_\mathrm{M}}$ and due to the $\varepsilon$ - tensor every index $0_\mathrm{M}, \{i_\mathrm{M}\}$ can always only appear once, i.e., the integrand is $2\, G^{1_\mathrm{M}2_\mathrm{M}} G^{3_\mathrm{M}0_\mathrm{M}} +$ permutations (note $\varepsilon_{1_\mathrm{M}2_\mathrm{M}3_\mathrm{M}0_\mathrm{M}} = 1$ and the factor $\frac{1}{2}$ is canceled due to the anti-symmetry of both $\varepsilon$ and $G$). Wick rotation yields $i\, G^{12} G^{34} +$ permutations and the factor $i$ combines with the factor $-i$ from Wick rotating the temporal measure $\mathrm{d}t \to -i\, \mathrm{d}\bar{t}$. Therefore, adding the $\theta$ - term in imaginary time equals to adding the same term in real time. [140]

We do not introduce the dilute gas approximation (DGA) for instantons at $T = 0$ and instead postpone it to section 2.4.4, where it is discussed in the context of finite - $T$ instantons, i.e., calorons. The reason for this is also discussed there.

### Topology at finite Temperature

After the above introduction to topology and instantons at finite temperatures, we now generalize to finite temperatures described by the spacetime $\mathbb{R}^3 \times S^1_{\mathrm{rad.} = \beta/2\pi}$ (cf. (2.2.23)). The intricacies of thermal $SU(N)$ - gauge theory topology are discussed at length in [54], which serves as the source for the following. It is shown that the topological charge (2.4.19) is no longer automatically quantized at finite $T$, but can instead take any value. In detail, it is given by

$$n = \frac{1}{16\pi^2} \mathrm{Tr}\big(\widetilde{G}^{\mu\nu} G^{\mu\nu}\big) = n' + \frac{1}{4\pi^2} \int_{\partial\mathbb{R}^3} \mathrm{d}^2\varphi \, n^i \mathrm{tr}\big(\ln(\Omega) B^i\big) = n' + \sum_{\alpha=0}^{\kappa} \frac{\ln(\lambda_\alpha^\infty)}{2\pi i} q_\alpha \, . \tag{2.4.35}$$

Here $n' \in \mathbb{Z}$ is the usual Pontryagin index (2.4.18), $\Omega(\vec{X})$ is the untraced Polyakov loop (2.2.29) and $\vec{B}$ is the chromo - magnetic field. The $\lambda_\alpha^\infty$, $\alpha = 1, \dots, \kappa$ are the gauge - invariant asymptotic, non - degenerate polyakov loop - eigenvalues at spatial infinity and the integers $q_\alpha = \frac{1}{4\pi\, i} \int_{\partial\mathbb{R}^3} \mathrm{d}^2\varphi \, n^i \, \mathrm{tr}(\mathrm{P}_\alpha B^i) \in \mathbb{Z}$ are the quantized chromo - magnetic fluxes; the $\mathrm{P}_\alpha$ are projectors onto the $\mathbb{R}^3 \times S^1_{\mathrm{rad.} = \beta/2\pi}$ - subspaces spanned by the $\lambda_\alpha^\infty$ - eigenvectors.

Actually, the $\Omega$ - eigenvalues $\lambda_{\alpha\, j}(X)$ have multiplicities $j = 1, \dots, m_\alpha$ and the $\mathrm{P}_\alpha$ project on the subspace spanned by the eigenvectors associated to these degenerate eigenvalues, but as $R \to \infty$, the eigenvalue degeneracy vanishes as $\lim_{R \to \infty} \lambda_{\alpha\, j} = \lambda_\alpha^\infty + \mathcal{O}(R^{-1/2})$ so that the Polyakov loop reads $\lim_{R \to \infty} \Omega(\vec{X}) = V(\vec{X}) \mathrm{diag}(\lambda_\alpha^\infty) V^{-1}(\vec{X}) + \mathcal{O}(R^{-1/2})$ with $V \in \frac{SU(N)}{G^\infty}$ and $G^\infty = U(1)^{\kappa+1} \otimes \prod_{\alpha=0}^{\kappa} SU(m_\alpha)$ the isotropy group of $\mathrm{diag}(\lambda_\alpha^\infty)$.

The Polyakov loop therefore provides a map $\partial\mathbb{R}^3 = S^2_\infty \to \frac{SU(N)}{G^\infty}$. Analogously to the maps $S^3_\infty \to SU(2)$ discussed for the gluon vacua, such maps form a homotopy group $\pi_2(SU(N)/G^\infty) = \pi_1(G^\infty) \cong \mathbb{Z}^{\kappa+1}$ and the $q_\alpha$ can be interpreted as the corresponding winding numbers.

For vacuum configurations the chromo - magnetic flux vanishes $q_\alpha = 0\ \forall\alpha$ and the $\lambda^\infty_\alpha$ distinguish gauge inequivalent vacua. We limit ourselves to the simplest choice $\mathrm{diag}(\lambda^\infty_\alpha) = \lim_{R\to\infty} \exp\big(\beta A^0(X)\big) = \mathbb{1}$. The reason is that for instantons at finite temperature, i.e., field configurations with $n' \neq 0$ and $q_\alpha = 0$, it turns out that only those with $\mathrm{diag}(\lambda^\infty_\alpha) = \mathbb{1}$ contribute to the partition function. Therefore, in the following, vacuum and instanton configurations at finite temperature are described by structurally identical topological invariants as at zero temperature.

### Calorons

Instantons at finite temperature are called *calorons* and their existence was first proven in [28]. As any boson they are periodic in (bounded) time $t$ (cf. (2.2.23)) and can thus be constructed by periodically summing up infinitely many identical “time - copies” of a single $T = 0$ - instanton separated purely in time $\bar{t}$ by units of $\beta$. The resulting caloron then has the same topological charge as carried by each of the time copies. For this summation and the subsequent compactification of spacetime in the temporal direction $\mathbb{R}^4 \to \mathbb{R}^3 \times S^1_{\text{rad.}={}^{\beta}\!/_{2\pi}}$ to make sense, one requires that each member of this “infinite string of instantons” carry its topological information at its center and not at the edge of $\mathbb{R}^4$, i.e., the summed up instantons have to be in singular gauge and the resulting caloron is as well. This procedure is illustrated in figure 2.11.[41]

The simplest such caloron with topological charge $n = \pm 1$ is called the *Harrington - Shepard* (HS) *(anti-)caloron* [147] and is constructed by summing up infinitely many singular gauge - BPST (anti-)instantons (2.4.27) according to (2.4.30) with $\rho_j = \rho$ and $C_j = C + j\beta\hat{e}_4$, $j \in \mathbb{Z}$. This sum can be performed and reads

$$\begin{aligned} 1 + \sum_{j\in\mathbb{Z}} \frac{\rho^2}{\big(X - (\vec{C}, C^4 + j\beta)\big)^2} &= \\ &= 1 + \frac{\pi\rho^2 \sinh(2\frac{\pi}{\beta}|\vec{X} - \vec{C}\,|)}{\beta\,|\vec{X} - \vec{C}\,|\big(\cosh(2\frac{\pi}{\beta}|\vec{X} - \vec{C}\,|) - \cos(2\frac{\pi}{\beta}(t - C^4)\big)} = \phi(X)\,. \qquad (2.4.36) \end{aligned}$$

Using the multi - BPST instanton form (2.4.30) together with (2.4.36) then yields the HS caloron of size $\rho$ centered at $C$:

---

[41] [54]

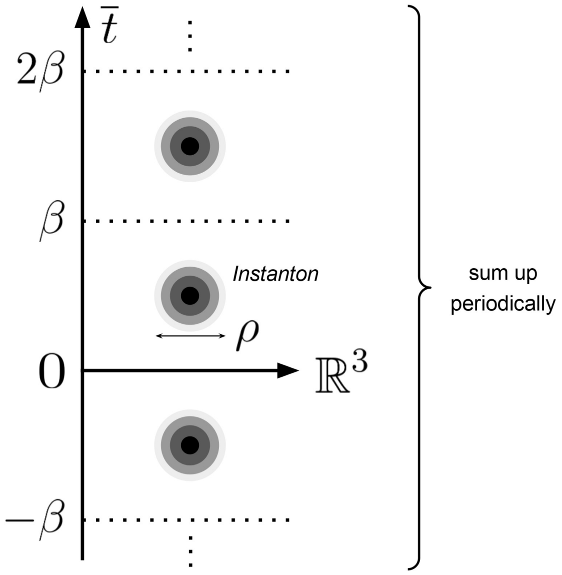
$\bar{t}$
$2\beta$
$\beta$
$0$
$-\beta$
Instanton
$\rho$
$\mathbb{R}^3$
sum up periodically

Figure 2.11: A caloron made up of an infinite sum of periodic instanton copies in the temporal direction. The instanton copies have identical properties and are separated in the $\bar{t}$ - direction of $\mathbb{R}^4$ by units of $\beta$. This summation yields an overall temporal $\beta$ - periodicity of the caloron, therefore essentially compactifying the spacetime $\mathbb{R}^4 \to \mathbb{R}^3 \times S^1_{\text{rad.}=\beta/2\pi}$.

$$A^{\mu}_{\text{HS}}(X) = -\bar{\eta}^{a\mu\nu}\partial^{\nu}\ln\big(\phi(X)\big)\frac{\sigma^a}{2} = A^{a\,\mu}_{\text{HS}}\,\frac{\sigma^a}{2} \tag{2.4.37}$$

and analogously with $\eta^{a\mu\nu}$ for the HS anti-caloron. The HS caloron is singular at its center and covariant under spatial rotations $SO(3) \subset SO(4)$. The singularity can for example be seen in $A^{2\,x}_{\text{HS}} = -\frac{\pi\rho^2(Z-C^z)\left(2\pi R\cosh(2\frac{\pi}{\beta}R)-2\pi\beta\sinh(2\frac{\pi}{\beta}R)\right)\left(\cosh(2\frac{\pi}{\beta}R)-\cos(2\frac{\pi}{\beta}t)\right)-2\pi R\sinh^2(2\frac{\pi}{\beta}R)}{\beta R^3\left(\cosh\left(\frac{2\pi R}{\beta}\right)-\cos\left(\frac{2\pi\tau}{\beta}\right)\right)\phi(X)}$: for $R = |\vec{X}-\vec{C}| \searrow 0$ it diverges as $R^{-1}$. The dependency on the coordinate $Z$ breaks rotational invariance, but, by the same reasoning founded on (anti-)'t Hooft symbol - based $SO(4)$ - generators as was discussed below (2.4.26), the caloron is again covariant under spatial rotations (since $\phi(X)$ is $SO(4)$ - invariant and $\partial^{\nu}$ transforms as a vector). The full $SO(4)$ - covariance is broken only by the boundedness of $t$. By design, the HS (anti-)caloron satisfies the (anti - )self - duality condition (2.4.22) as well as the equation of motion and has a classical YM action of $S_{\text{YM}}[A_{\text{(anti-)HS}}] = \pm\frac{8\pi^2}{g^2}$ (cf. (2.4.23)). Furthermore, as we stated in our discussion on topology at finite $T$, the caloron winding number is given by the same term $n = \frac{1}{16\pi^2}\text{Tr}\big(\widetilde{G}^{\mu\nu}G^{\mu\nu}\big)$ as for instantons. Finally, since $A_{\text{HS}} = A_{\text{HS},\,\mathfrak{su}(2)}$ like the BPST instanton or the vacuum configurations determined by the maps (2.4.16), the full $\mathfrak{su}(N)$ - configuration is again given by an embedding analogous to (2.4.13):[42]

$$A_{\text{HS},\,\mathfrak{su}(N)} = \left(\begin{array}{c|c} A_{\text{HS}} & 0_{2\times(N-2)} \\ \hline 0_{(N-2)\times 2} & 0_{(N-2)\times(N-2)} \end{array}\right). \tag{2.4.38}$$

In the limit of small distances $|(\vec{X},t)| \ll \beta$ the HS caloron takes the form of a BPST instanton in singular gauge

$$A^{\mu}_{\text{HS}} \overset{|X|\ll\beta}{\cong} \bar{\eta}^{a\mu\nu}\frac{2\tilde{\rho}^2}{(X-C)^2}\frac{(X-C)^{\nu}}{(X-C)^2+\tilde{\rho}^2}\frac{\sigma^a}{2}\Big(1+\mathcal{O}\big((|X|/\beta)^4\big)\Big) \tag{2.4.39}$$

(cf. (2.4.27)) with modified, reduced size

$$\tilde{\rho} = \frac{\rho}{\sqrt{1+\frac{\pi^2\rho^2}{3\beta^2}}}\,. \tag{2.4.40}$$

The same is true for the HS anti-caloron and BPST anti-instanton given in (2.4.28)). This means that on length scales much smaller than the temperature/periodicity scale the caloron is identical to an instanton with modified size $\tilde{\rho}$ and the actual $\beta$ periodicity is concealed in the far distance [43].

---

[42] [54, 140]

[43] [54]

The resulting field strength component $G^{\mu\nu}(A_{\text{HS}})$ is not rotationally invariant, either, but, as was noted below (2.4.27), the the $A_{\text{HS}}$ - singularity is now “only” a discontinuity at the caloron center $C$. Both of these properties are illustrated in figure 2.12 for the example of the $G^{1\,xy}$ - component. Note, however, that actual observables constructed from the field strength do turn out to be invariant under spatial rotations, as we are going to use repeatedly in the numerical integrations of section 3.1.3 and as we discuss in some more appendix 3.3.

Finally, note that, as temperature increases, calorons as tunneling solutions eventually become the subdominant topological transition process since eventually the mean thermal energy becomes comparable to the potential barrier between different vacuum sectors $A_{(\nu)}$ and $A_{(\nu')}$. This allows for real time topological transitions, so called sphalerons, to occur due to thermal fluctuations and dominate the tunneling transitions.[44]

### 2.4.3 Caloron Density with massive Quarks

After having discussed instantons and calorons at length in the two preceding sections 2.4.1 and 2.4.2, we now show how one proceeds to perform the quantization of a theory with massive quarks at finite temperature and a classical HS caloron background using the background field method as described in section 2.4.2. In detail, we show how one calculates the partition function up to second order in quantum fluctuations and thus obtains the caloron density function.

#### Caloron Density from the Partition Function

The caloron density $\mathcal{D}$ is a way of expressing the regularized, vacuum - normalized caloron partition function as

$$Z = \beta V\, \mathcal{D} + \mathcal{O}\big((\text{quantum fluctuations})^2\big) \tag{2.4.41}$$

up to 1 - loop order in the quantum fluctuations of the gluonic and matter fields. $\beta V$ is the volume of $\mathbb{R}^3 \times S^1_{\text{rad.}={}^{\beta}/_{2\pi}}$. Compare this to the instanton density in (2.4.7) for the toy model. The caloron density depends, as we show in the following, on the temperature, the strong interaction coupling strength, the regularization energy scale, the types and numbers of fields and their masses as well as the representation of the gauge group under which they transform.[45]

---

[44] [148, 149]

[45] [8, 33, 54, 132, 141]

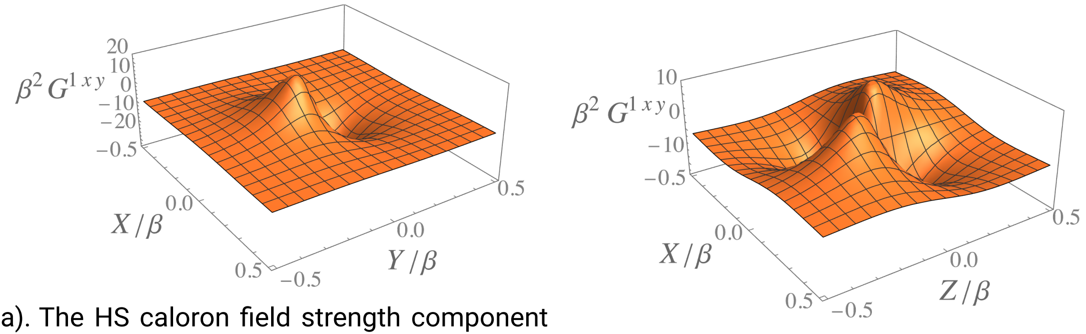

(a). The HS caloron field strength component $G^{1\,xy}(\rho = \frac{\beta}{2}, x, y, 0, t = \frac{\beta}{10})$.

(b). $G^{1\,xy}(\rho = \frac{\beta}{2}, x, 0, z, t = \frac{\beta}{10})$

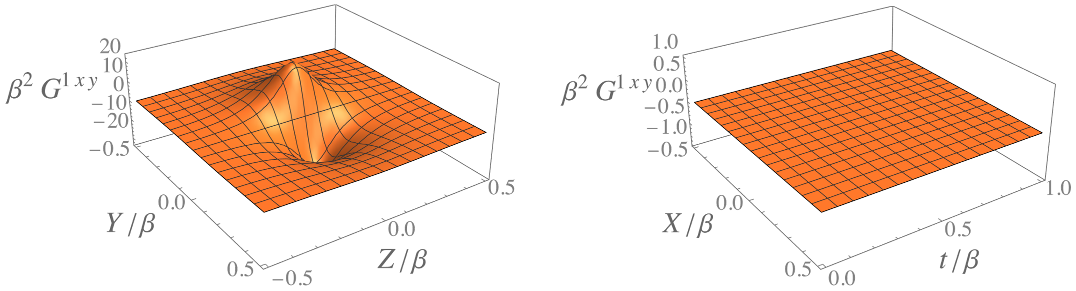

(c). $G^{1\,xy}(\rho = \frac{\beta}{2}, 0, y, z, t = \frac{\beta}{10})$

(d). $G^{1\,xy}(\rho = \frac{\beta}{2}, x, 0, 0, t)$

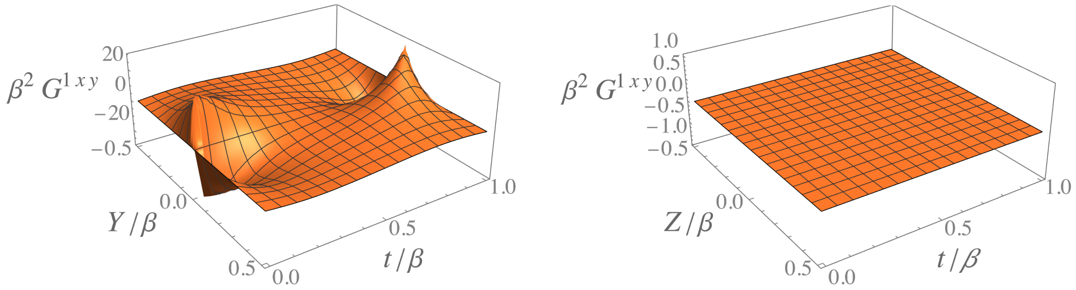

(e). $G^{1\,xy}(\rho = \frac{\beta}{2}, 0, y, 0, t)$

(f). $G^{1\,xy}(\rho = \frac{\beta}{2}, 0, 0, z, t)$

Figure 2.12: The HS caloron field strength component $G^{1\,xy}(\rho, X)$ in different planes of $\mathbb{R}^3 \times S^1_{\text{rad.}=\beta/2\pi}$ (here we set the caloron center to $C = 0$). If the field strength were rotationally invariant, figures 2.12a, 2.12b and 2.12c would be equal as well as figures 2.12d, 2.12e and 2.12f.

For a general discussion we therefore extend Euclidean QCD and consider a theory containing not only $N_f$ quarks $\psi_f$ and an $\mathfrak{su}(N)$ - gauge field $A^\mu$, but also $N_\phi$ real and $N_\varphi$ complex scalar fields, $\phi_i$ and $\varphi_j$, respectively. The real scalar fields are uncharged and therefore transform trivially under gauge rotations ($T_{SU(N),\,\text{triv}} = 0$), while the complex scalars can be taken to be composite objects containing numerous charged multiplets such that they form arbitrary representations of $SU(N)$ (compare [141]). We use a HS caloron with $n = 1$ (2.4.38) as a classical gauge field background for this extended theory and show how one obtains the important caloron density function $\mathcal{D}$ for this theory (following the notion of the temporal instanton density (2.4.7) discussed in section 2.4.1).

As we stated in section 2.4.2, the caloron is a solution to the classical equations of motion and thus describes a saddle point of the Euclidean YM action at finite temperature. Following the background field method analogously to the steps from (2.4.3) to (2.4.4), one considers a perturbative expansion, i.e., a saddle point approximation using Laplace's method, of the above theory in the caloron background, rewrites the partition function in terms of caloron - dependent differential operator determinants and calculates those. The gauge field then has the form $A^\mu = A^\mu_{\text{HS},\,\mathfrak{su}(N)} + A^\mu_{\text{qm}}$ and the scalar and fermion fields, having no classical background, are purely quantum/infinitesimal $\phi_i, \varphi_j, \psi_f = \phi_{i\,\text{qm}}, \varphi_{j\,\text{qm}}, \psi_{f\,\text{qm}}$. Additionally, the background gauge condition

$$\mathcal{G}_{\text{background}}(A^\mu_{\text{qm}}) = D^\mu(A^\mu_{\text{HS},\,\mathfrak{su}(N)})A^\mu_{\text{qm}} = 0 \tag{2.4.42}$$

is enforced, which means adding a pair of Faddeev - Popov ghosts $c, \bar{c} = c_{\text{qm}}, \bar{c}_{\text{qm}}$ to the theory (cf. (2.2.15) - (2.2.17)). These ghosts form an adjoint representation of $SU(N)$. As we stated, all interactions $\mathcal{O}(\phi_i, \varphi_j, \psi_f, A^\mu_{\text{qm}})^3$ are neglected in this approximation, i.e., one performs a 1st - order non-linear approximation of the full Lagrangian (2.2.26) up to 1 - loop level. All in all, the Lagrangian is:

$$\begin{aligned} \mathcal{L} + \mathcal{L}_\theta = \mathcal{L}_{\text{YM}}(A_{\text{HS}}) + \sum_{i,j,f} \frac{1}{2}\phi_i \mathfrak{M}_\phi(i)\phi_i + \varphi_j^* \mathfrak{M}_\varphi(j)\varphi_j + \bar{\psi}_f \mathfrak{M}_\psi(f)\psi_f + \\ + \frac{1}{2g^2}\text{tr}\big(A^\mu_{\text{qm}} \mathfrak{M}_A^{\mu\nu} A^\nu_{\text{qm}}\big) + \frac{1}{N}\text{tr}\big(\bar{c}\,\mathfrak{M}_{\text{gh}} c\big) - \frac{i\theta}{16\pi^2}\text{tr}\big(\widetilde{G}^{\mu\nu}G^{\mu\nu}\big)\,, \end{aligned} \tag{2.4.43}$$

with $\mathcal{L}_\theta = -i\theta q(x)$ (cf. (2.4.19)) and the differential operators

- $\mathfrak{M}_\phi(i) = -\partial_+^2 + M^2_{\phi_i}\,,$ (2.4.43.a)
- $\mathfrak{M}_\varphi(j) = -D^2_{+,\,\text{arb}}\big(A^\mu_{\text{HS},\,\mathfrak{su}(N)}\big) + M^2_{\varphi_j}\,,$ (2.4.43.b)
- $\mathfrak{M}_\psi(f) = i\not{D}_{\text{fund}}\big(A^\mu_{\text{HS},\,\mathfrak{su}(N)}\big) + M_{\psi_f} = i\not{D}(A_{\text{HS}}) + M_{\psi_f}\,,$ (2.4.43.c)

- $\mathfrak{M}_A^{\mu\nu} = \Big( - D_+^2 \big(A^\mu_{\text{HS},\, \mathfrak{su}(N)}\big)\delta^{\mu\nu} - 2G^{\mu\nu}_{\mathfrak{su}(N)}\Big)_{\text{adj}}$ (2.4.43.d)
- $\mathfrak{M}_{\text{gh}} = -D^2_{+,\,\text{adj}}\big(A^\mu_{\text{HS},\, \mathfrak{su}(N)}\big)\,,$ (2.4.43.e)

where the subscripts "$+/-$" denote $\beta$ - periodicity/anti-periodicity of the respective fields, the subscripts "arb", "fund" and "adj" denote the arbitrary, fundamental/defining and adjoint representation of $SU(2)$ (embedded in $SU(N)$), respectively, and the factor $\frac{1}{N}$ compensates the Dynkin index of the $SU(N)$ - adjoint representation (cf. (2.2.20)). In the following, $D$ is always to be read as $D(A_{\text{HS}})$. The partition function (neither normalized by a vacuum background $A_{\text{vac. background}} = 0$ nor renormalized) is given by

$$Z_{\text{HS}}(\theta) = e^{-\frac{8\pi^2}{g^2}+i\theta} \int \mathscr{D}[\phi_i, \varphi_j^*, \varphi_j, \overline{\psi}_f, \psi_f, A^\mu_{\text{qm}}, \bar{c}, c]\, e^{-\int^\beta \mathrm{d}^4X\,\mathcal{L}}\,, \tag{2.4.44}$$

where $S_{\text{YM}}[A_{\text{HS}}]$ was plugged in according to (2.4.23) and (2.4.19) was used. When referring to the above operators (2.4.43.a) - (2.4.43.e) in a vacuum background, we denote them with an additional subscript "0": $\mathfrak{M}_{\phi,\,\varphi,\,\psi,\,A,\,\text{gh},\,0}$. The caloron density is then given via $Z_{\text{HS}} = e^{i\theta}\,\beta V\,\mathcal{D}$.[46]

### Laplace's Method and Caloron Zero Modes

Following the procedure for the instanton toy model in section 2.4.1, one expands the quantum fields in bosonic eigenfunctions $\chi(X)$ of their corresponding $\mathfrak{M}$ - operators, $\phi_i(X) = \xi^\alpha_{\phi_i}\chi^\alpha_{\phi_i}$, $A^\mu(X) = \xi^\alpha_A \chi_A^{\alpha\,\mu}$, etc., with (c - number/Graßmannian) expansion coefficients $\xi^\alpha$, and eigenvalues $\lambda^\alpha$: $\mathfrak{M}\chi^\alpha = \lambda^\alpha\chi^\alpha$. The eigenfunctions are chosen orthogonal with respect to the inner product $\langle\chi^\alpha_{\phi_i}|\chi^\beta_{\phi_i}\rangle = \frac{1}{I(\phi_i)}\mathrm{Tr}\big(\chi^\alpha_{\phi_i}(X)\chi^\beta_{\phi_i}(X)\big) = u^\alpha_{\phi_i}\delta^{\alpha\beta}$, $\langle\chi_A^{\alpha\,\mu}|\chi_A^{\beta\,\mu}\rangle = \frac{1}{I(A)g^2}\mathrm{Tr}\big(\chi_A^{\alpha\,\mu}(X)\chi_A^{\beta\,\mu}(X)\big) = u^\alpha_A\delta^{\alpha\beta}$, etc., with $I$ the Dynkin index of the respective representation, e.g., $I(\text{def}) = I(A) = \frac{1}{2}$. Now the path integral functional measures can be rewritten as $\mathscr{D}\phi_i = \prod_\alpha \left(\frac{u^\alpha_{\phi_i}}{2\pi}\right)^{1/2} \mathrm{d}\xi^\alpha_{\phi_i}$, etc. (for the bosonic fields) and $\mathscr{D}\psi_f = \prod_\alpha \left(u^\alpha_{\psi_f}\right)^{-1/2}\mathrm{d}\xi^\alpha_{\psi_f}$, etc. (for the fermionic/Graßmannian fields).[47]

As in section 2.4.1, zero modes $Z^{\alpha_0} = \chi^{\alpha_0}$ with $\lambda'^{\alpha_0} = 0$ again need to be treated separately. Zero modes can only appear for $\mathfrak{M}_A$. To see this, consider the individual differential operators:

---

[46] [54, 140, 141, 150]
[47] [140]

**Scalar fields $\phi$, $\varphi$ and ghosts $c$:**
Just as the 4-dimensional Laplacian $-\partial_\pm^2$, $-D_\pm^2$ is also a positive operator [151, 152] and $M^2 > 0$, so that $\mathfrak{M}_{\phi,\,\varphi,\,\mathrm{gh}}$ cannot have zero eigenvalues.

**Quarks $\psi$:**
In an (anti-)self-dual background, $\mathfrak{M}_\psi$ and $-D_-^2 + M^2$ are isospectral, i.e., one can recast $\det \mathfrak{M}_\psi = \det(i\not{D} + M)$ in terms of $\det(-D_-^2 + M^2)$ and an exponential factor depending on the number of zero modes of $i\not{D}$. According to the above, the subscript "$-$" in $\det(-D_-^2 + M^2)$ means that the determinant is to be calculated with respect to only the anti-periodic eigenfunctions. An analogous transformation links $\det \mathfrak{M}_{\psi,\,0} = \det(i\not{\partial} + M)$ and $\det(-\partial_-^2 + M^2)$. By the same logic as for the scalar and ghost fields, $\mathfrak{M}_\psi$ then has no zero modes. We show this in three steps.

First, we use that $i\not{D} + c$, $c \in \mathbb{R}$ is self-adjoint with respect to the fermionic inner product, $(\psi(X), \psi'(X)) = \int_0^\beta \mathrm{d}t \int_{\mathbb{R}^3} \mathrm{d}^3X\, \overline{\psi}(X)\psi'(X) = \int^\beta \mathrm{d}^4X\, \psi^\dagger(X)\gamma^4\psi'(X)$, i.e.,

$$\begin{aligned}(i\not{D}\psi, \psi') &= \int^\beta \mathrm{d}^4X\, (\overline{i\not{D}\psi})\psi' = -\int^\beta \mathrm{d}^4X\, i\psi^\dagger D^{\mu\,\dagger}\gamma^{\mu\,\dagger}\gamma^4\psi' = \\ &= \int^\beta \mathrm{d}^4X\, i\psi^\dagger \begin{pmatrix} -\vec{D} \\ D^4 \end{pmatrix} \cdot \begin{pmatrix} \vec{\gamma}\,\gamma^4 \\ \gamma^4\gamma^4 \end{pmatrix} \psi' = \int^\beta \mathrm{d}^4X\, i\psi^\dagger \begin{pmatrix} -\vec{D} \\ D^4 \end{pmatrix} \cdot \begin{pmatrix} -\gamma^4\vec{\gamma} \\ \gamma^4\gamma^4 \end{pmatrix} \psi' = \\ &= \int^\beta \mathrm{d}^4X\, \overline{\psi} i\not{D}\psi' = (\psi, i\not{D}\psi')\,.\end{aligned} \tag{2.4.45}$$

Here, $\gamma^{\mu\,\dagger} = -\gamma^\mu$ and the anti-Hermiticity of the derivative in Minkowski spacetime $\partial_{\mu_\mathrm{M}}^\dagger = -\partial_{\mu_\mathrm{M}}$ (given that boundary terms do not contribute) were used. Two fermion fields, each $\beta$-anti-periodic, are again periodic and thus the boundary terms do indeed vanish. After Wick rotation of any vector $v^\mu = \begin{cases} v^{i_\mathrm{M}} \\ iv^{0_\mathrm{M}} \end{cases}$, especially $\partial^\mu$, one finds a mixed behavior of the components under Hermitian conjugation: $D^{\mu\,\dagger} = \begin{cases} -\vec{D} \\ iD^4 \end{cases}$. All in all, the determinant is therefore real: $\det(i\not{D} + M) = \det(\overline{i\not{D}} + M) = (\det(i\not{D} + M))^*$. Compare this with (2.1.16).

Second, from $\det(AB) = \det(A)\det(B)$, $(\gamma^5)^2 = \mathbb{1}$ and $\{\gamma^5, \gamma^\mu\} = 0$ it follows that

$$\det(i\not{D}+M) = \det((\gamma^5)^2(i\not{D}+M)) = \det(\gamma^5(-i\not{D}+M)\gamma^5) = \det(-i\not{D}+M)\,. \tag{2.4.46}$$

Thus, the fermionic determinants can be rewritten in terms of $\not{D}^2$ and $-\partial_-^2$:

$$\det(i\not{\partial}+M) = \sqrt{\det(i\not{\partial}+M)\det(-i\not{\partial}+M)} = \sqrt{\det(\not{\partial}^2+M^2)} = \big(\det(-\partial_-^2+M^2)\big)^2,$$
$$\det(i\not{D}+M) = \sqrt{\det(\not{D}^2+M^2)} = \sqrt{\det(-D_-^2 - \frac{i}{2}G^{\mu\nu}\gamma^\mu\gamma^\nu + M^2)}\,, \tag{2.4.47}$$

where the power of 4 (2 after the square - root) in the first line is due to the remaining $\mathbb{1}$ - matrix in Dirac space and $G^{\mu\nu} = i\,[D^\mu, D^\nu]$ was used. The operator $i\not{D}+M$ has no zero modes for finite $M > 0$ [140]. To verify that, assume $\psi_0(X)$ solves $(i\not{D}+M)\psi_0 = 0$ and act from the left with $(i\not{D}+M)\mathrm{P}_{\mathrm{R,L}}$ (c.f. (2.1.8)) for a $\begin{pmatrix}\text{self - dual (R)}\\ \text{anti - self - dual (L)}\end{pmatrix}$ caloron. Now anti-commute the right $(i\not{D}+M)$ to the left past $\mathrm{P}_{\mathrm{R,L}}$ to find $(\not{D}^2+M^2)\mathrm{P}_{\mathrm{R,L}}\psi_0 = 0$ and use that, for (anti-)self - dual field strengths, $\not{D}^2\mathrm{P}_{\mathrm{R,L}} = -D_-^2\mathrm{P}_{\mathrm{R,L}}$ [152, 153]. The resulting equation $(-D_-^2+M^2)\mathrm{P}_{\mathrm{R,L}}\psi_0 = 0$ has no solution. Either $(-D_-^2+M^2)\psi_0$ would have to yield 0, but, again, $-D_-^2$ is a positive operator and $M^2 > 0$, or one would require $\mathrm{P}_{\mathrm{R,L}}\psi_0 = 0$, but the eigenfunctions of $(i\not{D}+M)$ have no defined chirality, since $\{i\not{D}+M, \gamma^5\} \neq 0$. Thus, there can only be zero modes for $M = 0$. Then the eigenfunctions come in chirality pairs (as $\{i\not{D}, \gamma^5\} = 0$) and the zero modes have $\begin{pmatrix}\text{negative (L)}\\ \text{positive (R)}\end{pmatrix}$ chirality for $\begin{pmatrix}\text{self - dual}\\ \text{anti - self - dual}\end{pmatrix}$ caloron fields, i.e, they satisfy $\mathrm{P}_{\mathrm{R,L}}\psi_0^{\mathrm{L,R}} = 0$ [152, 153].

Third, the $G^{\mu\nu}$ - term can be dropped from the expression for $\det(\not{D}^2+M^2)$, i.e., the spin - dependency can be eliminated and $i\not{D}+M$ and $-D_-^2+M^2$ are isospectral [61]. We prove that using Jacobi's formula for the determinant of some matrix/operator $\mathcal{A}(s)$: $\mathrm{d}_s\det(\mathcal{A}(s)) = \det(\mathcal{A}(s))\,\mathrm{tr}\big(\mathcal{A}^{-1}(s)\,\mathrm{d}_s\mathcal{A}(s)\big)$. For the operator $\not{D}^2+M^2$ with parameter $M^2$ this means

$$\frac{\mathrm{d}}{\mathrm{d}M^2}\det(\not{D}^2+M^2) = \det(\not{D}^2+M^2)\,\mathrm{Tr}\left(\frac{1}{\not{D}^2+M^2}\right), \tag{2.4.48}$$

where $\mathrm{Tr}(\cdot)$ again denotes the operator trace $\int^\beta \mathrm{d}^4X\,\mathrm{tr}_{\text{Dirac, color(, etc.)}}\big(\langle X\,|\,(\;\cdot\;)\,|\,X\rangle\big)$. In [153] one finds the following expansion for the propagator of a massive fermion in a self - dual gauge field background:

$$\frac{1}{\not{D}^2+M^2} = \frac{1}{-D_-^2+M^2}\mathrm{P}_\mathrm{R} + \frac{1}{M^2}\left(\mathbb{1} - \not{D}\frac{1}{-D_-^2+M^2}\not{D}\right)\mathrm{P}_\mathrm{L}\,. \tag{2.4.49}$$

Compare the part in brackets of the second term with the projection operator into the subspace of $i\not{D}$ - zero modes, $\mathrm{P}_{\text{z. m.}} = \big(1 - \not{D}\frac{1}{-D_-^2}\not{D}\big)\mathrm{P}_\mathrm{R}$, found in [152, 153]. Expanding

$\frac{1}{-D_-^2+M^2} = \frac{1}{-D_-^2} - \frac{M^2}{-D_-^2(-D_-^2+M^2)}$, we can isolate this projector:

$$\frac{1}{\not{D}^2 + M^2} = \frac{1}{-D_-^2 + M^2}\mathrm{P_R} + \not{D}\frac{1}{-D_-^2(-D_-^2 + M^2)}\not{D}\,\mathrm{P_L} + \frac{\mathrm{P_{z.\,m.}}}{M^2}\,. \tag{2.4.50}$$

Finally, using the identities $\mathrm{tr_{Dirac}}(\gamma^\mu\gamma^\nu) = -4\delta^{\mu\nu}$, $\mathrm{tr_{Dirac}}(\gamma^5) = \mathrm{tr_{Dirac}}(\gamma^\mu\gamma^\nu\gamma^5) = 0$ and $\mathrm{tr}(\mathrm{P_{z.\,m.}}) = \mathrm{rank}(\mathrm{P_{z.\,m.}}) = \#(i\not{D}$ - zero modes$) = n_f$, we find for the trace in (2.4.48)

$$\mathrm{Tr}\left(\frac{1}{\not{D}^2 + M^2}\right) = 4\,\mathrm{Tr}\left(\frac{1}{-D_-^2 + M^2}\right) + \frac{n_f}{M^2}\,. \tag{2.4.51}$$

Solving the resulting differential equation for $\det(\not{D}^2 + M^2)$,

$$\frac{\mathrm{d}}{\mathrm{d}M^2}\det(\not{D}^2 + M^2) = \det(\not{D}^2 + M^2)\left(4\,\mathrm{Tr}\left(\frac{1}{-D_-^2 + M^2}\right) + \frac{n_f}{M^2}\right), \tag{2.4.52}$$

by separation of variables gives the desired overall result [60, 154]:

$$\begin{aligned} &\ln\det(\not{D}^2 + M^2) = 4\,\mathrm{Tr}\ln(-D_-^2 + M^2) + n_f\ln(M^2) = 4\ln\det(-D_-^2 + M^2) + \ln(M^{2n_f}) \\ \Leftrightarrow\quad &\det\mathfrak{M}_\psi(f) = \det(i\not{D} + M) = M^{n_f}\left(\det(-D_-^2 + M^2)\right)^2\,. \end{aligned} \tag{2.4.53}$$

Let's assume an additional integration constant $c$ appearing in the integration of the separation of variables - process. On the one hand, the same considerations with the identical integration constant $c$ hold for the vacuum case $A = 0$, since both $\int \mathrm{d}(\det)$ and $\int \mathrm{d}M^2$ work analogously ($-D_-^2 + M^2$ and $-\partial_-^2 + M^2$ have the same $M^2$ - dependency). On the other hand, $\det(\not{\partial}^2 + M^2)) = \left(\det(-\partial_-^2 + M^2)\right)^4$. Thus, we conclude that $c = 0$.[48]

It turns out that the number $n_f$ of $i\not{D}$ - zero modes is also determined by the caloron background. Expand the massless quark field $\psi = \xi_j\chi_j$, $\overline{\psi} = \bar{\xi}_j\chi_j^\dagger$ in a basis $\{\chi_j(X)\}$ of orthonormal $i\not{D}$ - eigenspinors, i.e., $i\not{D}\chi_j = \lambda_j\chi_j\,,\ (i\not{D}\chi_j)^\dagger = \chi_j^\dagger(-i\overleftarrow{\not{D}}) = \lambda_j\chi_j^\dagger$ and $\int^\beta \mathrm{d}^4X\,\chi_j^\dagger\chi_k = \delta_{jk}$, together with Graßmannian expansion coefficients $\xi_j$. A lengthy and very technical calculation involving the regularization of the infinite sum $\chi_j^\dagger\gamma^5\chi_j$ (see for example [3, 130]) shows that the caloron topological charge can be written as $n = -\int^\beta \mathrm{d}^4X\,\chi_j^\dagger\gamma^5\chi_j$ [151, 155]. Using $\gamma^5 = \mathrm{P_R} - \mathrm{P_L} = \mathrm{P_R^2} - \mathrm{P_L^2}$ (cf. (2.1.8)), $\chi_j^\dagger\gamma^5\chi_j$ can be written in terms of the right-/left - chiral 2 - spinors $\chi_{j\,\mathrm{R,L}}$ as $\chi_j^\dagger\gamma^5\chi_j = \chi_{j\,\mathrm{R}}^\dagger\chi_{j\,\mathrm{R}} - \chi_{j\,\mathrm{L}}^\dagger\chi_{j\,\mathrm{L}}$. Performing the $\int^\beta \mathrm{d}^4X$ - integral of these spinor products amounts to computing the scalar product of the Weyl spinor fields $(\chi_{j\,\mathrm{R,L}},\chi_{j\,\mathrm{R,L}}) = \int^{\beta}\mathrm{d}^4X\,\chi^{\dagger}_{j\,\mathrm{R,L}}\chi_{j\,\mathrm{R,L}}$ and since $\chi_{j\,\mathrm{R}}$ and $\chi_{j\,\mathrm{L}}$ are related via parity transformation, the above terms cancel except for either $\chi_{k\,\mathrm{R}} = 0$ or $\chi_{k\,\mathrm{L}} = 0$. This corresponds to 4 - spinor eigenfunctions of defined helicity $\mathrm{P}_{\mathrm{R,L}}\chi_{k,\pm} = \pm\chi_{k,\pm}$. Since $[\mathrm{P}_{\mathrm{R,L}}, i\not{D}] \neq 0$, the only $\chi_{k,\pm}$ to contribute can be zero modes with $\lambda_k = 0$. In that case, the two terms in $\int^{\beta}\mathrm{d}^4X\,\chi_j^{\dagger}\gamma^5\chi_j$ yield the number of right- and left - chiral $i\not{D}$ zero modes $n_{\mathrm{R,L}}$, respectively, and the caloron's topological charge fixes the net number of these zero modes [151, 155]:

---

[48] Any other value $c \neq 0$ would cancel anyway after regularization/normalization with the free theory, cf. (2.4.65) or (2.4.82).

$$\text{index}_{\,\text{topological}}(i\not{D}) = n = n_{\mathrm{L}} - n_{\mathrm{R}} = \text{index}_{\,\text{analytical}}(i\not{D})\,. \tag{2.4.54}$$

The relation (2.4.54) between the topological and analytical index of $i\not{D}$ is a special case of the *Atiyah - Singer index theorem* [156, 157] relating the topological and analytical indices of elliptic operators on compact manifolds (see also [135]). A caloron configuration of topological charge $n$ is thus accompanied by a net of $n_{\mathrm{L}} - n_{\mathrm{R}}$ unpaired left-/right - chiral zero modes of $i\not{D}$.

An alternative way of obtaining (2.4.54) is to note that since $\{\gamma^5, i\not{D}\} = 0$, the $\chi_j$ can be grouped in pairs $(\chi_j, \chi_{-j} = \gamma^5\chi_j)$ with opposite sign - eigenvalues $(\lambda_j, \lambda_{-j} = -\lambda_j)$. The $\chi_j$ are orthonormal by definition and thus the pairs $(\chi_j, \gamma^5\chi_j)$ are as well and do not contribute to the integrated sum except for $\lambda_k = 0$ when they share an eigenvalue.[49]

In the case of an HS (anti-)caloron with $n = \pm 1$, (2.4.54) sets $n_{\mathrm{L}} = n_{\mathrm{R}} \pm 1$ and since $i\not{D}$ in an (anti-)self - dual background has no (left - chiral) right - chiral zero modes, one finds

$$n_f \overset{\text{(anti-)self - dual background}}{=} |n| = 1\,. \tag{2.4.55}$$

All in all, $i\not{D} + m$ therefore has no zero modes and, equally importantly, it is sufficient to consider the determinants of $-D_{-}^2 + M^2$ (and $-\partial_{-}^2 + M^2$) for a (free) $\beta$ - anti-periodic scalar field in a HS caloron background field together with the zero mode of the massless Dirac operator $i\not{D}$ to calculate the fermionic contributions to the partition function.

### Gluon gauge field $A^{\mu}$:

The differential operator $\mathfrak{M}_A$ (2.4.43.d) has zero modes (as $-G^{\mu\nu}_{\mathfrak{su}(N),\,\mathrm{adj}}$ can contribute negatively). Just like in section 2.4.2, these correspond to the symmetries of the caloron and are parametrized by the corresponding collective coordinates $\gamma_A^{\alpha_0}$:

---

[49] [3, 116, 130]

- translation invariance of caloron center $\longleftrightarrow$ four collective coordinates $C^\mu$
- "dilatation symmetry" [50] $\longleftrightarrow$ collective coordinate $\rho$
- $\mathfrak{su}(2)$ - caloron $A_{\text{HS}}$ embedded in $\mathfrak{su}(N)$ - gauge field (2.4.38), i.e., $SU(N)$ - transformations can change embedded caloron or embedding itself
  - global ("rigid") $SU(2)$ - symmetry acts on caloron in on upper left corner: $A_{\text{HS}} \to U_{SU(2)}(\vec{\theta}\,)A_{\text{HS}}\, U^{-1}_{SU(2)}(\vec{\theta}\,)$
  - $SU(N-2)$ - transformations acting on "unoccupied" upper right and lower left corner leave caloron invariant, one generator ($\frac{\lambda^8}{2}$ for $SU(3)$) generates trivially commuting $U(1)$ - subgroup $\Rightarrow SU(N-2) \times U(1) \;=\;$ stability group of caloron embedding

    $\Rightarrow$ global "change of embedding symmetry" via $G = \frac{SU(N)}{SU(N-2)\times U(1)}$,

    $A_{\text{HS}} \to U_G(\vec{\vartheta}\,)A_{\text{HS}}U^{-1}_G(\vec{\vartheta}\,)$, $\dim(G) = N^2 - 1 - (N-2)^2 = 4N - 5$

  $\longleftrightarrow 4N-5$ collective coordinates $\{\Theta^A\} = \{\theta^a\}_{a\,=\,1,2,3} \cup \{\vartheta^i\}_{i\,=\,4,5,\ldots,4N-5}$

All in all, there are $4 + 1 + 4N - 5 = 4N$ zero modes $\chi^{\alpha_0\,\mu}_A$, $\alpha_0 = 1, \ldots, 4N$, for an $\mathfrak{su}(2)$ - caloron in $SU(N)$ - gauge theory, corresponding to $4N$ zero eigenvalues $\lambda^{\alpha_0}_A = 0$ and collective coordinates $\gamma^{\alpha_0}_A$. Analogously to $\mathrm{d}_{\bar{t}}\vec{\vec{X}}_{\text{cl}}$ in section 2.4.1, they are of the structure

$$\chi^{\alpha_0\,\mu}_A = Z^\mu_{\alpha_0}(X, \vec{\gamma}_A) = \frac{\partial A^\mu_{\text{HS},\,\mathfrak{su}(N)}(X, \vec{\gamma}_A)}{\partial \gamma^{\alpha_0}_A} + D^\mu \Delta_{\alpha_0}(X, \vec{\gamma}_A)\,, \tag{2.4.56}$$

where the function $\Delta_{\alpha_0}$ ensures the zero mode $Z_{\alpha_0}$ satisfy the background gauge condition (2.4.42). Unlike the $\lambda^\alpha \neq 0$ - modes, the caloron zero modes written in the form (2.4.56) are not orthogonal: $\langle Z^\mu_{\alpha_0} | Z^\mu_{\beta_0}\rangle = \frac{2}{g^2}\,\mathrm{Tr}\big(Z^\mu_{\alpha_0} Z^\mu_{\beta_0}\big) = U_{\alpha_0\beta_0}$. The factor $\frac{1}{g^2}$ in the zero mode - inner product is necessary because the Jacobian matrix $U$ can be understood as a metric in collective coordinate space and with this normalization the collective coordinate - action has the same $g^{-2}$ - prefactor as the YM action (cf. (2.1.22)).[51]

Continuity[52] fixes the integration measures for the zero mode expansion constants $\xi^{\alpha_0}_A$ analogously to the non - zero modes. Due to the non - orthogonality, the total zero mode integration measure reads $\prod_{\alpha_0} \frac{\mathrm{d}\xi^{\alpha_0}}{\sqrt{2\pi}} \sqrt{\det(U)}$. The integration over the zero modes is performed by converting the $\xi_A^{\alpha_0}$ - integrals into integrals over the known collective coordinates $\gamma_A^{\alpha_0}$. For that one inserts an identity into the $\xi_A^{\alpha_0}$ - integrals similarly to the Faddeev - Popov gauge fixing procedure (cf. (2.2.15) and (2.2.16))

---

[50] Due to the externally fixed scale $\beta$, there is no dilatation symmetry in the usual sense as for the instanton. In detail, under a rescaling $X \to cX$ one neither has $A \to c^\alpha A$, nor is the periodicity preserved. Instead, the combined transformation $X \to cX$, $\beta \to c\beta$ (constituting a scale transformation $\rho \to \frac{\rho}{c}$) yields the desired family of independent solutions and thus the collective coordinate and zero modes [158].

[51] [140, 150, 158]

[52] Infinitesimal changes to $\mathcal{L}$, e.g., the insertion of an infinitesimal mass for the gauge field, turn zero modes into non - zero modes for the calculation.

$$\begin{aligned} \mathrm{id} &= \int \prod_{\alpha_0\,=\,1}^{4N} \mathrm{d}\gamma_A^{\alpha_0}\, \delta^{(4N)}(\vec{f}(\vec{\gamma}_A)) \left|\det\left(\frac{\partial \vec{f}}{\partial \vec{\gamma}_A}\right)\right| , \\ \vec{f}(\vec{\gamma}_A) &= f_{\alpha_0}\hat{e}_{\alpha_0} = -\left\langle A^\mu_{\mathrm{qm}} \,\middle|\, Z^\mu_{\alpha_0}(\vec{\gamma}_A)\right\rangle \hat{e}_{\alpha_0} = \left\langle A^\mu_{\mathrm{HS}}(\vec{\gamma}_A) - A^\mu \,\middle|\, Z^\mu_{\alpha_0}(\vec{\gamma}\right\rangle \hat{e}_{\alpha_0} . \end{aligned} \tag{2.4.57}$$

Here $\delta^{(4N)}(\vec{f}) = \delta^{(4N)}(-U_{\beta_0\alpha_0}\xi^{\beta_0}\hat{e}_{\alpha_0}) = \delta^{(4N)}(U\vec{\xi}')$ and $\frac{\partial f_{\alpha_0}}{\partial \gamma_A^{\beta_0}}$ yields $\langle Z^\mu_{\beta_0}|Z^\mu_{\alpha_0}\rangle = U_{\beta_0\alpha_0}$ as well as a term $\mathcal{O}(A_{\mathrm{qm}})$ which first contributes at 2 - loop order, so $\det \frac{\partial \vec{f}}{\partial \vec{\gamma}_A} = \det U$. Performing the $\xi'^{\alpha_0}$ - integrals cancels the Jacobian determinant $\det U$ and the collective coordinate integrals remain. The partition function then reads

$$\begin{aligned} Z_{\mathrm{HS}}(\theta) &= e^{-\frac{8\pi^2}{g^2}+i\theta} \int \prod_{i,\,j,\,f} \prod_{\alpha} \sqrt{\frac{u^\alpha_{\phi_i}}{2\pi}\frac{u^\alpha_A}{2\pi}\frac{u^\alpha_{\varphi_j}}{2\pi}\frac{1}{u^\alpha_{\psi_f}}\frac{1}{u^\alpha_{\mathrm{gh}}}}\, \mathrm{d}\xi^\alpha_{\phi_i}\mathrm{d}\xi^{\alpha\,*}_{\varphi_j}\mathrm{d}\xi^\alpha_{\varphi_j}\mathrm{d}\bar{\xi}^\alpha_{\psi_f}\mathrm{d}\xi^\alpha_{\psi_f}\mathrm{d}\xi^\alpha_A\mathrm{d}\bar{\xi}^\alpha_{\mathrm{gh}}\mathrm{d}\xi^\alpha_{\mathrm{gh}} \times \\ &\quad \times \exp\Bigg( - \sum_{i,\,j,\,f}\sum_{\alpha}\bigg(\frac{1}{2}(\xi^\alpha_{\phi_i})^2\lambda^\alpha_{\phi_i}u^\alpha_{\phi_i} + \xi^{\alpha\,*}_{\varphi_j}\xi^\alpha_{\varphi_j}\lambda^\alpha_{\varphi_j}u^\alpha_{\varphi_j} + \bar{\xi}^\alpha_{\psi_f}\xi^\alpha_{\psi_f}\lambda^\alpha_{\psi_f}u^\alpha_{\psi_f} + \\ &\qquad + \frac{1}{2}(\xi^\alpha_A)^2\lambda^\alpha_A u^\alpha_A + \bar{\xi}^\alpha_{\mathrm{gh}}\xi^\alpha_{\mathrm{gh}}\lambda^\alpha_{\mathrm{gh}}u^\alpha_{\mathrm{gh}}\bigg)\Bigg) = \\ &= e^{-\frac{8\pi^2}{g^2}+i\theta} \prod_{i,\,j,\,f} \int \frac{\mathrm{d}\rho\,\mathrm{d}^4C\,\mathrm{d}^3\theta\,\mathrm{d}^{4N-8}\vartheta}{(\sqrt{2\pi})^{4N}} \sqrt{\det U}\big(\det \mathfrak{M}_\phi(i)\big)^{-1/2}\big(\det \mathfrak{M}_\varphi(j)\big)^{-1} \times \\ &\quad \times M_{\psi_f}\left(\det(-D_-^2 + M^2_{\psi_f})\right)^2 \big(\det{}' \mathfrak{M}_A\big)^{-1/2} \det \mathfrak{M}_{\mathrm{gh}} , \end{aligned} \tag{2.4.58}$$

where the Gaussian integrals were performed neglecting the vanishing eigenvalues $\lambda_A^{\alpha_0}$ as indicated by $\det{}'\mathfrak{M}_A$ and where (2.4.53) together with (2.4.55) was used for the $i\not{D}$ - determinant.[53]

---

[53] [140, 141, 150]

In detail, the caloron zero modes are given by

- $$Z^\mu_\rho = \frac{\partial A_{\text{HS}}}{\partial \rho} = -\frac{2}{\rho}\bar\eta^{a\mu\nu}\frac{\partial^\nu \phi}{\phi^2}\frac{\sigma^a}{2} \tag{2.4.59}$$
- $$Z^\mu_{C^\nu} = -\frac{\partial A_{\text{HS}}}{\partial X^\nu} + D^\mu A^\nu_{\text{HS}} = G^{\mu\nu} \tag{2.4.60}$$
- $$Z^\mu_{\theta^a} = D^\mu_{\text{adj}}(\phi^{-1})\,\frac{\sigma^a}{2} = -\frac{\delta^{ab}\partial^\nu\phi + \varepsilon^{abc}\bar\eta^{c\mu\nu}\partial^\nu\phi}{\phi^2}\frac{\sigma^b}{2} \tag{2.4.61}$$
- $$Z^\mu_{\vartheta^{j,k}} = D^\mu\left(\phi^{-\frac{1}{2}}\right)\frac{T^{j,k}}{2} - \text{h.c.} = -\left((i,\vec\sigma)\cdot\partial\right)\phi^{-\frac{1}{2}}(i,-\vec\sigma)^\mu\frac{T^{j,k}}{2} - \text{h.c.}\,, \tag{2.4.62}$$

with $\phi(X)$ as given in (2.4.36) and the $4N-8$ collective coordinates $\vartheta^i$ and generators $T^i$ relabeled with indices $j \in \{\pm1, \pm2\}$, $k = 3, \ldots, N$ such that $(T^{j\,>\,0,\,k})^{pq} = \delta^{jp}\delta^{kq}$ and $T^{j\,<\,0,\,k} = i\,T^{j\,>\,0,\,k}$. The zero modes are independent of the caloron gauge orientation described by the $\theta^a$ and $\vartheta^{j,k}$ and, in fact, orthogonal, so that the resulting $U$ - matrix is diagonal,

$$\begin{aligned} U &= \begin{pmatrix} U_{\rho\rho} & & & \\ & (U_{C^\mu C^\nu})_{\mu\nu} & & \\ & & (U_{\theta^a\theta^b})_{ab} & \\ & & & (U_{\vartheta^i\vartheta^j})_{ij} \end{pmatrix}_{4N\times 4N} = \\ &= \begin{pmatrix} \frac{16\pi^2}{g^2} & & & \\ & \frac{8\pi^2}{g^2}\mathbb{1}_{4\times4} & & \\ & & \frac{4\pi^2\rho^2}{g^2}\mathbb{1}_{3\times3} & \\ & & & \frac{2\pi^2\rho^2}{g^2}\mathbb{1}_{(4N-8)\times(4N-8)} \end{pmatrix}, \end{aligned} \tag{2.4.63}$$

and one has $\sqrt{\det U} = \frac{2^{2N+7}}{\rho^5}\left(\frac{\pi^2\rho^2}{g^2}\right)^{2N}$, which is again $\theta$ - $\vartheta$ - independent. If one considers only gauge - invariant correlation functions, one can therefore integrate out the gauge orientations[54] $\int \mathrm{d}^3\theta\,\mathrm{d}^{4N-8}\vartheta = \mathrm{vol}\left(\frac{SU(N)}{SU(N-2)\times U(1)}\right) = \frac{2^{4N-5}\pi^{2N-2}}{(N-1)!(N-2)!}$.[55]

Before plugging these results into the expression (2.4.65) for the partition function, one notes that the partition function is infinite without proper normalization with respect to a vacuum background and regularization/renormalization.

---

[54] This expression for the gauge group volume holds for the choice of Dynkin index $C_{\text{def}} = \frac{1}{2}$. A different choice alters the volume but leaves the overall density (2.4.66) invariant.

[55] [54, 140, 150, 158]

Renormalization is achieved by employing Pauli - Villars regularization [159], which introduces additional copies of all quantum fields with large mass $\Lambda \gg M_{\phi_i,\varphi_j,\psi_f}$ and minimal coupling only to the background. For the vector and ghost fields one introduces fields $A_{\text{heavy}}$ and $c_{\text{heavy}}$ which add to the Lagrangian as $\frac{1}{2}A^{\mu}_{\text{heavy}}\,\mathfrak{M}^{\mu\nu}_{A}(A_{\text{HS}})A^{\nu}_{\text{heavy}} - \Lambda^2 A^{\mu}_{\text{heavy}}A^{\mu}_{\text{heavy}}$ and $\bar{c}_{\text{heavy}}\mathfrak{M}_{\text{gh}}(A_{\text{HS}})c_{\text{heavy}} - \Lambda^2\bar{c}_{\text{heavy}}c_{\text{heavy}}$, respectively. Therefore all physics is understood as in relation to these heavy particles which probe physics at the asymptotically free UV - limit. UV divergences then cancel in the difference of two theories (at physical mass versus at $\Lambda$ - mass). Pauli - Villars regularization is required (instead of the more conventional dimensional methods), since, as we discussed in section 2.4.2, actual expressions for $SU(2)$ - instantons/calorons are only available in the 4 -/$3+1$ - dimensional spacetimes $\mathbb{R}^4$ and $\mathbb{R}^3 \times S^1_{\text{rad.}={}^{\beta}/_{2\pi}}$. The main drawback of Pauli Villars regularization, the fact that it violates gauge - invariance in non - Abelian gauge theories, does not pose a problem in this case, since for the background instanton/caloron fields the gauge is fixed prior to calculations. In this gauge, every zero mode $\chi^{\alpha_0}_{\phi_i,\,\varphi_j,\,A}$ is accompanied by a factor $\Lambda^2$ and every zero mode $\chi^{\alpha_0}_{\psi_f,\,\text{gh}}$ carries carries a factor $\Lambda$ so that one has to modify $\sqrt{\det U}$ by a factor $\sqrt{\Lambda^{8N}}$ and finds[56]

$$\sqrt{\det U} = \frac{2^{2N+7}}{\rho^5}\left(\frac{\pi^2\rho^2\Lambda^2}{g^2}\right)^{2N} . \tag{2.4.64}$$

Combining this determinant (2.4.64) with (2.4.58) and inserting normalization by a vacuum background (which, in this approximation, cancels the $\phi_i$ - contributions), the overall partition function and the thereby defined caloron density $\mathscr{D}$ thus read:

$$\begin{aligned} Z_{\text{HS}}(\theta) = e^{i\theta}\int_0^{\infty}\mathrm{d}\rho\int^{\beta}\mathrm{d}^4 Z\,\frac{4\,e^{-\frac{8\pi^2}{g^2}}}{\pi^2(N-1)!(N-2)!}\left(\frac{4\pi^2\rho^2\Lambda^2}{g^2}\right)^{2N}\frac{1}{\rho^5}\times \\ \times\prod_{j,\,f}\frac{\det\mathfrak{M}_{\varphi}(\Lambda)\,\det\mathfrak{M}_{\varphi,\,0}(M_{\varphi_j})}{\det\mathfrak{M}_{\varphi}(M_{\varphi_j})\,\det\mathfrak{M}_{\varphi,\,0}(\Lambda)}\,\frac{M_{\psi_f}}{\Lambda}\left(\frac{\det(-D_-^2+M_{\psi_f}^2)\,\det(-\partial_-^2+\Lambda^2)}{\det(-D_-^2+\Lambda^2)\,\det(-\partial_-^2+M_{\psi_f}^2)}\right)^2\times \\ \times\sqrt{\frac{\det'\mathfrak{M}_A(\Lambda)\,\det'\mathfrak{M}_{A,\,0}}{\det'\mathfrak{M}_A\,\det'\mathfrak{M}_{A,\,0}(\Lambda)}\,\frac{\det\mathfrak{M}_{\text{gh}}\,\det\mathfrak{M}_{\text{gh},\,0}(\Lambda)}{\det\mathfrak{M}_{\text{gh}}(\Lambda)\,\det\mathfrak{M}_{\text{gh},\,0}}} = \end{aligned} \tag{2.4.65}$$

$$= e^{i\theta}\,\beta V\int_0^{\infty}\mathrm{d}\rho\,\mathscr{d}(T,M_{\varphi_j},M_{\psi_f},\rho,\Lambda) = e^{i\theta}\,\beta V\,\mathscr{D}(T,M_{\varphi_j},M_{\psi_f},\Lambda) = \tag{2.4.66}$$

$$= \exp\big(-\Gamma_{\text{fermion, complex scalar, gluon and ghost}}(\theta)\big) = e^{i\theta}\,\beta V\int_0^{\infty}\mathrm{d}\rho\,e^{-\gamma(\rho)}\,, \tag{2.4.67}$$

---

[56] [141]

where $\beta V = \mathrm{vol}(\mathbb{R}^3 \times S^1_{\text{rad.}={}^{\beta}/_{2\pi}}) = \int^{\beta} \mathrm{d}^4 C$ and $\gamma(\rho) = -\ln(\mathscr{d})$ is the negative logarithmic caloron density, “log - caloron density” for short. We denote the log - caloron density by $\gamma$ since $\beta V\, e^{i\theta} \int_0^{\infty} \mathrm{d}\rho\, e^{-\gamma(\rho)} = e^{-\Gamma(\theta)}$.[57]

### Determinant Ratios and Relations

The instanton/caloron - density (2.4.66) was calculated for the simplified case of massless/almost massless scalar/fermionic fields at zero temperature in [141] and was extended to finite temperatures in [54].

For $T = 0$, $M_{\varphi_j} = 0$ and vanishingly small fermion masses $M_{\psi_f}\rho \ll 1$, the fermionic, vector and ghost determinants (2.4.43.c) - (2.4.43.e), using the background gauge and given a self - dual $SU(2)$ - background, are conveniently related. In detail, one has:

- $$\det{}' \mathfrak{M}_A = \big(\det(-D^2_{\text{adj}})\big)^4 = \Big(\det(-D^2_{\text{spin }1})\big(\det(-D^2)\big)^{2(N-2)}\Big)^4 , \tag{2.4.68}$$
- $$\det \mathfrak{M}_{\text{gh}} = \big(\det{}' \mathfrak{M}_A\big)^{\frac{1}{4}} = \det(-D^2_{\text{spin }1})\big(\det(-D^2_{\text{spin }1/2})\big)^{2(N-2)} , \tag{2.4.69}$$
- $$\left(\frac{\det(-D^2)\ \det(-\partial^2 + \Lambda^2)}{\det(-D^2 - \Lambda^2)\ \det(-\partial^2)}\right)_{\text{spin }1/2} = e^{\alpha\left(\frac{1}{2}\right) + \frac{1}{6}\ln(\Lambda\rho)} , \tag{2.4.70}$$
- $$\left(\frac{\det(-D^2)\ \det(-\partial^2 + \Lambda^2)}{\det(-D^2 - \Lambda^2)\ \det(-\partial^2)}\right)_{\text{spin }1} = e^{\alpha(1) + \frac{2}{3}\ln(\Lambda\rho)} , \tag{2.4.71}$$
- $$\frac{\det \mathfrak{M}_{\psi}(M_{\psi_f})\ \det \mathfrak{M}_{\psi,0}(\Lambda)}{\det \mathfrak{M}_{\psi}(\Lambda)\ \det \mathfrak{M}_{\psi,0}(M_{\psi_f})} \overset{(2.4.53)}{=} \frac{M_{\psi_f}}{\Lambda} \left(\frac{\det(-D^2 + M^2_{\psi_f})\ \det(-\partial^2 + \Lambda^2)}{\det(-D^2 + \Lambda^2)\ \det(-\partial^2 + M^2_{\psi_f})}\right)^2_{\text{spin }1/2} =$$
  $$\overset{M_{\psi_f}\rho \ll 1,\ (2.4.70)}{=} \frac{M_{\psi_f}}{\Lambda}\, e^{2\alpha\left(\frac{1}{2}\right) + \frac{1}{3}\ln(\Lambda\rho)} = M_{\psi_f}\rho\, e^{2\alpha\left(\frac{1}{2}\right) - \frac{2}{3}\ln(\Lambda\rho)} , \tag{2.4.72}$$
- $$\frac{\det \mathfrak{M}_{\varphi_j}\ \det \mathfrak{M}_{\varphi_j\,0}(\Lambda)}{\det \mathfrak{M}_{\varphi_j}(\Lambda)\ \det \mathfrak{M}_{\varphi_j\,0}} = e^{-\frac{1}{6}\ln(\Lambda\rho)\sum_{t_j} C(t_j) - \sum_{t_j}\alpha(t_j)} , \tag{2.4.73}$$

where the (not explicitly denoted) fundamental representation corresponds to spin $\frac{1}{2}$, $\alpha\left(\frac{1}{2}\right) \approx 0.145873$ and $\alpha(1) \approx 0.443307$, the $t_j$ are the spins of the $SU(2)$ - representations making up the composite fields $\varphi_j$, the corresponding Dynkin indices are given by $C(t_j) = \frac{2}{3} t_j (t_j + 1)(2t_j + 1)$ and the general expression for $\alpha(t_j)$ is given in [141, eq. (12.4)]. Furthermore, the instanton zero modes yield the same Jacobian matrix as (2.4.63) and thus the same Jacobian determinant. Given the above simplifications and relations one obtains the partition function:[58]

---

[57] [8, 54]

[58] [54, 141, 160]

$$
\begin{aligned}
&Z_{\mathrm{HS}}(T=0, M_{\varphi_j}=0, M_{\psi_f}\rho \ll 1, \theta) = \\
&= e^{i\theta}\,\beta V \int_0^\infty \mathrm{d}\rho\, \text{đ}(T=0, M_{\varphi_j}=0, M_{\psi_f}\rho \ll 1, \rho, \Lambda) = e^{i\theta}\,\beta V \int_0^\infty \mathrm{d}\rho\, e^{-\gamma(\rho)} = \\
&= e^{i\theta}\,\beta V \int_0^\infty \mathrm{d}\rho\, \frac{4\, e^{-\alpha(1)-2(N-2-N_f)\alpha\left(\frac{1}{2}\right)}}{\pi^2 (N-1)!(N-2)!} \left(\frac{4\pi^2}{g^2}\right)^{2N} \frac{1}{\rho^5} \prod_f M_{\psi_f}\rho \times \\
&\quad \times \exp\left(-\frac{8\pi^2}{g^2} + \frac{1}{3}\ln(\Lambda\rho)\left(11N - 2N_f - \frac{1}{2}\sum_{j,t_j} C(t_j)\right) - \sum_{j,t_j}\alpha(t_j)\right).
\end{aligned}
\tag{2.4.74}
$$

In the following we are going to focus on a description of QCD in a caloron background and thus drop the scalar fields $\varphi_j$ and shorten the notation $M_{\psi_f} \to M_f$. The remaining logarithm in the exponent, $\frac{1}{3}\ln(\Lambda\rho)(11N - 2N_f)$, coincides with the 1 - loop $\beta$ - function for the coupling constant of $SU(N)$ - YM theory coupled to $N_f$ fermions in the sense that $\frac{8\pi^2}{g^2} - \frac{1}{3}\ln(\Lambda\rho)(11N - 2N_f) = \frac{8\pi^2}{g^2(\mu=1/\rho)}$ is the 1 - loop regularized coupling at scale $\frac{1}{\rho}$ as given in (1.1.2). Therefore, the factor $g^{-4N}$ in (2.4.74) is often manually replaced by the running coupling $g^{-4N}(1/\rho)$.[59]

As was established for massless quarks in (2.4.77) and [54] and as we are going to verify for the general case (cf. figure 3.16), the preferred caloron size is small: $\rho T \approx 0.42$ in pure glue with $N = 3$, which goes own to $\rho T \approx 0.34$ in the case of four light quarks. We deduce that the replacement $g^{-4N} \to g^{-4N}(1/\rho)$ in (2.4.74) adds only small corrections: the large Pauli - Villars mass $\Lambda \gg T$ yields $\big(\ln(\Lambda\rho)\big)^{2N} = (\ln\Lambda)^{2N}\big(1 + 2N\epsilon + \mathcal{O}(\epsilon^2)\big)$, $\epsilon = \frac{\ln\rho}{\ln\Lambda}$. Therefore, we choose to neglect the $\rho$ - dependent $\epsilon$ - corrections and keep only the “constant”, i.e., $\rho$ - independent, term $\ln\Lambda$.

This identification of the running coupling also allows for the relation of the above result in Pauli - Villars regularization to other regularization schemes, for example the MS- or $\overline{\text{MS}}$ - scheme of dimensional regularization as described in [132, eqs. (82) - (89)] and [161, eqs. (3), (4)]. The $\overline{\text{MS}}$ - result was first established in [141]. Overall, the caloron density at $T = 0$ for vanishingly light quarks (in Pauli - Villars regularization) reads

$$
\text{đ} = \frac{2e^{-\alpha(1)+4\alpha\left(\frac{1}{2}\right)+\ln 2 - N\left(2\alpha\left(\frac{1}{2}\right)+2\ln 2\right)+2N_f\alpha\left(\frac{1}{2}\right)}}{\pi^2(N-1)!(N-2)!} \left(\frac{8\pi^2}{g^2}\right)^{2N} e^{-\frac{8\pi^2}{g^2(1/\varrho)}} \frac{\prod_f M_f\rho}{\varrho^5}
\tag{2.4.75}
$$

with the running coupling $g(\mu = 1/\rho)$ (1.1.2).

---

[59] Or even the renormalization group - improved running coupling (see [54]):
$\frac{8\pi^2}{g^2\left(\frac{1}{\rho}\right)} = -\frac{1}{3}\ln(\Lambda\rho)(11N - 2N_f) + \ln\left(\ln\left(\frac{1}{\Lambda\rho}\right)\right) \frac{17N^2 - \frac{N_f}{2N}(13N^2-3)}{11N - 2N_f} + \mathcal{O}\left(\frac{1}{\ln(\Lambda\rho)}\right).$

Compare the partition function (2.4.74) given in terms of $\mathcal{D} = \int_0^\infty \mathrm{d}\rho\, \mathscr{d}(\rho)$ and (2.4.75) with the remaining collective coordinate $\rho$ to (2.4.7) for the toy model. In the sense of (2.4.4), $\mathscr{d}(\rho)$ can be seen as the topological transition rate (per caloron size) [8].[60]

In order to extend the above to the physically interesting case of $T > 0$ and $M_f\rho \not\ll 1$ as well as $M_f\beta \not\ll 1$, the determinant relations must be reevaluated for these new parameters. For that the determinant relations in (2.4.65) are split into the parts with $T = 0$, $M_f\rho \ll 1$ and a correction factor $f$, i.e.,

$$\mathscr{d}(T, M_f, \rho, \Lambda) = \mathscr{d}(T = 0, M_f\rho \ll 1, \rho, \Lambda) \cdot f(T, M_f, \rho)\,, \tag{2.4.76}$$

and one uses the fact that (2.4.68) - (2.4.71) still hold at finite temperature [54].

For vanishing fermion masses but finite temperature this correction factor was calculated in [54] and reads $f(T, M_f\beta \ll 1, M_f\rho \ll 1, \rho) = f(T, M_f = 0, \rho)$:

$$f(T, 0, \rho) = \exp\Big(-\frac{(\pi\rho T)^2}{3}(2N + N_f) - A(\pi\rho T)\big(12 + 2(N - N_f)\big)\Big) \tag{2.4.77}$$

with $A(x) \approx -\frac{1}{12}\ln\left(1 + \frac{x^2}{3}\right) + a_1\big(1 + \frac{a_2}{x^{3/2}}\big)^{-8}$, $a_1 \approx 0.01289764$ and $a_2 \approx 0.15858$.

For zero temperature but non - vanishing fermion masses, the fermion determinant relation has also been evaluated and one finds analytical results for small mass- and large mass - expansions

$$f(0, M_f\rho) = \begin{cases} \prod\limits_f \exp\Big(M_f^2\rho^2\ln(M_f\rho) + (\gamma_\mathrm{E} - \ln 2)M_f^2\rho^2 + \mathcal{O}\big((M_f\rho)^4\big)\Big) & : M_f\rho \lesssim 0.5 \\ \prod\limits_f \dfrac{e^{-2\alpha(\frac{1}{2})}}{(M_f\rho)^{\frac{1}{3}}}\exp\Big(-\dfrac{2}{75\,(M_f\rho)^2} - \dfrac{34}{735\,(M_f\rho)^4} + \\ \qquad + \dfrac{464}{2835\,(M_f\rho)^6} - \dfrac{15832}{148225\,(M_f\rho)^8}\Big) & : M_f\rho \gtrsim 1.8 \end{cases} \tag{2.4.78}$$

as well as an interpolation between them, covering arbitrary masses, in [60]:

$$\begin{aligned} &f(0, M_f\rho) = \\ &= \prod_f \frac{e^{-2\alpha(\frac{1}{2})}}{(M_f\rho)^{\frac{1}{3}}}\exp\left(\frac{\frac{1}{3}\ln(M_f\rho) + 2\alpha\big(\frac{1}{2}\big) - \big(6\alpha\big(\frac{1}{2}\big) - \gamma_\mathrm{E} + \ln 2\big)\,(M_f\rho^2) - \frac{2}{5}(M_f\rho)^4}{1 - 3(M_f\rho)^2 + 20(M_f\rho)^4 + 15(M_f\rho)^6}\right). \end{aligned} \tag{2.4.79}$$

---

[60] [54, 132, 161]

Furthermore, an explicit numerical solution for arbitrary masses was found [61]:

$$f(0, M_f, \rho) = \prod_f e^{-2\alpha(\frac{1}{2})} \exp\Bigg( -2 \lim_{L\to\infty} \Bigg( \sum_{l=0,\frac{1}{2},\dots}^{L} (2l+1)(2l+2) P_{M_f,\,\rho}(l) + 2L^2 + 4L - \\ - \left(\frac{1}{6} + \frac{M_f^2\rho^2}{2}\right)\ln(L) + \frac{M_f^2\rho^2}{2}\big(\ln(M_f\rho) + 1 - 2\ln 2\big) + \frac{127}{72} - \frac{\ln 2}{3}\Bigg)\Bigg) , \tag{2.4.80}$$

where $P_{M_f,\,\rho}(l) = S^{l,l+\frac{1}{2}}_{M_f,\,\rho}(\overline{R}\to\infty) + S^{l+\frac{1}{2},l}_{M_f,\,\rho}(\overline{R}\to\infty)$ and $S^{l,j}_{M_f,\,\rho}(\overline{R})$ is the numerical solution to the ordinary differential equation

$$\frac{\mathrm{d}^2 S^{l,j}}{\mathrm{d}\overline{R}^2} + \left(\frac{\mathrm{d}S^{l,j}}{\mathrm{d}\overline{R}}\right)^2 + \left(\frac{1}{\overline{R}} + 2\frac{\mathrm{d}_{\overline{R}} I_{2l+1}(M_f\overline{R})}{I_{2l+1}(M_f\overline{R})}\right)\frac{\mathrm{d}S^{l,j}}{\mathrm{d}\overline{R}} = \frac{4(j-l)(j+l+1)}{\overline{R}^2+\rho^2} - \frac{3\rho^2}{\left(\overline{R}^2+\rho^2\right)^2} , \tag{2.4.81}$$

with $I_\alpha(x)$ the modified Bessel function of the first kind.

We aim to calculate the fermionic correction factor $f(T, M_f, \rho) = e^{-\gamma_{\text{ferm}}} \propto e^{-2\gamma_{\text{s},\,-}}$ for the general case of heavy quarks at finite temperatures. Here, $\gamma_{\text{ferm}}$ is the negative logarithmic caloron density due to a fermion and $\gamma_{\text{s},\,-}$ is the logarithmic density for an anti-periodic, complex scalar particle, i.e., the regularized, vacuum - normalized Klein - Gordon operator determinant in (2.4.65):

$$\begin{aligned} \gamma(\rho) \supset \gamma_{\text{fermion}}(\rho) &= -\ln\left(\frac{\det(i\not{D} + M_f)\,\det(i\not{\partial}) + \Lambda)}{\det(i\not{D} + \Lambda)\,\det(i\not{\partial}) + M_f)}\right) = \\ &= -2\ln\left(\frac{\det(-D_-^2 + M_f^2)\,\det(-\partial_-^2 + \Lambda^2)}{\det(-D_-^2 + \Lambda^2)\,\det(-\partial_-^2 + M_f^2)}\right) - \ln\left(\frac{M_f}{\Lambda}\right) = \\ &= -2\,\gamma_{\text{scalar, anti-periodic}}(\rho) - \ln\left(\frac{M_f}{\Lambda}\right) = -2\,\gamma_{\text{s},\,-}(\rho) - \ln\left(\frac{M_f}{\Lambda}\right) . \end{aligned} \tag{2.4.82}$$

A straight - forward calculation of $\gamma_{\text{s},\,-}$ in (2.4.82) would require us to solve a complicated, 2 - dimensional partial differential equation, which we derive in appendix A, compared to the ODE (2.4.81). This is due to the broken spacetime symmetry for thermal field theories described by the imaginary time formalism (cf. section 2.2.4) and the caloron - rotational covariance being restricted to spatial $\mathbb{R}^3$. We instead follow an alternative approach which was first used for $T = 0$ in [60] and that we adapt and generalize to finite temperatures. First, we calculate the correction factor $f(T, M_f, \rho)$ for large masses

($M \gg T$, cf. section 3.1) and light quarks ($M \ll T$, $M\rho \ll 1$, cf. section 3.2), obtaining

$$f(T, M_f, \rho) = \begin{cases} \exp\big(2\,\gamma_{\mathrm{s},\,-}(M_f\beta < 1, \rho)\big) & : \text{non - vanishigly small } M_f \\ \dfrac{e^{-2\alpha\left(\frac{1}{2}\right)}}{(\Lambda\rho)^{\frac{1}{3}}}\exp\big(2\,\gamma_{\mathrm{s},\,-}(M_f\beta > 1, \rho)\big) & : \text{large } M_f \end{cases} . \tag{2.4.83}$$

The factor $e^{-2\alpha\left(\frac{1}{2}\right)}(\Lambda\rho)^{-\frac{1}{3}}$ cancels $\{M\} \ll 1$ - terms in (2.4.75). Second, we interpolate between these mass regimes (cf. section 3.3) to obtain a result for arbitrary masses. This is the finite $T$ - generalization of (2.4.78) and (2.4.79).

As stated in section 1.3, our approach is motivated by the excellent agreement of $\gamma_{\mathrm{s},\,-}(M_f, \rho)$ at $T = 0$ as given by the interpolation (2.4.79) in [60] with the full numerical result (2.4.80) from [61] as shown in figure 6 of [61].

### 2.4.4 Dilute Gas Approximation for Calorons

So far, only BPST (anti-)instantons and HS (anti-)calorons of topological charge $n = \pm 1$ have been discussed. In general, topological configurations can carry any integer topological charge $n \in \mathbb{Z}$, however (even at finite $T$ only such configurations contribute, cf. section 2.4.2). While the general ADHM - construction for higher charge - instanton configurations is known and corresponding calorons could be constructed following [147], explicit expressions are only available for HS (anti-)calorons.

Given that small calorons $\rho \sim 0.35\beta$ dominate, however, (see [54] and our results in figure 3.16) it is reasonable to employ the *small constituent - approximation*, i.e., to describe more complicated background configurations as superpositions of spatially well - separated and thus non - interacting[61] single HS (anti-)calorons. At leading order, all higher charge - calorons can then be described this way. A general caloron background is populated by calorons of all topological charges and one describes $n$ - caloron configurations by the small constituent - approximation using $n_+$ HS calorons and $n_-$ HS anti-calorons with $n_+ - n_- = n$. This is the dilute gas approximation (DGA), as introduced for the periodic potential in section 2.4.1, employed for calorons.[62]

One defines again - analogously to the instanton case at $T = 0$ - the physical $\theta$ - vacuum $|\theta\rangle = \sum_{\nu\,\in\,\mathbb{Z}} e^{-i\nu\theta}\,|\nu\rangle$ and the operators $\mathrm{T}_\pm$ and $\mathrm{T}_n$ that change the vacuum winding number as $\mathrm{T}_\pm\,|\nu\rangle = |\nu \pm 1\rangle$ and $\mathrm{T}_n\,|\nu\rangle = |\nu + n\rangle$, i.e., $\mathrm{T}_n\,|\theta\rangle = e^{in\theta}\,|\theta\rangle$ (cf. (2.4.31) and

---

[61] Instanton and caloron interactions are short - ranged; e.g., for well - separated instantons at locations $Z_i$ with typical separation scale $d$, the interaction corrections compared to an exact solution are $\lesssim \frac{\rho^2}{d^3}$ in the "near region" $|X - Z_i| \lesssim \rho$ (for some $i$) and $\lesssim \frac{\rho^4}{d^5}$ in the "far region" $|X - Z_i| \gtrsim \rho\ \forall i$ [162].

[62] [8, 138, 163]

(2.4.32)). From the point of view of these operators, the DGA then implies

$$\mathrm{T}_n = \sum_{n_+,\, n_- \,\in\, \mathbb{N}} \frac{\delta_{n,n_+-n_-}}{n_+!\, n_-!} (\mathrm{T}_+)^{n_+} (\mathrm{T}_-)^{n_-} \quad \text{with} \quad [\mathrm{T}_\pm, \mathrm{T}_\mp] = 0\,, \tag{2.4.84}$$

where the factor $(n_+!\, n_-!)^{-1}$ accounts for the overcounting due to indistinguishable combinations of the HS (anti-)calorons. Compare this to figure 2.2b. Following (2.4.33) and (2.4.34) and using $Z_{\mathrm{HS}} = Z_{\overline{\mathrm{HS}}} = \beta V \mathcal{D}$ (cf. (2.4.66)), the DGA transition amplitude and the caloron background partition function $Z_{\mathrm{DGA}}(\theta)$ read

$$\begin{aligned}
&\langle\theta| \sum_{n\,\in\,\mathbb{Z}} e^{-H(A_{n\text{-cal}})\beta} |\theta\rangle = \sum_n \langle\theta\,|\,\mathrm{T}_n\,|\,\theta\rangle = \sum_{n,\, n_+,\, n_-} \frac{\delta_{n,n_+-n_-}}{n_+!\, n_-!} \langle\theta\,|\,(\mathrm{T}_+)^{n_+} (\mathrm{T}_-)^{n_-}\,|\,\theta\rangle = \\
&= \sum_{n_+,\, n_-} \frac{1}{n_+!\, n_-!} \int_0^{2\pi} \prod_{j\,=\,1}^{n_++n_--1} \mathrm{d}\theta_j \left\langle\theta \,\middle|\, \mathrm{T}_+ \,\middle|\, \theta_{n_++n_--1}\right\rangle \cdots \left\langle\theta_{1+n_-} \,\middle|\, \mathrm{T}_+ \,\middle|\, \theta_{n_-}\right\rangle \times \\
&\qquad\qquad\qquad\qquad \times \left\langle\theta_{n_-} \,\middle|\, \mathrm{T}_- \,\middle|\, \theta_{n_--1}\right\rangle \cdots \langle\theta_1\,|\,\mathrm{T}_-\,|\,\theta\rangle = \\
&= (2\pi)^{n_++n_-} \delta(0) \sum_{n_+\,, n_-} \frac{1}{n_+!\, n_-!} \left(e^{i\theta}\, Z_{\mathrm{HS}}\right)^{n_+} \left(e^{-i\theta}\, Z_{\overline{\mathrm{HS}}}\right)^{n_-} = \\
&= (2\pi)^{n_++n_-} \delta(0) \exp(e^{i\theta}\, \beta V \mathcal{D}) \exp(e^{-i\theta}\, \beta V \mathcal{D}) = (2\pi)^{n_++n_-} \delta(0) \underbrace{\exp(2\beta V \mathcal{D} \cos(\theta))}_{=\, Z_{\mathrm{DGA}}(\theta)}\,.
\end{aligned} \tag{2.4.85}$$

The overall factor $\delta(0)$ again reflects the infinite number of "starting point" $|\nu\rangle$ - vacua for the transition (cf. (2.4.34) with $\theta' = \theta$ so that $\sum_{\nu'} \to \infty$ or accordingly $\delta(\theta' - \theta) = \delta(0)$). This expression for $Z_{\mathrm{DGA}}(\theta)$ shows that it is fully sufficient to calculate the HS caloron density $\mathcal{D}(T)$ to obtain the full DGA partition function.[63]

The picture of a caloron tunneling process in imaginary time, connecting otherwise distinct $|\nu\rangle$ - vacua, which is invoked by the expression $\langle\theta| \sum_n e^{-H(A_{n\text{-cal}})\beta} |\theta\rangle$ and corresponds to the instanton case discussed in section 2.4.1 (cf. figure 2.10, (2.4.20) and (2.4.33)) is insufficient to discuss the DGA for calorons. For instantons with an infinite time scale for the "complete tunneling process" $\Delta\bar{t} \to \infty$, the usual reasoning behind the DGA is to assume temporally well - separated instantons $\overline{C}_i^4 - \overline{C}_j^4 \gg \delta\bar{t}\ \forall i, j$, where $\delta\bar{t}$ is the instanton size, i.e., time scale (e.g., see [8, 33, 38, 130, 132, 140]). At finite temperatures, the dominant caloron size is not much smaller than the temporal size of the system, however, and the calorons typically occupy most of the available space in the temporal direction [164]. Therefore, the usual reasoning for the applicability of the DGA fails. The caloronic

---

[63] [8, 116, 132]

DGA is based on a spatial separation of the small constituents to justify (2.4.84). This is realized by the caloron sizes $\rho_i$ being small enough, so that the field strengths fall off quickly (cf. figure 2.12) and for every HS (anti-)caloron $Z_i = \beta V \mathcal{D} \approx \beta V_i \mathcal{D}$ with disjoint volumes $V_i \subset \mathbb{R}^3$, $V_i \cap V_j = \emptyset$, $\cup_i V_i = \mathbb{R}^3$. This is also the reason why initially introducing the T - operators in (2.4.32) was important, as for calorons the topological transitions cannot be thought of as tunneling transitions in infinite time and thus require a general description independent of this interpretation.

[141] and [54] also show why we abstained from discussing the DGA for instantons in section 2.4.2 and only introduced it for calorons. Large caloron sizes are damped exponentially with temperature, called Debye screening (cf. (2.4.77)), so that at $T = 0$ infinitely large instantons populate the vacuum and dominate the instanton density. This leads to both the failure of the DGA and an infrared divergence of the partition function.

### 2.4.5 Topological Susceptibility

In section 2.4.2 we reviewed how the topologically non - trivial QCD vacuum structure and the presence of vacuum tunneling processes enforce the addition of the $\theta$ - term $-i\theta q(X) = -\frac{i\theta}{16\pi^2}\mathrm{tr}\big(\widetilde{G}^{\mu\nu} G^{\mu\nu}\big)$ to the Lagrangian and in the the above section 2.4.4 we presented the DGA, which shows that it is sufficient to consider only HS (anti-)calorons. The "strength" of the topological term is thus determined by the value of the angle $\theta$ and the "strength" of the topological fluctuations caused by caloron backgrounds is measured by the topological susceptibility $\chi_{\mathrm{top}}$. Analogously to, for example, the magnetic susceptibility, which measures the response of a system to (the strength of) an external magnetic field $B$, one defines the topological susceptibility $\chi_{\mathrm{top}}$ as the response of QCD to a topological background, the strength of which is determined by the fluctuation $\theta$ away from its VEV $\langle\theta\rangle \approx 0$ (the value predicted by both experiment and theory, for the latter cf. section 2.5.3). Given the magnetic susceptibility $\chi_{\mathrm{mag}} \propto \frac{\partial^2 \ln Z(B)}{\partial B^2}$ (e.g., see [6, p. 572/573]), the topological susceptibility is defined as (cf. (1.2.2))

$$\begin{aligned} \chi_{\mathrm{top}} &= -\frac{1}{\beta V}\frac{\partial^2 \ln\big(Z(\theta)\big)}{\partial\theta^2}\bigg|_{\theta=0} = \frac{\big(\langle n^2\rangle - \langle n\rangle^2\big)\big|_{\theta=0}}{\beta V} = \frac{\langle n^2\rangle|_{\theta=0}}{\beta V} = \\ &= \int^{\beta} \mathrm{d}^4X\, \mathrm{tr}\big(q(X)q(0)\big)\,, \end{aligned} \tag{2.4.86}$$

where it was used that $\langle n\rangle = 0$, since calorons and anti-calorons appear equally (they are linked via the flip $\theta \to -\theta$ ).[64]

---

[64] [4, 47, 49, 116, 165]

At temperatures $T > T_\text{c}$ above the critical temperature of chiral perturbation theory (cf. section 2.3), where gluons are a fundamental degree of freedom, the DGA yields a convenient expression for $\chi_\text{top}$. Using the DGA - partition function (2.4.85), which describes general caloron configurations at such temperatures, in the definition of $\chi_\text{top}$ (2.4.86), the topological susceptibility takes the convenient form:

$$\chi_\text{top}(T > T_\text{c}) \overset{\text{DGA}}{=} -\frac{1}{\beta V}\,\frac{\partial^2 \ln\big(Z_\text{DGA}(\theta)\big)}{\partial\theta^2}\bigg|_{\theta\,=\,0} = 2\mathcal{D}(T)\,, \tag{2.4.87}$$

with $\mathcal{D}(T)$ the HS caloron density (cf. (2.4.66) - (2.4.80)). From (2.4.75) and (2.4.77) a temperature dependency $\chi_\text{top} \propto T^{-a-N_f/3}$, $a \approx 7$ can be deduced. The exact coefficient of $\chi_\text{top}$ in this regime depends on chromo - magnetic and -electric screening and is not precisely known, however.[65]

At temperatures $T < T_\text{c}$, QCD as a perturbation theory fails and strong interaction matter is described chiral perturbation theory, which we introduced in section 2.3. For low temperatures and at leading order in chiral perturbation theory, the topological susceptibility reads

$$\chi_\text{top}(T < T_\text{c}) \overset{\text{chiral pert. theory}}{=} f_\pi^2(T) M_\pi^2(T)\,\frac{M_u M_d M_s}{(M_u + M_d)(M_u M_d + M_u M_s + M_d M_s)} \tag{2.4.88}$$

and has been calculated at zero temperature $\sqrt[4]{\chi_\text{top}(0)} = (75.44 \pm 0.34)$ MeV [51][66]. In the limit $M_s \gg M_{u,d}$ (2.4.88) simplifies to $\chi_\text{top}(T < T_\text{c}) \overset{M_s \gg M_{u,d}}{=} f_\pi^2(T) M_\pi^2(T)\,\frac{M_u M_d}{(M_u + M_d)^2}$.[67]

## 2.5 Observable Effects of Topology

After having discussed at length the role of topological effects and instantons (calorons) in QCD (at finite temperatures), we now present some of the most important and well - known phenomena that make the non - trivial topology of the QCD vacuum observable as well as their implications.

---

[65] [44, 49, 165, 166]

[66] This is in good agreement with other recent results as $\sqrt[4]{\chi_\text{top}(0)} = (75.6 \pm 0.6)$ MeV [52] or the $SU(2)$ - chiral perturbation theory result $\sqrt[4]{\chi_\text{top}(0)} = (75.5 \pm 0.5)$ MeV [44] and lattice QCD results $\sqrt[4]{\chi_\text{top}(0)} = (75.6 \pm 1.8_\text{statistical} \pm 0.9_\text{systematic})$ MeV [53], where the $b$ - quark was included.

[67] [44, 48, 52, 165]

### 2.5.1 Axial Anomaly and the missing Nambu - Goldstone Boson

In sections 1.2 and 2.3 we introduced the $\eta$ - $\eta'$ - puzzle: the large mass gap between the $\eta'$- and the $\eta$ - meson and especially between $\eta'$ and the pions. This mass gap seemingly disagrees with $\eta'$ being the singlet accompanying the light meson octet according to the $SU(3)_{\mathrm{V}}$ - product representation $3 \otimes \overline{3} = 8 \oplus 1$ and it directly disagrees with $\eta'$ serving as a pseudo - Nambu - Goldstone boson (pNG boson) for $U(1)_{\mathrm{A}}$ like the light octet for $SU(3)_{\mathrm{A}}$. The $\eta$ - $\eta'$ - puzzle is solved by an anomalous explicit breaking of the $U(1)_{\mathrm{A}}$ - symmetry, which is in turn explained by topological effects. This quantum anomaly is called the axial or chiral anomaly [29–31].[68]

The anomaly is due to $U(1)_{\mathrm{A}}$ - transformations $\psi_{f_l} \to e^{i\beta\gamma^{5_{\mathrm{M}}}}\psi_{f_l}$, $\overline{\psi}_{f_l} \to \overline{\psi}_{f_l} e^{i\beta\gamma^{5_{\mathrm{M}}}}$ of the, in general, $N_{f_l}$ light quark flavors $\psi_{f_l}$. These transformations leave the the quark Lagrangian (2.1.15) invariant/only lightly broken by terms $\propto M_{f_l}$ (cf. (2.3.9)), but actually change the path integral measure ((2.2.10), (2.2.19)) by a Jacobian determinant $\prod_{f_l} \mathscr{D}\overline{\psi}_{f_l}\, \mathscr{D}\psi_{f_l} \to \prod_{f} \mathscr{D}\overline{\psi}_{f_l}\, \mathscr{D}\psi_{f_l}\, J_{f_l}$ which turns out to add to the Lagrangian a term proportional to the topological charge density [167, 168]. To see this, one neglects the $M_{f_l}$ - terms (they are treated as perturbations in this approximation) and, using the Lagrangian $\overline{\psi}_{f_l} i\not{D}\psi_{f_l}$, expands the now equal quark flavors $\psi_f = \xi_j\chi_j$, $\overline{\psi}_f = \bar{\xi}_j\chi_j^\dagger$ in a basis $\{\chi_j(\text{ꭓ})\}$ of orthonormal $i\not{D}$ - eigenfunctions, i.e., $i\not{D}\chi_j = \lambda_j\chi_j$, $(i\not{D}\chi_j)^\dagger = \chi_j^\dagger(-i\overleftarrow{\not{D}}) = \lambda_j\chi_j^\dagger$ and $\int_{\mathbb{R}^{1,3}} \mathrm{d}^4\text{ꭓ}\, \chi_j^\dagger\chi_k = \delta_{jk}$, together with Graßmannian expansion coefficients $\xi_j$. The path integral measure $\prod_{f_l} \mathscr{D}\overline{\psi}_{f_l}\, \mathscr{D}\psi_{f_l} = \big(\prod_j \mathrm{d}\bar{\xi}_j\, \mathrm{d}\xi_j\big)^{N_{f_l}}$ can then be shown to change by the Jacobian determinant

$$\begin{aligned} J = (J_{f_l})^{N_{f_l}} &= \exp\left(-2iN_{f_l}\,\beta \int_{\mathbb{R}^{1,3}} \mathrm{d}^4\text{ꭓ}\, \chi_j^\dagger\gamma^{5_{\mathrm{M}}}\chi_j)\right) = \\ &= \exp\left(\frac{iN_{f_l}\,\beta}{8\pi^2} \int_{\mathbb{R}^{1,3}} \mathrm{d}^4\text{ꭓ}\, \mathrm{tr}\big(\widetilde{G}^{\mu_{\mathrm{M}}\nu_{\mathrm{M}}} G_{\mu_{\mathrm{M}}\nu_{\mathrm{M}}}\big)\right) = \exp\left(2iN_{f_l}\,\beta \int_{\mathbb{R}^4} \mathrm{d}^4\overline{X}\, q(\overline{X})\right). \end{aligned} \tag{2.5.1}$$

Below (2.4.34) it was shown that this topological term is covariant under Wick rotation and in (2.4.19) it was identified as the topological charge $n = \int_{\mathbb{R}^4} \mathrm{d}^4\overline{X}\, q(\overline{X})$ (analogously for calorons at finite $T$). Here one finds again the important relation between $n$ and the infinite sum $\chi_j^\dagger\gamma^5\chi_j$ mentioned above (2.4.54). In conclusion, the axial $U(1)_A$ - symmetry is no symmetry at all, not even for the light quarks, as it anomalously changes the Lagrangian the action by $-2N_{f_l}\,\beta n$. These terms are not small like the mass terms and thus cannot be neglected. The associated current (in Euclidean spacetime) is broken explicitly but lightly by mass terms as well as explicitly and strongly by a topological term:

---

[68] [3, 4, 33, 38, 111]

$$\partial^\mu j^\mu_{\mathrm{A}} = 2i \sum_{f_l} M_{f_l} \overline{\psi}_{f_l} \gamma^5 \psi_{f_l} + 2N_{f_l} \mathrm{tr}\big(\widetilde{G}^{\mu\nu} G^{\mu\nu}\big) = 2i \sum_{f_l} M_{f_l} \overline{\psi}_{f_l} \gamma^5 \psi_{f_l} + 2N_{f_l} q\,. \tag{2.5.2}$$

Compare this with the "naive" expression (2.3.9).[69]

In the truly massless case, the associated charge $Q_{\mathrm{A}}$ is therefore changed by $2N_{f_l}n$ units of axial charge[142]:

$$\Delta Q_{\mathrm{A}} = Q_{\mathrm{A}}(\bar{t} \to \infty) - Q_{\mathrm{A}}(\bar{t} \to -\infty) = \int_{\mathbb{R}^4} \mathrm{d}^4\overline{X}\, \partial^\mu j^\mu_{\mathrm{A}} = 2N_{f_l} n\,. \tag{2.5.3}$$

This can be shown analogously to the derivation of the Atiyah - Singer index theorem for $i\not{D}$ (2.4.54) in section 2.4.2. In detail, an instanton (caloron) of topological charge $n$ creates $2N_{f_l}n$ units of axial charge by creating/annihilating a net of $n_{\mathrm{L}}/n_{\mathrm{R}}$ unpaired left-/right - chiral zero modes of $i\not{D}$ (or by helicity flipping existing unpaired ones [141]).[70]

In the language of Feynman diagrams, the discussed breaking of $U(1)_{\mathrm{A}}$ can be understood via the triangle diagrams shown in figure 2.13 which describe the coupling an external axial vector current and two external photons via a loop of massless fermions. As it turns out, these diagrams are non - zero and the associated matrix element, describing the divergence of the axial vector current creating the two photons, is non - vanishing as well. This result is unchanged by renormalization, as there exists no regularization scheme that preserves the $U(1)_A$ - symmetry.[71]

Furthermore, topology also determines the mass of the $\eta'$ - meson via the Witten - Veneziano mechanism [34, 35]. Considering $N_{f_l}$ light quark flavors, the Witten - Veneziano relation for the $\eta'$ - mass at zero temperature reads

$$\frac{2N_{f_l}\, \chi_{\mathrm{top}}(N_{f_l}, 0)}{f_\pi^2(0)} = M_\eta^2 + M_{\eta'}^2 - 2M_K^2\,, \tag{2.5.4}$$

where $\chi_{\mathrm{top}}(N_{f_l}, 0)$ and $f_\pi(0)$ are the topological susceptibility and pion decay constant (cf. (2.3.10)) at zero temperature, respectively, and $M_K$ is the (average) kaon mass. In the chiral limit $M_{f_l} = 0\ \forall f_l$, where the chiral $SU(3)_{\mathrm{A}}$ - symmetry is restored, the non - anomalous mass contribution to $\eta'$ and the two other meson mass contributions largely cancel, so that only the anomalous mass contribution remains in (2.5.4): $M_{\eta'}^2\Big|_{M_{f_l}=0} = \frac{2N_f\, \chi_{\mathrm{top}}(0)}{f_\pi^2(0)}$. From the point of view of the light quarks, thermal field theory at high enough temperatures

---

[69] [3–5, 33, 38, 46, 116, 130, 140]

[70] [33, 116, 130]

[71] [3–5, 38, 111, 130]

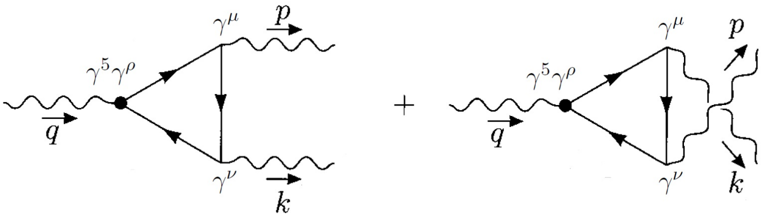

Figure 2.13: Taken from [3] and modified: A UV-divergent quark loop generating the according divergence of the axial vector current and the chiral anomaly, here in Euclidean spacetime. An axial vector current (momentum $q$) couples to a (diverging) loop of massless quarks - • marks an axial vector vertex $\gamma^5\gamma^\rho$ -, which in turn couples to two vector currents (momenta $p$ and $k$) - via vector vertices $\gamma^\mu$ and $\gamma^\nu$.

($T \gtrsim \Lambda_{\text{QCD}}$ or "no higher than $T \sim \Lambda_\chi$", for both cf. section 2.3) corresponds to the chiral limit, i.e., chiral perturbation theory has broken down, the light quarks are again fundamental degrees of freedom in the quark-gluon plasma and the thermal kinetic energy has grown much larger than the light quark masses, i.e., $m_{f_l} = \beta M_{f_l} \approx 0$. At such temperatures, it is therefore technically no longer sensible to speak of (light) baryons. Nevertheless, one can still look for the masses of excitations in the quark-gluon plasma with quantum numbers corresponding to the respective baryons (this can be implemented by corresponding external currents in correlation functions, for example [4, p. 402]). The excitations corresponding to the light octet of pNG bosons are all essentially massless at such temperatures and the mass of "$\eta'$-excitations" has to fall as well according to $\frac{N_f\,\chi_{\text{top}}(T)}{f_\pi^2(T)}$, where both $f_\pi(T)$ and $\chi_{\text{top}}(T)$ decrease with increasing temperatures. For example, at $T = 200\,\text{GeV}$, the mass of an "$\eta'$-excitation" was measured to be at least about $200\,\text{MeV}$ lower than the zero temperature mass $M_{\eta'}(T=0) \approx 958\,\text{MeV}$ [169, 170]. The thermal $\eta'$-mass therefore depends critically on how the pion decay constant and the topological susceptibility fall off at finite temperature and on how the system transitions into a quark-gluon plasma. Current theoretical predictions do not agree with experimental results, therefore a better understanding of $\chi_{\text{top}}(T)$ (and $f_\pi(T)$) at high temperatures is required.[72]

Topology thus explains both why $U(1)_\text{A}$ is not a symmetry, i.e., no ninth (fourth) pNG boson is required, and why the large mass of $\eta'$, not being a pNG boson, is not in contradiction with theory, i.e., it is indeed the singlet accompanying the light meson octet of pNG bosons. Furthermore, $U(1)_A$ - transformations flip a particle's helicity/parity, as can be seen by employing (2.1.10) and $\{\gamma^{5_\mathrm{M}}, \gamma^{0_\mathrm{M}}\} = 0$. If $U(1)_\mathrm{A}$ were actually a good approximate symmetry for the light quarks, all light hadrons made up of the light quarks would have to appear as parity - doublets of similar masses. This is not realized in nature, however - for example, the pions and $\rho$ - mesons would be such parity partners with identical quark content and opposite parity, but their mass difference is $\sim 640\,$MeV.[73]

---

[72] [129, 171]

This is the first important example of symmetry considerations - the chiral symmetry, in this case - leading to further developments of a seemingly established theory - the realization of the relation between anomalous $U(1)_\mathrm{A}$ - breaking and the $\eta$ - $\eta'$ - puzzle - which we was advertised at the beginning of section 2.1.

### 2.5.2 Strong CP Problem and its Resolution by Axions

While including the topological sector of QCD explains the axial anomaly and its consequences, it also creates problems, namely the strong CP problem: the topological $\theta$ - term in the Lagrangian is odd under combined charge conjugation C and parity transformation P, while, experimentally, QCD has proven to be invariant under the CP - transformation.

The $\theta$ - term in the Lagrangian is $\mathcal{L}_\theta = -i\theta q$ (cf. (2.4.19)). In section 2.4.2 it was shown that this term is covariant under Wick rotations. With the chromo - electric and -magnetic fields $E^{i_\mathrm{M}} = G^{0 i_\mathrm{M}}$ and $B^{i_\mathrm{M}} = \frac{1}{2}\varepsilon^{i_\mathrm{M}}{}_{j_\mathrm{M} k_\mathrm{M}} G^{j_\mathrm{M} k_\mathrm{M}}$, one can rewrite this term (using $\varepsilon_{0_\mathrm{M}}{}^{i_\mathrm{M}}{}_{j_\mathrm{M} k_\mathrm{M}} \varepsilon^{i_\mathrm{M}}{}_{j_\mathrm{M} k_\mathrm{M}} = 1$) as $\mathcal{L}_\theta = -\frac{i\theta}{4\pi^2}\mathrm{tr}(E^{i_\mathrm{M}} B_{i_\mathrm{M}})$. Under parity transformation P and the charge conjugation C

$$\mathrm{P} A^{\mu_\mathrm{M}}(x)\mathrm{P}^{-1} = \begin{Bmatrix} A^{0_\mathrm{M}}(t, -\vec{x}) \\ -\vec{A}(t, -\vec{x}) \end{Bmatrix} = A_{\mu_\mathrm{M}}(t, -\vec{x})\,, \quad \mathrm{C} A^{\mu_\mathrm{M}} \mathrm{C}^{-1} = -A^{\mu_\mathrm{M}} \tag{2.5.5}$$

the chromo - electric field picks up two factors of $-1$ (it is P- and C - odd), while the chromo - magnetic field picks up only one (it is C - odd but P - even, as it is a pseudo - vector). Therefore, the action term $S_\theta$ is CP - odd, $\mathrm{CP} S_\theta \mathrm{P}^{-1}\mathrm{C}^{-1} = -S_\theta$, and CP - invariance seems to be broken in QCD.[74]

As we discussed in the introductory section 1.2, the strong CP problem is the fine - tuning problem $|\theta| \lesssim 1.2 \cdot 10^{-10}$ by experimental results compared to the full range of theoretically possible values $\theta \in [-\pi, \pi)$. This also means that strong CP breaking cannot play a role in any CP violating process compared to CP violation by the weak interaction. To see this, one considers, for example, the decay of neural kaons. The neutral kaons $\overline{K}^0 = d\bar{s}$ and $\overline{K}^0 = s\bar{d}$ introduced in section 2.3 are not their own anti-particles (like $\pi^0 = \frac{1}{\sqrt{2}}(u\bar{u} - d\bar{d})$, for example), but they oscillate into each other $K^0 \leftrightarrow \overline{K}^0$ via box diagrams (figure 2.14) and are CP-partners $\mathrm{CP}K^0\mathrm{C}^{-1}\mathrm{P}^{-1} = \overline{K}^0$. This means they cannot be the true physical eigenstates of the theory. The linear superpositions $K_1 = \frac{1}{\sqrt{2}}(K^0 + \overline{K}^0)$ and $K_2 = \frac{1}{\sqrt{2}}(K^0 - \overline{K}^0)$ are each their own anti-particles, i.e., they are flavor eigenstates, and are CP eigenstates as well with $\mathrm{CP}K_{1,2}\mathrm{C}^{-1}\mathrm{P}^{-1} = \pm K_{1,2}$. However, due to small complex phases in the CKM matrix, CP is (slightly) broken by the weak interactions of the box diagram and the true physical/mass eigenstates are therefore given by $K^0_\mathrm{S} = \frac{1}{\sqrt{1+\varepsilon^2}}(K_1 + \varepsilon K_2)$ and $K^0_\mathrm{L} = \frac{1}{\sqrt{1+\varepsilon^2}}(K_2 + \varepsilon K_1)$ with $\varepsilon \approx 2.2 \cdot 10^{-3}$; this is called direct CP breaking. The names of these eigenstates correspond to the fact that $K^0_\mathrm{L}$ has a mean lifetime of circa $5 \cdot 10^{-8}$ s and is thus long lived compared to $K^0_\mathrm{S}$ with a 556-times shorter mean lifetime of approximately $9 \cdot 10^{-11}$ s. Additionally, there is also indirect CP breaking due to decays. In detail, the dominant CP conserving decay channels for the CP-even $K_1$ (or $K^0_\mathrm{S}$) are decays into two pseudoscalar pions, while the CP-odd $K_2$ (or $K^0_\mathrm{L}$) predominantly decays leptonically or into three pions. However, $K_2$ can also violate CP and decay into two-pion states. For kaons, this indirect CP violation is suppressed by a factor $\varepsilon' \approx 1.65\varepsilon \cdot 10^{-3}$, however. Therefore, the ration of decay rates $\frac{\Gamma(K^0_\mathrm{L} \to \pi^+\pi^-)}{\Gamma(K^0_\mathrm{S} \to \pi^+\pi^-)} = \varepsilon$ provides a good measure for the strength of (direct) CP breaking in weak interactions. From this ratio and the comparison to the upper bound $|\theta| \lesssim 1.2 \cdot 10^{-10}$ given above, one deduces the following: if either CP were actually conserved by weak interactions and instead strong CP breaking (in some loop process) were the source of $\varepsilon$ or if the weak interaction broke CP, but strong CP breaking were to actually play a role, a much higher value for $\theta$ would be required than is allowed by, for example, the neutron dipole moment bound.[75]

---

[73] [5, 33, 111]

[74] [3, 4, 6, 46, 116, 130, 140, 165]

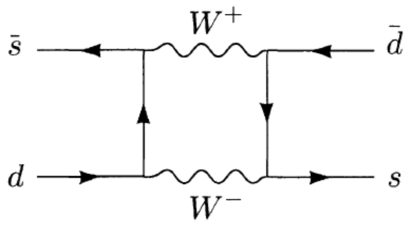

Figure 2.14: Taken from [3]: Kaon oscillations

Many ideas within the SM have been brought forward to solve the strong CP problem, e.g., a spontaneous CP-breaking modifying the Higgs mechanism and thereby the CKM matrix $Y$ so that $\theta \to \theta + \arg\det(Y)$ or a truly massless $u$-quark allowing for a $U(1)_\mathrm{A}$-transformation and a shift $\theta \to \theta - 2\beta n$ due to the Jacobian (2.5.1), but none has proven satisfactory. Both the Higgs and the CKM model of weak interactions work well and have been verified experimentally (for example by observation of the Higgs boson in the predicted mass range [19, 20]), with CP being explicitly broken in weak interactions, not spontaneously. The $u$-quark is not a truly massless particle (as would be required by a symmetry), so even if it were extremely light, this would just be a different fine-tuning problem, now for a vanishingly small $u$-mass.[76]

---

[75] [3, 4, 38, 46, 116]

A very promising solution of the strong CP problem is the extension of the SM in terms of the axion, the (p)NG boson of the $U(1)_{\text{Peccei Quinn}}$-symmetry, as discussed briefly in the introduction 1.2. The theory of axions, its role as a dark matter candidate, the dependency of its mass on the topology of the gluon field as well as experimental setups for axion detection are discussed in more detail in the following section 2.5.3. The strong CP-problem as a whole and the introduction of the axion as a possible resolution is the second example of symmetry shaping theory mentioned at the beginning of section 2.1.[77]

### 2.5.3 The Axion and its Relation to Topology

#### Standard Model - Extension, Resolution of the Strong CP - Problem and Axion as Dark Matter Candidate, Axion Mass and Topology

As stated before, the axion is introduced by extending the SM by the $U(1)_{\text{PQ}}$-symmetry. This has to be done such that this symmetry is unobservable in the current universe except for the existence and interactions of the axion. The two most important "benchmark" models that achieve this SM-extension are the *Kim-Shifman-Vainshtein-Zakharov* (KSVZ) *model* [172, 173] and the *Dine-Fischler-Srednicki-Zhitnitsky* (DFSZ) *model* [174, 175]. For this short overview on the theory of axions we employ the simpler KSVZ model and only briefly mention the DFSZ model at the end.[78]

The KSVZ model introduces the $U(1)_{\text{PQ}}$-symmetry via an additional vector-like quark $Q = Q_{\text{L}} \oplus Q_{\text{R}}$ and a complex, "SM-singlet" scalar field $\Phi$ which are both PQ-charged: $Q_{\text{L,R}}$ carries PQ-charge $\pm\frac{1}{2}$ and $\Phi$ has PQ-charge 1. For early-universe temperatures $T > f_a$, which is the very large energy scale setting spontaneous $U(1)_{\text{PQ}}$-symmetry breaking, the temperature-dependent Lagrangian reads

$$\mathcal{L} = \mathcal{L}_{\text{SM}} + \mathcal{L}_{\text{KSVZ}} = \mathcal{L}_{\text{SM}} + |\partial_{\mu_{\text{M}}}\Phi|^2 + i\overline{Q}\not{D}Q - (y\,\overline{Q}_{\text{L}}Q_{\text{R}}\Phi + \text{h.c.}) - V(\Phi,T)\,, \tag{2.5.6}$$

with:

- potential $$V(\Phi,T) = \frac{\lambda}{2}\left(|\Phi|^2 - \frac{f_a^2}{2}\right)^2 + \frac{\lambda}{3}T^2|\Phi|^2 \tag{2.5.7}$$
- $$D^\mu = \partial^\mu - iA^{i\,\mu}T^i_{SU(3)} - \frac{i}{2}V^{j\,\mu}T^j_{\text{SU(2)}} - iB^\mu\,. \tag{2.5.8}$$

Since $f_a \gg T_{\text{ew}} \approx 160\,\text{GeV}$, the electroweak symmetry breaking scale, the gauge bosons of the weak interaction are still massless and intermixed with the photon and the covariant derivative contains the gluon $A^i T^i_{SU(3)}$ as well as the gauge bosons $V^j T^j_{SU(2)}$ and $B$ of the electroweak symmetry group $SU(2)_\text{w} \otimes U(1)_Y$.[79] The additional quark $Q$ transforms under general representations of $SU(3)_\text{color}$ and $SU(2)_\text{w}$ described by the corresponding generators. The additional quark and scalar field interact via a Yukawa term; a detailed review of electroweak and Yukawa theory can be found in [3, sections 4 and 20] and [4, section 29], for example.[80]

---

[76] [3, 4, 6, 38, 46]
[77] [4, 6, 38, 46–50]
[78] [46, 47, 50]

Due to cooling of the universe, spontaneous symmetry breaking of $U(1)_\text{PQ}$ occurs at $T_\text{PQ} = \sqrt{\frac{3}{2}} f_a$. The scalar field then takes the form $\Phi = \frac{1}{\sqrt{2}} \left(F_a(T) + \phi(X)\right) e^{i \frac{a(X)}{F_a(T)}}$, with the temperature - dependent scale $F_a(T) = \sqrt{f_a^2 - \frac{2}{3} T^2}$ and axion field $a$ introduced as the corresponding Nambu - Goldstone boson. The KSVZ - Lagrangian is thus of the form

$$\begin{aligned} \mathcal{L}_\text{KSVZ} = & \frac{1}{2}(\partial^\mu \phi)^2 - \frac{\lambda F_a^2}{2} \phi^2 + \frac{1}{2}(\partial^\mu a)^2 + \frac{1}{F_a} \mathcal{L}^{(1)}_\text{int}\big((\partial a)^2, \phi, T\big) + \mathcal{L}^{(2)}_\text{int}(\phi, T) + \\ & + i \overline{Q} \not{D} Q - \Big(\frac{y}{\sqrt{2}} F_a \overline{Q}_\text{L} Q_\text{R}\, e^{i \frac{a}{F_a}} + \text{h.c.}\Big) + \mathcal{L}^{(3)}_\text{int}\big(\phi\, e^{i \frac{a}{F_a}}, \overline{Q} Q, T\big)\,. \end{aligned} \tag{2.5.9}$$

The axion is indeed massless, while the "radial excitation" field $\phi$ acquires a mass $M_\phi = \sqrt{\lambda} F_a(T)$, which grows from $M_\phi(T_\text{PQ}) = 0$ to be much larger than any SM - mass $M_\phi(T \ll f_a) \sim f_a \gg M_\text{SM}$ as the universe cools further. Now one performs an axion field - dependent axial $U(1)_\text{PQ}$ rotation[81] $Q \to e^{-i \frac{a(X)}{2 F_a(T)} \gamma^5} Q$, thereby removing the axion from both the $\phi$ - independent Yukawa term $\frac{y}{\sqrt{2}} F_a \overline{Q}_\text{L} Q_\text{R}\, e^{i \frac{a}{F_a}} + \text{h.c.} \to \frac{y}{\sqrt{2}} F_a \overline{Q}_\text{L} Q_\text{R} + \text{h.c.}$ and from $\mathcal{L}^{(3)}_\text{int}$, which originates from the Yukawa term. Therefore, the quark obtains a mass $M_Q(T) = \frac{y F_a(T)}{\sqrt{2}}$, which, as before, vanishes at $T_\text{PQ}$ and grows large at lower temperatures $M_Q(T \ll f_a) \sim \frac{y f_a}{\sqrt{2}} \gg M_\text{SM}$. Due to the anomalous nature of this axial transformation (cf. (2.5.1)), it introduces not only interactions of the axion with $Q$, but also axion - gauge boson interaction terms; after a proper normalization of the axion field one has

$$\begin{aligned} \delta \mathcal{L}_\text{KSVZ} = & - \frac{i}{16 \pi^2} \frac{a}{F_a(T)} \widetilde{G}^{i\,\mu\nu} G^{i\,\mu\nu} - \frac{i\, I(V)}{16 \pi^2 I(A)} \frac{a}{F_a(T)} \widetilde{V}^{j\,\mu\nu} V^{j\,\mu\nu} - \\ & - \frac{i}{16 \pi^2 I(A)} \frac{a}{F_a(T)} \widetilde{B}^{\mu\nu} B^{\mu\nu} + \frac{1}{F_a(T)} \mathcal{L}^{(4)}_\text{int}(\partial a, \overline{Q} \gamma \gamma^5 Q)\,, \end{aligned} \tag{2.5.10}$$

---

[79] The weak electroweak coupling strength $g_\text{weak}$ and the $U(1)$ - charge $Y$ were absorbed into the $V$ - and $B$ - boson, respectively, following the geometrical normalization for the gluon.

[80] [47, 50, 176, 177]

[81] The derivation of the axial anomaly in section 2.5.1 is actually performed using a local angle $\beta(\chi)$, so this axion - valued transformation is legitimate.

where $I(A)$ and $I(V)$ are the Dynkin indices of the $SU(3)_{\text{color}}$- and $SU(2)_{\text{w}}$ - representation and $V^{\mu\nu}$ and $B^{\mu\nu}$ are the field strength tensors. Their appearance is due to an analogous axial anomaly in the electroweak sector as was discussed in section 2.5.1 (e.g., see [3, section 19]).[82]

At temperatures below the electroweak symmetry breaking scale but above the critical temperature of chiral perturbation theory (cf. section 2.3) $T_{\text{c}} < T < T_{\text{ew}} \ll f_a$ - i.e., $F_a(T) \approx f_a$ and quarks and gluons are the degrees of freedom - the additional fields $Q$ and $\phi$ form a decoupled sector of super heavy particles that can be integrated out.[83] Also, the fields $V$ and $B$ form the $W^{\pm}$- and $Z$- bosons, which gain a mass via the Higgs mechanism, and the massless photons $A_{(\gamma)}$ (e.g., see [3, section 20], [4, section 29], [5, section VII.2] or [6, section 10]). (2.5.10) then yields $f_a^{-1}$ - damped coupling of the axion to gauge bosons

$$\begin{aligned}\delta\mathcal{L}_{\text{KSVZ}} = &- \frac{i}{16\pi^2}\frac{a}{f_a}\widetilde{G}^{i\,\mu\nu}G^{i\,\mu\nu} - \frac{i\,I(V)}{16\pi^2 I(A) s_{\text{w}}^2}\frac{a}{f_a}\widetilde{W}^{+\,\mu\nu}W^{-\,\mu\nu} - \\ &- \frac{i\,I(V)}{16\pi^2 I(A) s_{\text{w}}^2 c_{\text{w}}^2}\frac{a}{f_a}\widetilde{Z}^{\mu\nu}Z^{\mu\nu} - \frac{i}{16\pi^2 I(A)}\frac{a}{f_a}\widetilde{A}^{\mu\nu}_{(\gamma)}A^{\mu\nu}_{(\gamma)} - \\ &- \frac{i\,I(V)}{16\pi^2 I(A) s_{\text{w}} c_{\text{w}}}\frac{a}{f_a}\widetilde{A}^{\mu\nu}_{(\gamma)}Z^{\mu\nu}\,,\end{aligned} \tag{2.5.11}$$

where $W^{\pm\,\mu\nu}$, $Z^{\mu\nu}$, $A^{\mu\nu}_{(\gamma)}$ are the respective field strength tensors and $s_{\text{w}}$, $c_{\text{w}}$ are short-hand notations for the sine and cosine of the weak mixing/Weinberg angle given as $\sin^2(\theta_{\text{w}}) \approx 0.23$ [2] $\Rightarrow \cos^2(\theta_{\text{w}}) \approx 0.77$. $\mathcal{L}^{(4)}_{\text{int}}$ has been removed, since the quark $Q$ and scalar $\Phi$ are considered as integrated out of the now effective theory. These interactions (2.5.11) allow for experimental searches of the axion, as we are going to discuss below.[84]

As the temperature falls below $T_{\text{c}}$, strong interaction matter is no longer described by quarks and gluons as the degrees of freedom, but by light hadrons. The topological term and thus also the axion interaction with the hadrons is retained by performing a transformation of the light quarks and thus of the light quark mass matrix (cf. (2.1.24) and (2.3.11))

$$\begin{aligned}&\begin{pmatrix} u \\ d \\ s \end{pmatrix} \to e^{i\theta_{\text{eff}}(X)\,\gamma^5 A}\begin{pmatrix} u \\ d \\ s \end{pmatrix}\,,\ \theta_{\text{eff}}(X) = \theta + \frac{a(X)}{f_a}\,,\ \text{tr}(A) = 1 \\ \Rightarrow \quad & M_{q_l} \to e^{i\theta_{\text{eff}}\,\gamma^5 A} M_{q_l} e^{i\theta_{\text{eff}}\,\gamma^5 A} = M_{q_l}(a)\,,\end{aligned} \tag{2.5.12}$$

---

[82] [46, 47, 176]

[83] The resulting effective theory without $Q$ and $\Phi$ is already valid in the wide temperature range $T_{\text{ew}} < T \ll f_a$, the only difference is that the electroweak symmetry is still intact.

[84] [47, 176]

so that the axion - modified Lagrangian of chiral perturbation theory now contains a mass or interaction term $-\frac{\langle\bar{q}q\rangle}{3}\mathrm{tr}\big(M_{ql}(a)U^\dagger + UM_{ql}^\dagger(a)\big)$. The other interaction terms in (2.5.11) remain intact, as there is electroweak confinement. The axial transformation (2.5.12) is justified, as the axion can also couple to SM - quarks, either directly as in the DFSZ model which we briefly discuss below, or via loop level interactions in the KSVZ model (the interaction is then still $\mathcal{O}(f_a^{-1})$, but one should include a damping factor in the exponential to account for the higher order nature of the interaction). [85]

The above axion - gauge boson interactions (2.5.11) contain the topological charge densities for the gauge bosons. The $U(1)$ - topology of photons is trivial: $\int^\beta \mathrm{d}^4X\, \widetilde{A}^{\mu\nu}_{(\gamma)} A^{\mu\nu}_{(\gamma)} = 0$ and the photon vacuum is always homeomorphic to 0. Thus there are no photonic instantons/calorons, but this term does constitute an interaction $a\,\vec{E}_{(\gamma)}\cdot\vec{B}_{(\gamma)}$, the so - called Primakoff effect or Primakoff conversion. The $SU(2)$ - theory describing the weak interactions is topologically non - trivial, analogous to QCD, but its effects are exponentially suppressed as $e^{-g_{\text{weak}}^{-2}+g_{\text{strong}}^{-2}}$ due to the classical action of the electroweak calorons compared to the gluonic ones. Furthermore, electroweak calorons only contribute in baryon- and lepton - number violating processes. All in all, electroweak calorons could only have been relevant during the phase of baryo- and leptogenesis at very high temperatures in the early universe. The gluonic topological interaction term in (2.5.11) is therefore the dominant interaction term. It becomes significant for temperatures $\lesssim \Lambda_{\text{QCD}}$, where the non - perturbative topological effects of QCD become significant, i.e., calorons start to matter.[86]

At temperatures $T_{\text{c}} < T < T_{\text{ew}}$, the interaction of axions with calorons determined by $\mathcal{L} \supset -i\theta q - i\frac{a}{f_a}q = -i\theta_{\text{eff}}\, q$ yields an effective potential for the axion. This can be seen by following the discussion in section 2.4.4. The axion - modified DGA partition function (cf. (2.4.85)) reads $Z_{\text{DGA}}(\theta_{\text{eff}}) = N\exp\big(2\beta V\mathcal{D}\,\cos(\theta_{\text{eff}})\big)$ and the effective action is $\Gamma[\langle a\rangle] = -\ln(Z_{\text{DGA}}) = -\ln(N) + 2\beta V\mathcal{D}\,\cos(\theta_{\text{eff}})$. Comparing this with the definition of the effective potential (2.2.28), the effective axion potential, normalized by a vacuum containing no calorons and thus also only fully decoupled axions, reads

$$V_{\text{eff, DGA}}(\langle a\rangle) = \frac{1}{\beta V}\Big(-\ln\big(Z_{\text{DGA}}(\theta_{\text{eff}})\big) + \ln\big(Z_{\text{DGA}}(0)\big)\Big) = 2\mathcal{D}(T)\Big(1-\cos\Big(\theta+\frac{\langle a\rangle}{f_a}\Big)\Big), \tag{2.5.13}$$

where the normalization in terms of fully decoupled axions canceled the term $-\ln(N)$ and the HS caloron density $\mathcal{D}(T)$ is to be obtained as discussed in section 2.4.3. Comparing this expression for the axion effective potential with the topological susceptibility in the

---

[85] [44]

[86] [38, 178]

DGA (2.4.87), one notes that $V_{\text{eff}}(\langle a\rangle)$ can also be written as

$$V_{\text{eff, DGA}}(\langle a\rangle) = \chi_{\text{top}}(T)\big(1-\cos(\theta_{\text{eff}})\big)\,, \quad \theta_{\text{eff}} = \theta + \frac{\langle a\rangle}{f_a}\,. \tag{2.5.14}$$

At temperatures $T < T_{\text{c}}$ one can also derive an axion effective potential from chiral perturbation theory, which reads

$$V_{\text{eff, chPT}}(\langle a\rangle) = -M_\pi^2(T)f_\pi^2(T)\sqrt{1-\frac{\chi_{\text{top}}(T)}{M_\pi^2(T)f_\pi^2(T)}\sin^2(\theta_{\text{eff}})}\,, \tag{2.5.15}$$

with the chiral susceptibility in chiral perturbation theory as given in (2.4.88).[87]

Due to its effective potential (2.5.14) and (2.5.15) the axion settles into its VEV $\langle a\rangle = -f_a\theta$, thus minimizing $V_{\text{eff}}(\langle a\rangle)|_{\langle a\rangle=-f_a\theta} = 0$ and canceling the angle $\theta$, so that the overall effective angle vanishes $\theta_{\text{eff}}|_{\langle a\rangle=-f_a\theta} = 0$ and the strong CP problem is resolved. Furthermore, the axion also picks up a very small mass (cf. (1.2.1))

$$\begin{aligned} M_a^2(T \ll f_a) &= \left.\frac{\partial^2 V_{\text{eff}}(\langle a\rangle)}{\partial\langle a\rangle^2}\right|_{\langle a\rangle = f_a\theta} = \frac{1}{f_a^2}\left.\frac{\partial^2 V_{\text{eff}}(\theta_{\text{eff}})}{\partial\theta_{\text{eff}}^2}\right|_{\theta_{\text{eff}}=0} = \frac{\chi_{\text{top}}(T)}{f_a^2} = \\ &= \frac{1}{f_a^2}\cdot\begin{cases} 2\mathcal{D}(T) & : T > T_{\text{c}} \\ f_\pi^2(T)M_\pi^2(T)\,\dfrac{M_uM_dM_s}{(M_u+M_d)(M_uM_d+M_uM_s+M_dM_s)} & : T < T_{\text{c}} \end{cases}, \end{aligned} \tag{2.5.16}$$

which slowly grows as the temperature falls. We gave the current available evaluations of $\chi_{\text{top}}(0)$ and $M_a(0)$ in section 1.2.[88]

From the point of view of the $\Phi$ - potential (2.5.7), the “creation” of the axion mass via interactions can be understood intuitively as a tilt of the Mexican hat potential. This is sketched in figure 2.15.

All of the above features make the axion an excellent candidate for dark matter: Firstly, all its interactions are, at current low temperatures $T \ll f_a$, strongly damped as $f_a^{-1}$, making it de facto non - interacting with SM - particles. Secondly, it is a very light boson and would constitute cold, i.e., slow - moving, dark matter, which is favored by cosmology and astrophysics. Thirdly, the detection of the Higgs boson [19, 20] proved that the process of spontaneous symmetry breaking is realized in nature, validating the axion as the pNG boson associated to the spontaneous $U(1)_{\text{PQ}}$ - breaking.[89]

---

[87] [44, 46, 49, 52, 165]

[88] [39, 44, 49, 52, 165, 179]

[89] [43]

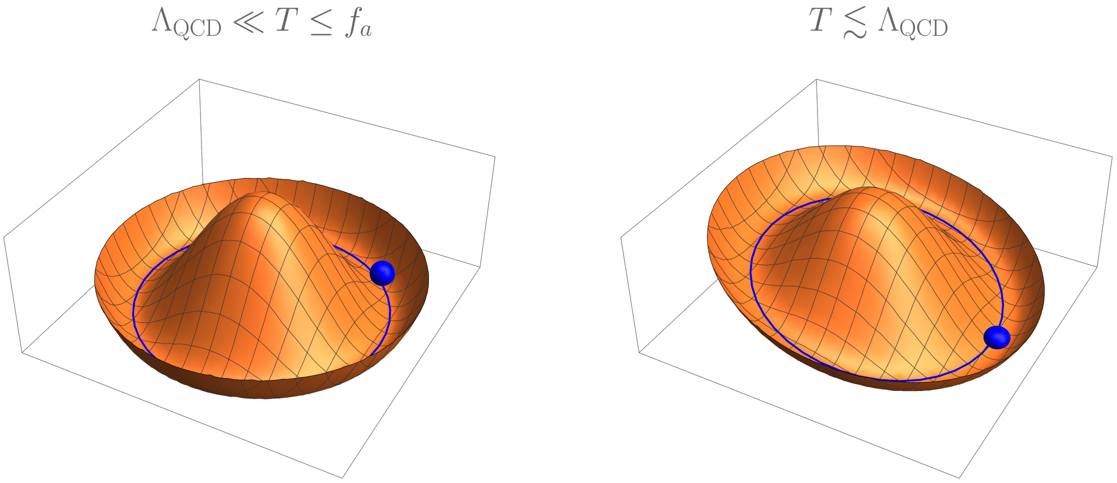

$\Lambda_{\mathrm{QCD}} \ll T \leq f_a$

$T \lesssim \Lambda_{\mathrm{QCD}}$

Figure 2.15: (Tilted) potential $V(\Phi)$ at high and low temperatures. For temperatures $\Lambda_{\mathsf{QCD}} \ll T < T_{\mathsf{PQ}}$, the spontaneously broken potential $V$ allows for a massless axion (●) as the excitation of angular propagation along the potential minimum (◯). As temperatures fall, $T \lesssim \Lambda_{\mathsf{QCD}}$, and QCD topology becomes relevant, the axion - caloron interactions effectively tilt $V$, associating a mass to the angular axion trajectories.

The discussion so far used the KSVZ axion model. Instead, the DFSZ model could also have been employed. Just like the KSVZ model it introduces a SM - singlet complex scalar $\Phi$, such that the axion is the Nambu - Goldstone boson of the spontaneously broken $U(1)_{\text{PQ}}$ - symmetry in the $\Phi$ - potential. Also, the $\Phi$ - radial mode becomes $f_a$ - heavy at low temperatures and decouples it from the theory. The DFSZ model is more intricate than the KSVZ model, however, as in DFSZ the SM - quarks are PQ - charged as well, just as an additional Higgs doublet interacting with $\Phi$ and with the SM - quarks (via Yukawa terms). The interaction of the axion with gauge bosons then enters via an axion - valued axial transformation of the SM - quarks, similar to the KSVZ model. The DFSZ model is discussed in more detail in [47], for example. Qualitatively and as far as the free - axion Lagrangian is concerned, the DFSZ model agrees with the KSVZ model. One of the main differences is that the DFSZ model includes tree level interaction terms of the axion with chiral currents of SM quarks $\propto \frac{\partial^\mu a}{F_a(T)} \overline{\psi}_f \gamma^\mu \gamma^5 \psi_f$, while in the KSVZ model such interactions happen only at loop level (nevertheless at first order in $f_a^{-1}$).[90].

### Experimental Searches for the Axion

A nice overview of the most important (current and future) experimental ventures on detecting the axion/measuring its mass and coupling strengths as well the experimental results is given in [50], which serves as a general reference for the following. We briefly present the concepts for a small selection of experiments employing the Primakoff effect - interaction of the axion with photons $a\, \vec{E}_{(\gamma)} \cdot \vec{B}_{(\gamma)}$, i.e., the conversion of axions into photons/light in the presence of a (strong) magnetic field - and vice versa.

The basic idea of “Light shining through Walls” - experiments, as illustrated in [50, figure 4], is to use a high intensity laser to inject photons into a cavity with a strong magnetic field, at the end of which an opaque wall absorbs the laser. By means of the Primakoff effect, some photons get converted into axions which, due to their weak interactions, pass through the wall unhindered and get converted back into photons in a second magnetic cavity behind the wall. Two photon sensors then detect whatever photons might have passed through the wall (through radiation or otherwise) and the surplus of photons after the back conversion chamber which was produced by the axions. The goal of such Light shining through Walls - experiments therefore is to measure the squared axion - photon coupling, which is proportional to $f_a^{-2}$.

Another type of experiments, so - called “Dark Matter Haloscopes”, make use of the fact that axions, as dark matter, should be present as a background even in local physics. The galactic dark matter halo has local energy density density $\epsilon \sim 0.2$ to $0.56\, \frac{\text{GeV}}{\text{cm}^3}$ [180,

---

[90] [44, 47]

181]. Assuming dark matter to be made up entirely of axions and using the axion mass $26.2\,\mu$eV, the local cold axion density then is $n_{\text{axion}} \sim (7.6 \text{ to } 21) \cdot 10^6 \, \frac{\text{axions}}{\text{cm}^3}$. In the standard halo model, the axions move "slowly" (given their small mass) with a virial velocity (i.e., purely due to galactic gravitation) of $v \approx 10^{-3}\, c$. All in all, the global collective of dark matter axions is then best described by a classical field (rather than a gas). The field is coherent over length scales comparable to the non-relativistic de Broglie wavelength $\lambda_{\text{axion}} = \frac{h}{M_a(0)v} \approx 1.240\,\text{m} \left(\frac{1\,\mu\text{eV}}{M_a(0)\,[\mu\text{eV}]}\right) \approx 47.3\,\text{m}$ and thus spatially constant on laboratory length scales. Furthermore, it oscillates with a frequency given by the axion mass $\nu \approx \frac{M_a(0)c^2}{h} \approx 2.42 \cdot 10^9 \, \frac{1}{\text{s}} \left(\frac{M_a(0)\,[\mu\text{eV}]}{1\,\mu\text{eV}}\right) \approx 6.34 \cdot 10^{10} \, \frac{1}{s}$, with a frequency spread of about $\delta\nu/\nu \sim 10^{-6}$. The idea of dark matter haloscopes shown in [50, figure 5] is to convert the dark matter axions into photons in a magnetic cavity via the Primakoff effect and detect these using a low-noise photon amplifier and a photon detector. If the resonance frequency of the magnetic cavity matches the axion frequency in the narrow bandwidth given by $\delta\nu/\nu$, the production of photons from dark matter axions is resonantly enhanced by a factor $\sim (\delta\nu/\nu)^{-1}$. By fine-tuning the magnetic resonance frequencies, dark matter haloscopes thus aim to measure the axion mass.

The third type of axion detection experiments we wish to mention are "Axion Helioscope" experiments, which aim to detect axions produced by the sun. In the strong magnetic fields inside the sun, produced by the high density of charged particles, axions are produced from solar core photons via the Primakoff effect. The typical core photon energies $\sim 3\,$keV (corresponding to the core temperature of $\sim 1\,$keV, for the factor $3$ cf. the discussion concerning $T_{\text{c}}$ in section 2.3) yield highly relativistic axions with energies $\sim 3\,\text{keV} \gg M_a(T \sim 1\,\text{keV})$ which leave the sun as an axion flux independent of $M_a$. As illustrated in [50, figure 9], axion helioscopes aim a magnetic cavity with subsequent X-ray optics and photon detectors at the sun, hoping to partially convert this flux of solar axions back into photons via the Primakoff effect and detect these photons. This way, the axion-photon coupling is to be measured.

# 3 Caloron Density for heavy Fermions – Large and Small Mass - Expansion

In the following, we now show how to obtain $\gamma_{\mathrm{s},\,-}$ in (2.4.82) including (non - vanishingly) heavy quarks. For that, we perform the expansions in (2.4.83).

## 3.1 Large Mass - Expansion of the Caloron Density

### 3.1.1 Schwinger Proper Time - Representation

First we consider a heavy quark and expand the fermionic log - caloron density (2.4.82) in powers of the inverse mass $(M\beta)^{-2k}$, $\mathbb{N} \ni k \geq 1$. For that, let the fermion mass $M$ be an energy scale much larger than the temperature: $M^2 \gg T^2 = \beta^{-2}$. We start by rescaling the fermion and regulator masses $M$, $\Lambda \to m = M\beta$, $\lambda = \Lambda\beta$ as well as the caloron size $\rho \to \varrho = \rho\beta^{-1}$ to dimensionless properties and by transforming the dimensionful $X$ - coordinates of $\mathbb{R}^3 \times S^1_{\text{rad.}\,=\,\beta/2\pi}$ to dimensionless $x$ - coordinates of $\mathbb{R}^3 \times S^1_{\text{rad.}\,=\,1/2\pi}$ centered on the caloron located at $C$:

$$X = (\vec{X}, t) \to x = \big(\vec{x} = \beta^{-1}(\vec{X} - \vec{C}\,), \tau = \beta^{-1}(t - C^4)\big)\,. \tag{3.1.1}$$

This change of coordinates also makes explicit the dimensions of integration and differentiation - $\int^\beta \mathrm{d}^4X \to \beta^4 \int^1 \mathrm{d}^4x$ and $\partial_X \to \beta^{-1}\partial_x$. Furthermore, it implies the introduction of $\beta$ - rescaled and therefore dimensionless fermion and gauge fields: $\psi(X) \to \beta^{-3/2}\psi(x)$ and $A^\mu_{\text{HS}}(X) \to \beta^{-1}A^\mu_{\text{HS}}(x) = -\beta^{-1}\,\bar{\eta}^{a\mu\nu}\partial^\nu \ln(\phi(x))\frac{\sigma^a}{2}$ with $\phi(x) = 1 + \frac{\pi\varrho^2\sinh(2\pi r)}{r(\cosh(2\pi r) - \cos(2\pi\tau))}$ (cf. (2.4.37) and (2.4.36), respectively). We use the same symbols for these fields and the ($\beta$ - )dimensionality is made clear by the $X$- or $x$ - dependency. Accordingly, we also have the field strength $G^{\mu\nu}(X) \to \beta^{-2}G^{\mu\nu}(x)$. In the following, we use the rescaled fields exclusively. The fermionic part of (2.4.82) is dimensionless and thus remains unchanged by all of the above (i.e., it can safely be reformulated in terms of the dimensionless coordinates and parameters $m$, $\lambda$, $\varrho$). In order to discuss the "dimensions" of such rescaled properties and of final expressions as well as for dimensionally verifying our results, we assign each object in this dimensionless picture the "$\beta$ - dimension" of its non - rescaled counterpart, e.g., $m$ is of $\beta$ - dimension $[m]_\beta = \text{Length}^{-2}$.

The determinants of the free Klein - Gordon operator $-\partial_-^2 + m^2$ and the one in a caloron background $-D_-^2 + m^2$ are inherently divergent. To regularize and renormalize these divergences, employ the *Schwinger proper time* $(s)$ - representation of the (anti-periodic, scalar) log - caloron density (see [4] for a good review of Schwinger proper time and [60, 154] for the $T = 0$ - case):

$$\begin{aligned}\gamma_{\text{scalar, anti-periodic}}(\varrho) = \gamma_{\text{s, }-}(\varrho) = \ln\left(\frac{\det(-D_-^2 + m^2)\,\det(-\partial_-^2 + \lambda^2)}{\det(-D_-^2 + \lambda^2)\,\det(-\partial_-^2 + m^2)}\right) = \\ = -\int_0^\infty \frac{\mathrm{d}s}{s}\left(e^{-m^2 s} - e^{-\lambda^2 s}\right)\int^1 \mathrm{d}^4x\,\mathrm{tr}\left\langle x\,\middle|\,\left(e^{-(-D_-^2)s} - e^{-(-\partial_-^2)s}\right)\middle|\,x\right\rangle\,. \qquad (3.1.2)\end{aligned}$$

In this representation, the mass is separated from the now purely caloron - dependent operator $-D_-^2$ and from $-\partial_-^2$. Note that the proper time $s$ is also $\beta$ - rescaled and thus dimensionless with $\beta$ - dimension $[s]_\beta = \text{Length}^2$. $\langle x|e^{-(-D_-^2)s}|y\rangle = \langle xs\,|\,y\rangle^-$ and $\langle x|e^{-(-\partial_-^2)s}|y\rangle = \langle xs\,|\,y\rangle_0^-$ are the anti-periodic proper time - Green's functions, i.e., they satisfy proper time - Schrödinger equations: $-\partial_s\,\langle xs\,|\,y\rangle^- = -D_{x,\,-}^2\,\langle xs\,|\,y\rangle^-$ and analogously for $\langle xs\,|\,y\rangle_0^-$. These Green's functions describe a propagation from $y$ to $x$ in proper time $s$. From them, the ordinary anti-periodic propagators from $y$ to $x$ in Euclidean time are reproduced by $s$ - integration: $\Delta^-(x, y, m^2) = \langle x|\frac{1}{-D_-^2 + m^2}|y\rangle = \int_0^\infty \mathrm{d}s\,\langle xs\,|\,y\rangle^-\,e^{-m^2 s}$ (analogously for $\Delta_0^-(x, y, m^2)$). As the ordinary propagator has $[\Delta_{(0)}^\pm]_\beta = \text{Length}^{-2}$ and the $s$ - integration is of $\beta$ - dimension $[\mathrm{d}s]_\beta = \text{Length}^2$, the proper time - Green's functions must be $[\langle xs\,|\,y\rangle_{(0)}^\pm]_\beta = \text{Length}^{-4}$. This is confirmed by the fact that their $\beta$ - 4 - dimensional $x$ - integration then yields a dimensionless quantity. All in all, the proper time - representation allows us to consider the proper time - Green's function of a massless, anti-periodic boson. The proper time - Green's function is also called the *heat kernel* of the operator, here of $-D_-^2$ and $-\partial_-^2$, with respect to proper time.[1]

The log - caloron density (3.1.2) is then given by the spacetime integral over all traced, closed loop - propagators of the anti-periodic scalar in a periodic spacetime with a caloron background. This is illustrated in figure 3.1. Closed loop propagators are called coincident propagators and they diverge. In order to regularize the caloron density, one performs an asymptotic expansion in the inverse mass, the so - called *heat kernel expansion*, of the coincident proper time - Greens functions. Said expansion is possible, because the term $e^{-m^2 s}$ in $\gamma$, together with the large fermion mass, leads to an exponential suppression of large proper time - regions, i.e., only very small $s \lesssim m^{-2} \ll 1$ contribute to $\gamma$. Thus, the heat kernel expansion, which is valid for $s \searrow 0$, can be employed. We discuss this expansion in detail in the next section 3.1.2 and perform it numerically in section 3.1.3.

---

[1] [154, 182]

### 3.1.2 Heat Kernel Expansion at finite Temperature

#### Heat Kernel Expansion at zero Temperature

We first present the details of the heat kernel expansion at $T = 0$, i.e., in infinite, dimensionless 4 - dimensional Euclidean spacetime[2] $\mathbb{R}^4_{\text{dim.less}}$ with coordinates $\bar{x}^\mu$ (the barred notation again denotes the $T = 0$ - case), and a BPST instanton background $\overline{A}_{\text{BPST}}$ (2.4.27), as discussed in [60, 154, 182–184]. To emphasize the difference to the finite temperature heat kernel expansion in the following section, we also employ the $T = 0$ - barred notation for the BPST instanton $\overline{A}^\mu_{\text{BPST}}$ and its field strength $\overline{G}^{\mu\nu}$. The coincident heat kernel in $\mathbb{R}^4$ can be expanded as

$$\langle \bar{x} s \,|\, \bar{x} \rangle = \left\langle \bar{x} \,\middle|\, e^{-(-\overline{D}^2)s} \,\middle|\, \bar{x} \right\rangle \overset{s \searrow 0}{\cong} \sum_{k \,\in\, \mathbb{N}} \frac{s^{k-2}}{(4\pi)^2}\, \bar{a}_{2k}\big(\overline{A}_{\text{BPST}}(\bar{x})\big) \tag{3.1.3}$$

in terms of *Seeley - DeWitt* heat kernel *coefficients* $\bar{a}_{2k}$; and analogously for $-\bar{\partial}^2$. The large - mass expansion corresponds to inserting the series expansion (3.1.3) in (3.1.2), switching the order of the $k$ - sum and $s$ - integral, and performing the $s$ - integral followed by the operator trace. The uniform convergence properties needed to exchange sum and integral are not generally fulfilled, so the large - mass $k$ - summation is generally only asymptotic. Therefore, it is valid to consider only its first few terms. The known Seeley - DeWitt heat kernel coefficients for $-\overline{D}^2$ read

$$\begin{aligned}
\bar{a}_0 &= \mathbb{1}_{2\times 2}\,, \quad \bar{a}_2 = 0\,, \quad \bar{a}_4(\bar{x}) = -\frac{1}{12}\overline{G}^{\mu\nu}\overline{G}^{\mu\nu}\,, \\
\bar{a}_6 &= -\frac{1}{6}\Big(\frac{2i}{15}\overline{G}^{\mu\nu}\overline{G}^{\nu\kappa}\overline{G}^{\kappa\mu} - \frac{1}{20}\overline{G}^{\nu\kappa;\,\mu}\overline{G}^{\nu\kappa;\,\mu}\Big)\,, \\
\bar{a}_8 &= \frac{1}{24}\Big( -\frac{1}{21}\overline{G}^{\mu\nu}\overline{G}^{\nu\kappa}\overline{G}^{\kappa\lambda}\overline{G}^{\lambda\mu} + \frac{11}{420}\overline{G}^{\mu\nu}\overline{G}^{\kappa\lambda}\overline{G}^{\mu\nu}\overline{G}^{\kappa\lambda} + \frac{2}{35}\overline{G}^{\mu\nu}\overline{G}^{\mu\nu}\overline{G}^{\kappa\lambda}\overline{G}^{\kappa\lambda} + \\
&+ \frac{4}{35}\overline{G}^{\mu\nu}\overline{G}^{\nu\kappa}\overline{G}^{\mu\lambda}\overline{G}^{\lambda\kappa} + \frac{6i}{35}\overline{G}^{\kappa\lambda}\overline{G}^{\lambda\nu;\mu}\overline{G}^{\nu\kappa;\mu} + \frac{8i}{105}\overline{G}^{\kappa\lambda}\overline{G}^{\mu\nu;\kappa}\overline{G}^{\mu\nu;\lambda} - \frac{1}{70}\overline{G}^{\kappa\lambda;\nu\mu}\overline{G}^{\kappa\lambda;\mu\nu}\Big)\,,
\end{aligned} \tag{3.1.4}$$

$\bar{a}_{10}$ is given in appendix B and $\bar{a}_{12}$ in [183], the $\bar{a}_{2k\,>\,12}$ are unknown. Here we use the notation $\overline{G}^{\mu\nu;\kappa} = \overline{D}^\kappa\overline{G}^{\mu\nu} = [\overline{D}^\kappa, \overline{G}^{\mu\nu}]$, $\overline{G}^{\mu\nu;\kappa\lambda} = \overline{G}^{\mu\nu;\kappa;\lambda} = \overline{D}^\lambda\overline{D}^\kappa\overline{G}^{\mu\nu}$, etc.

---

[2] $\beta$ - rescaled and centered around $Z$ for consistency

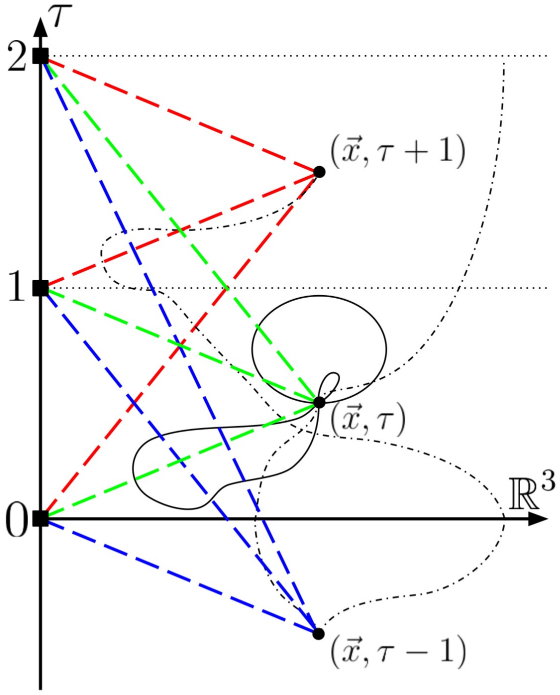

Figure 3.1: Some closed loop - propagators in the periodic spacetime $\mathbb{R}^3 \times S^1_{\text{rad.}={}^1\!/_{2\pi}}$ as they appear in the log - caloron density (3.1.2). The periodicity of the spacetime is made explicit by showing all the time copies of the boson and BPST instanton making up the thermal boson and HS caloron, respectively.
The anti-periodic boson copies are located at (•) $x + j\hat{e}_4$, $j \in \mathbb{Z}$ and are connected by closed loops; the solid lines (——) show "aperiodically closed loops" which do not encounter the spacetime periodicity, the dash - dotted lines (—·—·—) show loops which encounter the periodicity $j$ times and close (anti-)periodically for $j$ even (odd). The caloron is made up of periodic instanton copies located at (■) $0 + j\hat{e}_4$.
All boson copies and all connecting, closed loop - propagators are affected by all periodic copies of the instanton; this is symbolized by the dashed red, green and blue lines (– – –) connecting the instanton and boson copies.

The “traced integral - heat kernel coefficients” $\bar{b}_{2k}$, i.e., those appearing in the traced and integrated heat kernel expansion used in the log - caloron density

$$\mathrm{Tr}\big(\langle \bar{x}s \,|\, \bar{x}\rangle\big) = \mathrm{Tr}\Big(\Big\langle \bar{x}\,\Big|\, e^{-(-\overline{D}^2)s}\,\Big|\,\bar{x}\Big\rangle\Big) \overset{s\searrow 0}{\cong} \sum_{k\,\in\,\mathbb{N}} \frac{s^{k-2}}{(4\pi)^2} \int_{\mathbb{R}^4} \mathrm{d}^4\bar{x}\ \mathrm{tr}\Big(\bar{b}_{2k}\big(\overline{A}_{\mathrm{BPST}}(\bar{x})\big)\Big)\,, \tag{3.1.5}$$

can be simplified using trace cyclicity, IBP as well as the equation of motion and the Bianchi identity.[3] These traced integral - coefficients are

$$\begin{aligned}
\bar{b}_0 &= \bar{a}_0\,, \quad \bar{b}_2(\bar{x}) = \bar{a}_2\,, \quad \bar{b}_4(\bar{x}) = \bar{a}_4\,, \quad \bar{b}_6 = \frac{i}{90}\overline{G}^{\mu\nu}\overline{G}^{\mu\kappa}\overline{G}^{\nu\kappa}\,,\\
\bar{b}_8 &= \frac{1}{24}\left(\frac{17}{210}\overline{G}^{\mu\nu}\overline{G}^{\mu\nu}\overline{G}^{\kappa\lambda}\overline{G}^{\kappa\lambda} + \frac{2}{35}\overline{G}^{\mu\nu}\overline{G}^{\mu\kappa}\overline{G}^{\nu\lambda}\overline{G}^{\kappa\lambda} + \frac{1}{105}\overline{G}^{\mu\nu}\overline{G}^{\nu\kappa}\overline{G}^{\kappa\lambda}\overline{G}^{\lambda\mu} + \right.\\
&\qquad\qquad \left. + \frac{1}{420}\overline{G}^{\mu\nu}\overline{G}^{\kappa\lambda}\overline{G}^{\mu\nu}\overline{G}^{\kappa\lambda}\right),\\
\bar{b}_{10} &= \frac{1}{120}\left(\frac{i}{945}\overline{G}^{\mu\nu}\overline{G}^{\kappa\lambda}\overline{G}^{\alpha\mu}\overline{G}^{\nu\kappa}\overline{G}^{\lambda\alpha} - \frac{47i}{126}\overline{G}^{\mu\nu}\overline{G}^{\mu\nu}\overline{G}^{\kappa\lambda}\overline{G}^{\lambda\alpha}\overline{G}^{\alpha\kappa} + \right.\\
&\quad + \frac{i}{126}\overline{G}^{\mu\nu}\overline{G}^{\kappa\lambda}\overline{G}^{\mu\nu}\overline{G}^{\lambda\alpha}\overline{G}^{\alpha\kappa} + \frac{i}{63}\overline{G}^{\mu\nu}\overline{G}^{\nu\kappa}\overline{G}^{\mu\lambda}\overline{G}^{\lambda\alpha}\overline{G}^{\alpha\kappa} - \frac{11i}{189}\overline{G}^{\mu\nu}\overline{G}^{\kappa\lambda}\overline{G}^{\lambda\nu}\overline{G}^{\mu\alpha}\overline{G}^{\alpha\kappa} + \\
&\quad + \frac{37i}{945}\overline{G}^{\mu\nu}\overline{G}^{\nu\kappa}\overline{G}^{\kappa\lambda}\overline{G}^{\lambda\alpha}\overline{G}^{\alpha\mu} + \frac{4}{189}\overline{G}^{\nu\alpha}\overline{G}^{\alpha\lambda}\overline{G}^{\nu\kappa;\mu}\overline{G}^{\kappa\lambda;\mu} - \frac{2}{63}\overline{G}^{\kappa\lambda}\overline{G}^{\nu\alpha;\mu}\overline{G}^{\nu\alpha}\overline{G}^{\kappa\lambda;\mu} - \\
&\quad - \frac{2}{189}\overline{G}^{\kappa\lambda}\overline{G}^{\nu\alpha;\mu}\overline{G}^{\alpha\lambda}\overline{G}^{\nu\kappa;\mu} + \frac{4}{63}\overline{G}^{\kappa\lambda}\overline{G}^{\kappa\lambda}\overline{G}^{\nu\alpha;\mu}\overline{G}^{\nu\alpha:\mu} + \frac{2}{63}\overline{G}^{\mu\kappa}\overline{G}^{\kappa\lambda}\overline{G}^{\nu\alpha;\mu}\overline{G}^{\nu\alpha;\lambda} + \\
&\quad \left. + \frac{4}{189}\overline{G}^{\kappa\lambda}\overline{G}^{\lambda\nu}\overline{G}^{\nu\alpha;\mu}\overline{G}^{\alpha\kappa;\mu}\right).
\end{aligned} \tag{3.1.6}$$

For $\bar{a}_{12}$ the corresponding simplification to $\bar{b}_{12}$ is unknown, i.e., $\bar{b}_{12} = \bar{a}_{12}$.

Counting $\beta$ - dimensions in the heat kernel expansion, the heat kernel coefficients (regular and traced integral) have to be $[\bar{a}_{2k}]_\beta = \mathrm{Length}^{-2k} = \mathrm{Mass}^{2k}$ to reproduce the $\beta$ - dimension of the proper time - Green’s functions. In general, the expansion of the heat kernel $\Big\langle \bar{x}\,\Big|\, e^{-\overline{\mathcal{D}}s}\,\Big|\,\bar{x}\Big\rangle$ for some general second order differential operator of Laplace type $\overline{\mathcal{D}} = -\bar{g}_{\mu\nu}(\overline{\nabla}^\mu - i\overline{A}^\mu)(\overline{\nabla}^\nu - i\overline{A}^\nu) + f(\bar{x})$, with metric $g$, geometrical covariant derivative $\nabla$ and some gauge - invariant matrix - valued function $f(\bar{x})$, has its coefficients $\bar{a}_k$ constructed from all possible invariants formed using $f$, the Riemann, Ricci and scalar curvature, the gauge field strength and their covariant derivatives. All these tensors are of $\beta$ - dimension $\mathrm{Length}^{-2}$ and of even rank 0, 2 or 4. Therefore, odd Seeley - DeWitt coefficients $\bar{a}_{2k+1}$

---

[3] $\overline{G}^{\mu\nu;\mu} = 0$ and $\varepsilon^{\nu\mu\kappa\lambda}\overline{G}^{\kappa\lambda;\mu} = 0 \Leftrightarrow \overline{G}^{\kappa\lambda;\mu} + \overline{G}^{\mu\kappa;\lambda} + \overline{G}^{\lambda\mu;\kappa} = 0$, respectively.

corresponding to $s^{k+\frac{1}{2}-2}$ cannot be constructed, as they would be $[\bar{a}_{2k+1}]_\beta = \text{Length}^{-2k-1}$ which requires an odd number of covariant derivatives that cannot be contracted with tensors of even rank to form an invariant. As can be seen above, in the case of $\overline{\mathcal{D}} = -\overline{D}^2$ in flat spacetime, all invariants are constructed from the field strength.

Since regions of larger (i.e., "non - infinitesimal") proper time give strongly exponentially damped contributions, it is reasonable to both truncate the heat kernel expansion after the first few (or finitely many) terms and keep the full $s$ - integral over $\mathbb{R}$.

The free coincident proper time - Green's function is described by a single heat kernel coefficient $\langle \bar{x} s \,|\, \bar{x} \rangle_0 = \langle \bar{x} | e^{-(-\bar{\partial}^2)s} | \bar{x} \rangle \overset{s \searrow 0}{\cong} \frac{s^{-2}}{(4\pi)^2} \, \bar{a}_0(0)$ with $\bar{a}_0(0) = \bar{a}_{\text{free}} = \bar{b}_{\text{free}} = \mathbb{1}_{2\times 2}$.[4]

### Structure of the Expansion at finite Temperature

At finite temperature $T$ and for the $\beta$ - rescaled spacetime $\mathbb{R}^3 \times S^1_{\text{rad.} = {}^1/_{2\pi}}$ containing a HS caloron background $A_{\text{HS}}(x)$ (2.4.37), the coincident heat kernel expansion reads (analogously to (3.1.3))

$$\langle xs \,|\, x \rangle^- = \left\langle x \,\middle|\, e^{-(-D_-^2)s} \,\middle|\, x \right\rangle \overset{s \searrow 0}{\cong} \sum_{k \,\in\, \mathbb{N} \,\cup\, \mathbb{N} + \frac{1}{2}} \frac{s^{k-2}}{(4\pi)^2} \, a_{2k}\big(A_{\text{HS}}(x)\big) \tag{3.1.7}$$

with heat kernel coefficients of $\beta$ - dimension $[a_{2k}]_\beta = \text{Length}^{-2k}$ [185, 186].

These heat kernel coefficients $a_{2k}$ are given by linear combinations of, firstly, the $T = 0$ - coefficients $\bar{a}_{2k}$ and, secondly, the chromo - electric and -magnetic fields $E^i = G^{i4}$ and $B^i = \frac{1}{2}\varepsilon^{ijk} Gjk$ and their covariant derivatives, together with matrix - valued combination coefficient functions

$$\varphi_l(\vec{x}, \varrho, s) = \sum_{\alpha \,\in\, \mathbb{Z}} \sqrt{4\pi} \, s^{\frac{l+1}{2}} \left(i p_\alpha^{\text{bos/ferm}} - \ln \Omega(\vec{x}, \varrho)\right)^l e^{s\left(i p_\alpha^{\text{bos/ferm}} - \ln \Omega(\vec{x}, \varrho)\right)^2} , \tag{3.1.8}$$

where $p_\alpha^{\text{bos/ferm}} = \beta \omega_\alpha^{\text{bos/ferm}} = \begin{pmatrix} 2\pi\alpha \\ 2\pi(\alpha + {}^1/_2) \end{pmatrix}$, $\alpha \in \mathbb{Z}$, are the $\beta$ - rescaled $\begin{pmatrix} \text{bosonic} \\ \text{fermionic} \end{pmatrix}$ Matsubara frequencies (cf. (2.2.24) and (2.2.27)) with $[p^{\text{bos/ferm}}]_\beta = \text{Length}^{-1}$ and

$$\Omega(\vec{x}, \varrho) = \mathrm{T} \exp\left(i \int_0^1 \mathrm{d}\tau \, A^4_{\text{HS}}(\vec{x}, \tau)\right) \tag{3.1.9}$$

is the untraced Polyakov loop (2.2.29). The coefficient functions $\varphi_l$ are dimensionless - see [185, 186] for the non - $\beta$ - rescaled expressions. Note that now also odd $a_{2k}$ with half-integer $k$ are possible. They can be constructed using temporal derivatives that do not have to be contracted and the chromo-electric and -magnetic fields, which are tensors with $[E]_\beta = [B]_\beta = \text{Length}^{-2}$ and rank 1. For $-D_-^2$ the finite-$T$ heat kernel coefficients have the structure $a_{2k\,\text{even}} = \varphi_0\, \bar{a}_{2k\,\text{even}} + \mathcal{A}_{2k\,\text{even}}(\varphi_{l\,\text{even}}, D^{(a)}E, D^{(b)}B)$ and $a_{2k\,\text{odd}} = \mathcal{A}_{2k\,\text{odd}}(\varphi_{l\,\text{odd}}, D^{(a)}E, D^{(b)}B)$, with fermionic Matsubara frequencies in the $\varphi_l$ to encode the anti-periodicity of the corresponding eigenfunctions and $\mathcal{A}_{2k}$ denoting the finite-$T$ terms.

---

[4] [60, 154, 182–184]

The traced integral-heat kernel coefficients $b_{2k}$ in the operator trace (cf. (3.1.5))

$$\text{Tr}\big(\, \langle xs \,|\, x\rangle^- \,\big) = \text{Tr}\Big( \Big\langle x \,\Big|\, e^{-(-D_-^2)s} \,\Big|\, x \Big\rangle \Big) \overset{s \searrow 0}{\cong} \sum_{k \,\in\, \mathbb{N} \,\cup\, \mathbb{N}+\frac{1}{2}} \frac{s^{k-2}}{(4\pi)^2} \int^1 \mathrm{d}^4x \, \text{tr}\Big( b_{2k}\big(A_{\text{HS}}(x)\big)\Big)\,, \tag{3.1.10}$$

are of the same structure as the $a_{2k}$-coefficients, but contain simpler finite-$T$ terms $\mathcal{B}_{2k}(\varphi_l, D^{(a)}E, D^{(b)}B)$ and the traced integral-heat kernel coefficients at $T = 0$:

$$\begin{aligned}
b_0(A_{\text{HS}}) &= \varphi_0 = \varphi_0 \bar{b}_0\,, \qquad b_4(A_{\text{HS}}) = \varphi_0 \bar{b}_4 - \frac{\varphi_0 + 2\varphi_2}{6} E^i E^i\,,\\
b_6(A_{\text{HS}}) &= \varphi_0 \bar{b}_6 + \frac{\varphi_0 + 2\varphi_2}{60}\Big( \big(E^{i;i}\big)^2 + \big(G^{ij;4}\big)^2 - 2E^i G^{ij} E^j \Big) - \\
&\qquad - \left( \frac{\varphi_0}{15} + \frac{\varphi_2}{3} + \frac{2\varphi_4}{15} \right) \big(E^{i;4}\big)^2\,,\\
b_{6\,<\,2k\,\leq\,12}(A_{\text{HS}}) &= \varphi_0 \bar{b}_{2k} + \text{“unknown”}\,;
\end{aligned} \tag{3.1.11}$$

the other coefficients either vanish in general ($2k \in \{1,3\}$) or in this case ($2k \in \{2,5\}$), are unknown beyond $\varphi_0 \bar{b}_{2k}$ ($6 < 2k \leq 12$ and $2k =$ even) or are completely undetermined ($2k > 6$ and $2k =$ odd). In appendix D.1 and the ancillary files we present our method to find the detailed functional forms of the known coefficients $\bar{b}_{0\,\leq\,2k\,\leq\,12}(A_{\text{HS}})$ and finite temperature terms $\mathcal{B}_{0\,\leq\,2k\,\leq\,6}(A_{\text{HS}})$ as given in (3.1.11); for that we use the *OGRe*-package [187] for *Mathematica*.[5]

The free contribution resulting from $-\partial_-^2$ can be calculated more straightforwardly, i.e., without employing the elaborated techniques described in [185, 186] that lead to the coefficient function-structure. Instead, a simpler method from [185, 186] can be utilized, where the temporal part of the asymptotic expansion, that is, the expansion in Matsubara frequencies, is split off and the heat kernel expansion is only performed in the 3-dimensional spatial part for $-\vec{\partial}^2$. This yields

---

[5] [185, 186]

$$\begin{aligned}\langle xs\,|\,x\rangle_0^- &= \left\langle x \left| e^{-(-\partial_-^2)s} \right| x \right\rangle = \sum_{\alpha\,\in\,\mathbb{Z}} \left\langle \vec{x} \left| e^{-\left(-\vec{\partial}^{\,2}-(ip_\alpha^{\text{ferm}})^2\right)s} \right| \vec{x} \right\rangle = \\ &\overset{s\searrow 0}{\cong} \sum_{\alpha\,\in\,\mathbb{Z}} e^{-(p_\alpha^{\text{ferm}})^2 s} \frac{1}{(4\pi s)^{\frac{3}{2}}}\, \mathbb{1}_{2\times 2} = \frac{1}{(4\pi s)^2}\, \varphi_0(\vec{x},0,s)\mathbb{1}_{2\times 2}\,,\end{aligned} \tag{3.1.12}$$

with $\Omega(\vec{x},0) = \mathbb{1}$ in the free case. This is equal to a 4 - dimensional heat kernel expansion with the $-\partial_-^2$ - heat kernel coefficient $a_{\text{free}} = b_{\text{free}} = \varphi_0|_{A=0} = \mathbb{1}$.[6]

The coefficient function $\varphi_0$ can be transformed using the Poisson summation formula [185, 186]. Treating $\tilde{f}(p) = \exp\left((ip - \ln\Omega)^2\right)$ as a continuous, aperiodic function of $p \in \mathbb{R}$ with a Fourier transform $f(\tau)$, one has $\sum_{p\,\in\,\mathbb{Z}} \tilde{f}(p) = \sum_{j\,\in\,\mathbb{Z}} f(j)$, i.e.,

$$\varphi_0 = \sum_{\alpha\,\in\,\mathbb{Z}} \sqrt{4\pi s}\, e^{s\left(ip_\alpha^{\text{bos/ferm}} - \ln(\Omega)\right)^2} = \sum_{j\,\in\,\mathbb{Z}} (\pm 1)^j\, \Omega^j\, e^{-\frac{j^2}{4s}} \tag{3.1.13}$$

with $\pm 1$ for the $\begin{pmatrix}\text{bosonic}\\\text{fermionic}\end{pmatrix}$ case. Therefore, for small $s$ all terms with $j \neq 0$ are exponentially suppressed such that $\varphi_0 \overset{s\searrow 0}{\longrightarrow} \mathbb{1}_{2\times 2}$ with $\mathbb{1}_{2\times 2}$ the identity in $SU(2)$ - color space. This Fourier back - transformation connects the momentum space of Matsubara frequencies back to Euclidean time. This means that modes with $j = 0$ correspond to loops in the heat kernel expansion that close "aperiodically", i.e., without crossing the (anti-)periodic boundary at $\tau = 1 \mathrel{\widehat{=}} 0$, while $j \neq 0$ - modes correspond to loops which close by "(anti-)periodically" crossing the boundary $j$ times, cf. figure 3.1.

Furthermore, reintroducing the explicit dimensionalities we observe an exponential damping factor $e^{-\frac{j^2\beta^2}{4s}}$ which, in the zero temperature limit $\beta \to \infty$, goes to 0 for $j \neq 0$, i.e, in this limit all finite $T$ - effects vanish as expected.

We can also use the Poisson summation formula to calculate higher $\varphi_{l\,>\,0}$. For that, notice that by modifying the coefficient functions as $\varphi_l(a) = \sum_p \sqrt{4\pi}\, s^{(l+1)/2}\, Q^l e^{sQ^2 + aQ}$ with $Q = ip - \ln(\Omega)$, we have the general form $\varphi_l = s^{l/2}\,(\partial_a^{(l)}\varphi_0(a))|_{a\,=\,0}$. Now we Fourier transform $\varphi_0(a)$, employ the Poisson formula and perform the $a$ - derivatives before finally setting $a = 0$. For the first few coefficient functions up to $l = 4$ and the combinations appearing in the known traced Seeley - DeWitt coefficients (3.1.11) we find:

---

[6] The sum over the $n$ - modes (and thus over the Matsubara frequencies) gives a well - defined object, the 2nd Jacobi theta function $\vartheta_2(0, e^{-4\pi^2 s})$.

$$
\begin{aligned}
\varphi_1 &= -\sum_{j\,\in\,\mathbb{Z}} (\pm 1)^j\, \Omega^j\, e^{-\frac{j^2}{4s}}\, \frac{j}{2s^{1/2}}\,, &
\varphi_2 &= \sum_{j\,\in\,\mathbb{Z}} (\pm 1)^j\, \Omega^j\, e^{-\frac{j^2}{4s}}\, \frac{j^2-2s}{4s}\,,\\
\varphi_3 &= -\sum_{j\,\in\,\mathbb{Z}} (\pm 1)^j\, \Omega^j\, e^{-\frac{j^2}{4s}}\, \frac{j(j^2-6s)}{8s^{3/2}}\,, &
\varphi_4 &= \sum_{j\,\in\,\mathbb{Z}} (\pm 1)^j\, \Omega^j\, e^{-\frac{j^2}{4s}}\, \frac{j^4-12j^2s+12s^2}{16s^2}\,,\\
\varphi_0 + 2\varphi_2 &= \sum_{j\,\in\,\mathbb{Z}} (\pm 1)^j\, \Omega^j\, e^{-\frac{j^2}{4s}}\, \frac{j^2}{2s}\,, \\
\frac{\varphi_0}{15} + \frac{\varphi_2}{3} + \frac{2\varphi_4}{15} &= \sum_{j\,\in\,\mathbb{Z}} (\pm 1)^j\, \Omega^j\, e^{-\frac{j^2}{4s}}\, \frac{j^2(j^2-2s)}{120s^2}\,.
\end{aligned}
\tag{3.1.14}
$$

We note a general structure: $\varphi_{l\ \text{even/odd}}$ contains terms $\frac{j^c}{s^{c/2}}$ with even/odd $0 \le c \le l$. Again all modes $j \neq 0$ are exponentially suppressed and for $\varphi_{l\ \text{odd}}$ the $j = 0$ - mode vanishes identically (i.e., they contain only terms with $c > 0$). The limit $s \searrow 0$ produces the $j = 0$ - mode: $\varphi_2 \xrightarrow{s \searrow 0} -\frac{1}{2}\mathbb{1}_{2\times 2}$, $\varphi_4 \xrightarrow{s\searrow 0} \frac{3}{4}\mathbb{1}$, ($\varphi_6 \xrightarrow{s\searrow 0} -\frac{15}{8}\mathbb{1}$, $\varphi_8 \xrightarrow{s\searrow 0} \frac{105}{16}\mathbb{1}$) and $\varphi_{1,3(,5,7)} \xrightarrow{s\searrow 0} 0$ as well as $\varphi_0 + 2\varphi_2 \xrightarrow{s\searrow 0} 0$ and $\frac{\varphi_0}{15} + \frac{\varphi_2}{3} + \frac{2\varphi_4}{15} \xrightarrow{s\searrow 0} 0$. From this we can also see that the (known) finite $T$ - terms, which contain only $j \neq 0$ - modes, vanish for $\beta \to \infty$, just as was discussed for $\varphi_0$ above.

The $j$-th powers of the untraced Polyakov loop $\Omega$ appearing in the $\varphi_l$ - coefficient functions can be calculated straightforwardly. For that, we first perform the $\tau$ - integral of $A^4_{\text{HS}} = -\overline{\eta}^{a4\nu}\partial^\nu \ln(\phi(r,\tau))\frac{\sigma^a}{2} = -\vec{\partial}\ln\phi \cdot \frac{\vec{\sigma}}{2} = -\frac{\partial_r\phi}{\phi}\,\frac{\vec{x}\cdot\vec{\sigma}}{2r}$ (result confirmed in [188]):

$$
\begin{aligned}
-i\int_0^1 \mathrm{d}\tau\, \frac{\partial_r\phi}{\phi} &= 2\pi i \left( 1 - \frac{\varrho^2\big(2\pi r\cosh(2\pi r) - \sinh(2\pi r)\big) + 2r^2\sinh(2\pi r)}{r\sqrt{2(r^2+\pi^2\varrho^4)\big(\cosh(4\pi r)-1\big) + 4\pi\varrho^2 r\sinh(4\pi r)}} \right) = \\
&= 2\pi i\,\omega(r,\varrho)\,.
\end{aligned}
\tag{3.1.15}
$$

The untraced Polyakov loop then reads $\Omega = \exp\big(i\pi\,\omega\,\frac{\vec{x}\cdot\vec{\sigma}}{r}\big)$. As shown in figure 3.2, $\omega(r,\varrho) \ge 0\ \forall\, r,\varrho \ge 0$, especially $\omega(0,\varrho) = 1$ and $\omega(r,0) = 0$ (the latter correctly reproduces the vacuum background case) with an according discontinuity at $r = \varrho = 0$ that we can make obvious by a simultaneous Taylor expanding of $\omega(r\varepsilon,\varrho\varepsilon)$ for $\varepsilon \searrow 0$. This expansion yields $\omega = \big((r^2+\varrho^2)^{1/2} - r\big)(r^2+\varrho^2)^{-1/2} + \mathcal{O}(\varepsilon^2)$ and we see that now taking $r \searrow 0$ yields 1 while $\varrho \searrow 0$ produces 0. Furthermore, $\omega$ falls off quickly at large

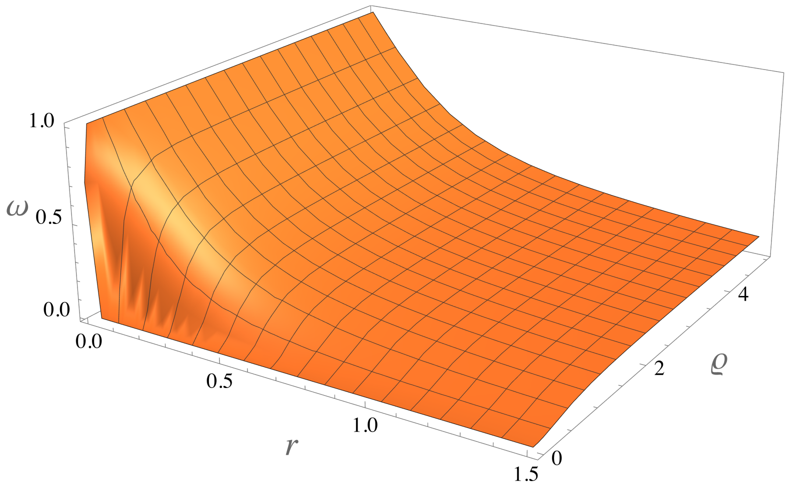

Figure 3.2: $\omega(r,\varrho)$ as it appears in the untraced Polyakov loop $\Omega = \exp\left(i\pi\,\omega\,\frac{\vec{x}\cdot\vec{\sigma}}{r}\right)$.

radii; by expanding[7] we find $\omega = \frac{\varrho^4\pi^2}{r^2} + \mathcal{O}\big((\frac{\varrho}{r})^2\big)$. Second, we expand $\Omega$ using $\left(\frac{\vec{x}\cdot\vec{\sigma}}{r}\right)^2 = \mathbb{1}$ and find $\Omega(\vec{x},\varrho) = \cos\big(\pi\,\omega(r,\varrho)\big)\,\mathbb{1}_{2\times 2} + i\sin\big(\pi\,\omega(r,\varrho)\big)\frac{\vec{x}\cdot\vec{\sigma}}{r}$. The inverse is therefore given by $\Omega^{-1} = \exp\left(-\,i\pi\,\omega\,\frac{\vec{x}\cdot\vec{\sigma}}{r}\right) = \cos\big(\pi\,\omega(r,\varrho)\big)\,\mathbb{1} \;-\; i\sin\big(\pi\,\omega(r,\varrho)\big)\frac{\vec{x}\cdot\vec{\sigma}}{r}$ and the general $j$-th power reads

$$\Omega^j(\vec{x},\varrho) = \cos\big(j\pi\,\omega(r,\varrho)\big)\,\mathbb{1}_{2\times 2} + i\sin\big(j\pi\,\omega(r,\varrho)\big)\frac{\vec{x}\cdot\vec{\sigma}}{r} \quad \forall j \in \mathbb{Z}\,. \tag{3.1.16}$$

Since $\omega \overset{r\,\rightarrow\infty}{\rightarrow} 0$, $\Omega^j$ approaches the free case $\Omega^j(\vec{x},0) = \mathbb{1}\ \forall j$ at large (enough) distances from the caloron as expected.

It is important to note that the leading terms of (3.1.11), i.e., those given by $\bar{b}_{2k}$ times $\mathbb{1} \subset \varphi_0$ (cf. $j=0$ in (3.1.13)), yield the same expansion structure as at $T=0$. Here, “leading” means dominant compared to the $j \neq 0$ - modes of $\varphi_0$ and $\varphi_l$, which are due to finite temperature, exponentially suppressed as $s \searrow 0$ (cf. (3.1.14)) and which we find below to be of $\mathcal{O}(m^b e^{-m})$, $b \sim 1$. Therefore, the leading expansions are equivalent for the periodic and anti-periodic operators $D_+^2$ and $D_-^2$, while the summations should actually differ. The exponentially damped $\mathcal{B}$ - terms, which introduce boundary condition - dependency, cannot be thought of as the required corrections, however, as they are of the order of the typical ambiguity associated with summing an asymptotic series like the heat kernel series.

---

[7] $\omega \overset{r\,\rightarrow\infty}{\rightarrow} 1 - \frac{r^2 e^{2\pi r} + \varrho^2\pi r e^{2\pi r}}{r\sqrt{r^2 e^{4\pi r} + 2\varrho^2\pi r e^{4\pi r}}} = 1 - \frac{1+\frac{\varrho^2\pi}{r}}{\sqrt{1+\frac{2\varrho^2\pi}{r}}} = \frac{\varrho^4\pi^2}{r^2} + \mathcal{O}\big((\frac{\varrho}{r})^2\big)$

The finite - $T$ terms in (3.1.11) are therefore uncertainties in the summation and we have to ensure that $m$ is large enough to allow us to neglect such terms. The exponential damping of the finite - $T$ terms is due to heavy quarks $m \gg 1$ exploring $\mathbb{R}^3 \times S^1_{\text{rad.}={}^1\!/_{2\pi}}$ on length scales $m^{-1} \ll 1$, i.e., essentially as they would $\mathbb{R}^4$. Figure 3.3 sketches this: a typical caloron $\varrho \approx 0.5$ (gray) and the heavy quark - propagation range (red). Temperature then only enters in the way that it modifies the caloron fields; the short - range propagation only feels the boundary conditions in an exponentially suppressed fashion because propagation of a heavy field over a distance $\beta \mathrel{\widehat{=}} 1$ is exponentially small.

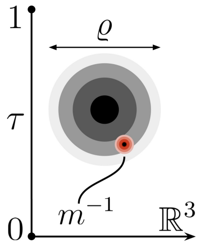

Figure 3.3

In the end we also connect the large - $m$ expansion to the small - $m$ one which, as we are going to see in section 3.2, contains explicit boundary condition information and thus serves as a “boundary condition” itself for the interpolation between small - $m$ and large - $m$ expansion (cf. (2.4.83) and the short outlook below), ensuring the correct anti-periodic properties.

### 3.1.3 Heat Kernel Expansion Order by Order - Numerical Results

Now we plug the finite temperature - heat kernel coefficients with the above $\varphi_l$ into the log - caloron density of the heavy, anti-periodic scalar particle in a HS caloron background:

$$\gamma_{\text{s},-} = -\int_0^\infty \frac{\mathrm{d}s}{s}\left(e^{-m^2 s} - e^{-\lambda^2 s}\right)\int^1 \mathrm{d}^4x\ \mathrm{tr}\left(\sum_{k\,\in\,\mathbb{N}\,\cup\,\mathbb{N}+\frac{1}{2}} \frac{s^{k-2}}{(4\pi)^2}\, b_{2k}\big(A_{\text{HS}}(x)\big) - b_{\text{free}}\right). \tag{3.1.17}$$

We note that only the leading contributions of the coefficients (3.1.11) contain “actual physical information”, while we use the finite - $T$ uncertainties to find a lower limit on the large masses.

As we stated before, we perform the $s$ - integrals first. In general, these integrals are of the structure (analogously for $\lambda^2$ instead of $m^2$)

$$I\Big(m^2, k, j^2; \frac{c}{2}\Big) = \int_0^\infty \mathrm{d}s\ e^{-m^2 s - \frac{j^2}{4s}}\, s^{k-3-\frac{c}{2}}\,, \tag{3.1.18}$$

with $c$ the semi-positive definite integer resulting from the $\varphi_l$ in (3.1.14). For $j = 0$, i.e., the non - suppressed/leading modes, this integer is $c = 0$ and the integrals are

$$I(m^2,k,0;0)\begin{cases}\to\ \infty & : k\in\{0,1,2\}\\ =\dfrac{1}{m^{2k-4}}\widetilde{\Gamma}(k-2)=\dfrac{(k-3)!}{m^{2k-4}} & : \mathbb{N}\ni k\geq 3\end{cases}, \tag{3.1.18.a}$$

where by $\widetilde{\Gamma}$ we denote the Gamma function [189]. Note that there are no leading contributions for half-integer $k$. To parametrize the divergences in (3.1.18.a), one introduces a a small-scale cut-off $\varepsilon_s$ for the $s$-integral and finds [189]

$$I(m^2,0\leq k\leq 2,0;0)=\lim_{\varepsilon_s\searrow 0}\int_{\varepsilon_s}^{\infty}\mathrm{d}s\, e^{-m^2 s}\, s^{k-3}=$$

$$=\begin{cases}\dfrac{e^{-m^2\varepsilon_s}(1-m^2\varepsilon_s)}{2\varepsilon_s^2}+\dfrac{m^4}{2}\left(\ln(m^2\varepsilon_s)+\gamma_{\mathrm{E}}+\mathcal{O}(m^2\varepsilon_s)\right) & : k=0\\ \dfrac{e^{-m^2\varepsilon_s}}{\varepsilon_s}+m^2\left(\ln(m^2\varepsilon_s)+\gamma_{\mathrm{E}}+\mathcal{O}(m^2\varepsilon_s)\right) & : k=1\\ \lim\limits_{\varepsilon_s\searrow 0}\widetilde{\Gamma}(0,m^2\varepsilon_s)=-\ln(m^2\varepsilon_s)-\gamma_{\mathrm{E}}+\mathcal{O}(m^2\varepsilon_s) & : k=2\end{cases}, \tag{3.1.18.b}$$

where $\gamma_{\mathrm{E}}$ is the Euler-Mascheroni-constant and $\widetilde{\Gamma}(0,z)$ is the upper incomplete Gamma function. For $j\neq 0$ with general $c\neq 0$ we obtain

$$I\left(m^2,k,j^2;\frac{c}{2}\right)=2^{-(k-3-\frac{c}{2})}\left(\frac{|j|}{m}\right)^{k-2-\frac{c}{2}}K_{|k-2-\frac{c}{2}|}(|j|m)\overset{m^2\gg 1}{\sim}$$

$$\sim 2^{-(k-\frac{5}{2}-\frac{c}{2})}\sqrt{\pi}\,\frac{|j|^{k-\frac{5}{2}-\frac{c}{2}}}{m^{k-\frac{3}{2}-\frac{c}{2}}}e^{-|j|m}\left(1+\sum_{u\,\in\,\mathbb{N}^+}\frac{\prod_{v\,=\,1}^{u}\left(4(k-2-\frac{c}{2})^2-(2v-1)^2\right)}{u!(8|j|m)^u}\right), \tag{3.1.18.c}$$

with $K_\alpha(x)$ the modified Bessel function of the second kind. Since the $K_\alpha$-expansion is an asymptotic one, it is justified for large (enough) $|j|m$ to keep only the first few terms. The integrals $I\left(m^2,k,j^2;\frac{c}{2}\right)$ are $e^{-m}$-exponentially suppressed, but part of the infinite summation over all $j\neq 0$-modes of the coefficient functions $\varphi_l$. Therefore, one cannot simply neglect them and we compute the total finite-$T$ terms to quantify the large enough masses required to keep these terms suppressed compared to the leading contributions. Note also that for the $j$-summation $I\left(m^2,k,j^2;\frac{c}{2}\right)$ has to be multiplied by the corresponding factor $\propto j^c$ from the coefficient functions (cf. (3.1.14)).

In the following we consider the different orders of the traced integral-heat kernel expansion and present our analytical and numerical results for the resulting log-caloron density contributions. A detailed description of our numerical methods can be found in the appendices D.1 and D.2 and the ancillary files.

**Order $k = 0$:**

The leading $j = 0$ - modes of both $b_0(A_{\text{HS}}) = \varphi_0(A_{\text{HS}})\mathbb{1} = \sum_{j \in \mathbb{Z}}(-1)^j \Omega^j e^{-\frac{j^2}{4s}}$ (3.1.13) and the vacuum term $b_{\text{free}} = \varphi_0(0) = \sum_{j \in \mathbb{Z}}(-1)^j e^{-\frac{j^2}{4s}}\mathbb{1}$ both give rise to quadratically divergent contributions $I(m^2, 0, 0; 0)$ (cf. (3.1.18.b)) and multiply the spacetime volume spacetime $V = \text{vol}(\mathbb{R}^3 \times S^1_{\text{rad.} = {}^1/_{2\pi}}) = \int^1 \mathrm{d}x^4$. These divergent contributions therefore cancel identically and the leading $k = 0$ - contribution to the log - caloron density (3.1.17) vanishes: $\gamma_0 = 0$ (we denote $j = 0$ - mode terms from $\varphi_0 \bar{b}_{2k}$ as $\gamma_{2k}$ ).

For the $j \neq 0$ - modes of $b_0(A_{\text{HS}})$ and $b_0(0)$ we find finite $s$ - integrals $I(m^2, 0, j^2; 0)$. Plugging these $s$ - integrals into the infinite $j$ - summation of $\varphi_0$ (3.1.13), we find the contributions from $b_0(A_{\text{HS}})$ to be given by

$$\sum_{j \in \mathbb{Z}\setminus\{0\}} (-1)^j \Omega^j \, 2^{\frac{5}{2}} \sqrt{\pi} \frac{m^{\frac{3}{2}}}{|j|^{\frac{5}{2}}} e^{-|j|m} \Big(1 + \frac{15}{8|j|m} + \mathcal{O}(m^{-2})\Big) . \tag{3.1.19}$$

Here and in the proceeding treatment of the large $m$ - expansion's finite - temperature terms we drop all contributions which are additionally (to the overall $e^{-m}$ - damping) mass damped by inverse powers of $m$ with respect to the leading $j = 0$ - mode: for $k = 0$ the "leading" term is $0$ and thus $\mathcal{O}(m^0)$, therefore, we neglect all terms $\mathcal{O}(m^{-1/2})$ and lower in (3.1.19).

We plug in $\Omega^j$ (3.1.16), keeping only the traceful part of $\Omega^j$, i.e., $\cos(j\pi\,\omega)\,\mathbb{1}$, which is denoted as "$=_{\text{tr}}$", and perform the $j$ - summation:

$$\begin{aligned}
&\sum_{j \in \mathbb{Z}\setminus\{0\}} (-1)^j \Omega^j \, 2^{\frac{5}{2}} \sqrt{\pi} \frac{m^{\frac{3}{2}}}{|j|^{\frac{5}{2}}} e^{-|j|m} \Big(1 + \frac{15}{8|j|m}\Big) =_{\text{tr}} \\
&=_{\text{tr}} \sum_{j \in \mathbb{N}^+} (-1)^j \cos(j\pi\,\omega)\, 2^{\frac{7}{2}} \sqrt{\pi} \frac{m^{\frac{3}{2}}}{j^{\frac{5}{2}}} e^{-jm} \Big(1 + \frac{15}{8jm}\Big) \mathbb{1} = \\
&= 2^{\frac{7}{2}} \sqrt{\pi} \bigg( m^{\frac{3}{2}} \,\text{Re}\big(\text{Li}_{\frac{5}{2}}(-e^{i\pi\omega - m})\big) + \frac{15\, m^{\frac{1}{2}}}{8} \,\text{Re}\big(\text{Li}_{\frac{7}{2}}(-e^{-i\pi\omega - m})\big) \bigg) \mathbb{1} = \\
&= 2^{\frac{7}{2}} \sqrt{\pi} \Big( \text{L}_{\frac{3}{2},\frac{5}{2}}\big(m, \omega(r,\varrho)\big) + \frac{15}{8} \text{L}_{\frac{1}{2},\frac{7}{2}}\big(m, \omega(r,\varrho)\big) \Big) \, \mathbb{1} \, ,
\end{aligned} \tag{3.1.20}$$

where $\text{Li}_b(z)$ is the polylogarithm[8] and we abbreviate a (hereafter) often recurring pattern by introducing the function

$$\text{L}_{a,b}\big(m, \omega(r,\varrho)\big) = m^a \,\text{Re}\Big(\text{Li}_b\big(-\, e^{i\pi\omega(r,\varrho) - m}\big)\Big) . \tag{3.1.21}$$

---

[8] Not to be confused with the polylogarithmic function.

For leading order mass terms $\mathcal{O}(m^d)$ our rule about dropping mass damped terms thus translates to neglecting all contributions $\mathrm{L}_{a,b}$ with $a < d$.

The free case for $b_0(0)$ is calculated analogously with $\Omega = \mathbb{1} \Leftrightarrow \omega = 0$ and we obtain the contribution

$$2^{\frac{7}{2}}\sqrt{\pi}\left(m^{\frac{3}{2}}\,\mathrm{Li}_{\frac{5}{2}}(-e^{-m}) + \frac{15\,m^{\frac{1}{2}}}{8}\,\mathrm{Li}_{\frac{7}{2}}(-e^{-m}) + \mathcal{O}\big(m^{-\frac{1}{2}}\big)\right)\mathbb{1}\,. \tag{3.1.22}$$

The overall contribution to the log-caloron density is therefore given by the space(time) integral (additional factor of $(2\pi)^{-1}$ due to a factor of 2 from $\mathrm{tr}(\mathbb{1}_{2\times 2})$, the heat kernel expansion prefactor $(4\pi)^{-2}$, the volume element $4\pi r^2\,\mathrm{d}r$ and the integral $\int_0^1 \mathrm{d}\tau$ trivially yielding $1$)

$$\begin{aligned}\gamma_0^{\varphi_0}(m,\varrho) = \frac{2^{\frac{5}{2}}}{\sqrt{\pi}}\int_0^\infty \mathrm{d}r\, r^2\Big(\mathrm{L}_{\frac{3}{2},\frac{5}{2}}(m,\omega(r,\varrho)) + \frac{15}{8}\,\mathrm{L}_{\frac{1}{2},\frac{7}{2}}(m,\omega(r,\varrho)) -\\ - m^{\frac{3}{2}}\,\mathrm{Li}_{\frac{5}{2}}(-e^{-m}) - \frac{15\,m^{\frac{1}{2}}}{8}\,\mathrm{Li}_{\frac{7}{2}}(-e^{-m})\Big)\,.\end{aligned} \tag{3.1.23}$$

By $\gamma_{2k}^{\varphi_0}(m,\varrho)$ we denote the finite temperature contribution to the log-caloron density at heat kernel expansion order $k$ coming from the $j \neq 0$-modes of $\varphi_0\bar{b}_{2k}$. The corresponding terms from $\mathcal{B}_{2k}$ we denote as $\gamma_{2k}^{\mathcal{B}}$ (here obviously $\gamma_0^{\mathcal{B}} = 0$).

Note that $\omega$ falls off quickly with increasing $r$, so that the caloron background-terms in $\gamma_0^{\varphi_0}$ quickly approach the $r$-independent vacuum terms which renders the overall spacetime integral finite. To see this, first note that $\gamma_0^{\varphi_0}$ is a positive definite function which we prove by employing the Fermi-Dirac integral-representation of the polylogarithm function [190]:

$$\mathrm{Li}_b(-e^{-z}) = -\widetilde{\Gamma}^{-1}(b)\int_0^\infty \mathrm{d}u\,\frac{u^{b-1}}{e^{u+z}+1}\,. \tag{3.1.24}$$

This holds $\forall\,\mathrm{Re}(b) > 0$ and $\forall z \in \mathbb{C}$, $z \neq \pm i\pi + x$, $x \leq 0$.[9] In our case this excludes only the pathological combination $r = 0 \,\wedge\, m \leq 0$. The $\mathcal{O}(m^a)$-terms of $\gamma_0^{\varphi_0}$ $(a = \frac{3}{2}, \frac{1}{2})$ are then determined (up to positive prefactors $m^a \cdot \text{const.}$) by the integral

$$\widetilde{\Gamma}^{-1}(b)\int_0^\infty \mathrm{d}u\, u^{b-1}\left(\frac{1}{e^{u+m}+1} - \frac{1+e^{u+m}\cos(\pi\omega)}{e^{2(u+m)}+2e^{u+m}\cos(\pi\omega)+1}\right) \tag{3.1.25}$$

with $b = a+1, 2$. This integrand is positive $\forall\, u+m > 0 \wedge \omega \in [0,1]$. In the limit $r \searrow 0 \Rightarrow \omega \nearrow 1 \Rightarrow \cos(\pi\omega) \to -1$ it simplifies to $\frac{2u^{b-1}e^{u+m}}{e^{2(u+m)}-1}$ which is finite given $u \geq 0$, $m > 1$. In

---

[9] I.e., it holds $\forall z \in \mathbb{C}$ except $z \in \mathbb{R} \wedge z \leq -1$.

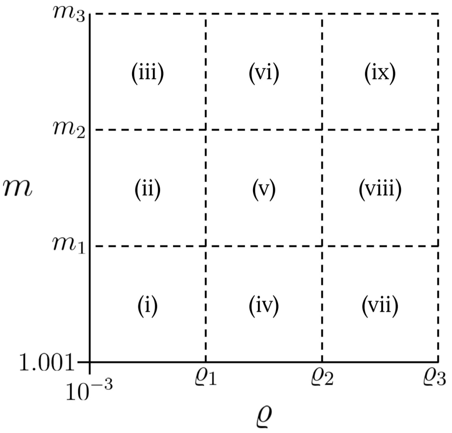

Figure 3.4: The general splitting of the $m$ - $\varrho$ - plane required for parametrizing the finite temperature heat kernel corrections (3.1.27), (3.1.29), (3.1.34) and (3.1.35).

the limit $r \to \infty \Rightarrow \omega \searrow 0$, the integrand falls off as $\omega^2 \propto r^{-4}$ (cf. below (3.1.15)) and for large $u$ as $u^{b-1} e^{-u}$, rendering the $u$ - integral finite and $\gamma_0^{\varphi_0}$ as a whole "$\int_0^\infty \mathrm{d}r\, r^{-2}$ - finite".

In the ancillary files we provide the data for $\gamma_0^{\varphi_0}(m, \varrho)$, which we obtained using the *SymPy* [191] and *mpmath* [192] packages[10]. It is difficult to provide a good functional fit to this data - and indeed for all finite temperature corrections; the best approximation for the finite temperature ambiguities is given by the function

$$\zeta(m, \tilde{\varrho}, \varrho\,;\, \tilde{a}, \tilde{b}, \tilde{c}, a, b, c) = e^{-m} \left( \tilde{a}\, m^{\tilde{b}}\, \tilde{\varrho}^{\,\tilde{c}} + a\, m^b \varrho^c \right), \tag{3.1.26}$$

where the choice of $\tilde{\varrho}$ or $\varrho$ depends on the $\varrho$ - value as we see in the following ($\tilde{\varrho} = \frac{\tilde{\rho}}{\beta}$ (2.4.40) describes HS (anti-)calorons at length scales $r \ll 1$, where they resemble BPST (anti-)instantons of modified size $\tilde{\varrho}$ (cf. (2.4.39)). We compute $\gamma_0^{\varphi_0}$ on an $m$ - $\varrho$ - grid of 15000 points formed by 100 fermion masses $m \in \{1.001 \cdot (\frac{200}{1.001})^{\frac{i}{99}} \,|\, \mathbb{N} \ni i \leq 99\}$ "times" 150 caloron sizes $\varrho \in \{10^{-3} \cdot (\frac{200}{10^{-3}})^{\frac{i}{149}} \,|\, \mathbb{N} \ni i \leq 149\}$ with $m_{\text{min}} = 1.001$, $\varrho_{\text{min}} = 10^{-3}$ and $m_{\text{max}} = \varrho_{\text{max}} = 200$, splitting the $m$ - $\varrho$ - plane in nine sectors (i) - (ix) as shown in figure 3.4. The coefficients $\tilde{a}$, $\tilde{b}$, $\tilde{c}$, $a$, $b$, $c$ in these sectors as well as the sector boundaries are given in table 3.1. We write this using the short - hand notation

$$\gamma_0^{\varphi_0}(m, \varrho) \overset{(3.1.26)}{=} \zeta(m, \tilde{\varrho}, \varrho\,;\, \tilde{a}, \tilde{b}, \tilde{c}, a, b, c)\Big|_{\text{Table 3.1}}\,. \tag{3.1.27}$$

---

[10] These packages allows us to handle polylogarithms in symbolic and numerical *Python* - calculations, respectively.

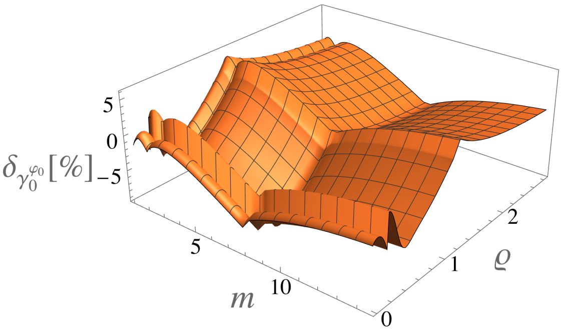

Figure 3.5: Relative error $\delta_{\gamma_0^{\varphi_0}}$ of the fitting function (3.1.27).

| | (i) | (ii) | (iii) | (iv) | (v) | (vi) | (vii) | (viii) | (ix) |
|---|---|---|---|---|---|---|---|---|---|
| $\tilde a$ | 8.878 | 8.107 | 5.000 | $\tilde a_0^{(1)}(\varrho)$ | $\tilde a_0^{(2)}(\varrho)$ | $\tilde a_0^{(3)}(\varrho)$ | 0 | 0 | 0 |
| $\tilde b$ | 1.03 | 1.17 | 1.42 | 1.03 | 1.17 | 1.42 | 0 | 0 | 0 |
| $\tilde c$ | 3.00 | 3.00 | 3.00 | 3.13 | 3.13 | 3.13 | 0 | 0 | 0 |
| $a$ | 0 | 0 | 0 | $a_0^{(1)}(\varrho)$ | $a_0^{(2)}(\varrho)$ | $a_0^{(3)}(\varrho)$ | 3.075 | 2.823 | 1.700 |
| $b$ | 0 | 0 | 0 | 1.04 | 1.18 | 1.42 | 1.04 | 1.18 | 1.43 |
| $c$ | 0 | 0 | 0 | 2.25 | 2.26 | 2.26 | 2.00 | 2.00 | 2.00 |

Table 3.1: The $(m,\varrho)$-sector boundaries corresponding to figure 3.4 are $m_1 \approx 2$, $m_2 \approx 8$, $\varrho_1 \approx 0.22$ and $\varrho_2 \approx 1.2$, the upper values are $m_3 = \varrho_3 = 200$. The $\tilde a$ and $a$ functions in sectors (iv) - (vi) are required due to the rapid transition of small-caloron ($\tilde\varrho$) to large-caloron description ($\varrho$); they contain step functions for which we choose the logistic function approximation $\Theta_l(\varrho,u) = \big(1+e^{-2u\varrho}\big)^{-1}$: $\tilde a_0^{(1)} = 11.24\big(1-\Theta_l(\varrho-0.4,7.5)\big)$, $\tilde a_0^{(2)} = 10.29(1-\Theta_l)$, $\tilde a_0^{(3)} = 6.350(1-\Theta_l)$, $a_0^{(1)} = 2.904\,\Theta_l(\varrho-0.4,7.5)$, $a_0^{(2)} = 2.657\,\Theta_l$, $\tilde a_0^{(3)} = 1.650\,\Theta_l$.

The boundaries in table 3.1 are roughly set by hand to minimize the fitting error, which is shown in figure 3.5.

Concerning the $\lambda^2$-regulator terms: the $j=0$-modes cancel again like for $m^2$ and the $j\neq 0$-mode contribution $\gamma_0^{\varphi_0}(\lambda,\varrho)$ vanishes exponentially as $\lambda\to\infty$.

All in all, the diverging $j=0$-modes in the caloron and the vacuum background cancel, just like for $T=0$ (where $\bar b_0(\bar A_{\text{Instanton}}) = \mathbb{1} = \bar b_0(0)$) and we find the finite-temperature term $-\gamma_0^{\varphi_0}(m,\varrho)$.

**Order $k = \frac{1}{2}$:**
The coefficient $b_1$ is always 0.

**Order $k = 1$:**
For $-D_-^2$ (and $-\partial_-^2$) the coefficient $b_2$ vanishes (just as for instantons).

**Order $k = \frac{3}{2}$:**
The coefficient $b_3$ is always 0.

**Order $k = 2$:**
The $j = 0$ - mode of $b_4$ is given by $\varphi_0 \bar{b}_4$ (again only the traceful part of $\varphi_0$ contributes) and diverges logarithmically as $I(m^2, 2, 0; 0) \propto \widetilde{\Gamma}(0)$ (cf. (3.1.18.b)). This logarithmic divergence is canceled by the Pauli - Villars - regulator term (see [60, 154] for $T = 0$ - case); the $\gamma_{\mathrm{E}}$ - terms cancel as well. Thus the physical $j = 0$ - mode contribution at asymptotic order $k = 2$ reads

$$\gamma_4(m, \lambda) = \ln\left(\frac{\lambda^2}{m^2}\right) \frac{1}{(4\pi)^2} \operatorname{Tr}\left(\bar{b}_4\right) = \ln\left(\frac{m^2}{\lambda^2}\right) \frac{1}{12(4\pi)^2} \int^1 \mathrm{d}^4 x \operatorname{tr}\left(G^{\mu\nu} G^{\mu\nu}\right) = \frac{1}{6} \ln\left(\frac{m}{\lambda}\right), \tag{3.1.28}$$

where it was used that integrating $\operatorname{tr}\left(\bar{b}_4(A_{\mathrm{HS}})\right)$ yields the caloron's topological charge: $\frac{1}{(4\pi)^2} \operatorname{Tr}\left(\bar{b}_4(A_{\mathrm{HS}})\right) = n = 1$. This result is analogous to the instanton - case in [60].

In order to verify our numerical methods, we also perform the $x$ - integral numerically for 35 $\varrho$ - values ranging over several orders of magnitude $\varrho \in \{0.005 \cdot 1.5^i \,|\, \mathbb{N} \ni i \leq 34\}$ with $\varrho_{\text{max}} = 4853.70$ and find excellent agreement with the analytical value. As can be seen in figure 3.6, and our data in the ancillary files, the relative error of the numerical integration with respect to $\frac{1}{12}$ never exceeds $|\delta_{\gamma_4,\,\text{max}}| \approx 2.3 \cdot 10^{-5}\%$.

The $j \neq 0$ - ambiguities from $b_4 = \varphi_0 \bar{b}_4 - \frac{\varphi_0 + 2\varphi_2}{6} E^i E^i$ come from $\varphi_0$ with $c = 0$, i.e., from the integral $I(m^2, 2, j^2; 0)$, and from $\frac{1}{6}(\varphi_0 + 2\varphi_2)$, where $\frac{j^2}{12s}$ means $c = 2$ and the integral in question thus is $I(m^2, 2, j^2; 1)$. For both $\bar{b}_4 \propto G^{\mu\nu} G^{\mu\nu}$ and $E^i E^i$ only the traceful part $\cos(j\pi\omega)\mathbb{1}$ of $\Omega^j$ in $\varphi_0$ and $\varphi_0 + 2\varphi_2$ contributes. The traceless part $i \sin(j\pi\omega) \frac{x^a \sigma^a}{r}$ yields: $\frac{i}{4} \sin(j\pi\omega) \frac{x^a}{r} G^{b\,\mu\nu} G^{c\,\mu\nu} \sigma^a \sigma^b \sigma^c =_{\mathrm{tr}} -\frac{1}{2} \sin(j\pi\omega) \frac{x^a}{r} G^{b\,\mu\nu} G^{c\,\mu\nu} \varepsilon^{abc} \mathbb{1} = 0$ due to the exchange symmetry for the field strength - analogously for the chromo - electric field. Performing the $j$ - summation in the first term gives $2^{3/2} \sqrt{\pi} \left(\mathrm{L}_{-\frac{1}{2}, \frac{1}{2}} + \ldots\right) \bar{b}_4$ and we neglect this contribution completely as it contains a mass damping. The second term yields (mind the factor $\frac{j^2}{12}$ in this $j$ - summation) $-2^{5/2} \sqrt{\pi} (\frac{1}{12} \mathrm{L}_{\frac{1}{2}, -\frac{1}{2}} + \ldots) E^i E^i$, where $\operatorname{tr}(\mathbb{1}\, E^i E^i) = E^{a\,i} E^{b\,i} \operatorname{tr}\left(\frac{\sigma^a}{2} \frac{\sigma^b}{2}\right) = \frac{1}{2} E^{a\,i} E^{a\,i}$ gave a factor of $\frac{1}{2}$, so that we obtain the overall

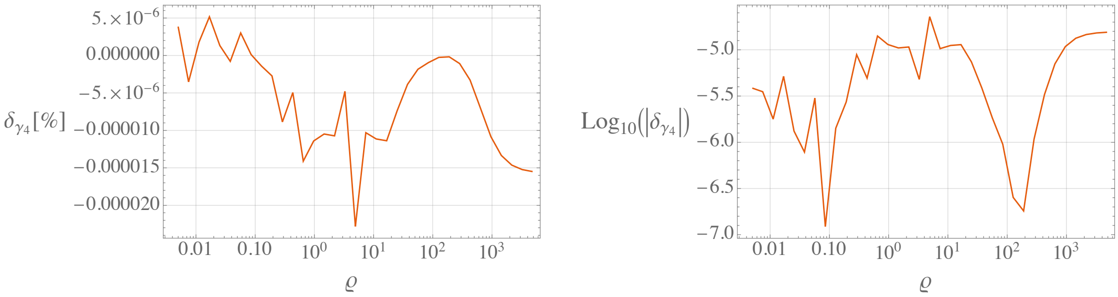

Figure 3.6: Relative error $\delta_{\gamma_4}$ of (3.1.28) compared to the theoretical value of $\frac{1}{12}$.

finite temperature contribution

$$\begin{aligned}\gamma_4^{\mathcal{B}}(m,\varrho) &= -\frac{1}{2^{\frac{5}{2}}\cdot 3\sqrt{\pi}}\int_0^1 \mathrm{d}\tau \int_0^\infty \mathrm{d}r\, r^2\, \mathrm{L}_{\frac{1}{2},-\frac{1}{2}}\big(m,\omega(r,\varrho)\big)\big(E^{a\,i}E^{a\,i}\big)(r,\tau,\varrho) = \\ &\overset{(3.1.26)}{=} \zeta(m,\tilde{\varrho},\varrho\,;\,\tilde{a},\tilde{b},\tilde{c},a,b,c)\Big|_{\text{Table 3.2}} .\end{aligned} \tag{3.1.29}$$

| | (i) | (ii) | (iii) | (iv) | (v) | (vi) | (vii) | (viii) | (ix) |
|---|---|---|---|---|---|---|---|---|---|
| $\tilde{a}$ | 0 | 0 | 0 | 0 | 0 | 0 | 0 | 0 | 0 |
| $\tilde{b}$ | 0 | 0 | 0 | 0 | 0 | 0 | 0 | 0 | 0 |
| $\tilde{c}$ | 0 | 0 | 0 | 0 | 0 | 0 | 0 | 0 | 0 |
| $a$ | -0.092 | -0.069 | -0.069 | -0.088 | -0.061 | -0.061 | -0.085 | -0.057 | -0.057 |
| $b$ | 0.27 | 0.50 | 0.50 | 0.23 | 0.50 | 0.50 | 0.17 | 0.50 | 0.50 |
| $c$ | 0 | 0 | 0 | 0.05 | 0.10 | 0.10 | 0 | 0 | 0 |

Table 3.2: The sector boundaries corresponding to figure 3.4 are $m_1 \approx 3.4$, $m_2 \approx 8$, $m_3 = 45$ and $\varrho_1 \approx 0.3$, $\varrho_3 \approx 2$, $\varrho_3 = 45$.

Here 55 fermion mass values $m \in \{1.001\cdot(\frac{45}{1.001})^{\frac{i}{54}}\,|\,\mathbb{N}\ni i\leq 54\}$ and 85 caloron size values $\varrho \in \{10^{-3}\cdot 10^{\frac{3i}{49}}\,|\,\mathbb{N}\ni i \leq 50\}\cup\{10^{-3}\cdot 10^{\frac{150}{49}}\cdot 39.083^{\frac{i}{34}}\,|\,\mathbb{N}^+\ni i\leq 34\}$ form a grid of 4675 points. The corresponding data and the relative fitting error of (3.1.29) are to be found in the ancillary files.

This integral (3.1.29) is finite - just as (3.1.28) and the other heat kernel contributions, because the field strength and thus the chromo - electric and -magnetic fields vanish fast enough for $r\to\infty$ (cf. figure 2.12).

Overall, the contribution to $\gamma_{\text{s},-}$ is $-\gamma_4(m,\lambda)$ with a finite - $T$ uncertainty $-\gamma_4^{\mathcal{B}}(m,\varrho)$.

**Order $k = \frac{5}{2}$:**
For $-D_-^2$ the coefficient $b_5$ vanishes.

**Order $k = 3$:**
$I\big(m^2, k, j^2; \frac{c}{2}\big)$ is always finite for $k \geq 3$, e.g., $I(m^2, 3, 0; 0) = m^{-2}$. Here we find the physical $\gamma_{\text{s},\,-}$ - contribution

$$\frac{\gamma_6(\varrho)}{m^2} = I(m^2, 3, 0; 0)\,\frac{1}{(4\pi)^2}\,\mathrm{Tr}\big(\bar{b}_6\big) = -\frac{1}{1440\pi\, m^2}\int_0^1 \mathrm{d}\tau \int_0^\infty \mathrm{d}r\, r^2\, \varepsilon^{abc}\, G^{a\,\mu\nu} G^{b\,\mu\kappa} G^{c\,\nu\kappa}\,. \tag{3.1.30}$$

The corresponding $\lambda$ - terms thus vanish as $\lambda \to \infty$. We calculate $\gamma_6$ for 150 caloron sizes $\varrho \in \{10^{-3} \cdot 1.1^i \,|\, \mathbb{N} \ni i \leq 100\} \cup \{10^{-3} \cdot 1.1^{100} \cdot 1.075^i \,|\, \mathbb{N}^+ \ni i \leq 49\}$ with $\varrho_{\text{max}} \approx 476.74$ and obtain

$$\frac{\gamma_6(\varrho)}{m^2} = \begin{cases} \dfrac{0.013}{\tilde{\varrho}^{2.00} m^2} & : 0 < \varrho \leq 0.267 \\[2ex] \dfrac{0.128\tilde{\varrho}^{1.55}}{m^2} + \dfrac{0.021}{\varrho^{1.78} m^2} & : 0.267 < \varrho \leq 1.844\,, \\[2ex] \dfrac{0.008}{\varrho^{2.00} m^2} + \dfrac{0.052}{m^2} & : 1.844 < \varrho \end{cases} \tag{3.1.31}$$

where $0.013 \approx \frac{1}{75}$ is the prefactor of the corresponding instanton heat kernel expansion [60] - in fact, the full numerical result agrees with $\frac{1}{75} = 0.01\bar{3}$ to eight decimal places. Furthermore, the difference between "$x$" and "$x.00$" in (3.1.31) and other numerical results is that the former denotes the exact integer number (either obtained by analytical calculation or set by hand), while the latter means a numerical result that is given to two decimal places. The data and fitting function as well as the latter's relative error compared to the data are shown in figures 3.7a and 3.7b, respectively and can be found in the ancillary files.

In (3.1.31) we can identify three $\varrho$ - regions: for small caloron sizes or low temperatures $\varrho = \rho T \leq 0.267$ the heat kernel coefficient $\gamma_6$ is best described by $\tilde{\varrho}$ (2.4.40); for large caloron sizes or large temperatures $\rho T > 1.844$, $\varrho$ describes the coefficient; in the intermediate region, both $\varrho$ and $\tilde{\varrho}$ play a role. This means that for $\rho \ll \beta$ the caloron is small enough to only effect physics on length scales much smaller than the temperature scale. Therefore, such a small caloron essentially behaves like an instanton. As the caloron gets larger, its actual periodic nature becomes increasingly important for its effect on particles.

The $j \neq 0$ - modes at $k = 3$ are due to (I) $\varphi_0$ with $I(m^2, 3, j^2; 0)$, (II) $\frac{1}{60}(\varphi_0 + 2\varphi_2)$ with $I(m^2, 3, j^2; 1)$, where we study the terms (II.1) $\frac{1}{60}(\varphi_0 + 2\varphi_2)\Big(\big(E^{i;i}\big)^2 + \big(G^{ij;4}\big)^2\Big)$ and (II.2) $-\mathrm{tr}\big(\frac{1}{60}(\varphi_0 + 2\varphi_2)\, 2E^i G^{ij} E^j\big)$ separately, and (III) $-\big(\frac{\varphi_0}{15} + \frac{\varphi_2}{3} + \frac{2\varphi_4}{15}\big)$ with

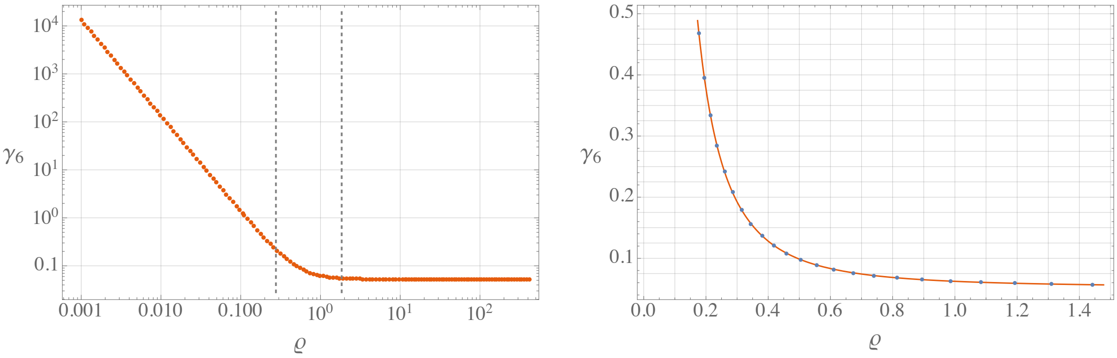

(a). $m^{-2}$ - coefficient $\gamma_6$ (3.1.31) of $\gamma_{\text{s},-}$ (3.1.17): our data (orange) on the left, data points (blue) and fitting function (orange) on right. The vertical, dashed gray lines again mark the boundaries of the piecewise defined function (3.1.31).

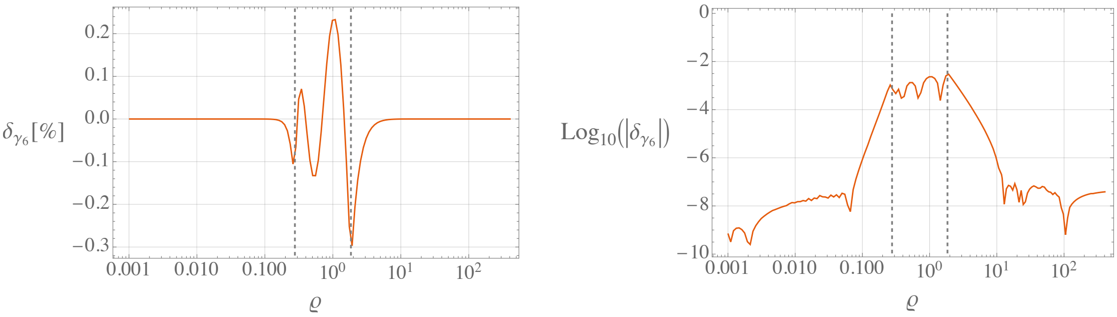

(b). Relative error $\delta_{\gamma_6}$ of (3.1.31) compared to our data in %. Again, the vertical lines mark the boundaries in the fitting function. We see good agreement in the physically relevant region $0.1 \lesssim \varrho \lesssim 1$.

Figure 3.7

(III.1) $I(m^2,3,j^2;1)$ and (III.2) $I(m^2,3,j^2;2)$. For the $j$-summation we use that in all (I) - (III.2) only $\cos(j\pi\omega)\mathbb{1} \subset \Omega^j$ contributes. For the traceless part we find: (I) $x^a G^{b\,\mu\nu} G^{c\,\mu\kappa} G^{d\,\nu\kappa} \sigma^a\sigma^b\sigma^c\sigma^d =_{\mathrm{tr}} 2x^a\big(G^{a\,\mu\nu}G^{b\,\mu\kappa}G^{b\,\nu\kappa} + (\nu \leftrightarrow \kappa) + (\mu \leftrightarrow \kappa)\big) = 0$ because of index symmetries; (II.1), (III.1) and (III.2) give vanishing contributions due to $\sigma^a\sigma^b\sigma^c =_{\mathrm{tr}} 2i\,\varepsilon^{abc}$ together with exchange symmetries in $G$ and $E$; (II.2) yields $x^a E^{b\,i} G^{c\,ij} E^{d\,j} \sigma^a\sigma^b\sigma^c\sigma^d =_{\mathrm{tr}} 2x^a\big(E^{a\,i}G^{b\,ij}E^{b\,j} - (i \leftrightarrow j) - E^{b\,i}G^{a\,ij}E^{b\,j}\big)$, where the first two terms cancel and the third again vanishes owing to index symmetry. Finally, the corresponding traceful contributions with all mass damped terms neglected are:

(I) $\sqrt{2\pi}\,\mathrm{L}_{-\frac{3}{2},-\frac{1}{2}}\,\bar{b}_6 =_{\mathrm{tr}} \frac{\sqrt{\pi}}{2^{7/2}\cdot 45}\,\mathrm{L}_{-\frac{3}{2},-\frac{1}{2}}\,\varepsilon^{abc}G^{a\,\mu\nu}G^{b\,\mu\kappa}G^{c\,\nu\kappa}\,\mathbb{1}\,,$

(II.1) $\frac{\sqrt{\pi}}{2^{7/2}\cdot 15}\big(\mathrm{L}_{-\frac{1}{2},-\frac{3}{2}} - \frac{1}{8}\,\mathrm{L}_{-\frac{3}{2},-\frac{1}{2}}\big)\big((E^{a\,i;i})^2 + (G^{a\,ij;4})^2\big)\mathbb{1}\,,$

(II.2) $-\frac{\sqrt{\pi}}{2^{7/2}\cdot 15}\big(\mathrm{L}_{-\frac{1}{2},-\frac{3}{2}} - \frac{1}{8}\,\mathrm{L}_{-\frac{3}{2},-\frac{1}{2}}\big)\varepsilon^{abc}E^{a\,i}G^{b\,ij}E^{c\,j}\,\mathbb{1}\,,$

(III.1) $\frac{\sqrt{\pi}}{2^{5/2}\cdot 15}\big(\mathrm{L}_{-\frac{1}{2},-\frac{3}{2}} - \frac{1}{8}\,\mathrm{L}_{-\frac{3}{2},-\frac{1}{2}}\big)\big(E^{a\,i;4}\big)^2\,\mathbb{1}\,,$

(III.2) $-\frac{\sqrt{\pi}}{2^{5/2}\cdot 15}\big(\mathrm{L}_{\frac{1}{2},-\frac{5}{2}} + \frac{3}{8}\,\mathrm{L}_{-\frac{1}{2},-\frac{3}{2}} - \frac{15}{128}\,\mathrm{L}_{-\frac{3}{2},-\frac{1}{2}}\big)\big(E^{a\,i;4}\big)^2\,\mathbb{1}\,.$

Performing the trace and plugging the result in the spacetime integral we find the finite temperature corrections at $k = 3$:

$$\gamma_6^{\varphi_0}(m,\varrho) = \frac{1}{2^{\frac{9}{2}}\cdot 45\sqrt{\pi}}\int_0^1 \mathrm{d}\tau \int_0^\infty \mathrm{d}r\, r^2\, \mathrm{L}_{-\frac{3}{2},-\frac{1}{2}}\,\varepsilon^{abc}G^{a\,\mu\nu}G^{b\,\mu\kappa}G^{c\,\nu\kappa}\,, \tag{3.1.32}$$

$$\begin{aligned}\gamma_6^{\mathcal{B}}(m,\varrho) = \frac{1}{2^{\frac{7}{2}}\cdot 15\sqrt{\pi}}\int_0^1 \mathrm{d}\tau \int_0^\infty \mathrm{d}r\, r^2 \Bigg(\frac{1}{2}\big(\mathrm{L}_{-\frac{1}{2},-\frac{3}{2}} - \frac{1}{8}\,\mathrm{L}_{-\frac{3}{2},-\frac{1}{2}}\big)\big((E^{a\,i;i})^2 + (G^{a\,ij;4})^2 - \\ - \varepsilon^{abc}E^{a\,i}G^{b\,ij}E^{c\,j}\big) - \big(\mathrm{L}_{\frac{1}{2},-\frac{5}{2}} - \frac{5}{8}\,\mathrm{L}_{-\frac{1}{2},-\frac{3}{2}} + \frac{1}{128}\,\mathrm{L}_{-\frac{3}{2},-\frac{1}{2}}\big)\big(E^{a\,i;4}\big)^2\Bigg)\,.\end{aligned} \tag{3.1.33}$$

The numerical values for these ambiguities

$$\gamma_6^{\varphi_0}(m,\varrho) = \text{non-trivial function}(m,\varrho)\cdot e^{-m} \tag{3.1.34}$$

$$\gamma_6^{\mathcal{B}}(m,\varrho) \overset{(3.1.26)}{=} \zeta(m,\tilde{\varrho},\varrho\,;\,\tilde{a},\tilde{b},\tilde{c},a,b,c)\Big|_{\text{Table 3.3}} \tag{3.1.35}$$

were again obtained on the grid of 4675 $(m,\varrho)$-points $m \in \{1.001\cdot(\frac{45}{1.001})^{\frac{i}{54}}\,|\,\mathbb{N} \ni i \leq 54\}$ and $\varrho \in \{10^{-3}\cdot 10^{\frac{3i}{49}}\,|\,\mathbb{N} \ni i \leq 50\} \cup \{10^{-3}\cdot 10^{\frac{150}{49}}\cdot 39.083^{\frac{i}{34}}\,|\,\mathbb{N}^+ \ni i \leq 34\}$ and can be found in the ancillary files. Note that the "non - trivial function" of $\gamma_6^{\varphi_0}$ contains a transition from negative to positive values and is therefore difficult to describe by the function (3.1.26).

|  | (i) | (ii) | (iii) | (iv) | (v) | (vi) | (vii) | (viii) | (ix) |
|---|---|---|---|---|---|---|---|---|---|
| $\tilde{a}$ | 0.012 | 0.009 | 0.003 | $\tilde{a}_6^{(1)}(\varrho)$ | $\tilde{a}_6^{(2)}(\varrho)$ | $\tilde{a}_6^{(3)}(\varrho)$ | 0 | 0 | 0 |
| $\tilde{b}$ | -0.04 | 0.03 | 0.68 | 0.07 | -0.16 | 0.61 | 0 | 0 | 0 |
| $\tilde{c}$ | -1.99 | -2.00 | -2.00 | -2.27 | -1.90 | -1.63 | 0 | 0 | 0 |
| $a$ | 0 | 0 | 0 | $a_6^{(1)}(\varrho)$ | $a_6^{(2)}(\varrho)$ | $a_6^{(3)}(\varrho)$ | 0.029 | 0.048 | 0.012 |
| $b$ | 0 | 0 | 0 | 0.66 | -0.11 | 0.65 | 0.62 | -0.25 | 0.74 |
| $c$ | 0 | 0 | 0 | -0.08 | -0.16 | -0.28 | -0.00 | -0.25 | -0.02 |

Table 3.3: The sector boundaries corresponding to figure 3.4 are $m_1 \approx 2.2$, $m_2 \approx 3.5$, $m_3 = 45$ and $\varrho_1 \approx 0.2$, $\varrho_2 \approx 2.5$, $\varrho_3 = 45$. The $\tilde{a}$ and $a$ functions are: $\tilde{a}_6^{(1)} = 0.007\big(1 - \Theta_l(\varrho - 0.65, 7.5)\big)$, $\tilde{a}_6^{(2)} = 0.013(1 - \Theta_l)$, $\tilde{a}_6^{(3)} = 0.007(1 - \Theta_l)$, $a_6^{(1)} = 0.030\,\Theta_l(\varrho - 0.65, 7.5)$, $a_6^{(2)} = 0.050\,\Theta_l$, $\tilde{a}_6^{(3)} = 0.020\,\Theta_l$.

The relative fitting error of (3.1.35) on the above $m$ - $\varrho$ - grid is also provided in the ancillary files.

We find the $k = 3$ - contribution to the log - caloron density $-\frac{\gamma_6(\varrho)}{m^2}$ with boundary condition dependent ambiguities $-\gamma_6^{\varphi_0}(m, \varrho) - \gamma_6^{\mathcal{B}}(m, \varrho)$.

We showed, that despite the infinite $j$ - summation, the finite $T$ - ambiguities at $k = 0, 2, 4$ are not only exponentially damped for small $s$, but also for large $m$, and decrease in importance. In keeping with the nature of an asymptotic expansion, we can therefore neglect all further finite $T$ - terms, where the $\mathcal{B}_{2k>6}$ are unknown.

All in all "the finite temperature corrections are negligible in the ultraviolet region" and "temperature does not modify the renormalization properties" [185]. In figure 3.10 and (3.1.40) we quantify how large a mass is necessary to limit the particle to said UV region.

We now continue the heat kernel expansion up to higher orders. Due to expected computational cost in calculating the explicit form of $\bar{b}_{12}(x, \varrho)$ and performing the integration of this term, we compute the physical terms only up to $k = 5$, leaving out the last known $k = 6$ - contribution. All the following results are also documented in the ancillary files. We find the $\gamma_{s,-}$ - contributions:

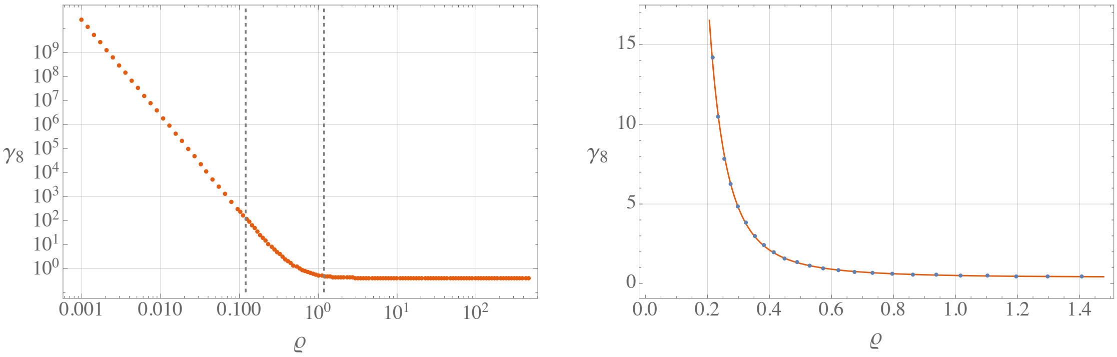

(a). $m^{-4}$ - coefficient $\gamma_8$ (3.1.36) of $\gamma_{\mathrm{s},-}$ (3.1.17).

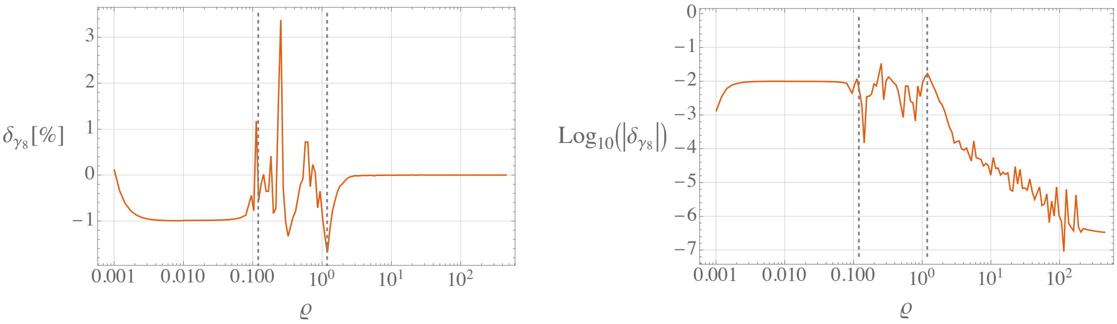

(b). Relative error $\delta_{\gamma_8}$ of (3.1.36) compared to our data.

Figure 3.8

**Order $k=4$:**

$$\frac{\gamma_8(\varrho)}{m^4} = I(m^2,4,0;0)\frac{1}{(4\pi)^2}\,\mathrm{Tr}\big(\bar{b}_8\big) = \\ = \begin{cases} \dfrac{0.023}{\tilde{\varrho}^4 m^4} & : 0<\varrho\leq 0.120 \\ \dfrac{0.090}{\tilde{\varrho}^{2.34} m^4} + \dfrac{0.021}{\varrho^{4.03} m^4} & : 0.120<\varrho\leq 1.183\ , \\ \dfrac{0.020}{\varrho^{3.11} m^4} + \dfrac{0.096}{\varrho^{1.99} m^4} + \dfrac{0.388}{m^4} & : 1.183<\varrho \end{cases} \tag{3.1.36}$$

plotted in figures 3.8a and 3.8b. The full small - $\varrho$ coefficient in (3.1.36) fits the expected instanton coefficient $\frac{17}{735}$ [60] up to $1\%$. For the numerical calculation of (3.1.36) we used

130 caloron sizes $\varrho \in \{10^{-3} \cdot 1.2^i \,|\, \mathbb{N} \ni i \leq 25\} \cup \{10^{-3} \cdot 1.2^{25} \cdot 1.085^i \,|\, \mathbb{N}^+ \ni i \leq 104\}$ with $\varrho_{\text{max}} \approx 461.56$.

**Order $k = 5$:**

$$\frac{\gamma_{10}(\varrho)}{m^6} = I(m^2, 5, 0; 0) \frac{1}{(4\pi)^2} \operatorname{Tr}\big(\bar{b}_{10}\big) = \\ = \begin{cases} -\dfrac{0.082}{\tilde{\varrho}^6 m^6} & : 0 < \varrho \leq 0.298 \\ -\dfrac{0.463}{\tilde{\varrho}^{3.87} m^6} + \dfrac{0.267}{\varrho^{5.33} m^6} & : 0.298 < \varrho \leq 1.348 \\ -\dfrac{2.280}{\varrho^{2.15} m^6} - \dfrac{5.106}{m^6} & : 1.348 < \varrho \end{cases} , \tag{3.1.37}$$

which is plotted in figure 3.9. The small-$\varrho$ coefficient here agrees with the instanton coefficient $\frac{232}{2385}$ up to $-0.21\%$.[11]

Finally, we give the large mass expansion of the log-caloron density for an anti-periodic scalar particle in a HS caloron background (3.1.17) up to $m^{-6}$:

$$\gamma_{\text{s},-}(m \text{ large}, \varrho, \lambda) = \frac{1}{6} \ln\left(\frac{\lambda}{m}\right) - \left(\frac{\gamma_6(\varrho)}{m^2} + \frac{\gamma_8(\varrho)}{m^4} + \frac{\gamma_{10}(\varrho)}{m^6}\right) + \mathcal{O}(m^b e^{-m}) \,, \quad b \sim 1 \,. \tag{3.1.38}$$

In order to estimate the validity of (3.1.38), we modify the idea of [60] and demand that the expansion (3.1.38) be asymptotic, i.e., that each additional expansion order contribute less to the existing expansion than the one before. For that, we find the "lightest heavy mass" so that 1) $\frac{\gamma_6}{m^2} \geq \frac{\gamma_8}{m^4}$ and 2) $\frac{\gamma_8}{\gamma_6 m^2} \geq \frac{\gamma_{10}}{\gamma_6 m^4 + \gamma_8 m^2}$. Additionally, the finite-temperature ambiguities in (3.1.38) need to be small compared to the physical expansion and we therefore demand 3) $\left|\frac{\gamma_6(\varrho)}{m^2} + \frac{\gamma_8(\varrho)}{m^4} + \frac{\gamma_{10}(\varrho)}{m^6}\right| > 1.2(\gamma_0^T(m,\varrho) + \gamma_4^T(m,\varrho) + \gamma_6^T(m,\varrho)$, where the factor $1.2$ gives a conservative estimate and we abbreviate the full $T > 0$-uncertainties at order $2k$ as $\gamma_{2k}^T$. We consider conditions 1) and 2) for 650 caloron sizes $\varrho \in \{10^{-3\left(1-\frac{j}{249}\right)} \cdot 0.15^{\frac{j}{249}} \,|\, \mathbb{N} \ni j \leq 249\}$, $\varrho \in \{0.153^{1-\frac{j}{249}} \cdot 1.5^{\frac{j}{249}} \,|\, \mathbb{N} \ni j \leq 249\}$ and $\varrho \in \{1.514^{1-\frac{j}{149}} \cdot 100^{\frac{j}{249}} \,|\, \mathbb{N} \ni j \leq 249\}$ with minimal caloron size $0.001$ and maximum size $100$ an find the combined, conservative (meaning that in 1) and 2) the higher order term contributes at most about $67\%$ of the existing series) restriction:

---

[11] We would like to specifically thank Simon Stendebach for setting up the code for the numerical $x$-integration of $\operatorname{tr}(\bar{b}_{10})$ in (3.1.37) and performing the integrals (using the *Cubature* package [193–196] to handle the highly oscillatory integrand $\operatorname{tr}(\bar{b}_{10})$).

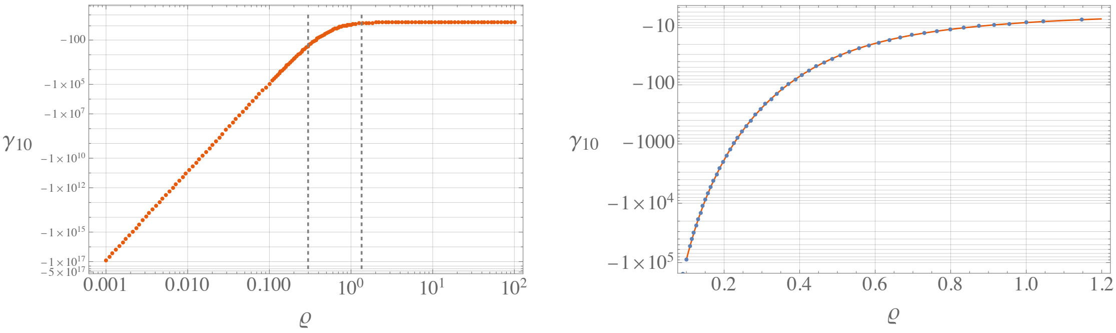

(a). $m^{-6}$ - coefficient $\gamma_{10}$ (3.1.37) of $\gamma_{\text{s},-}$ (3.1.17).

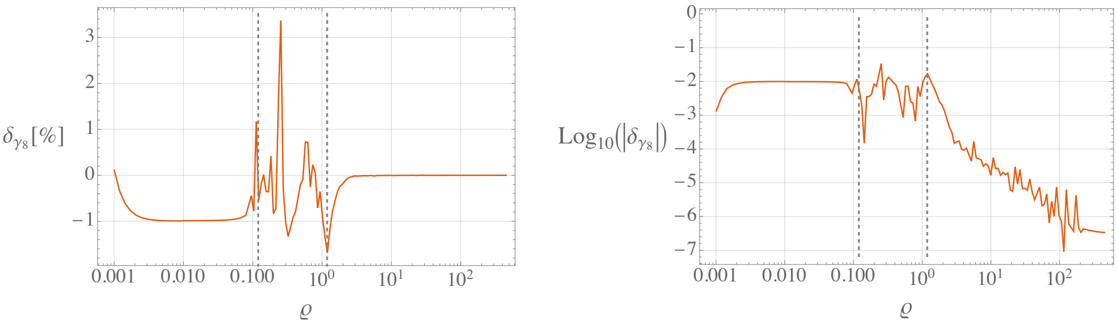

(b). Relative error $\delta_{\gamma_{10}}$ of (3.1.37) compared to our data.

Figure 3.9

$$m_{\text{large, min, (1,2)}}(\varrho) = \begin{cases} 1.7\tilde{\varrho}^{-1} & : 0 < \varrho \leq 0.094 \\ 2.1\varrho^{-0.9} + 0.5 & : 0.094 < \varrho \leq 0.44 \\ 1.7\tilde{\varrho}^{-1} - 2.3\varrho^{-0.1} + 22.4 & : 0.44 < \varrho \leq 1.39 \\ 0.16\varrho^{-2.1} + 3.4 & : 1.39 < \varrho \end{cases} . \tag{3.1.39}$$

Condition 3) cannot be inverted and we show the numerical results, obtained for 650 sizes $\varrho \in \{0.31^{1-\frac{j}{249}} \cdot 0.6^{\frac{j}{249}} \,|\, \mathbb{N} \ni j \leq 249\}$, $\varrho \in \{0.601^{1-\frac{j}{249}} \cdot 3^{\frac{j}{249}} \,|\, \mathbb{N} \ni j \leq 249\}$ and $\varrho \in \{3.019^{1-\frac{j}{149}} \cdot 25^{\frac{j}{249}} \,|\, \mathbb{N} \ni j \leq 249\}$ with minimal caloron size $0.31$ (for smaller $\varrho$, condition 3) is satisfied, see figure 3.10a) and maximum size $25$, in figure 3.10b.

All in all, the lightest quark mass for which our heat kernel expansion is valid is

$$m_{\text{large, min}}(\varrho) = \max\left(m_{\text{large, min, (1,2)}}(\varrho), m_{\text{large, min, 3}}(\varrho)\right) . \tag{3.1.40}$$

Our large mass result (3.1.38) together with the estimate for the minimal mass (3.1.40) gives the large $m$ - correction factor $f$ according to (2.4.83) - compare also the $T = 0$ result (2.4.78):

$$\begin{aligned} f_{\text{large}}(m \geq m_{\text{large, min}}(\varrho), \varrho) &= \frac{e^{-2\alpha\left(\frac{1}{2}\right)}}{(\lambda\varrho)^{\frac{1}{3}}} e^{2\gamma_{\text{s},-}} = \\ &= \frac{e^{-2\alpha\left(\frac{1}{2}\right)}}{(m\varrho)^{\frac{1}{3}}} \exp\left(-\frac{2\gamma_6(\varrho)}{m^2} - \frac{2\gamma_8(\varrho)}{m^4} - \frac{2\gamma_{10}(\varrho)}{m^6}\right) \end{aligned} \tag{3.1.41}$$

## 3.2 Small Mass - Expansion of the Caloron Density

### 3.2.1 Expansion Strategy

After analyzing heavy quarks the the large - mass heat kernel expansion, we now consider light fermions with $m \ll 1$, but non - vanishing. The straightforward procedure in this limit is a Taylor expansion of the log - caloron density (2.4.82) up to first order in $m^2$ using $\frac{\mathrm{d}}{\mathrm{d}m^2} \ln\det(-D_-^2 + m^2) = \frac{\mathrm{d}}{\mathrm{d}m^2} \mathrm{Tr}\ln(-D_-^2 + m^2) = \mathrm{Tr}\left(\frac{1}{-D_-^2+m^2}\right) = \int^1 \mathrm{d}^4x\, \mathrm{tr}\langle x| \frac{1}{-D_-^2+m^2} |x\rangle$ with the massive anti-periodic closed loop - propagator $\Delta^-(x, x, m^2) = \langle x| \frac{1}{-D_-^2+m^2} |x\rangle$. Including higher orders in the Taylor expansion would require convolutions of such propagators and we thus avoid them.

Since these closed loop - propagators are naturally divergent, we achieve regularization via point splitting, i.e., by considering "almost closed loop" - propagation $\Delta^-(x', x, m^2)$

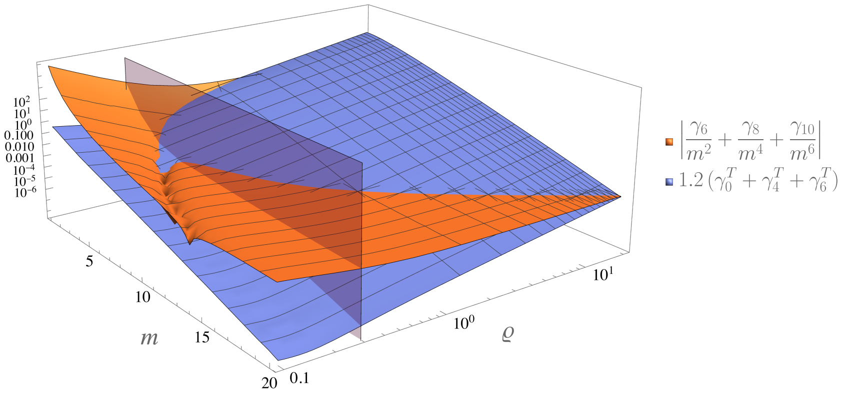

(a). The leading heat kernel expansion $\left|\frac{\gamma_6(\varrho)}{m^2}+\frac{\gamma_8(\varrho)}{m^4}+\frac{\gamma_{10}(\varrho)}{m^6}\right|$ shown in orange compared to $1.2(\gamma_0^T+\gamma_4^T+\gamma_6^T)$ depicted in blue (the factor 1.2 allows for a conservative restriction). The $\varrho = 0.31$ - plane shows that for smaller caloron sizes the finite - $T$ ambiguities are always smaller, while for $\varrho \gtrsim 0.31$ a large enough quark mass is required.

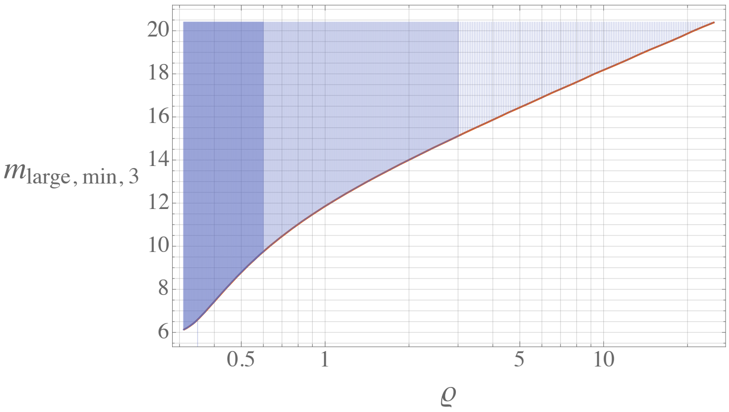

(b). The minimal, i.e., lightest, possible heavy mass $m_{\text{large, min, 3}}(\varrho)$ determined from condition 3). We choose it conservative so that $\left|\frac{\gamma_6}{m^2}+\frac{\gamma_8}{m^4}+\frac{\gamma_{10}}{m^6}\right|$ exceeds $\gamma_0^T+\gamma_4^T+\gamma_6^T$ by at least $20\%$. The blue lines mark data points and fill the area of allowed masses. We identify a roughly logarithmic growth of $m_{\text{large, min, 3}}(\varrho)$.

Figure 3.10

from $x$ to $x' = x+\varepsilon$, $\varepsilon \to 0$.[12] To retain the gauge invariance of $\gamma_{\text{ferm}}$, an appropriate Wilson line $\mathrm{P}\exp\left(i\int_x^{x'}\mathrm{d}z^\mu A^\mu_{\text{HS}}(z)\right) = \mathbb{1} + iA^\mu_{\text{HS}}(x)\,\varepsilon^\mu + \frac{1}{2}\left(i\,\partial^\mu A^\nu_{\text{HS}}\big|_x - (A^\mu_{\text{HS}}A^\nu_{\text{HS}})(x)\right)\varepsilon^\mu\varepsilon^\nu + \mathcal{O}(\varepsilon^3)$ (2.1.28) has to be added to the propagator. Using also (2.4.77), we find the Taylor expansion up to $\mathcal{O}(m^2)$:[13]

$$\begin{aligned}\gamma_{\text{ferm}} = &-\frac{1}{3}\ln(\lambda\varrho) - 2\alpha\left(\frac{1}{2}\right) + \frac{1}{3}(\pi\varrho)^2 - 2A(\pi\varrho) - \\ &- 2m^2 \lim_{\varepsilon\to 0}\mathrm{Tr}\left(\left\langle x' \left| \frac{1}{-D_-^2} \right| x\right\rangle \mathrm{P}\exp\left(i\int_x^{x'}\mathrm{d}z^\mu A^\mu_{\text{HS}}(z)\right) - \left\langle x' \left| \frac{1}{-\partial_-^2} \right| x\right\rangle\right).\end{aligned} \tag{3.2.1}$$

Such a Taylor expansion is not possible in the limit $T \searrow 0 \Leftrightarrow \beta \to \infty$. At zero temperature the known result for $\gamma_{\text{s},-}$ contains a term $(M\rho)^2\ln(M\rho)$ [60], which is non-analytical at $M\rho = 0$. This IR non-analyticity corresponds to eigenmodes of $-\overline{D}^2$ with arbitrarily low momenta that get effected arbitrarily strongly by the introduction of even an infinitesimal mass. At finite energy, however, particles in equilibrium always carry a non-zero thermal energy with typical energies $\sim T$; in detail, fermions have anti-periodic boundary conditions which raise the lowest fluctuation frequencies in $D_-^2$ to the lowest fermionic Matsubara frequency $\omega_0^{\text{ferm}} = \pi T$ (cf. 2.2.27)). Therefore, as long as $M \ll T \searrow 0 \Rightarrow m = M\beta \ll 1$, the introduction of a such small mass only infinitesimal effects on the particles and the fluctuation determinant. Therefore, the above Taylor expansion is justified, but its convergence radius in $m$ will drop to 0 in the limit $T \searrow 0 \Leftrightarrow \beta \to \infty$. In other words, the lower $T$ gets, the smaller $M$ and thus also $m$ have to be to ensure convergence of the Taylor series.

In order to verify the Taylor series expansion, one could also also adapt the procedure developed in [60], which is suitable to produce the non-analytical expansion at $T = 0$, to finite temperatures and compare the result to the Taylor expansion. For this, $\gamma_{\text{s},-}$ is used in its Schwinger proper time representation (3.1.2) and $\gamma_{\text{ferm}}$ is expanded in $m^2$ as

$$\gamma_{\text{ferm}} = \gamma_{\text{ferm}}\big|_{m=0} - 2\int_0^{m^2}\mathrm{d}\widetilde{m}^2\left(\frac{\partial\gamma_{\text{s},-}[\widetilde{m}^2]}{\partial\widetilde{m}^2}\right)_{s\text{-regularized}} - \ln\left(\frac{m}{\lambda}\right), \tag{3.2.2}$$

with the integration only up to $m^2 \ll 1$ and the $\widetilde{m}^2$-derivative regularized not via point splitting, but by using instead a lower integration cut-off $\varepsilon_s \ll 1$ in the $s$-integration. We discuss this approach in a bit more detail in appendix C.

---

[12] Technically speaking, the $\mathrm{d}_{m^2}$-derivative above cannot be performed, before the diverging integral (without $\lambda$) is regularized, via point splitting or otherwise. This is of importance in appendix C.

[13] [54, 60, 141]

For the Taylor expansion (and the alternative expansion in appendix C), the massless anti-periodic scalar propagator in a caloron and a vacuum background are required. In general, any (anti-)periodic propagator $\Delta^{\pm}_{(0)}(x,y,m^2)$ can be obtained from the corresponding aperiodic propagator $\overline{\Delta}_{(0)}(\overline{x},\overline{y},m^2)$ in $\mathbb{R}^4$ by adding up time copies [54]:

$$\Delta^{\pm}_{(0)}(x,y,m^2) \;=\; \sum_{j\,\in\,\mathbb{Z}} (\pm 1)^j \overline{\Delta}_{(0)}(\overline{x},\overline{y}+j\hat{e}_4,m^2) \tag{3.2.3}$$

Also compare this with the construction of the caloron from instantons described in section 2.4.2, especially (2.4.36). Performing the time - copy sums amounts to compactifying the spacetime in the temporal direction $\mathbb{R}^4 \to \mathbb{R}^3 \times S^1_{\text{rad.}\,=\,{}^1\!/_{2\pi}}$, therefore the bars are dropped: $\overline{\Delta} \to \Delta$, $|\vec{\overline{x}}|, |\vec{\overline{y}}| \to r_x, r_y$, $\overline{x}^4, \overline{y}^4 \to \tau_x, \tau_y$, etc. The (almost-)closed loop propagators in (3.2.1) correspond again to the system sketched in figure 3.1. Thus, before proceeding, we have to obtain these massless propagators.

### 3.2.2 Periodic and anti-periodic massless scalar Propagator in a HS Caloron Background

#### Aperiodic Propagator

First we calculate the aperiodic $\mathbb{R}^4$ - propagator for a scalar field in a HS caloron background. An ansatz for this propagator can be found by employing the results of [152]:

$$\begin{aligned} \overline{\Delta}(\overline{x},\overline{y}) \;&=\; \frac{1}{\sqrt{\phi(x)}}\,\frac{F(\overline{x},\overline{y})}{4\pi^2(\overline{x}-\overline{y})^2}\,\frac{1}{\sqrt{\phi(y)}}\;, \qquad \phi(x) \;=\; 1 + \frac{\pi\varrho^2\sinh(2\pi r_x)}{r_x(\cosh(2\pi r_x)-\cos(2\pi\tau_x))}\,, \\ F(\overline{x},\overline{y}) \;&=\; \mathbb{1} + \varrho^2 \sum_{k\,\in\,\mathbb{Z}} \frac{\sigma^\mu(\overline{x}-k\,\hat{e}_4)^\mu}{(\overline{x}-k\,\hat{e}_4)^2}\,\frac{\sigma^{\dagger\,\nu}(\overline{y}-k\,\hat{e}_4)^\nu}{(\overline{y}-k\,\hat{e}_4)^2}\,, \end{aligned} \tag{3.2.4}$$

where $\sigma^\mu = (\vec{\sigma}, i)$ and $\vec{\sigma}$ are the Pauli matrices. Since $\phi$ is periodic in the $\overline{x}^4$ - direction, the $\overline{x}$ - and $x$ - coordinates are equivalent for $\phi$. All of the summations (3.2.3) and (3.2.4) performed in the following are presented in detail in the ancillary files.

We expand $F(\overline{x},\overline{y})$ and compute its traceful and traceless parts separately, beginning with the traceful part. For that, we denote $\overline{x}-\overline{y} = \overline{\Delta}$ with $\overline{x}^4 - \overline{y}^4 = \overline{\Delta}^4$:

$$
\begin{aligned}
&F = \\
&= \mathbb{1} + \varrho^2 \sum_{k\,\in\,\mathbb{Z}} \frac{\vec{\bar{x}}\cdot\vec{\bar{y}} + (\bar{x}^4 - k)(\bar{y}^4 - k) + i(\bar{x}^4 - k)\vec{\bar{y}}\cdot\vec{\sigma} - i(\bar{y}^4 - k)\vec{\bar{x}}\cdot\vec{\sigma} + i(\vec{\bar{x}}\times\vec{\bar{y}}\,)\cdot\vec{\sigma}}{\vec{\bar{x}}^{\,2}\,\vec{\bar{y}}^{\,2} + \vec{\bar{x}}^{\,2}(\bar{y}^4 - k)^2 + \vec{\bar{y}}^{\,2}(\bar{x}^4 - k)^2 + (\bar{x}^4 - k)^2(\bar{y}^4 - k)^2} =_{\mathrm{tr}} \\
&=_{\mathrm{tr}} \mathbb{1} + \mathbb{1}\varrho^2 \sum_{k\,\in\,\mathbb{Z}} \frac{\vec{\bar{x}}\cdot\vec{\bar{y}} + (\bar{x}^4 - k)(\bar{y}^4 - k)}{\vec{\bar{x}}^{\,2}\,\vec{\bar{y}}^{\,2} + \vec{\bar{x}}^{\,2}(\bar{y}^4 - k)^2 + \vec{\bar{y}}^{\,2}(\bar{x}^4 - k)^2 + (\bar{x}^4 - k)^2(\bar{y}^4 - k)^2} = \\
&= \mathbb{1} + \mathbb{1}\varrho^2\,\mathrm{Re}\left(\frac{i\,\vec{\bar{x}}\cdot\vec{\bar{y}} - |\vec{\bar{x}}|(i\,|\vec{\bar{x}}| + \overline{\Delta}^4)}{|\vec{\bar{x}}|\,\left(\vec{\bar{y}}^{\,2} - (|\vec{\bar{x}}| - i\overline{\Delta}^4)^2\right)}\left(\psi(-\bar{x}^4 - i\,|\vec{\bar{x}}|) - \psi(1 + \bar{x}^4 + i\,|\vec{\bar{x}}|)\right)\right) + (\bar{x} \leftrightarrow \bar{y})\,,
\end{aligned}
\tag{3.2.5}
$$

with $\psi(z) = \frac{\mathrm{d}_z\widetilde{\Gamma}(z)}{\widetilde{\Gamma}(z)}$ the digamma function; $\widetilde{\Gamma}(z)$ again represents the Gamma function. Employing $\psi(1-z) = \psi(z) + \pi\cot(\pi z)$ (reflection formula for the digamma function [189]) with $1 - z = -\bar{x}^4 - i|\vec{\bar{x}}| \Leftrightarrow z = 1 + \bar{x}^4 + i\,|\vec{\bar{x}}|$ as well as the periodicity of the cotangent $\cot(a + \pi) = \cot(a)$ gives

$$
\begin{aligned}
F \;&=_{\mathrm{tr}} \mathbb{1} + \mathbb{1}\varrho^2\,\mathrm{Re}\Bigg(\frac{i\,\vec{\bar{x}}\cdot\vec{\bar{y}} - |\vec{\bar{x}}|(i\,|\vec{\bar{x}}| + \overline{\Delta}^4)}{|\vec{\bar{x}}|\,\left(\vec{\bar{y}}^{\,2} - (|\vec{\bar{x}}| - i\overline{\Delta}^4)^2\right)}\times \\
&\qquad\times\left(\psi(1 + \bar{x}^4 + i\,|\vec{\bar{x}}|) + \pi\cot(\pi(\bar{x}^4 + i\,|\vec{\bar{x}}|)) - \psi(1 + \bar{x}^4 + i\,|\vec{\bar{x}}|)\right)\Bigg) + (\bar{x} \leftrightarrow \bar{y})\,,
\end{aligned}
\tag{3.2.6}
$$

so that the $\psi$ - terms now cancel. The cotangent of a complex argument can be expanded $\cot(\pi(\bar{x}^4 + i\,|\vec{\bar{x}}|)) = \frac{\sin(2\pi\bar{x}^4)}{\cosh(2\pi|\vec{\bar{x}}|) - \cos(2\pi\bar{x}^4)} - i\frac{\sinh(2\pi|\vec{\bar{x}}|)}{\cosh(2\pi|\vec{\bar{x}}|) - \cos(2\pi\bar{x}^4)}$ and we obtain

$$
\begin{aligned}
F(\bar{x},\bar{y}) \;&=_{\mathrm{tr}} \mathbb{1} + \mathbb{1}\pi\varrho^2\,\mathrm{Re}\left(\frac{i\,\vec{\bar{x}}\cdot\vec{\bar{y}} - |\vec{\bar{x}}|(i\,|\vec{\bar{x}}| + \overline{\Delta}^4)}{|\vec{\bar{x}}|\,\left(\vec{\bar{y}}^{\,2} - (|\vec{\bar{x}}| - i\overline{\Delta}^4)^2\right)}\cot\big(\pi(\bar{x}^4 + i\,|\vec{\bar{x}}|)\big)\right) + (\bar{x} \leftrightarrow \bar{y}) = \\
&= \mathbb{1} + \mathbb{1}\frac{\pi\varrho^2}{c_1(|\vec{\bar{x}}|,\bar{x}^4)\,d(|\vec{\bar{x}}|,|\vec{\bar{y}}|,\bar{x}^4,\bar{y}^4)}\Big(-\overline{\Delta}^4(\overline{\Delta})^2\sin(2\pi\bar{x}^4) + \\
&\quad + \left(|\vec{\bar{x}}|(\overline{\Delta})^2 + \hat{e}_{\vec{\bar{x}}}\cdot\vec{\bar{y}}\,(\overline{\Delta})^2 + 2|\vec{\bar{x}}|(\hat{e}_{\vec{\bar{x}}}\cdot\vec{\bar{y}}\,)^2 - 2|\vec{\bar{x}}|\,\vec{\bar{y}}^{\,2}\right)\sinh(2\pi|\vec{\bar{x}}|)\Big) + (\bar{x} \leftrightarrow \bar{y})\,,
\end{aligned}
\tag{3.2.7}
$$

where we shortened our notation by introducing the functions

$$
c_1(z_1, z_2) = \cosh(2\pi z_1) - \cos(2\pi z_2)\,, \tag{3.2.8}
$$

$$
d(|\vec{\bar{x}}|,|\vec{\bar{y}}|,\bar{x}^4,\bar{y}^4) = \left((|\vec{\bar{x}}| - |\vec{\bar{y}}|)^2 + (\bar{x}^4 - \bar{y}^4)^2\right)\left((|\vec{\bar{x}}| + |\vec{\bar{y}}|)^2 + (\bar{x}^4 - \bar{y}^4)^2\right). \tag{3.2.9}
$$

Now we consider only the traceless part - denoted by "$=_{\backslash\mathrm{tr}}$":

$$
\begin{aligned}
F \;&=_{\backslash\mathrm{tr}}\; i\varrho^2 \sum_{k\,\in\,\mathbb{Z}} \frac{(\bar{x}^4-k)\vec{\sigma}\cdot\vec{\bar{y}}-(\bar{y}^4-k)\vec{\sigma}\cdot\vec{\bar{x}}+(\vec{\bar{x}}\times\vec{\bar{y}}\,)\cdot\vec{\sigma}}{\vec{\bar{x}}^{\,2}\,\vec{\bar{y}}^{\,2}+\vec{\bar{x}}^{\,2}(\bar{y}^4-k)^2+\vec{\bar{y}}^{\,2}(\bar{x}^4-k)^2+(\bar{x}^4-k)^2(\bar{y}^4-k)^2} = \\
&= i\varrho^2\,\mathrm{Re}\left(\frac{\pi(i\,|\vec{\bar{y}}|+\overline{\Delta}^4)\coth\big(\pi(|\vec{\bar{y}}|+i\bar{y}^4)\big)}{|\vec{\bar{y}}|\Big(\big(|\vec{\bar{x}}|-|\vec{\bar{y}}|+i\overline{\Delta}^4\big)\big(|\vec{\bar{x}}|+|\vec{\bar{y}}|-i\overline{\Delta}^4\big)\Big)}-\right. \\
&\qquad\left.-\frac{\psi(-\bar{x}^4-i\,|\vec{\bar{x}}|)-\psi(1+\bar{x}^4+i\,|\vec{\bar{x}}|)}{\big(|\vec{\bar{x}}|-|\vec{\bar{y}}|-i\overline{\Delta}^4\big)\big(|\vec{\bar{x}}|+|\vec{\bar{y}}|-i\overline{\Delta}^4\big)}\right)\vec{\bar{y}}\cdot\vec{\sigma}+(\bar{x}\leftrightarrow\bar{y})- \qquad (3.2.10)\\
&\quad+i\pi\varrho^2\,\mathrm{Re}\left(-\frac{\coth\big(\pi(|\vec{\bar{x}}|+i\bar{x}^4)\big)}{|\vec{\bar{x}}|\big(|\vec{\bar{x}}|-|\vec{\bar{y}}|+i\overline{\Delta}^4\big)\big(|\vec{\bar{x}}|+|\vec{\bar{y}}|+i\overline{\Delta}^4\big)}+\right. \\
&\qquad\left.+\frac{\coth\big(\pi(|\vec{\bar{y}}|+i\bar{y}^4)\big)}{|\vec{\bar{y}}|\big(|\vec{\bar{x}}|-|\vec{\bar{y}}|+i\overline{\Delta}^4\big)\big(|\vec{\bar{x}}|+|\vec{\bar{y}}|-i\overline{\Delta}^4\big)}\right)(\vec{\bar{x}}\times\vec{\bar{y}}\,)\cdot\vec{\sigma}\,.
\end{aligned}
$$

Using again the digamma function reflection formula, the cotangent periodicity and complex expansion as well as $\coth\big(\pi(|\vec{\bar{y}}|+i\,\bar{y}^4)\big)=i\cot(\pi(-\bar{y}^4+i\,|\vec{\bar{y}}|))$ we obtain

$$
\begin{aligned}
F(x,y) \;&=_{\backslash\mathrm{tr}}\; i\pi\varrho^2\left(\frac{\vec{\bar{x}}^{\,2}-\vec{\bar{y}}^{\,2}-(\overline{\Delta}^4)^2}{d(|\vec{\bar{x}}|,|\vec{\bar{y}}|,\bar{x}^4,\bar{y}^4)}\frac{\sin(2\pi\bar{y}^4)}{c_1(|\vec{\bar{y}}|,\bar{y}^4)}+\frac{\overline{\Delta}^4\big(\vec{\bar{x}}^{\,2}+\vec{\bar{y}}^{\,2}+(\overline{\Delta}^4)^2\big)}{|\vec{\bar{y}}|\,d(|\vec{\bar{x}}|,|\vec{\bar{y}}|,\bar{x}^4,\bar{y}^4)}\frac{\sinh(2\pi|\vec{\bar{y}}|)}{c_1(|\vec{\bar{y}}|,\bar{y}^4)}-\right.\\
&\left.-\frac{\vec{\bar{x}}^{\,2}-\vec{\bar{y}}^{\,2}-(\overline{\Delta}^4)^2}{d(|\vec{\bar{x}}|,|\vec{\bar{y}}|,\bar{x}^4,\bar{y}^4)}\frac{\sin(2\pi\bar{x}^4)}{c_1(|\vec{\bar{x}}|,\bar{x}^4)}-\frac{2\,|\vec{\bar{x}}|\overline{\Delta}^4}{d(|\vec{\bar{x}}|,|\vec{\bar{y}}|,\bar{x}^4,\bar{y}^4)}\frac{\sinh(2\pi|\vec{\bar{x}}|)}{c_1(|\vec{\bar{x}}|,\bar{x}^4)}\right)\vec{\bar{y}}\cdot\vec{\sigma}-(\bar{x}\leftrightarrow\bar{y})+\\
&+i\pi\varrho^2\left(\frac{\overline{\Delta}^4}{d(|\vec{\bar{x}}|,|\vec{\bar{y}}|,\bar{x}^4,\bar{y}^4)}\frac{\sin(2\pi\bar{x}^4)}{c_1(|\vec{\bar{x}}|,\bar{x}^4)}-\frac{\vec{\bar{x}}^{\,2}-\vec{\bar{y}}^{\,2}-(\overline{\Delta}^4)^2}{2\,|\vec{\bar{x}}|\,d(|\vec{\bar{x}}|,|\vec{\bar{y}}|,\bar{x}^4,\bar{y}^4)}\frac{\sinh(2\pi|\vec{\bar{x}}|)}{c_1(|\vec{\bar{x}}|,\bar{x}^4)}-\right.\\
&\left.-\frac{\overline{\Delta}^4}{d(|\vec{\bar{x}}|,|\vec{\bar{y}}|,\bar{x}^4,\bar{y}^4)}\frac{\sin(2\pi\bar{y}^4)}{c_1(|\vec{\bar{y}}|,\bar{y}^4)}-\frac{\vec{\bar{y}}^{\,2}-\vec{\bar{x}}^{\,2}-(\overline{\Delta}^4)^2}{2\,|\vec{\bar{y}}|\,d(|\vec{\bar{x}}|,|\vec{\bar{y}}|,\bar{x}^4,\bar{y}^4)}\frac{\sinh(2\pi|\vec{\bar{y}}|)}{c_1(|\vec{\bar{y}}|,\bar{y}^4)}\right)(\vec{\bar{x}}\times\vec{\bar{y}})\cdot\vec{\sigma}\,. \qquad (3.2.11)
\end{aligned}
$$

The aperiodic scalar propagator reads $\overline{\Delta}(\bar{x},\bar{y})=\frac{F(\bar{x},\bar{y})}{4\pi^2(\bar{x}-\bar{y})^2}\frac{1}{\sqrt{\phi(x)\phi(y)}}$ with the traceful (diagonal) and traceless (off-diagonal) parts of $F(\bar{x},\bar{y})$ as given above. Note that the diagonal part of $\overline{\Delta}(\bar{x},\bar{y})$ is $\bar{x}\leftrightarrow\bar{y}$ - symmetric, while the off-diagonal part is $\bar{x}\leftrightarrow\bar{y}$ - antisymmetric. Taking the limit $\rho\to 0\Rightarrow\varrho\to 0$ (no caloron), the free aperiodic propagator $\overline{\Delta}(\bar{x},\bar{y})=\frac{\mathbb{1}}{4\pi^2(\bar{x}-\bar{y})^2}$ is reproduced.

We use this result to calculate the (free) periodic and anti-periodic propagator $\Delta^{\pm}_{(0)}(x,y)$

by performing the summation over time copies as described at the end of section 3.2.1:

$$\Delta^{\pm}(x,y) = \frac{1}{\sqrt{\phi(x)\phi(y)}} \sum_{j\,\in\,\mathbb{Z}} (\pm 1)^j \frac{F\big(\bar{x}, \bar{y} + j\hat{e}_4)\big)}{4\pi^2(\overline{\Delta} - j\hat{e}_4)^2}\,. \tag{3.2.12}$$

Note that $\phi(\bar{y} + j\hat{e}_4) = \phi(\bar{y})\ \forall j \in \mathbb{Z}$ (cf. (2.4.36)), i.e., the $\phi$ can be pulled out of any time copy sums due to their periodicity.

We can also obtain the $\mathbb{R}^4$ - propagator for $T = 0$ from the aperiodic propagator by reverting the (coordinate) transformation (in (3.1.1)), $\big(\vec{\bar{x}}, \bar{x}^4\big) = \big(\beta^{-1}\vec{X}, \beta^{-1}\bar{x}^4\big)$, $\varrho = \frac{\rho}{\beta}$ (keep the caloron centered at the origin) with the bars again denoting the zero temperature case, and taking the limit $\beta \to \infty$:

$$\begin{aligned} &\lim_{\beta\,\to\,\infty} \frac{F(\beta^{-1}\overline{X}, \beta^{-1}\overline{Y}, \beta^{-1}\rho)}{4\pi^2(\overline{X} - \overline{Y})^2} \frac{1}{\sqrt{\phi((\overline{X}, \rho, \beta)\phi((\overline{Y}, \rho, \beta)}} =_{\text{tr}} \\ &=_{\text{tr}}\ \mathbb{1}\, \frac{|\overline{X}|\,|\overline{Y}| + \rho^2\,\hat{e}_{\overline{X}} \cdot \hat{e}_{\overline{Y}}}{4\pi^2(\overline{X} - \overline{Y})^2 \sqrt{\big(\overline{X}^2 + \rho^2\big)\big(\overline{Y}^2 + \rho^2\big)}}\,. \end{aligned} \tag{3.2.13}$$

This is shown in the ancillary files.

### Periodic Propagator

For calculating the traceful part of the periodic propagator in a caloron background with the caloron centered at the origin according to (3.2.12) and using (3.2.7), we identify three types of periodic time copy sums:

$$\begin{aligned} (1)^+ &= \sum_{j\,\in\,\mathbb{Z}} \frac{1}{4\pi^2(\overline{\Delta} - j\hat{e}_4)^2}\,, \\ (2)^+_{x,y} &= \sum_{j\,\in\,\mathbb{Z}} \frac{-(\overline{\Delta}^4 - j)}{4\pi\, d(|\vec{\bar{x}}|, |\vec{\bar{y}}|, \bar{x}^4, \bar{y}^4 + j)}\,, \\ (3)^+_{x,y} &= \sum_{j\,\in\,\mathbb{Z}} \frac{(\pm 1)^j\,\big(|\vec{\bar{x}}|(\overline{\Delta} - j\hat{e}_4)^2 + \hat{e}_{\vec{\bar{x}}} \cdot \vec{\bar{y}}\,(\overline{\Delta} - j\hat{e}_4)^2 + 2|\vec{\bar{x}}|(\hat{e}_{\vec{\bar{x}}} \cdot \vec{\bar{y}}\,)^2 - 2|\vec{\bar{x}}|\,\vec{\bar{y}}^{\,2}\big)}{4\pi(\overline{\Delta} - j\hat{e}_4)^2\, d(|\vec{\bar{x}}|, |\vec{\bar{y}}|, \bar{x}^4, \bar{y}^4 + j)}\,, \end{aligned} \tag{3.2.14}$$

where $(2)^+_{x,y}$ and $(3)^+_{x,y}$ are not (explicitly) $x \leftrightarrow y$ - symmetric and a factor $\pi$ was absorbed into these terms. The traceful part of the full periodic propagator thus reads:

$$
\begin{aligned}
\Delta^+(x,y) =_{\mathrm{tr}} \mathbb{1} \Bigg( (1)^+ + \varrho^2 \left( (2)^+_{x,y} \frac{\sin(2\pi\tau_x)}{c_1(r_x,\tau_x)} + (2)^+_{y,x} \frac{\sin(2\pi\tau_y)}{c(r_y,\tau_y)} \right) + \\
+ \varrho^2 \left( (3)^+_{x,y} \frac{\sinh(2\pi r_x)}{c(r_x,\tau_x)} + (3)^+_{y,x} \frac{\sinh(2\pi r_y)}{c_1(r_y,\tau_y)} \right) \Bigg) \frac{1}{\sqrt{\phi(x)\phi(y)}} \, .
\end{aligned}
\tag{3.2.15}
$$

Here we dropped the barred notation, because performing the $j$-summation describes the transition from $\mathbb{R}^4$ to $\mathbb{R}^3 \times S^1_{\text{rad.}={}^1/_{2\pi}}$.

Explicitly, we find for the periodic case, denoting similarly to above $\tau_x - \tau_y = \Delta\tau$, $r_x - r_y = \Delta r$, and $\vec{x} - \vec{y} = \vec{\Delta}$:

$$
(1)^+ = \frac{\sinh(2\pi|\vec{\Delta}|)}{4\pi|\vec{\Delta}|\, c_1(|\vec{\Delta}|,\Delta\tau)} \, , \tag{3.2.16}
$$

$$
(2)^+_{x,y} = -\frac{\sinh(2\pi r_x)\sinh(2\pi r_y)\sin(2\pi\Delta\tau)}{8 r_x r_y\, c_1(r_x+r_y,\Delta\tau)\, c_1(\Delta r,\Delta\tau)} \, , \tag{3.2.17}
$$

$$
(3)^+_{x,y} = \frac{1}{16 r_x} \left( \frac{\sinh(2\pi\Delta r)}{r_y\, c_1(\Delta r,\Delta\tau)} - \frac{\sinh(2\pi(r_x+r_y))}{r_y\, c_1(r_x+r_y,\Delta\tau)} + \frac{2\sinh(2\pi|\vec{\Delta}|)}{|\vec{\Delta}|\, c_1(|\vec{\Delta}|,\Delta\tau)} \right) . \tag{3.2.18}
$$

Plugging our results (3.2.16) - (3.2.18) into (3.2.15) yields the traceful (diagonal) part of the full massless, periodic propagator:

$$
\begin{aligned}
\Delta^+(x,y) =_{\mathrm{tr}} & \frac{\mathbb{1}}{\sqrt{\phi(x)\phi(y)}} \Bigg[ \frac{\sinh(2\pi|\vec{\Delta}|)}{4\pi|\vec{\Delta}|\, c_1(|\vec{\Delta}|,\Delta\tau)} + \\
& + \varrho^2 \big( \cosh(2\pi r_x)\sin(2\pi\tau_y) - \cosh(2\pi r_y)\sin(2\pi\tau_x) + \sin(2\pi\Delta\tau)) \big) \times \\
& \times \frac{\sin(2\pi\Delta\tau)\sinh(2\pi r_x)\sinh(2\pi r_y)}{8 r_x r_y\, c_1(r_x,\tau_x)\, c_1(r_y,\tau_y)\, c_1(r_x+r_y,\Delta\tau)\, c_1(\Delta r,\Delta\tau)} + \\
& + \varrho^2 \Bigg( \frac{1}{16 r_x} \left( \frac{\sinh(2\pi\Delta r)}{r_y\, c_1(\Delta r,\Delta\tau)} - \frac{\sinh(2\pi(r_x+r_y))}{r_y\, c_1(r_x+r_y,\Delta\tau)} + \frac{2\sinh(2\pi|\vec{\Delta}|)}{|\vec{\Delta}|\, c_1(|\vec{\Delta}|,\Delta\tau)} \right) \frac{\sinh(2\pi r_x)}{c_1(r_x,\tau_x)} + \\
& + \frac{1}{16 r_y} \left( -\frac{\sinh(2\pi\Delta r)}{r_x\, c_1(\Delta r,\Delta\tau)} - \frac{\sinh(2\pi(r_x+r_y))}{r_x\, c_1(r_x+r_y,\Delta\tau)} + \frac{2\sinh(2\pi|\vec{\Delta}|)}{|\vec{\Delta}|\, c_1(|\vec{\Delta}|,\Delta\tau)} \right) \frac{\sinh(2\pi r_y)}{c_1(r_y,\tau_y)} \Bigg) \Bigg] .
\end{aligned}
\tag{3.2.19}
$$

As a quick check for our method, we we show in the ancillary files that the back-transformation $(\vec{\bar{x}}, \bar{x}^4) = (\beta^{-1}\vec{\overline{X}}, \beta^{-1}\bar{x}^4)$, $\varrho = \frac{\rho}{\beta}$ and limit $\beta \to \infty$ of our result (3.2.19) reproduce the result in (3.2.13).

The free periodic propagator by is obtained taking $\varrho \to 0$:

$$\Delta_0^+(x,y) \;=_{\mathrm{tr}}\; \mathbb{1} \sum_{j\,\in\,\mathbb{Z}} \frac{1}{4\pi^2(\overline{\Delta} - j\hat{e}_4)^2} \;=\; \mathbb{1}\,(1)^+ \;=\; \frac{\sinh(2\pi|\vec{\Delta}|)}{4\pi|\vec{\Delta}|\,c(|\vec{\Delta}|,\Delta\tau)} \tag{3.2.20}$$

and in the limit of zero temperature we reproduce the well - known free $\mathbb{R}^4$ - propagator: $\Delta_0^+(X,Y) \;=_{\mathrm{tr}}\; \mathbb{1}\, \frac{\beta\sinh(2\pi|\vec{X}-\vec{Y}|\beta^{-1})}{4\pi|\vec{X}-\vec{Y}|\left(\cosh(2\pi|\vec{X}-\vec{Y}|\beta^{-1})-\cos(2\pi(t_X-t_Y)\beta^{-1}\right)} \overset{\beta\,\to\,\infty}{\to} \frac{\mathbb{1}}{4\pi^2\left(\overline{X}-\overline{Y}\right)^2}$.

### Anti-periodic Propagator

In the anti-periodic, traceful case of (3.2.12), we are interested in the following anti-periodic time copy sums of (3.2.7):

$$\begin{aligned}
(1)^- \;\;&= \sum_{j\,\in\,\mathbb{Z}} \frac{(-1)^j}{4\pi^2(\overline{\Delta} - j\hat{e}_4)^2}\,,\\
(2)^-_{x,y} &= \sum_{j\,\in\,\mathbb{Z}} \frac{-(-1)^j(\overline{\Delta}^4 - j)}{4\pi\, d(|\vec{\overline{x}}|,|\vec{\overline{y}}|,\overline{x}^4,\overline{y}^4+j)}\,,\\
(3)^-_{x,y} &= \sum_{j\,\in\,\mathbb{Z}} \frac{(-1)^j\left(|\vec{\overline{x}}|(\overline{\Delta} - j\hat{e}_4)^2 + \hat{e}_{\vec{\overline{x}}}\cdot\vec{\overline{y}}\,(\overline{\Delta} - j\hat{e}_4)^2 + 2|\vec{\overline{x}}|(\hat{e}_{\vec{\overline{x}}}\cdot\vec{\overline{y}}\,)^2 - 2|\vec{\overline{x}}|\,\vec{\overline{y}}^{\,2}\right)}{4\pi(\overline{\Delta} - j\hat{e}_4)^2\, d(|\vec{\overline{x}}|,|\vec{\overline{y}}|,\overline{x}^4,\overline{y}^4+j)}\,,
\end{aligned} \tag{3.2.21}$$

where $(2)^-_{x,y}$ and $(3)^-_{x,y}$ are again not (explicitly) $x \leftrightarrow y$ - symmetric and contain the factor $\pi$. The traceful part of the full anti-periodic propagator thus reads

$$\begin{aligned}
\Delta^-(x,y) \;=_{\mathrm{tr}}\; \mathbb{1}\,\Bigg((1)^- + \varrho^2\left((2)^-_{x,y}\frac{\sin(2\pi\tau_x)}{c(r_x,\tau_x)} + (2)^-_{y,x}\frac{\sin(2\pi\tau_y)}{c_1(r_y,\tau_y)}\right) +\\
+\;\varrho^2\left((3)^-_{x,y}\frac{\sinh(2\pi r_x)}{c_1(r_x,\tau_x)} + (3)^-_{y,x}\frac{\sinh(2\pi r_y)}{c(r_y,\tau_y)}\right)\Bigg)\,\frac{1}{\sqrt{\phi(x)\phi(y)}}\,.
\end{aligned} \tag{3.2.22}$$

For numerical reasons we have to split up the sum $(3)^-_{x,y}$ into three parts/individual sums: $(3.1)^-_{x,y} = \sum_{j\,\in\,\mathbb{Z}} \frac{(-1)^j\left(|\vec{\overline{x}}| + \hat{e}_{\vec{\overline{x}}}\cdot\vec{\overline{y}}\right)}{4\pi\, d(|\vec{\overline{x}}|,|\vec{\overline{y}}|,\overline{x}^4,\overline{y}^4+j)}$, $(3.2)^-_{x,y} = \sum_j \frac{(-1)^j|\vec{\overline{x}}|\left(\hat{e}_{\vec{\overline{x}}}\cdot\vec{\overline{y}}\right)^2}{2\pi(\overline{\Delta}-j\hat{e}_4)^2\, d(|\vec{\overline{x}}|,|\vec{\overline{y}}|,\overline{x}^4,\overline{y}^4+j)}$ as well as $(3.3)^-_{x,y} = -\sum_j \frac{(-1)^j\,|\vec{\overline{x}}|\,\vec{\overline{y}}^{\,2}}{2\pi(\overline{\Delta}-j\hat{e}_4)^2\, d(|\vec{\overline{x}}|,|\vec{\overline{y}}|,\overline{x}^4,\overline{y}^4+j)}$. Additionally, we introduce the function $c_2(z_1,z_2) = \cosh^2(\pi z_1) - \cos^2(\pi z_2)$. We find:

$$(1)^- \;\;= \frac{\sinh(\pi|\vec{\Delta}|)\cos(\pi\Delta\tau)}{2\pi|\vec{\Delta}|\,c_1(|\vec{\Delta}|,\Delta\tau)}\,, \tag{3.2.23}$$

$$(2)^{-}_{x,y} = -\frac{\big(\cosh(2\pi r_x) + \cosh(2\pi r_y) + \cos(2\pi\Delta\tau) + 1\big)\sinh(\pi r_x)\sinh(\pi r_y)\sin(\pi\Delta\tau)}{16 r_x r_y\, c_2(r_x + r_y, \Delta\tau)\, c_2(\Delta r, \Delta\tau)}\,, \tag{3.2.24}$$

$$\begin{aligned}(3)^{-}_{x,y} = -\Bigg(&\frac{(1 - \hat{e}_{\vec{x}}\cdot\hat{e}_{\vec{y}})\sinh(\pi(r_x + r_y))}{(r_x + r_y)c_2(r_x + r_y, \Delta\tau)} + \frac{(1 + \hat{e}_{\vec{x}}\cdot\hat{e}_{\vec{y}})\sinh(\pi\Delta r)}{\Delta r\, c_2(\Delta r, \Delta\tau)} - \frac{2\sinh(\pi|\vec{\Delta}|)}{|\vec{\Delta}|\, c_2(|\vec{\Delta}|, \Delta\tau)} - \\ &- (r_x + r_y\,\hat{e}_{\vec{x}}\cdot\hat{e}_{\vec{y}})\left(\frac{\sinh(\pi(r_x + r_y))}{r_y(r_x + r_y)\, c_1(r_x + r_y, \Delta\tau)} + \frac{\sinh(\pi|\Delta r|)}{c_1(\Delta r, \Delta\tau)}\right)\Bigg)\frac{\cos(\pi\Delta\tau)}{16 r_x}\,. \end{aligned} \tag{3.2.25}$$

Using again (3.2.15) yields the massless, anti-periodic scalar propagator's diagonal part. As it is very lengthy and not needed for this work, we do do not present it in full, however; especially because we only find one simplification for the explicit form:

$$\begin{aligned}&(2)^{-}_{x,y}\frac{\sin(2\pi\tau_x)}{c_1(r_x, \tau_x)} + (2)^{-}_{y,x}\frac{\sin(2\pi\tau_y)}{c_1(r_y, \tau_y)} = \\ &= \big(\cosh(2\pi r_x)\sin(2\pi\tau_y) - \cosh(2\pi r_y)\sin(2\pi\tau_x) + \sin(2\pi\Delta\tau)\big)\times \\ &\quad\times\frac{\big(\cosh(2\pi r_x) + \cosh(2\pi r_y) + \cos(2\pi\Delta\tau) + 1\big)\sinh(\pi r_x)\sinh(\pi r_y)\sin(\pi\Delta\tau)}{16 r_x r_y\, c_1(r_x, \tau_x)\, c_1(r_y, \tau_y)\, c_2(r_x + r_y, \Delta\tau)\, c_2(\Delta r, \Delta\tau)}\,.\end{aligned} \tag{3.2.26}$$

Analogously to the periodic case, we find for the free anti-periodic propagator:

$$\Delta^{-}_{0}(x, y) =_{\text{tr}} \mathbb{1}\sum_{j\,\in\,\mathbb{Z}}\frac{(-1)^j}{4\pi^2(\overline{\Delta} - j\hat{e}_4)^2} = \mathbb{1}\,(1)^{-}_{x,y} = \frac{\sinh(\pi|\vec{\Delta}|)\cos(\pi\Delta\tau)}{2\pi|\vec{\Delta}|\, c(|\vec{\Delta}|, \Delta\tau)}\,. \tag{3.2.27}$$

For $T = 0$, this also yields the familiar free $\mathbb{R}^4$ - propagator: $\Delta^{-}_{0}(X, Y) \overset{\beta\,\to\,\infty}{\to} \frac{\mathbb{1}}{4\pi^2\left(\overline{X} - \overline{Y}\right)^2}$.

### Closed Loop - Propagators

Finally, we calculate the finite and infinite parts of the coincident (anti-)periodic propagator $\Delta^{\pm}(x, x)$ (3.2.3), which correspond to (anti-)periodically ($j \neq 0$) and aperiodically ($j = 0$) closed loops, respectively. Compare this to figure 3.1, where these anti-periodic propagators are shown and discussed.

For the finite part of the coincident propagator, first set $\vec{x} = \vec{y}$ in the calculation of the aperiodic propagator's traceful part and include $j \neq 0$. This drastically simplifies the calculation of $F$ as given in (3.2.4) (cf. also (3.2.5)):

$$\begin{aligned} F(\bar{x}, \bar{x} + j\,\hat{e}_4) &=_{\text{tr}} \\ =_{\text{tr}} \mathbb{1} + \sum_{k\,\in\,\mathbb{Z}} &\frac{\mathbb{1}\,\varrho^2\big(\vec{\bar{x}}^{\,2} + (\bar{x}^4 - k)(\bar{x}^4 + j - k)\big)}{\vec{\bar{x}}^{\,4} + \vec{\bar{x}}^{\,2}(\bar{x}^4 - k)^2 + \vec{\bar{x}}^{\,2}(\bar{x}^4 + j - k)^2 + (\bar{x}^4 - k)^2(\bar{x}^4 + j - k)^2} = \\ = \mathbb{1}\left(1 + \frac{4\pi\varrho^2\vec{\bar{x}}^{\,2}\sinh(2\pi|\vec{\bar{x}}|)}{(4\,\vec{\bar{x}}^{\,2} + j^2)\,c(|\vec{\bar{x}}|, \bar{x}^4)}\right)&. \end{aligned} \tag{3.2.28}$$

We can now perform the $j$ - summation according to (3.2.12) and find the traceful finite part of the coincident (anti-)periodic propagator:

$$\begin{aligned} \sum_{j\,\in\,\mathbb{Z}\backslash\{0\}} (\pm 1)^j \overline{\Delta}(\bar{x}, \bar{x} + j\hat{e}_4) &= \sum_{j\,\in\,\mathbb{Z}\backslash\{0\}} \frac{(\pm 1)^j F(\bar{x}, \bar{x} + j\hat{e}_4)}{4\pi^2 j^2\,\phi(x)} =_{\text{tr}} \\ =_{\text{tr}} \sum_{j\,\in\,\mathbb{Z}\backslash\{0\}} \frac{(\pm\mathbb{1})^j}{4\pi^2\,\phi(x)} &\left(\frac{1}{j^2} + \left(\frac{1}{j^2} - \frac{1}{4\,\vec{\bar{x}}^{\,2} + j^2}\right)\frac{\pi\varrho^2\sinh(2\pi|\vec{\bar{x}}|)}{|\vec{\bar{x}}|\,c(|\vec{\bar{x}}|, \bar{x}^4)}\right) = \\ = \left\{\begin{matrix} \dfrac{\mathbb{1}}{12} \\ -\dfrac{\mathbb{1}}{24} \end{matrix}\right\} + \frac{\mathbb{1}\,\varrho^2\sinh(2\pi r_x)}{16\pi r_x^3\,c_1(r_x, \tau_x)\,\phi(x)} &\left(1 - 2\pi r_x \cdot \left\{\begin{matrix} \coth(2\pi r_x) \\ \operatorname{csch}(2\pi r_x) \end{matrix}\right\}\right), \end{aligned} \tag{3.2.29}$$

where we used that $\frac{1}{j^2(4\vec{\bar{x}}^{\,2}+j^2)} = \frac{1}{4\,\vec{\bar{x}}^{\,2}j^2} - \frac{1}{4\,\vec{\bar{x}}^{\,2}(4\,\vec{\bar{x}}^{\,2}+j^2)}$. We abbreviate $\{\frac{1}{12}, -\frac{1}{24}\} = C^{\pm}$. This finite contribution contains the corresponding finite contribution to the free propagator

$$\sum_{j\,\in\,\mathbb{Z}\backslash\{0\}} (\pm 1)^j \overline{\Delta}_0(\bar{x}, \bar{x} + j\hat{e}_4) = \sum_{j\in\mathbb{Z}} \frac{(\pm\mathbb{1})^j}{4\pi^2 j^2} = \mathbb{1}\,C^{\pm}\,. \tag{3.2.30}$$

Second, the finite traceless part vanishes. To see that, we calculate the traceless part (again with the general formulae (3.2.4) and (3.2.5))

$$\begin{aligned} F(\bar{x}, \bar{x} + j\hat{e}_4) \;=_{\backslash\text{tr}} \sum_{k\,\in\,\mathbb{Z}} &\frac{-i\varrho^2 j\,\vec{\bar{x}}\cdot\vec{\sigma}}{\vec{\bar{x}}^{\,4} + \vec{\bar{x}}^{\,2}(\bar{x}^4 - k)^2 + \vec{\bar{x}}^{\,2}(\bar{x}^4 + j - k)^2 + (\bar{x}^4 - k)^2(\bar{x}^4 + j - k)^2} = \\ = -&\frac{2i\pi\varrho^2\sinh(2\pi|\vec{\bar{x}}|)\,\hat{e}_{\bar{x}}\cdot\vec{\sigma}}{c(|\vec{\bar{x}}|, \bar{x}^4)}\,\frac{j}{4\,\vec{\bar{x}}^{\,2} + j^2} \end{aligned} \tag{3.2.31}$$

and note that it is odd in $j$, i.e., the time copy sums vanish:

$$\sum_{j\,\in\,\mathbb{Z}\backslash\{0\}} (\pm 1)^j \overline{\Delta}\big(\bar{x}, \bar{x} + j\hat{e}_4)\big) \propto_{\backslash\text{tr}} \sum_{j\,\in\,\mathbb{Z}\backslash\{0\}} \frac{(\pm 1)^j j}{(4\,\vec{\bar{x}}^{\,2} + j^2)j^2} = 0\,. \tag{3.2.32}$$

Note that the connection to dimensionful coordinates and parameters $\vec{X}, t, \rho$ for the finite contributions is achieved by rescaling $j \to j\beta$ before performing the $j$ - summations. This introduces an overall factor of $\beta^{-2}$ in (3.2.29) so that the caloron background term reads $\frac{\mathbb{1}\,\rho^2 \sinh(2\pi|\vec{X}|\beta^{-1})}{16\pi\beta|\vec{X}|^3\, c\left(|\vec{X}|\beta^{-1}, \bar{t}\beta^{-1}\right)\, \phi(X)} \left(1 - 2\pi|\vec{X}|\beta^{-1} \cdot \{...\}\right)$. As expected, (3.2.29) vanishes as $\beta \to \infty \Rightarrow T \searrow 0$.

Third, we turn to the infinite (or rather, regularized) parts. We cannot employ the Schwinger proper time representation and heat kernel expansion in this case, as there is no large parameter to take the place of $m \gg 1$ and enforce $s \searrow 0$ as in section 3.1, which would ensure convergence. As discussed section 3.2.1, point splitting can instead provide regularization. We choose a temporal splitting $\bar{x}' = \bar{x} + \bar{\varepsilon}_\tau\, \hat{e}_4$, $\bar{\varepsilon}_\tau \searrow 0$ to find the regularized part of the coincident propagator from $\bar{x}$ to $\bar{x}'$. Note that this procedure for the $j = 0$ - mode is equivalent for the periodic and anti-periodic case. In temporal point splitting regularization, the traceful part of $F(\bar{x}', \bar{x})$ as given in (3.2.4) and (3.2.5) reads

$$\begin{aligned}
F(\bar{x}', \bar{x}) \;&=_{\mathrm{tr}} \\
&=_{\mathrm{tr}} \mathbb{1} + \mathbb{1} \sum_{k\,\in\,\mathbb{Z}} \frac{\varrho^2\left(\vec{\bar{x}}^{\,2} + (\bar{x}^4 + \bar{\varepsilon}_\tau - k)(\bar{x}^4 - k)\right)}{\vec{\bar{x}}^{\,4} + \vec{\bar{x}}^{\,2}(\bar{x}^4 - k)^2 + \vec{\bar{x}}^{\,2}(\bar{x}^4 + \bar{\varepsilon}_\tau - k)^2 + (\bar{x}^4 + \bar{\varepsilon}_\tau - k)^2(\bar{x}^4 - k)^2} = \\
&= \mathbb{1} + \frac{\mathbb{1}\pi\varrho^2}{4\,\vec{\bar{x}}^{\,2} + \bar{\varepsilon}_\tau^2}\Big(2\,|\vec{\bar{x}}|\sinh(4\pi|\vec{\bar{x}}|) - 2\,|\vec{\bar{x}}|\sinh(2\pi|\vec{\bar{x}}|)\big(\cos(2\pi\bar{x}^4) + \cos(2\pi(\bar{x}^4 + \bar{\varepsilon}_\tau))\big) - \\
&\qquad\qquad - \bar{\varepsilon}_\tau\cosh(2\pi|\vec{\bar{x}}|)\big(\sin(2\pi(\bar{x}^4 + \bar{\varepsilon}_\tau)) - \sin(2\pi\bar{x}^4)\big) + \bar{\varepsilon}_\tau\sin(2\pi\bar{\varepsilon}_\tau)\Big) \times \\
&\qquad\qquad \times \frac{1}{c(|\vec{\bar{x}}|, \bar{x}^4)\,c(|\vec{\bar{x}}|, \bar{x}^4 + \bar{\varepsilon}_\tau)}
\end{aligned} \tag{3.2.33}$$

and for the traceless part described in (3.2.4) and (3.2.10) we find

$$\begin{aligned}
F(\bar{x}', \bar{x}) \;&=_{\backslash\mathrm{tr}} \sum_{k\,\in\,\mathbb{Z}} \frac{i\varrho^2\,\bar{\varepsilon}_\tau\,\vec{\bar{x}}\cdot\vec{\sigma}}{\vec{\bar{x}}^{\,4} + \vec{\bar{x}}^{\,2}(\bar{x}^4 - k)^2 + \vec{\bar{x}}^{\,2}(\bar{x}^4 + \bar{\varepsilon}_\tau - k)^2 + (\bar{x}^4 + \bar{\varepsilon}_\tau - k)^2(\bar{x}^4 - k)^2} = \\
&= \frac{i\pi\varrho^2\,\hat{e}_{\vec{\bar{x}}}\cdot\vec{\sigma}}{4\,\vec{\bar{x}}^{\,2} + \bar{\varepsilon}_\tau^2}\Big(\bar{\varepsilon}_\tau\sinh(4\pi|\vec{\bar{x}}|) + 2\,|\vec{\bar{x}}|\cosh(2\pi|\vec{\bar{x}}|)\big(\sin(2\pi(\bar{x}^4 + \bar{\varepsilon}_\tau)) - \sin(2\pi\bar{x}^4)\big) - \\
&\qquad\qquad - \bar{\varepsilon}_\tau\sinh(2\pi|\vec{\bar{x}}|)\big(\cos(2\pi\bar{x}^4) + \cos(2\pi(\bar{x}^4 + \bar{\varepsilon}_\tau))\big) - 2\,|\vec{\bar{x}}|\sin(2\pi\bar{\varepsilon}_\tau)\Big) \times \\
&\qquad \times \frac{1}{c(|\vec{\bar{x}}|, \bar{x}^4)\,c(|\vec{\bar{x}}|, \bar{x}^4 + \bar{\varepsilon}_\tau)}\,.
\end{aligned} \tag{3.2.34}$$

Finally, we obtain the full coincident propagator at finite temperature, regularized via point splitting in the temporal direction, by plugging (3.2.29) - (3.2.34) into (3.2.3), performing a Taylor expansion in $\bar{\varepsilon}$ and dropping the subscript "$x$" for clarity of notation:

$$
\begin{aligned}
&\Delta^{\pm}(x' = x + \varepsilon_\tau\, \hat{e}_4, x) = \frac{F(\bar{x}', \bar{x})}{4\pi^2\, \bar{\varepsilon}_\tau^{\,2} \sqrt{\phi(x')\phi(x)}} + \sum_{j\, \in\, \mathbb{Z}\setminus\{0\}} \frac{(\pm 1)^j F(\bar{x}, \bar{x} + j\hat{e}_4)}{4\pi^2 j^2\, \phi(x)} = \\
&= \frac{\mathbb{1}}{4\pi^2\, \varepsilon_\tau^2} + \mathbb{1}\, C^{\pm} + \frac{\mathbb{1}\, \varrho^2 \sinh(2\pi r) \left(1 - 2\pi r \cdot \begin{Bmatrix} \coth(2\pi r) \\ \operatorname{csch}(2\pi r) \end{Bmatrix}\right)}{16\pi r^3 \big(\cosh(2\pi r) - \cos(2\pi\tau)\big)\phi(x)} - \\
&\quad - \frac{\mathbb{1}\, \varrho^2}{64\pi r^3} \Bigg( \sinh(6\pi r) + 4\pi r \cosh(4\pi r)\cos(2\pi\tau) - \sinh(2\pi r) \times \\
&\quad \times \left( \frac{8\pi^3 \varrho^2 r \sinh(2\pi r)\sin^2(2\pi\tau)}{\big(\cosh(2\pi r) - \cos(2\pi\tau)\big)\phi(x)} - 2\cos(2\pi\tau) - 3 \right) - 4\big(\sinh(4\pi r) - 3\pi r\big)\cos(2\pi\tau) - \\
&\quad - 4\pi r \cosh(2\pi r)(\cos(4\pi\tau) + 3) \Bigg) \left( \big(\cosh(2\pi r) - \cos(2\pi\tau)\big)^3 \phi(x) \right)^{-1} + \\
&\quad + \frac{i\varrho^2\, \sigma^r(x)}{64\pi r^3\, \varepsilon_\tau} \Bigg( r\sinh(8\pi r) + \pi\varrho^2 \cosh(8\pi r) + \big((4\pi^2\varrho^2 - 6) r \sinh(6\pi r) + \\
&\quad + 4\pi(r^2 - \varrho^2)\cosh(6\pi r)\big)\cos(2\pi\tau) - 2\pi\Big((4r^2 - \varrho^2)\big(2 + \cos(4\pi\tau)\big) + \varrho^2\Big)\cosh(4\pi r) - \\
&\quad - 12\pi^2\varrho^2 r \sinh(4\pi r) + 8r\sinh(4\pi r) - 2(2\pi^2\varrho^2 - 3) r \sinh(4\pi r)\cos(4\pi\tau) + \\
&\quad + 4\pi\cosh(2\pi r)\big((14r^2 + \varrho^2)\cos(2\pi\tau) + r^2\cos(6\pi\tau)\big) - 2r\sinh(2\pi r)\cos(6\pi\tau) + \\
&\quad + 4(5\pi^2\varrho^2 - 3) r \sinh(2\pi r)\big)\cos(2\pi\tau) - \pi(8r^2 + \varrho^2)(2\cos(4\pi\tau) + 3) \Bigg) \cdot \\
&\quad \cdot \left( \big(\cosh(2\pi r) - \cos(2\pi\tau)\big)^4 \phi^2(x) \right)^{-1} - \\
&\quad - \frac{i\varrho^2\, \sigma^r(x)}{64\pi r^3} \Bigg( 2\pi r\big(2\pi r \cosh(6\pi r) + 8\pi^2\varrho^2 \sinh^3(2\pi r) + \sinh(6\pi r)\big)\sin(2\pi\tau) - \\
&\quad - 4\pi r \sinh(4\pi r) - 4\pi^2 r^2 \cosh(2\pi r)\big(6\sin(2\pi\tau) + \sin(6\pi\tau)\big) + \\
&\quad + 2\pi r \sinh(2\pi r)\big(2\sin(4\pi\tau) + \sin(6\pi\tau)\big) + 16\pi^2 r^2 \sin(4\pi\tau) \Bigg) \times \\
&\quad \cdot \left( \big(\cosh(2\pi r) - \cos(2\pi\tau)\big)^4 \phi^2(x) \right)^{-1} + \mathcal{O}(\varepsilon_\tau)\,, \qquad (3.2.35)
\end{aligned}
$$

with $C^{\pm} = \{\frac{1}{12}, -\frac{1}{24}\}$, $\vec{x}\cdot\vec{\sigma} = r\,\sigma^r(x)$ and $\sigma^r(x) = \hat{e}_r(x)\cdot\vec{\sigma} = \begin{pmatrix} \cos(\theta) & \sin(\theta)e^{-i\varphi} \\ \sin(\theta)e^{i\varphi} & -\cos(\theta) \end{pmatrix}$ a function of only the polar and azimuthal angles $\theta$, $\varphi$ of $\vec{x}$. Note: $\mathrm{tr}(\sigma^r) = 0$ and $(\sigma^r)^2 = \mathbb{1}$.

The first two (constant) diagonal terms in $\Delta^{\pm}(x', x)$ correspond to the periodic/anti-periodic free field coincident propagator $\Delta_0^{\pm}(x', x) = \Delta^{\pm}(x', x)\big|_{\varrho=0} = \frac{\mathbb{1}}{4\pi^2\,\varepsilon_\tau^2} + \mathbb{1}\,C^{\pm}$. The spacetime - dependent diagonal terms (third and fourth term) we write as $\mathbb{1}\,\Delta^{\pm}_{\text{diag, finite}}(x)$. In the periodic case, this finite contribution due to the caloron centered at the origin $x = 0$ vanishes polynomially as $\Delta^{+}_{\text{diag, finite}} \overset{r\,\to\,\infty}{\propto} -\frac{\varrho^2}{8r^2}$ for large distances from the caloron, while for the anti-periodic scalar of interest this term falls off exponentially as $\Delta^{-}_{\text{diag, finite}} \overset{r\,\to\,\infty}{\propto} -\frac{\varrho^2}{2r^2}\,e^{-2\pi r}\cos^2(\pi\tau)$. The off-diagonal part of the coincident propagator (fifth and sixth term) contains an "$\varepsilon_\tau \searrow 0$ - diverging" term and a finite one, which we denote as $i\sigma^r(x)\,\varepsilon_\tau^{-1}\Delta_{\text{off-diag, infinite}}(x)$ and $i\sigma^r(x)\,\Delta_{\text{off-diag, finite}}(x)$, respectively. They fall off as $\Delta_{\text{off-diag, infinite}} \overset{r\,\to\,\infty}{\propto} \frac{\varrho^2}{8\pi r^2}$ and $\Delta_{\text{off-diag, finite}} \overset{r\,\to\,\infty}{\propto} -\frac{\pi\varrho^2}{2r}\,e^{-2\pi r}\sin(2\pi\tau)$.

The fact that the anti- periodic propagator falls off exponentially at large separation, but the periodic one does not, explains why it is possible to perform an $m^2$ - expansion in the anti- periodic but not the periodic case. For periodic boundary conditions, the lowest Matsubara frequency is zero, and the logarithmic IR effects present in vacuum become more severe, appearing as a linear divergence in the $m^2$ - coefficient. We expect the true $m^2$ - dependency to be non - analytic $\propto m$, similar to what happens in the finite - $m$ expansion of the pressure [197].

Close to the caloron center, i.e., for $r \searrow 0$, the coincident propagator - terms scale as: $\Delta^{+}_{\text{diag, finite}} \overset{r\,\searrow\,0}{\propto} -\frac{\pi^2\varrho^2(1+\pi^2\varrho^2)}{2\left(2\pi^2\varrho^2+1-\cos(2\pi\tau)\right)^2}$, $\Delta^{-}_{\text{diag, finite}} \overset{r\,\searrow\,0}{\propto} -\frac{\pi^2\varrho^2\cos^2(\pi\tau)}{2\left(2\pi^2\varrho^2+1-\cos(2\pi\tau)\right)^2}$ for the (anti-)periodic traceful terms and $\Delta_{\text{off-diag, infinite}} \overset{r\,\searrow\,0}{\propto} r\,\frac{\pi^2\varrho^2\left(2+\cos(2\pi\tau)\right)\csc^2(\pi\tau)}{6\left(2\pi^2\varrho^2+1-\cos(2\pi\tau)\right)}$ as well as $\Delta_{\text{off-diag, finite}} \overset{r\,\searrow\,0}{\propto} -r\,\frac{\pi^3\varrho^2\left(12\pi^2\varrho^2+9-8\cos(2\pi\tau)-\cos(4\pi\tau)\right)\cot(\pi\tau)\,\csc^2(\pi\tau)}{12\left(2\pi^2\varrho^2+1-\cos(2\pi\tau)\right)^2}$ for the traceless parts.

Using all the above abbreviations, we write the closed loop - propagator (3.2.35) as

$$\begin{aligned} \Delta^{\pm}(x', x) = \frac{\mathbb{1}}{4\pi^2\,\varepsilon_\tau^2} + \mathbb{1}\,C^{\pm} + \mathbb{1}\,\Delta^{\pm}_{\text{diag, finite}}(r, \tau) + \frac{i\sigma^r(x)}{\varepsilon_\tau}\,\Delta_{\text{off-diag, infinite}}(r, \tau) + \\ + i\sigma^r(x)\,\Delta_{\text{off-diag, finite}}(r, \tau) + \mathcal{O}(\varepsilon_\tau)\,. \end{aligned} \tag{3.2.36}$$

### 3.2.3 Taylor Expansion

Now obtain the Taylor expansion as described in section 3.2.1, using the results from section 3.2.2. According to the temporal point splitting employed above, we have to include a temporal Wilson line. Using again $A^4_{\text{HS}}(x) = -\frac{\partial_r \phi}{\phi} \frac{\sigma^r(x)}{2}$ we find an expression for this temporal line

$$\begin{aligned} e^{i\int_\tau^{\tau+\varepsilon_\tau} \mathrm{d}\tau \, A^4_{\text{HS}}(\vec{x},\tau)} &= \mathbb{1} + iA^4_{\text{HS}}(x)\,\varepsilon_\tau + \frac{1}{2}\Big(i\,\partial_\tau A^4_{\text{HS}}\big|_x - \big(A^4_{\text{HS}}(x)\big)^2\Big)\varepsilon_\tau^2 + \mathcal{O}(\varepsilon_\tau^3) = \\ &= \mathbb{1}\Big(1 - \frac{1}{8}\Big(\frac{\partial_r\phi}{\phi}\Big|_x\Big)^2\varepsilon_\tau^2\Big) - i\,\frac{\sigma^r(x)}{2}\,\Big(\frac{\partial_r\phi}{\phi}\,\varepsilon_\tau + \frac{\partial_\tau\partial_r\phi}{2\phi}\,\varepsilon_\tau^2 - \frac{\partial_\tau\phi\,\partial_r\phi}{2\phi^2}\,\varepsilon_\tau^2\Big)\Big|_x \,. \end{aligned} \tag{3.2.37}$$

We note the large and small distance behavior of the caloron field: $A^4_{\text{HS}} \propto \frac{\partial_r\phi}{\phi} \overset{r\to\infty}{\propto} -\frac{\pi\varrho^2}{r^2}$ and $\frac{\partial_r\phi}{\phi} \overset{r\searrow 0}{\propto} -r\,\frac{8\pi^4\varrho^2\big(2+\cos(2\pi\tau)\big)}{3\big(2\pi^2\varrho^2+1-\cos(2\pi\tau)\big)\big(1-\cos(2\pi\tau)\big)}$.

With this, the $m^2$ - coefficient of $\gamma_{\text{ferm}}$ reads

$$\begin{aligned} &-2\lim_{\varepsilon_\tau\searrow 0}\int^1 \mathrm{d}^4x\,\mathrm{tr}\,\Big(\frac{\mathbb{1}}{4\pi^2\,\varepsilon_\tau^2} + \mathbb{1}\,C^- - \frac{\mathbb{1}}{32\pi^2}\Big(\frac{\partial_r\phi}{\phi}\Big|_x\Big)^2 + \mathbb{1}\,\Delta^-_{\text{diag, finite}}(r,\tau) + \\ &\qquad\qquad + \frac{\mathbb{1}}{2}\,\Delta_{\text{off-diag, infinite}}(r,\tau)\,\frac{\partial_r\phi}{\phi}\Big|_x - \Delta^-_0(x',x)\Big) = \\ &= -\int_0^1 \mathrm{d}\tau \int_0^\infty \mathrm{d}r\, r^2\,\Big(-\frac{1}{2\pi}\Big(\frac{\partial_r\phi}{\phi}\Big|_x\Big)^2 + 16\pi\,\Delta^-_{\text{diag, finite}}(r,\tau) + \\ &\qquad\qquad + 8\pi\,\Delta_{\text{off-diag, infinite}}(r,\tau)\,\frac{\partial_r\phi}{\phi}\Big|_x\Big) = \\ &= -\int_0^1 \mathrm{d}\tau \int_0^\infty \mathrm{d}r\;\mathrm{int}^-(\varrho,r,\tau) = -2\gamma^{\text{small}}_{\text{s},\,-}(\varrho) \end{aligned} \tag{3.2.38}$$

$$\Rightarrow \quad \gamma_{\text{ferm}} = \gamma_{\text{ferm}}\big|_{m\,=\,0} - 2m^2\gamma^{\text{small}}_{\text{s},\,-}(\varrho) + \mathcal{O}(m^4), \tag{3.2.39}$$

with $\gamma_{\text{ferm}}\big|_{m\,=\,0}$ given in (3.2.1). Due to the aforementioned large- and small - distance behaviors of $\frac{\partial_r\phi}{\phi}$, $\Delta^+_{\text{diag, finite}}$ and $\Delta^+_{\text{off-diag, infinite}}$, the integral $\gamma^{\text{small}}_{\text{s},\,-}(\varrho)$ is finite and we can calculate it numerically for different values of the parameter $\varrho$. In the periodic case, the corresponding integral $\gamma^{\text{small}}_{\text{s},\,+}$ is linearly divergent, as we discussed before. This is due to $\Delta^+_{\text{diag, finite}}(r,\tau)$ scaling as $r^{-2}$ for large distances.

The set $\varrho \in \{5\cdot 10^{-4}\cdot 1.075^j\,|\,\mathbb{N}\ni j \leq 30\} \cup \{5\cdot 10^{-4}\cdot 1.075^{30}\cdot 1.12^k\,|\,\mathbb{N}\ni k \leq 79\}$ of 110 $\varrho$ - caloron sizes - with a minimal and maximal caloron size of $\varrho_{\text{min}} = 5\cdot 10^{-4}$ and

$\varrho_{\text{max}} \approx 33.8$ - is chosen for the numerical integration of (3.2.38). Detailed information on the numerical procedure is provided in appendix D.2 and the ancillary files:[14]

$$\gamma_{\text{s},-}^{\text{small}}(\varrho) = \begin{cases} -0.500\tilde{\varrho}^2 \ln(0.946\tilde{\varrho}) & : 0 \leq \varrho \leq 0.082 \\ -0.85\varrho^{1.80} + 0.59\tilde{\varrho}^{1.28} & : 0.082 < \varrho \leq 1.045 \, , \\ -0.76\varrho^{2.00} & : 1.045 < \varrho \end{cases} \tag{3.2.40}$$

where, as explained in section 3.1.3, "$x.00$" again means the coefficient is numerically given to two decimal places in comparison to "$x$" which is the coefficient set to the exact integer. The $\varrho$ - boundaries $0.082$ and $1.045$ again separate the regions of small, intermediate and large caloron sizes. The fitting function (3.2.40) and our data as well as the fit's relative error are shown in figures 3.11a and 3.11b.

We gauge the validity of our expansion (3.2.39) with $-2\gamma_{\text{s},-}^{\text{small}}$ as in (3.2.40) by modifying the method proposed in [60]: we compare (3.2.40) with the expected terms of $\mathcal{O}(m^4)$ in the Taylor series:

$$\frac{m^4}{2}\, \frac{\mathrm{d}^2\gamma_{\text{ferm}}}{\mathrm{d}^2 m^2}\bigg|_{m=0} = m^4 \cdot \begin{cases} c_1\tilde{\varrho}^4 & : 0 \leq \varrho \leq 0.1 \\ c_2\rho^4 + c_3\tilde{\varrho}^4 & : 0.1 < \varrho \leq 1 \ . \\ c_4\varrho^4 & : 1 < \varrho \end{cases} \tag{3.2.41}$$

The coefficients $c_1$, $c_4$ and $c_2 + c_3$ are expected to be of $\mathcal{O}(1)$ and we set them as $c_1 = c_4 = 1$ and $c_2 = 0.8$, $c_3 = 0.2$ ($c_2$ and $c_3$ are chosen as such for later convenience). The boundaries $0.1$ and $1$ are set to simplified versions of their counterparts in (3.2.40). We estimate the upper limit of the Taylor expansion by determining the maximum $m$ - value $m_{\text{small, max, 1}}(\varrho)$ such that the $\mathcal{O}(m^4)$ - contribution (3.2.41) is at maximum about $\frac{2}{3}$ of the $\mathcal{O}(m^2)$ - one (this value of $\frac{2}{3}$ is chosen in accordance with [60], where it is used as the maximum for the $m^4$ - instanton contribution). We obtain this maximum $m$ - value for 750 caloron sizes given by the sets $\varrho \in \{10^{-3\left(1-\frac{j}{249}\right)} \cdot 0.1^{\frac{j}{249}} \,|\, \mathbb{N} \ni j \leq 249\}$, $\varrho \in \{0.102^{1-\frac{j}{249}} \cdot 1^{\frac{j}{249}} \,|\, \mathbb{N} \ni j \leq 249\}$ and $\varrho \in \{1.009^{1-\frac{j}{249}} \cdot 50^{\frac{j}{249}} \,|\, \mathbb{N} \ni j \leq 249\}$ with minimal and maximal caloron sizes $0.001$ and $50$; the coefficients $c_2$ and $c_3$ were chosen by hand such that jumps in the $m_{\text{small, max, 1}}$ - values are minimized as well as possible. We obtain the conservative, simplified fit for $m_{\text{small, max, 1}}$:

---

[14] To improve the interpolation function we added the apparent point $(\varrho, -2\gamma_{\text{s},-}^{\text{small}}) = (0, 0)$ to the interpolation data set only. It turns out that this point is also covered by the resulting interpolation function.

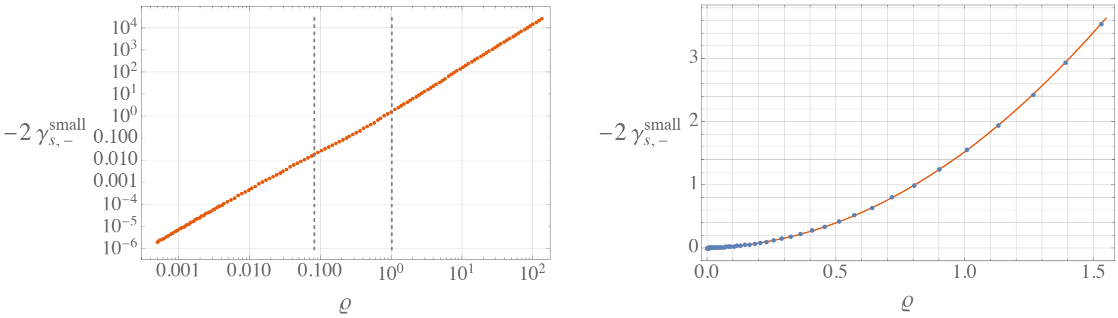

(a). $m^2$ - coefficient $-2\gamma^{\text{small}}_{\text{s},-}$ of the fermionic determinant ratio (3.2.39). Our data and the boundaries of (3.2.40) are shown in orange on the left and the right figure shows the data points in blue together with fitting function in orange.
Despite the deceiving similarity to a simple quadratic function, even close to $\varrho = 0$, such an ansatz becomes an arbitrarily bad fit to the data as $\varrho \to 0$. $\gamma^{\text{small}}_{\text{s},-}$ is is non - analytical at $\varrho = 0$, just as the small mass expansion at $T = 0$ given in [60], which contains the term $(M\rho)^2 \ln(M\rho)$, is non - analytical at $\rho = 0$. This is shown explicitly below in figure 3.11c.

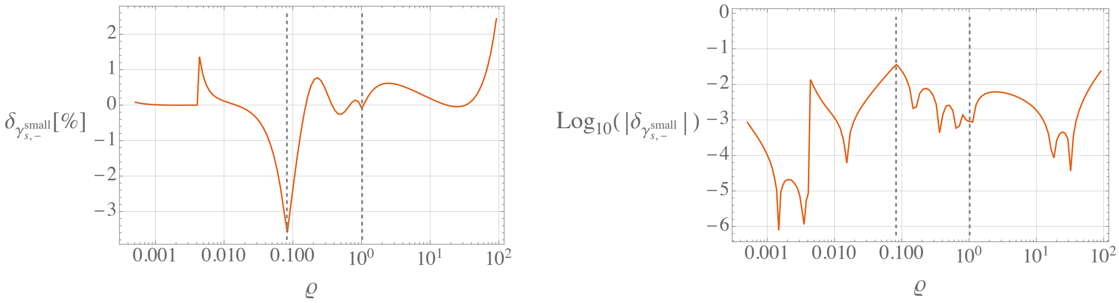

(b). Relative error $\delta_{\gamma^{\text{small}}_{\text{s},-}}$ of (3.2.40) compared to our data in %.

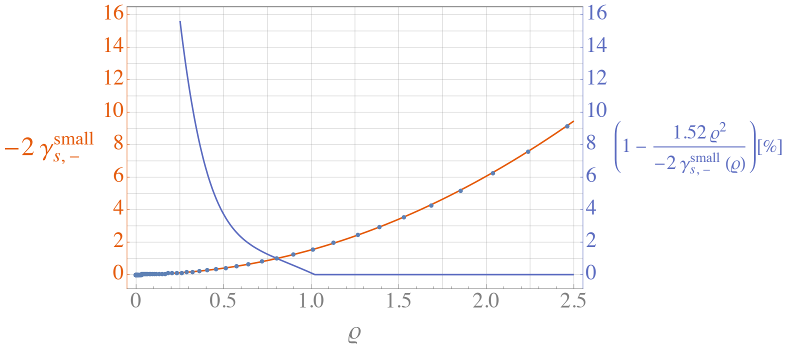

(c). The non - analyticity of $\gamma_{\text{s},-}$ for small $\varrho$. Despite looking very similar to a quadratic even for small caloron sizes, this fit becomes arbitrarily bad as $\varrho \searrow 0$.

Figure 3.11

$$m_{\text{small, max, 1}}(\varrho) = \begin{cases} \sqrt{-\frac{5}{8}\ln(\tilde{\varrho})\tilde{\varrho}^{-2}} & : 0 < \varrho \leq 0.07 \\ 0.35\tilde{\varrho}^{-1.38} + 5.3\varrho^{-0.17} - 5.3 & : 0.07 < \varrho \leq 1.00 \\ \varrho^{-1} & : 1.00 < \varrho \end{cases} . \tag{3.2.42}$$

Additionally, this small mass Taylor expansion requires $M$ to be small compared to $T$, which gives a second upper bound $m \leq m_{\text{small, max, 2}} = \delta$, where we chose $\delta = 0.5$. All in all, the full maximum mass which limits the “small mass regime” and thus the Taylor expansion's applicability is

$$m_{\text{small, max}}(\varrho) = \min\left(m_{\text{small, max, 1}}(\varrho), m_{\text{small, max, 2}}\right) . \tag{3.2.43}$$

Our small mass result (3.2.39) together with (3.2.40), the finite $T$ - corrections at $M = 0$ (2.4.77) and the estimate for the minimal mass (3.2.43) gives the small $m$ - correction factor $f$ according to (2.4.83) - compare also the $T = 0$ result (2.4.78):

$$f_{\text{small}}(m \leq m_{\text{small, max}}(\varrho), \varrho) = f(T,0)\, e^{-\gamma_{\text{ferm}}} = \exp\left(-\frac{(\pi\varrho)^2}{3} + 2A(\pi\varrho) - 2m^2\gamma^{\text{small}}_{\text{s, -}}(\varrho)\right) . \tag{3.2.44}$$

## 3.3 Interpolation between Mass Regimes and Topological Susceptibility

Having performed the large and small mass - expansions, we can now insert the corresponding correction factors (3.1.41) and (3.2.44) into the general correction factor (2.4.83), which we define in terms of an exponent $p(m_{f_{\text{h}}}, \varrho)$:

$$\begin{aligned} f(m_{f_{\text{h}}}, \varrho) &= e^{-2\alpha\left(\frac{1}{2}\right) - p(m_{f_{\text{h}}}, \varrho)} = e^{-2\alpha\left(\frac{1}{2}\right)} \left\{ \begin{matrix} e^{2\alpha\left(\frac{1}{2}\right)} f_{\text{small}} & : m_{f_{\text{h}}} \leq m_{\text{small, max}}(\varrho) \\ e^{2\alpha\left(\frac{1}{2}\right)} f_{\text{large}} & : m_{f_{\text{h}}} \geq m_{\text{large, min}}(\varrho) \end{matrix} \right\} = \\ &= e^{-2\alpha\left(\frac{1}{2}\right)} \begin{cases} \exp\left(2\alpha\left(\frac{1}{2}\right) - \frac{(\pi\varrho)^2}{3} + 2A(\pi\varrho) - 2m_{f_{\text{h}}}^2 \gamma^{\text{small}}_{\text{s, }-}(\varrho)\right) & : m_{f_{\text{h}}} \leq m_{\text{small, max}}(\varrho) \\ \frac{1}{(m_{f_{\text{h}}}\varrho)^{\frac{1}{3}}} \exp\left(-\frac{2\gamma_6(\varrho)}{m_{f_{\text{h}}}^2} - \frac{2\gamma_8(\varrho)}{m_{f_{\text{h}}}^4} - \frac{2\gamma_{10}(\varrho)}{m_{f_{\text{h}}}^6}\right) & : m_{f_{\text{h}}} \geq m_{\text{large, min}}(\varrho) \end{cases} \end{aligned} \tag{3.3.1}$$

We use the function $p(m_{f_{\text{h}}}, \varrho)$ to interpolate between the regimes of small and large masses, i.e., we demand it produce the correct form in these limits. For that, we make the “Padé - like” approximant ansatz

$$p(m,\varrho) = \frac{\sum_{i=0}^{K} p_i(\varrho)\, m^{2i}}{\prod_{j=1}^{K+1}\left(1+\mathcal{P}_j(\varrho)\, m^2\right)} + \frac{1}{6}\ln\!\left(m^2\varrho^2+\xi^2(\varrho)\right), \quad \mathcal{P}_j > 0\,\forall j,\varrho\,. \tag{3.3.2}$$

For $m \ll 1$ this ansatz approaches an $m$ - independent function of $\varrho$ with $\mathcal{O}(m^2)$ - corrections and for $m \gg 1$ the logarithm correctly reproduces the corresponding term in (3.3.1), while the rational part falls off as $m^{-2}$. (3.3.2) contains $2K+3$ $\varrho$ - dependent coefficient functions $p_0(\varrho), \ldots, p_K(\varrho), \mathcal{P}_1(\varrho), \ldots, \mathcal{P}_{K+1}(\varrho)$ and $\xi(\varrho)$, which we fix in terms of the five functions available in (3.3.1): $-2\alpha\left(\frac{1}{2}\right) + \frac{(\pi\varrho)^2}{3} - 2A(\pi\varrho)$, $\gamma_{\mathrm{s},-}^{\mathrm{small}}$ and $\gamma_6$, $\gamma_8$, $\gamma_{10}$. This means we have to set $K=1$. In order to fix the coefficient functions, we perform a Taylor expansion of (3.3.2) up to $\mathcal{O}(m^2)$ for small masses as well as a Laurent expansion up to $\mathcal{O}(m^{-6})$ for large masses and identify these expansions with the corresponding ones in (3.3.1) by equating the $\varrho$ - dependent coefficients. This yields a non - linear, but solvable system of equations.

It is important to note that one cannot write an ansatz of the structure (3.3.2) with an even number of coefficients. Therefore, if one has a large $m$ - expansion up to, for example, $\frac{\gamma_{12}(\varrho)}{m^8}$, one cannot extend the general $p$ - expansion up to higher $K>1$, but is limited to solving an over - determined system of equations for the five $p$ - coefficient functions.

With $p$ we can then describe the full caloron density (2.4.76), using (2.4.75) and the factor $f(N_{f_l}, N, \varrho)$ (2.4.77) due to light quarks and the gauge and ghost sector. For, in general, $N_{f_l}$ light and $N_{f_\mathrm{h}}$ heavy fermions, $N_{f_l}+N_{f_\mathrm{h}} = N_f$, in $SU(N)$ - gauge theory we have:

$$\begin{aligned} d(m_{f_l}, m_{f_\mathrm{h}}, \varrho, \lambda) = {} & \frac{2e^{-\alpha(1)+4\alpha\left(\frac{1}{2}\right)+\ln 2-N\left(2\alpha\left(\frac{1}{2}\right)+2\ln 2\right)+2N_{f_l}\alpha\left(\frac{1}{2}\right)}}{\pi^2(N-1)!(N-2)!}\left(\frac{\ln\lambda(11N-2N_f)}{3}\right)^{2N} \times \\ & \times e^{-\frac{8\pi^2}{g^2(N_f,N,1/\varrho)}}\,\frac{\prod_f m_f\varrho}{\varrho^5}\, f(N_{f_l}, N, \varrho)\prod_{f_\mathrm{h}} e^{-p(m_{f_\mathrm{h}},\varrho)} \end{aligned} \tag{3.3.3}$$

with $g(1/\varrho)$ given in (1.1.2) and with the replacement of $g^{-4N}$ by only the $\lambda$ - dependent part as discussed below (2.4.74).

With $K=1$ in (3.3.2) our ansatz reads

$$p(m_{f_\mathrm{h}},\varrho) = \frac{p_0(\varrho)+p_1(\varrho)\, m_{f_\mathrm{h}}^2}{\left(1+\mathcal{P}_1(\varrho)\, m_{f_\mathrm{h}}^2\right)\left(1+\mathcal{P}_2(\varrho)\, m_{f_\mathrm{h}}^2\right)} + \frac{1}{6}\ln\!\left(m_{f_\mathrm{h}}^2\varrho^2+\xi^2(\varrho)\right), \quad \mathcal{P}_{1,2} > 0\,\forall\varrho. \tag{3.3.4}$$

Performing the Taylor and Laurent expansions of (3.3.4) for small and large $m_{f_\mathrm{h}}$, respectively, and equating them to the respective expansions in (3.3.1) we find:

small $m_{f_\mathrm{h}}$ :

$$p_0 + \frac{1}{3}\ln(\xi) + \left(p_1 - p_0\mathcal{P}_1 - p_0\mathcal{P}_2 + \frac{\varrho^2}{6\xi^2}\right) m_{f_\mathrm{h}}^2 \overset{!}{=} -2\alpha\left(\frac{1}{2}\right) + \frac{(\pi\varrho)^2}{3} - 2A - 2m_{f_\mathrm{h}}^2\gamma_{\mathrm{s},\,-}^{\mathrm{small}}\,, \tag{3.3.5}$$

large $m_{f_\mathrm{h}}$ :

$$\begin{aligned}&\frac{1}{3}\ln(m_{f_\mathrm{h}}\varrho) + \frac{6p_1\varrho^2 + \mathcal{P}_1\mathcal{P}_2\xi^2}{6\mathcal{P}_1\mathcal{P}_2\, m_{f_\mathrm{h}}^2\,\varrho^2} + \frac{12p_0\mathcal{P}_1\mathcal{P}_2\varrho^4 - 12p_1\mathcal{P}_1\varrho^4 - 12p_1\mathcal{P}_2\varrho^4 - \mathcal{P}_1^2\mathcal{P}_2^2\xi^4}{12\mathcal{P}_1^2\mathcal{P}_2^2\, m_{f_\mathrm{h}}^4\,\varrho^4} - \\ &- \frac{18p_0\mathcal{P}_1^2\mathcal{P}_2\varrho^6 + 18p_0\mathcal{P}_1\mathcal{P}_2^2\varrho^6 - 18p_1\mathcal{P}_1^2\varrho^6 - 18p_1\mathcal{P}_1\mathcal{P}_2\varrho^6 - 18p_1\mathcal{P}_2^2\varrho^6 - \mathcal{P}_1^3\mathcal{P}_2^3\xi^6}{18\mathcal{P}_1^3\mathcal{P}_2^3\, m_{f_\mathrm{h}}^6\,\varrho^6} \overset{!}{=} \\ &\overset{!}{=} \frac{1}{3}\ln(m_{f_\mathrm{h}}\varrho) + \frac{2\gamma_6}{m_{f_\mathrm{h}}^2} + \frac{2\gamma_8}{m_{f_\mathrm{h}}^4} + \frac{2\gamma_{10}}{m_{f_\mathrm{h}}^6}\,.\end{aligned} \tag{3.3.6}$$

Using the $m^2$ -, $m^{-2}$ -, $m^{-4}$ - and $m^{-6}$ - coefficient, we analytically solve for $p_0\big(\varrho,\xi(\varrho)\big)$, $p_1\big(\varrho,\xi(\varrho)\big)$, $\mathcal{P}_1\big(\varrho,\xi(\varrho)\big)$ and $\mathcal{P}_2\big(\varrho,\xi(\varrho)\big)$ and finally, using the $\mathcal{O}(m^0)$ - terms, obtain $\xi(\varrho)$ numerically. We find the following analytical results:

$$\begin{aligned}p_0\big(\varrho,\xi(\varrho)\big) &= \frac{\sqrt{2}}{12\big(-18\gamma_{10}\varrho^6 + \xi^6\big)}\left(\frac{3}{\sqrt{2}}\big(6\gamma_6\varrho^2 - \xi^2\big)\big(12\gamma_8\varrho^4 + \xi^4\big) + \frac{1}{\xi\varrho}\sqrt{q_1(\varrho,\xi)}\;\times\right.\\ &\quad\left.\times\sqrt{-6\gamma_{\mathrm{s},\,-}^{\mathrm{small}}\big(\xi^8 - 18\gamma_{10}\xi^2\varrho^6\big) - 2\xi^6\varrho^2 + 18\gamma_6\xi^4\varrho^4 - 54\gamma_6^2\xi^2\varrho^6 + 9\gamma_{10}\varrho^8}\right),\end{aligned} \tag{3.3.7}$$

$$\begin{aligned}p_1\big(\varrho,\xi(\varrho)\big) &= \frac{6\gamma_6\varrho^2 - \xi^2}{3\left(\frac{q_5(\varrho,\xi)}{q_1} - \frac{\sqrt{3q_3(\varrho,\xi)}\big(12\gamma_8\varrho^4+\xi^4\big)}{|q_1|}\right)}\left(\frac{q_2(\varrho,\xi)}{q_1} - \frac{\varrho^2\sqrt{3q_3}}{|q_1|}\right)\times\\ &\quad\times\left(\frac{q_4(\varrho,\xi)}{q_1} + \frac{\sqrt{3q_3}\big(6\gamma_6\varrho^2 - \xi^2\big)}{|q_1|}\right),\end{aligned} \tag{3.3.8}$$

$$\mathcal{P}_1\big(\varrho,\xi(\varrho)\big) = \frac{q_2}{q_1} - \frac{\varrho^2\sqrt{3q_3}}{|q_1|}\,, \tag{3.3.9}$$

$$\mathcal{P}_2\big(\varrho,\xi(\varrho)\big) = \frac{2\varrho^2}{\frac{q_5}{q_1} - \frac{\sqrt{3q_3}\big(12\gamma_8\varrho^4+\xi^4\big)}{|q_1|}}\left(\frac{q_4}{q_1} + \frac{\sqrt{3q_3}\big(6\gamma_6\varrho^2 - \xi^2\big)}{|q_1|}\right) \tag{3.3.10}$$

with

$$q_1(\varrho,\xi) = \xi^8 - 24\gamma_6\xi^6\varrho^2 - 72\gamma_8\xi^4\varrho^4 - 72\gamma_{10}\xi^2\varrho^6 - 432\big(\gamma_8^2 - \gamma_6\gamma_{10}\big)\varrho^8\,, \tag{3.3.11}$$

$$q_2(\varrho,\xi) = 3\left(-\big(1+4p_0^2\big)\xi^6\varrho^2 + \gamma_6\xi^4\varrho^4 - 12\gamma_8\xi^2\varrho^6 + 72(\gamma_6\gamma_8 + \gamma_{10}p_0)\varrho^8\right), \tag{3.3.12}$$

$$\begin{aligned} q_3(\varrho,\xi) = {}&\big(7+36p_0+48p_0^2\big)\xi^{12} - 36\gamma_6(5+12p_0)\xi^{10}\varrho^2 + 108\big(13\gamma_6^2 - 2\gamma_8 - 4\gamma_8 p_0\big)\xi^8\varrho^4 - \\ &- 144\Big(24\gamma_6^3 - 18\gamma_6\gamma_8(1-2p_0) + \gamma_{10}\big(2+9p_0+12p_0^2\big)\Big)\xi^6\varrho^6 - \\ &- 1296\big(6\gamma_6^2\gamma_8 - 2\gamma_6\gamma_{10}(2+3p_0) + \gamma_8^2(1+12p_0)\big)\xi^4\varrho^8 + \\ &+ 15552\big(\gamma_6\gamma_8^2 - 2\gamma_6^2\gamma_{10} - \gamma_8\gamma_{10}p_0\big)\xi^2\varrho^{10} - \\ &- 15552\Big(3\gamma_6^2\gamma_8^2 - 4\gamma_6^3\gamma_{10} - 6\gamma_6\gamma_8\gamma_{10}p_0 + p_0\big(4\gamma_8^2 - \gamma_{10}^2 p_0\big)\Big)\varrho^{12}\,, \end{aligned} \tag{3.3.13}$$

$$\begin{aligned} q_4(\varrho,\xi) = {}&-3\Big((1+2p_0)\xi^8 - 12\gamma_6(1-2p_0)\xi^6\varrho^2 + 12\big(3\gamma_6^2 + \gamma_8 + 12\gamma_8 p_0\big)\xi^4\varrho^4 - \\ &- 72(2\gamma_6\gamma_8 - \gamma_{10}p_0)\xi^2\varrho^6 + 432\big(\gamma_6^2\gamma_8 + 2\gamma_8^2 p_0 - \gamma_6\gamma_{10}p_0\big)\varrho^8\Big)\,, \end{aligned} \tag{3.3.14}$$

$$\begin{aligned} q_5(\varrho,\xi) = {}&-(5+12p_0)\xi^{10} + 78\gamma_6\xi^8\varrho^2 - 72\big(4\gamma_6^2 - \gamma_8(1-2p_0)\big)\xi^6\varrho^4 - \\ &- 72\big(6\gamma_6\gamma_8 - \gamma_{10}(2+3p_0)\big)\xi^4\varrho^6 + 432\big(\gamma_8^2 - 4\gamma_6\gamma_{10}\big)\xi^2\varrho^8 - \\ &- 2592\big(\gamma_6\gamma_8^2 - 2\gamma_6^2\gamma_{10} - \gamma_8\gamma_{10}p_0\big)\varrho^{10} \end{aligned} \tag{3.3.15}$$

and the numerical results for $\xi$ as shown in figure 3.12a. The full set of 750 $\varrho$-values for which we obtained $\xi$ is the same as the one used to determine (3.2.42). In figure 3.12b we also show the parameters $\mathcal{P}_1$ and $\mathcal{P}_2$ and verify that they are indeed positive-definite functions as demanded in (3.3.4).

Finally, in figures 3.13 and 3.14 we present the full result of the "Padé-like" interpolation and the agreement with the small and large mass results given in (3.3.1).

Having determined $p(m_{f_\mathrm{h}},\varrho)$, we can obtain the caloron density $d$ as given in (3.3.3) for the case of $N=3$, $N_{f_l}=4$ and $N_{f_\mathrm{h}}=1$ (i.e., the light quarks are the $u$-, $d$-, $s$- and $c$-quark and the heavy quark is the $b$-quark). To depict $d$, we normalize it by the maximum density of the asymptotic case $m_b \to \infty$, which cancels any renormalization scale ($\lambda$) dependency. Here it is important to make sure that the caloron densities we compare describe theories which agree in the accessible IR limit, as we briefly stated in section 1.3. This means we have to ensure that both theories yield equal $N_{f_l}$-flavor effective theories in the IR. In order to do this, we define the running coupling constant (1.1.2) for the

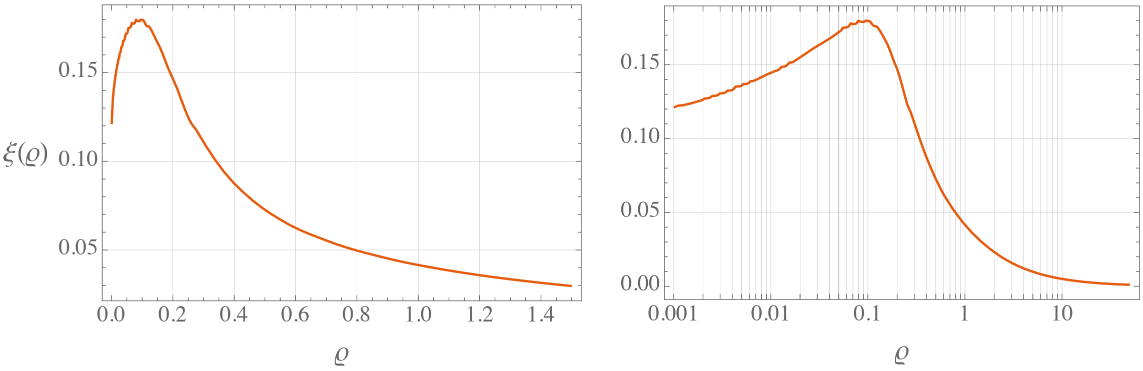

(a). Numerical values for the parameter $\xi(\varrho)$ of the “Padé - like” approximation (3.3.4), shown for the physically relevant caloron sizes $\varrho$ (left) and for the full set of $\varrho$ - values (right).

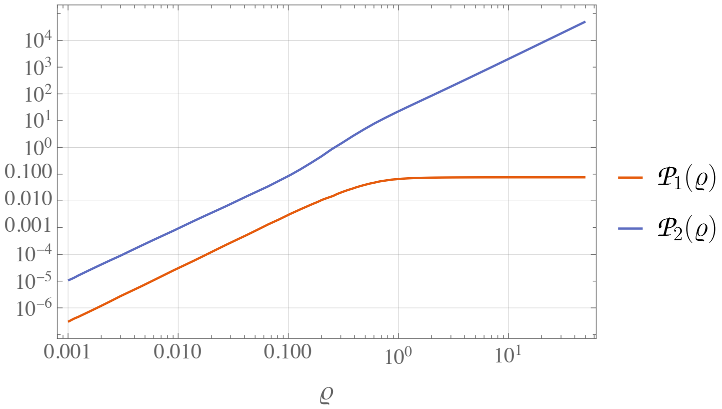

(b). The parameters $\mathcal{P}_1(\varrho)$ and $\mathcal{P}_2(\varrho)$ of (3.3.4), shown for the full set of $\varrho$ - values; the parameters are positive - definite functions as demanded.

Figure 3.12: The parameters $\xi(\varrho)$, $\mathcal{P}_1(\varrho)$ and $\mathcal{P}_2(\varrho)$ or the “Padé - like” interpolation (3.3.4).

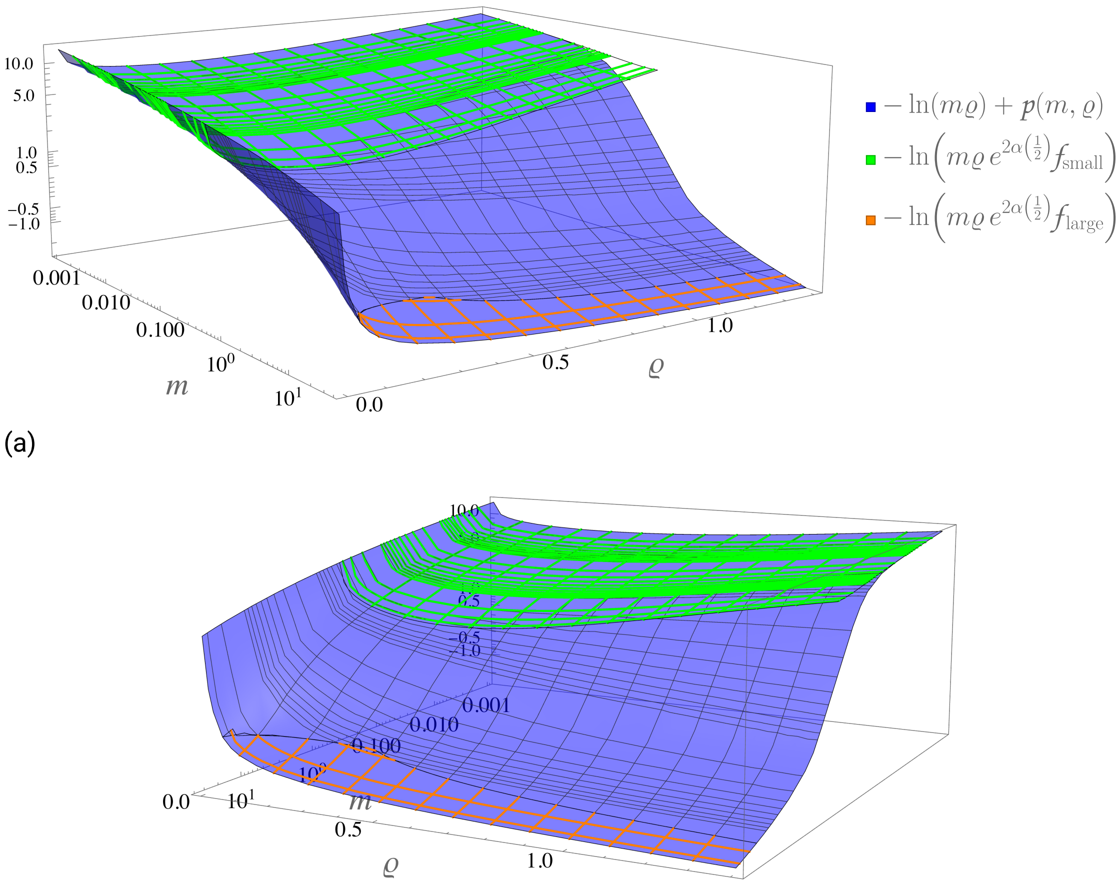

(a)

(b)

Figure 3.13: The negative caloron density logarithm corresponding to the heavy quark $-\ln\left(d(m,\varrho)\right) \supset -\ln\left(m\varrho\, e^{2\alpha\left(\frac{1}{2}\right)} f(m,\varrho)\right)$ (cf. (3.3.3) with (3.3.1); $m_{f_{\mathsf{h}}} = m$ for short.

The “Padé-like” interpolation function $-\ln(m\varrho) + p(m,\varrho)$ ((3.3.4) with coefficients (3.3.7) - (3.3.10) together with (3.3.11) - (3.3.15) as well as figure 3.12a) is shown in blue. The small- and large-mass exponents $-\ln(m\varrho) - 2\alpha\left(\frac{1}{2}\right) - \ln\left(f_{\mathsf{small,\,large}}\right)$ given in (3.3.1) are depicted as green and orange grids, respectively.

For large and small masses the interpolation agrees well with the numerical results for these regimes, in between it provides a reasonable analytical interpolation. This is shown in for several $\varrho$-values in figure 3.14.

As we can see here and in figures 3.14f - 3.14i, the choice $\delta = 0.5$ for $m_{\mathsf{small,\,max,\,2}}$ in (3.2.43) is actually too large for large $\varrho$, but this does not effect our interpolation.

theory containing asymptotically heavy quarks by

$$\frac{8\pi^2}{g^2_{\text{asy}}(N_f, N, 1/\varrho, \lambda)} = \underbrace{\frac{8\pi^2}{g^2_{\text{phys}}(N_f, N, 1/\varrho, \lambda)}}_{-\frac{1}{3}\ln(\lambda\varrho)(11N-3N_f)} + \frac{2}{3}\sum_{f_{\text{h}}} \ln\left(\frac{m_{f_{\text{h, asy}}}}{m_{f_{\text{h}}}}\right). \tag{3.3.16}$$

This is illustrated and described in figure 3.15. In figure 3.16 we now show the normalized caloron density. These results also verify the small constituent - approximation, as introduced in the section 2.4.4, for finite $T$ and with heavy quarks.

Using the full caloron density (3.3.3), we can employ (2.4.85) to obtain the partition function in the DGA and then use (2.4.87) to find the resulting topological susceptibility given purely in terms of the (integrated) caloron density $\chi_{\text{top}} = 2\mathcal{D}(T, m_{f_l}, m_{f_{\text{h}}}, \lambda)$. We are interested in the effects of a physically heavy $b$ - compared to a system of four light quarks ($u$, $d$, $c$, $s$) together with an asymptotically heavy fifth quark (i.e., with the modified coupling (3.3.16)), which is well - understood due to lattice QCD; all with a background of dilute $SU(3)$ - calorons. For that purpose, we consider the ratio of topological susceptibilities:

$$\begin{aligned}\kappa(m_{f_{\text{h}}}, N_{f_l}, N_{f_{\text{h}}}, N) &= \frac{\chi_{\text{top}}\big(N, m_{f_l}, m_{f_{\text{h}}}, g_{\text{phys}}\big)}{\chi_{\text{top}}\big(N, m_{f_l}, m_{f_{\text{h, asy}}}, g_{\text{asy}}\big)} = \\ &= \frac{\displaystyle\int_0^\infty \mathrm{d}\varrho\, \varrho^{\frac{11N+N_f}{3}-5} f(N_{f_l}, N, \varrho) \prod_{f_{\text{h}}} \sqrt[3]{m_{f_{\text{h}}}}\, e^{-p(m_{f_{\text{h}}},\varrho)}}{\displaystyle\int_0^\infty \mathrm{d}\varrho\, \varrho^{\frac{11N+N_{f_l}}{3}-5} f(N_{f_l}, N, \varrho)}\end{aligned} \tag{3.3.17}$$

with $f(N_{f_l}, N, \varrho)$ (2.4.77) the factor due to the light quarks, gluons and gauge ghosts.

We calculate (3.3.17) for the physical case $\kappa(m_b, 4, 1, 3)$ and 160 bottom quark - masses given by $m_b \in \{0.1 \cdot 10^{\frac{j}{49}} \,|\, \mathbb{N} \ni j \leq 49\}$, $m_b \in \{1.048^{1-\frac{j}{49}} \cdot 2^{\frac{j}{49}} \,|\, \mathbb{N} \ni j \leq 49\}$ and $m_b \in \{2.027^{1-\frac{j}{49}} \cdot 10^{\frac{j}{49}} \,|\, \mathbb{N} \ni j \leq 49\}$, together with the large and small outliers $m_b \in \{0.01, 0.025, 0.05, 12, 14, 16, 18, 20, 22.5, 25\}$. This is our main result shown in figure 3.17. We see that for the temperature range of main interest for axion physics, $400\,\text{MeV} \lesssim T \lesssim 1.1\,\text{GeV}$ (the temperature most important for the cosmological history of axions, see [55] and the discussion in the introduction 1.2), and thus the mass range $4 \lesssim m_b \lesssim 11$, the difference between the physically heavy $b$ and its asymptotically heavy counterpart used in lattice QCD is $\lesssim 5\%$, i.e., $\kappa \gtrsim 0.95$. Only for high temperatures $m_b \lesssim 2$ do we see $\kappa \lesssim 0.9$ and an appreciable ($\gtrsim 10\%$) difference between the topological susceptibilities of finite temperature $2+1+1+1$ theory (including a dynamical $b$ quark) and the $2+1+1$ case of lattice QCD.

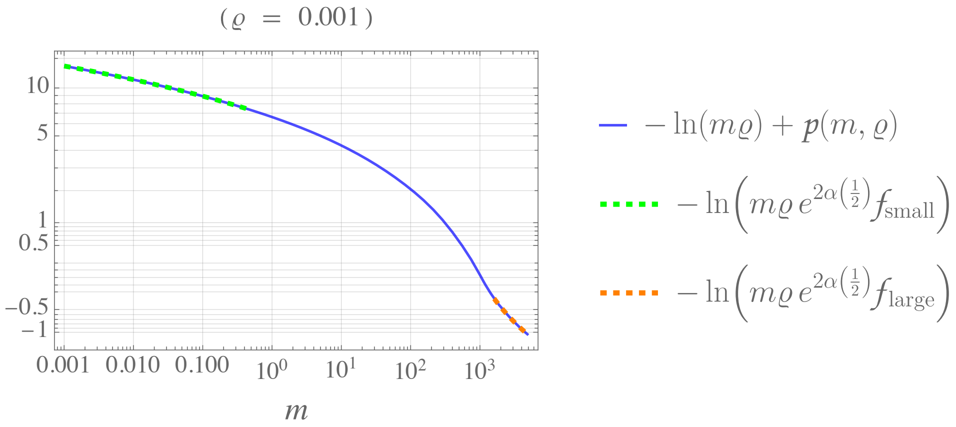
(ϱ = 0.001)
10
5
1
0.5
−0.5
−1
0.001 0.010 0.100 $10^0$ $10^1$ $10^2$ $10^3$
m
$-\ln(m\varrho) + p(m,\varrho)$
$-\ln\left(m\varrho\, e^{2\alpha(\frac{1}{2})} f_{\text{small}}\right)$
$-\ln\left(m\varrho\, e^{2\alpha(\frac{1}{2})} f_{\text{large}}\right)$

(a)

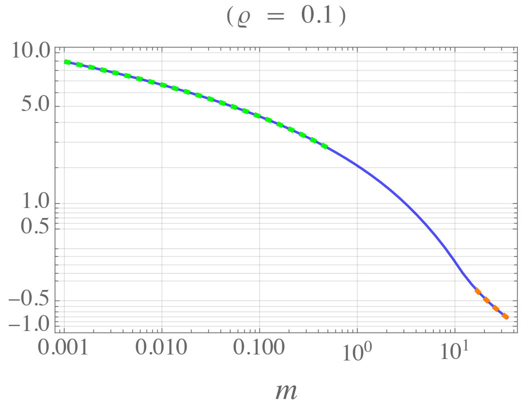
(ϱ = 0.1)
10.0
5.0
1.0
0.5
−0.5
−1.0
0.001 0.010 0.100 $10^0$ $10^1$
m

(b)

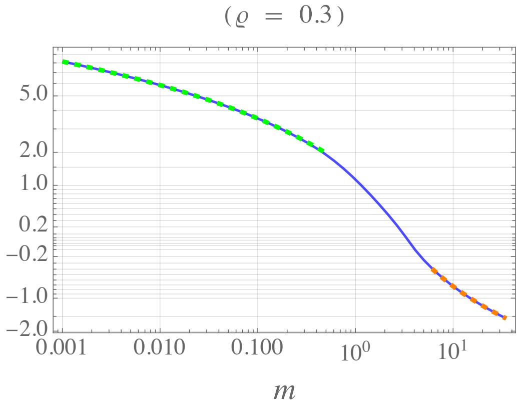
(ϱ = 0.3)
5.0
2.0
1.0
0.2
−0.2
−1.0
−2.0
0.001 0.010 0.100 $10^0$ $10^1$
m

(c)

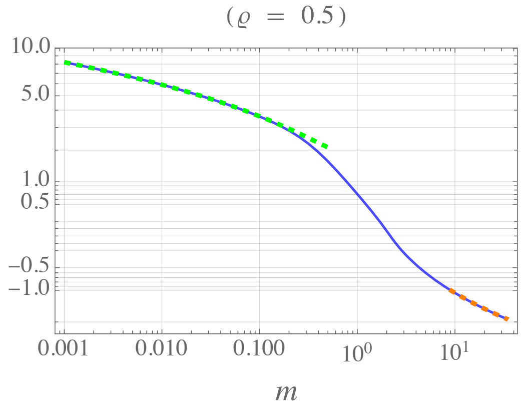
(ϱ = 0.5)
10.0
5.0
1.0
0.5
−0.5
−1.0
0.001 0.010 0.100 $10^0$ $10^1$
m

(d)

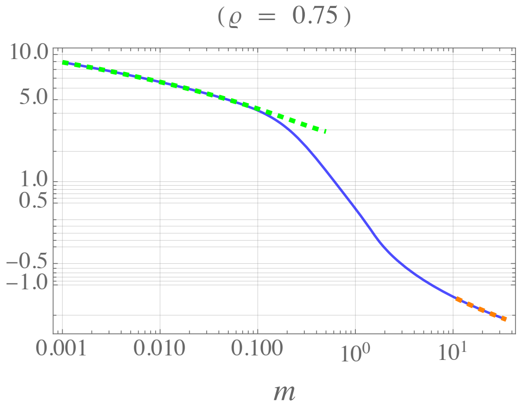
(ϱ = 0.75)
10.0
5.0
1.0
0.5
−0.5
−1.0
0.001 0.010 0.100 $10^0$ $10^1$
m

(e)

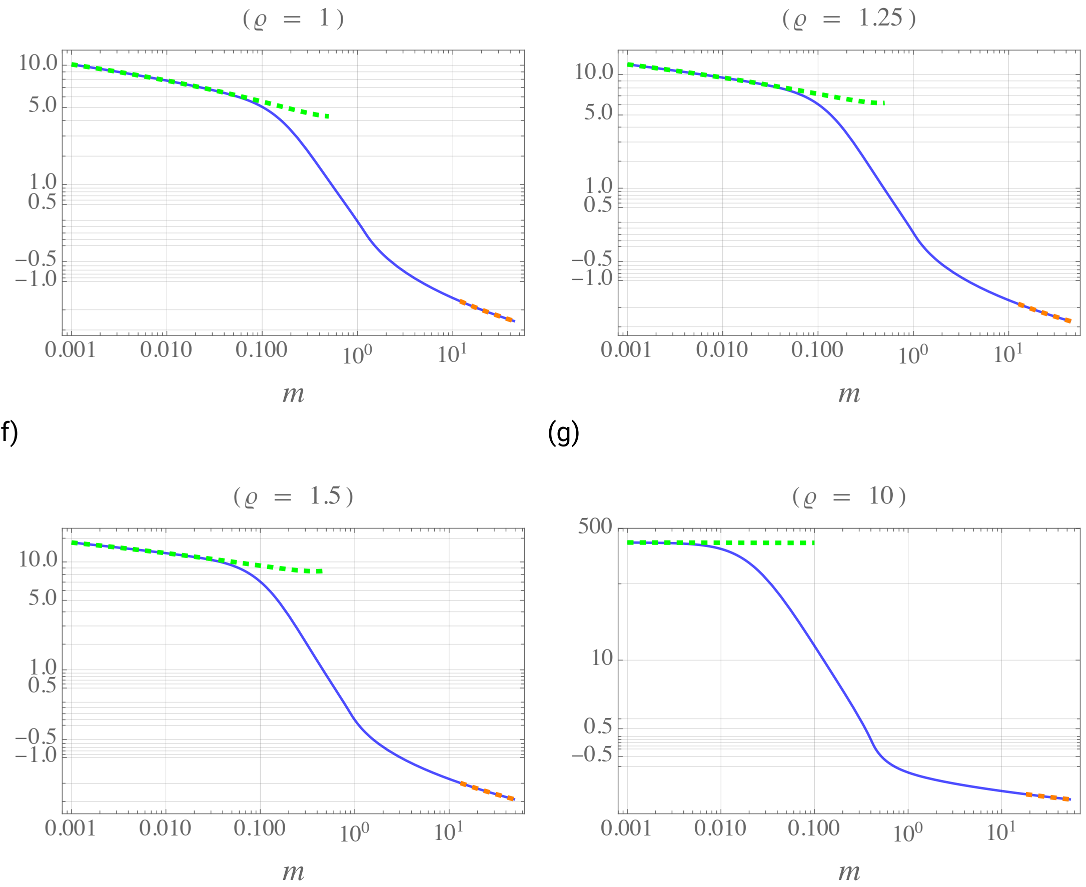

(f) (g) (h) (i)

Figure 3.14: The caloron density term $-\ln\left(m\varrho\, e^{2\alpha\left(\frac{1}{2}\right)} f(m,\varrho)\right)$ (cf. (3.3.3) and (3.3.1)) shown in figure 3.13 presented for several caloron sizes.
The agreement of the small-mass (- - -) and large-mass (- - -) results with the Padé approximation (—) and the latter's interpolation between the mass regimes is shown for several caloron sizes in the physically interesting region $0.1 \lesssim \varrho \lesssim 1$ as well as for a vanishingly small caloron $\varrho = 0.001$ and some "unphysically large" calorons $\varrho = 1.25$, $\varrho = 1.5$ and $\varrho = 10$.

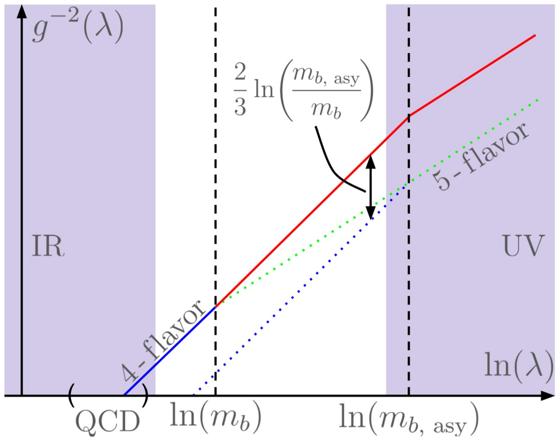

Figure 3.15: The running coupling $g^{-2}(\lambda)$ for a theory with four light and a heavy $b$ quark. At large energy scales $\gg m_b$ one has a 5 - flavor running (- - -) which switches to 4 - flavor running at the energy scale $m_b$ (——). For a theory with an asymptotically heavy $b$ quark, the switch occurs at the UV scale $m_{b,\text{ asy}}$ (- - -) and the two theories disagree in the IR, with the asymptotic $b$ - theory failing to describe known 4 - flavor QCD/IR theory.
In order to compare the $m_b$ - and $m_{b,\text{ asy}}$ - theory with matching IR physics, we modify the coupling $g_{\text{asy}}$ and describe it in terms of the coupling $g_{\text{phys}}$ (3.3.16) for scales $> m_b$ (——). Overall, $g_{\text{asy}}$ is thus given by (——). This is arbitrarily off compared to the physical description in the UV (which is, however, inaccessible to reasonable physical description anyway), but agrees in the IR and thus corresponds better to what happens in a $2+1+1$ - flavor lattice calculation.

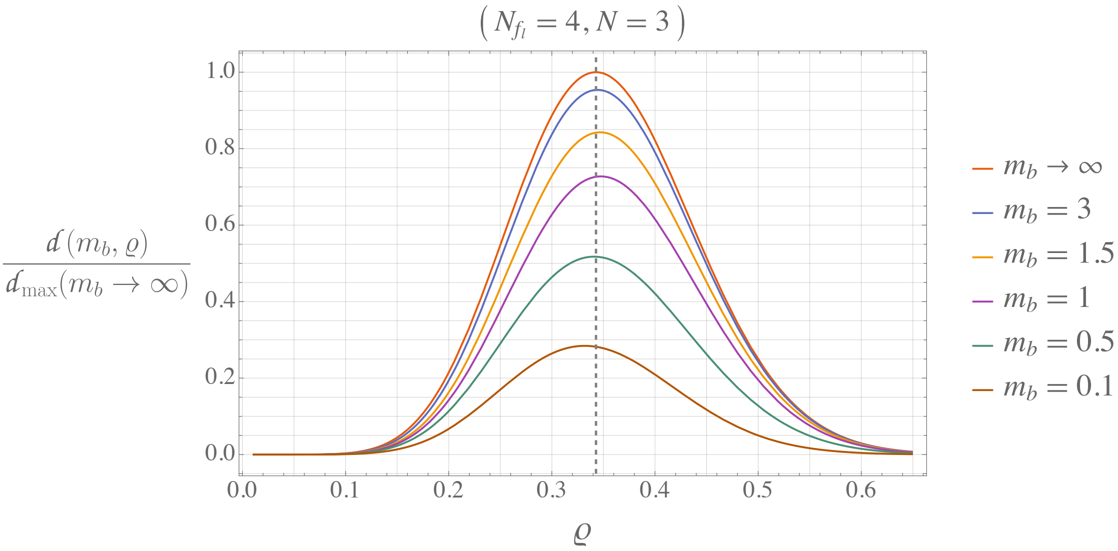

Figure 3.16: The caloron density $đ(N_{f_l} = 4, N = 3, m_b, \varrho, \lambda)$ (3.3.3) with the correction factor $e^{-2\alpha\left(\frac{1}{2}\right) - p(m,\varrho)}$ (3.3.1). We normalize it by the maximum density of 4-flavor theory, represented by $đ_{\text{max}}(m_b \to \infty, g_{\text{asy}})$ with $g_{\text{asy}}$ as in (3.3.16), which is located at $\varrho \approx 0.3428$. This value is marked by the dashed line. We see a decline of the maximum caloron density with decreasing $m_b$ and a slight shift of the density peak: for finite $m_b \gtrapprox 1.073$ the peak moves to higher $\varrho$-values as $m_b$ decreases and then progresses back down to smaller sizes (for $m_b \approx 0.569$ the peak is again located at $\varrho \approx 0.3428$).

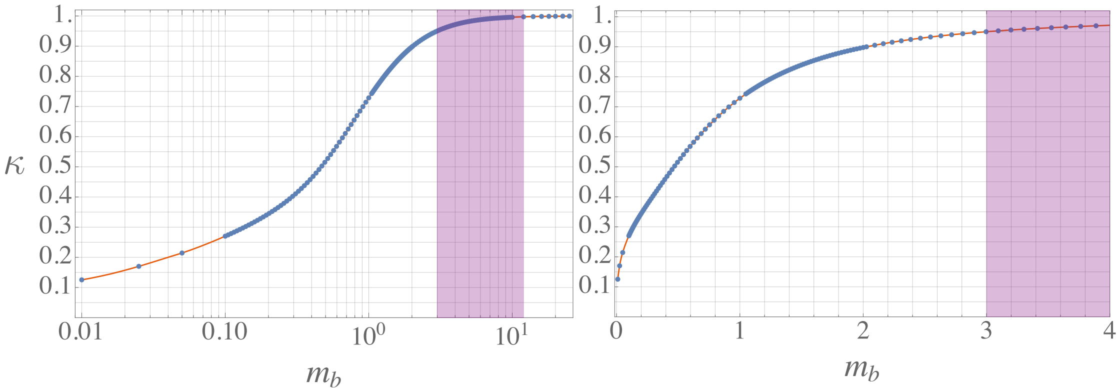

Figure 3.17: The ratio of topological susceptibilities $\kappa(m_b, 4, 1, 3)$ (3.3.17) comparing a theory with a four light and a physical $b$ quark in $SU(3)$ gauge theory to lattice QCD, where the $b$ quark is asymptotically heavy. Due to the modification of the running coupling (3.3.16), $\kappa$ depends only on the physical quark mass $m_b$. The interesting mass range $3 \lesssim m_b \lesssim 12$, chosen to be slightly wider than the physically relevant temperature range $400$ MeV $\lesssim T \lesssim 1.1$ GeV - given a dimensionful $b$ - mass $m_b \approx 4.2$ MeV [2] -, is marked marked in purple.

# Appendices

# A. Partial Differential Equation

In order to solve the full problem of the topological susceptibility's quark mass dependency at finite temperatures, one has to compute the determinant ratio $\frac{\det(-D_-^2+m_f^2)\,\det(-\partial_-^2+\lambda^2)}{\det(-D_-^2+\lambda^2)\,\det(-\partial_-^2+m_f^2)}$ (cf. (2.4.65) with dimensionless coordinates (3.1.1), masses, etc.), i.e., one has to solve the eigenvalue problem

$$(-D_-^2 + m^2)\psi_n = \lambda_n \psi_n \tag{A.1}$$

given in terms of coupled ordinary and partial differential equations (ODEs and PDEs). We derive these differential equations in the following.

Following [54], the spacetime $\mathbb{R}^3 \times S^1_{\text{rad.}={}^1\!/_{2\pi}}$ can be separated into three regions as depicted in figure A.1: the "instanton region" I with $|(\vec{x},\tau)| = \sqrt{r^2+\tau^2} \ll 1$, the "asymptotic region" III with $r = \sqrt{\vec{x}^{\,2}} \gg 1$, and the "transition region" II in between.

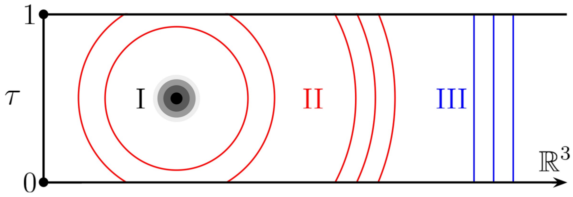

Figure A.1: The three spacetime regions important for solving (A.1). As in figure 3.3, the caloron is shown as a graded gray sphere. In the "instanton region" I the caloron resembles a 4 - dimensional radially symmetric instanton; in the "asymptotic region" III the caloron is reduced to a 3 - dimensional, radially symmetric object. The topology of $\mathbb{R}^3 \times S^1_{\text{rad.}={}^1\!/_{2\pi}}$ with its distinct, bounded time direction and open space directions and the resulting broken down symmetry group (cf. the discussion in section 2.2.4) are relevant in the asymptotic region III as well as the "transition region" II.

In the instanton region I the caloron $A^{a\,\mu}_{\text{HS}} = -\bar{\eta}^{a\mu\nu}\partial^\nu \ln(\phi)$ (2.4.37) resembles an instanton of modified size $\tilde{\varrho}$ (cf. (2.4.39) and (2.4.40)). The behavior of individual solutions to (A.1) in this region is the same as for an instanton. This determines the small - radius boundary conditions for the solutions in the transition region.

In the asymptotic region III we can expand $\phi \overset{r\gg 1}{\rightarrow} 1 + \frac{\pi\varrho^2}{r} + \pi^2\varrho^2\,\mathcal{O}(re^{-\pi r})$. This obeys 3 - dimensional radial symmetry and the resulting asymptotic caloron components read $A^{a\,4}_{\text{HS}} \overset{r\gg 1}{\rightarrow} \frac{1}{1+\frac{r}{\pi\varrho^2}}\frac{x^a}{r^2} = a^{\text{III}}_{\varrho}(r)\frac{x^a}{r^2}$ and $A^{a\,i}_{\text{HS}} \overset{r\gg 1}{\rightarrow} a^{\text{III}}_{\varrho}(r)\,\varepsilon^{aij}\frac{x^j}{r^2}$; the caloron is static in $\tau$. We can thus exploit this radial symmetry by adapting the approach developed in [141]:

we use the regular angular momentum operators $L^a = -i\,\varepsilon^{aij} x^i \partial^j$ and define the isospin operators $\mathcal{T}^a = \frac{\sigma^a}{2}$ as well as the "spin + isospin" operators $J^a = L^a + \mathcal{T}^a$. This means that $L^2$ has eigenvalues $l(l+1)$, $l \in \mathbb{N} \cup \mathbb{N} + \frac{1}{2}$, $\mathcal{T}^2$ has the eigenvalue $\frac{3}{4}$, and $J^2$ has eigenvalues $j(j+1)$, $j = |l \pm \frac{1}{2}|$. Using this, we find the $-D_-^2$ - operator in region III:

$$\begin{aligned} -D_-^2 &= -\partial_r^2 - \frac{2}{r}\partial_r + \frac{L^2}{r^2} + 2a_\varrho^{\text{III}}(r)\frac{\vec{L}\cdot\vec{\mathcal{T}}}{r^2} + \frac{\left(a_\varrho^{\text{III}}(r)\right)^2}{r^2}\mathcal{T}^2 - \partial_\tau^2 + \frac{2ia_\varrho^{\text{II}}(r)}{r}\,\hat{e}_r\cdot\vec{\mathcal{T}}\,\partial_\tau = \\ &= -\partial_r^2 - \frac{2}{r}\partial_r + \frac{l(l+1)}{r^2} + a_\varrho^{\text{III}}\frac{(j-l)(j+l+1)}{r^2} - \frac{3}{4}\frac{\left(a_\varrho^{\text{III}}\right)^2}{r\pi\varrho^2} - \partial_\tau^2 + \frac{2ia_\varrho^{\text{III}}}{r}\,\hat{e}_r\cdot\vec{\mathcal{T}}\,\partial_\tau\,, \end{aligned} \tag{A.2}$$

where we used a separation ansatz for the eigenfunction $\psi_{n,l,j}(x) = \chi_{l,j}(\theta,\varphi)\Psi_{n,l,j}(r,\tau)$ with $\chi_{l,j}$ a function and $\widetilde{\Psi}_{n,l,j}$ a 2 - spinor. Furthermore, in the asymptotic limit $r \gg 1$ with $\tau$ - independent calorons any $\psi_n$ can be expanded in terms of fermionic Matsubara frequencies $p^{\text{ferm}}_{\alpha\,\in\,\mathbb{Z}} = 2\pi\left(\alpha + \frac{1}{2}\right)$, i.e., $\psi_{n,l,j}(x) = \chi_{l,j}(\theta,\varphi)\sum_{\alpha\,\in\,\mathbb{Z}}\widetilde{\Psi}_{n,l,j,\alpha}(r,p^{\text{f}}_\alpha)e^{-ip^{\text{f}}_\alpha\tau}$. This gives us the $-D_-^2$ - operator as it acts on $\widetilde{\Psi}_{n,l,j,\alpha}$:

$$-D_-^2 = -\partial_r^2 - \frac{2}{r}\partial_r + \frac{l(l+1)}{r^2} + a_\varrho^{\text{III}}\frac{(j-l)(j+l+1)}{r^2} + \frac{3}{4}\frac{\left(a_\varrho^{\text{III}}\right)^2}{r\pi\varrho^2} - (p^{\text{f}}_\alpha)^2 + \frac{2a_\varrho^{\text{III}}p^{\text{f}}_\alpha}{r}\,\hat{e}_r\cdot\vec{\mathcal{T}}\,. \tag{A.3}$$

Note that (A.3) gives a coupled system of two ODEs due to the isospin operators $\mathcal{T}^a$ (alternatively: $\hat{e}_r\cdot\vec{\mathcal{T}} = \frac{\sigma^r}{2}$). Together with (A.1) this is the eigenvalue problem in the asymptotic region which gives the boundary conditions for the transition region solutions.

For the transition region II we again introduce $L^a$ and $\mathcal{T}^a$ together with the separation ansatz $\psi_{n,l,j}(x) = \chi_{l,j}(\theta,\varphi)\Psi_{n,l,j}(r,\tau)$. Additionally, we define the function $\Phi = \frac{\phi(r,\tau)}{r}$, so that $A^{a\,4}_{\text{HS}} = -\left(1 + r\frac{\partial_r\Phi}{\Phi}\right)\frac{x^a}{r^2} = -a_\varrho^{\text{II}}(r,\tau)\frac{x^a}{r^2}$ and $A^{a\,i}_{\text{HS}} = -a_\varrho^{\text{II}}(r,\tau)\,\varepsilon^{aij}\frac{x^j}{r^2} + \delta^{ai}\frac{\partial_\tau\Phi}{\Phi}$. We thus find the differential operator acting on $\Psi_{n,l,j}$:

$$\begin{aligned} -D_-^2 = &- \partial_r^2 - \frac{2}{r}\partial_r + \frac{L^2}{r^2} + 2a_\varrho^{\text{II}}(r,\tau)\frac{\vec{L}\cdot\vec{\mathcal{T}}}{r^2} + i\,\partial_r\frac{\partial_\tau\Phi}{\Phi}\,\hat{e}_r\cdot\vec{\mathcal{T}} - i\,\partial_\tau\frac{\partial_r\Phi}{\Phi} + \\ &+ \frac{\left(a_\varrho^{\text{II}}(r,\tau)\right)^2}{r^2}\mathcal{T}^2 + \left(\frac{\partial_\tau\Phi}{\Phi}\right)^2\mathcal{T}^2 - \partial_\tau^2 - \frac{2ia_\varrho^{\text{II}}(r,\tau)}{r^2}\,\hat{e}_r\cdot\vec{\mathcal{T}}\,\partial_\tau = \end{aligned} \tag{A.4}$$

$$\begin{aligned} = &- \partial_r^2 - \frac{2}{r}\partial_r + \frac{l(l+1)}{r^2} + a_\varrho^{\text{II}}\frac{(j-l))(j+l+1)}{r^2} + i\,\partial_r\frac{\partial_\tau\Phi}{\Phi}\,\hat{e}_r\cdot\vec{\mathcal{T}} - \\ &- i\,\partial_\tau\frac{\partial_r\Phi}{\Phi} + \frac{3}{4}\frac{a_\varrho^{\text{II}}}{r}\frac{\partial_r\Phi}{\Phi} + \frac{3}{4}\left(\frac{\partial_\tau\Phi}{\Phi}\right)^2 - \partial_\tau^2 - \frac{2ia_\varrho^{\text{II}}}{r^2}\,\hat{e}_r\cdot\vec{\mathcal{T}}\,\partial_\tau\,. \end{aligned} \tag{A.5}$$

Since $\Psi_{n,l,j}$ cannot be expanded in terms of Matsubara frequencies in this region, the transition region - eigenvalue problem given by (A.5) and (A.1) is posed in terms of a

2 - dimensional, coupled system of PDEs.[15] These are to be matched at small and large $\sqrt{r^2+\tau^2}$ to the asymptotic forms in the other two regions.

## B. Heat Kernel Coefficient $\bar{a}_{10}$

The heat kernel coefficient $\bar{a}_{10}$ for our case reads [183] (with the barred notation used just as described in section 3.1.2, especially as used in (3.1.4) and (3.1.6)):

$$\begin{aligned}
\bar{a}_{10} = \frac{1}{120}\Bigg(&\frac{1}{9}\overline{G}^{\kappa\lambda}\overline{G}^{\lambda\mu}\overline{G}^{\kappa\rho;\nu}\overline{G}^{\rho\mu;\nu} - \frac{i}{18}\overline{G}^{\kappa\lambda}\overline{G}^{\nu\rho;\lambda\mu}\overline{G}^{\rho\nu;\mu\kappa} - \frac{1}{189}\overline{G}^{\kappa\lambda}\overline{G}^{\lambda\mu}\overline{G}^{\nu\rho;\kappa}\overline{G}^{\rho\nu;\mu} + \\
&+ \frac{1}{252}\overline{G}^{\nu\rho;\kappa\lambda\mu}\overline{G}^{\rho\nu;\mu\lambda\kappa} + \frac{1}{378}\overline{G}^{\kappa\lambda}\overline{G}^{\nu\rho;\lambda\mu}\overline{G}^{\mu\kappa}\overline{G}^{\rho\nu} - \frac{2i}{21}\overline{G}^{\lambda\mu;\kappa}\overline{G}^{\mu\rho;\kappa\nu}\overline{G}^{\rho\lambda;\nu} + \\
&+ \frac{2}{63}\overline{G}^{\kappa\lambda}\overline{G}^{\nu\rho;\mu}\overline{G}^{\lambda\kappa}\overline{G}^{\rho\nu;\mu} + \frac{2i}{945}\overline{G}^{\kappa\lambda}\overline{G}^{\lambda\nu}\overline{G}^{\mu\nu}\overline{G}^{\nu\rho}\overline{G}^{\rho\kappa} - \frac{4i}{63}\overline{G}^{\kappa\lambda}\overline{G}^{\lambda\rho;\mu\nu}\overline{G}^{\rho\kappa;\nu\mu} - \\
&- \frac{5}{63}\overline{G}^{\kappa\lambda}\overline{G}^{\lambda\mu}\overline{G}^{\mu\rho;\nu}\overline{G}^{\rho\kappa;\nu} + \frac{5}{63}\overline{G}^{\kappa\lambda}\overline{G}^{\lambda\nu;\mu}\overline{G}^{\kappa\rho}\overline{G}^{\rho\nu;\mu} + \frac{5}{63}\overline{G}^{\kappa\lambda}\overline{G}^{\nu\rho;\mu}\overline{G}^{\rho\lambda}\overline{G}^{\nu\kappa;\mu} - \\
&- \frac{5i}{126}\overline{G}^{\lambda\mu;\kappa}\overline{G}^{\nu\rho;\mu\kappa}\overline{G}^{\rho\nu;\lambda} - \frac{5i}{126}\overline{G}^{\lambda\mu;\kappa}\overline{G}^{\nu\rho;\mu}\overline{G}^{\rho\nu;\lambda\kappa} + \frac{8i}{63}\overline{G}^{\kappa\lambda}\overline{G}^{\lambda\mu}\overline{G}^{\kappa\nu}\overline{G}^{\mu\rho}\overline{G}^{\rho\nu} - \\
&- \frac{8}{189}\overline{G}^{\kappa\lambda}\overline{G}^{\mu\nu;\lambda}\overline{G}^{\kappa\rho;\nu}\overline{G}^{\rho\mu} - \frac{10}{189}\overline{G}^{\kappa\lambda}\overline{G}^{\mu\nu;\lambda}\overline{G}^{\nu\rho}\overline{G}^{\mu\kappa;\rho} - \frac{10}{189}\overline{G}^{\kappa\lambda}\overline{G}^{\lambda\nu;\mu}\overline{G}^{\mu\rho}\overline{G}^{\rho\nu;\kappa} + \\
&+ \frac{11}{189}\overline{G}^{\kappa\lambda}\overline{G}^{\lambda\kappa;\mu}\overline{G}^{\nu\rho}\overline{G}^{\rho\nu;\mu} + \frac{11}{189}\overline{G}^{\kappa\lambda}\overline{G}^{\nu\rho;\mu}\overline{G}^{\rho\nu}\overline{G}^{\lambda\kappa;\mu} - \frac{11}{378}\overline{G}^{\kappa\lambda}\overline{G}^{\lambda\mu}\overline{G}^{\nu\rho;\mu\kappa}\overline{G}^{\rho\nu} + \\
&+ \frac{13}{252}\overline{G}^{\kappa\lambda}\overline{G}^{\lambda\kappa}\overline{G}^{\nu\rho;\mu}\overline{G}^{\rho\nu;\mu} - \frac{16}{63}\overline{G}^{\kappa\lambda}\overline{G}^{\mu\nu;\lambda}\overline{G}^{\nu\rho}\overline{G}^{\rho\mu;\kappa} - \frac{16}{189}\overline{G}^{\kappa\lambda}\overline{G}^{\lambda\mu}\overline{G}^{\nu\rho}\overline{G}^{\rho\nu;\mu\kappa} - \\
&- \frac{16i}{945}\overline{G}^{\kappa\lambda}\overline{G}^{\mu\nu}\overline{G}^{\lambda\rho}\overline{G}^{\nu\kappa}\overline{G}^{\rho\mu} - \frac{19}{756}\overline{G}^{\kappa\lambda}\overline{G}^{\mu\nu;\lambda}\overline{G}^{\kappa\rho}\overline{G}^{\nu\mu;\rho} - \frac{19}{756}\overline{G}^{\kappa\lambda}\overline{G}^{\nu\rho;\mu}\overline{G}^{\mu\lambda}\overline{G}^{\rho\nu;\kappa} - \\
&- \frac{22i}{189}\overline{G}^{\kappa\lambda}\overline{G}^{\lambda\mu}\overline{G}^{\kappa\nu}\overline{G}^{\nu\rho}\overline{G}^{\rho\mu} + \frac{25}{189}\overline{G}^{\kappa\lambda}\overline{G}^{\lambda\nu;\mu}\overline{G}^{\kappa\rho;\mu}\overline{G}^{\rho\nu} - \frac{26}{189}\overline{G}^{\kappa\lambda}\overline{G}^{\lambda\nu;\mu}\overline{G}^{\mu\kappa;\rho}\overline{G}^{\rho\nu} - \\
&- \frac{31i}{378}\overline{G}^{\kappa\lambda}\overline{G}^{\lambda\nu}\overline{G}^{\nu\rho}\overline{G}^{\mu\kappa}\overline{G}^{\rho\nu} - \frac{34}{189}\overline{G}^{\kappa\lambda}\overline{G}^{\mu\nu;\lambda}\overline{G}^{\nu\kappa;\rho}\overline{G}^{\rho\mu} - \frac{41}{378}\overline{G}^{\kappa\lambda}\overline{G}^{\lambda\mu}\overline{G}^{\nu\rho;\mu}\overline{G}^{\rho\nu;\kappa} - \\
&- \frac{53i}{378}\overline{G}^{\kappa\lambda}\overline{G}^{\lambda\kappa}\overline{G}^{\mu\nu}\overline{G}^{\nu\rho}\overline{G}^{\rho\mu} + \frac{61}{756}\overline{G}^{\kappa\lambda}\overline{G}^{\lambda\kappa;\mu}\overline{G}^{\nu\rho;\mu}\overline{G}^{\rho\nu} + \frac{61}{756}\overline{G}^{\kappa\lambda}\overline{G}^{\mu\nu}\overline{G}^{\lambda\kappa;\rho}\overline{G}^{\nu\mu;\rho}\Bigg) .
\end{aligned} \tag{B.1}$$

---

[15] If one aims to solve this eigenvalue problem, one could expand $\Phi(r,\tau)$ in terms of radial and temporal variables $u, v$ given by $r = 1 + u$ and $\tau = 1 - v$, respectively. This simplifies the coefficient functions in (A.5) to rational functions of $u$ and $v$, thus possibly simplifying calculations, reducing numerical cost and/or making possible the application of certain theorems from the theory or partial differential equations.

# C. Alternative Small - Mass Expansion

In order to obtain a small $m$ - expansion which is sensitive to possible non - analytical contributions, we propose an alternative procedure following [60] and using techniques from [154]: we propose to calculate

$$\gamma_{\text{ferm}} = \gamma_{\text{ferm}}\big|_{m\,=\,0} - 2\int_0^{m^2} \mathrm{d}\widetilde{m}^2\, \frac{\mathrm{d}\gamma_{\text{s},\,-}(\widetilde{m}^2)}{\mathrm{d}\widetilde{m}^2} - \ln\left(\frac{m}{\lambda}\right), \tag{C.1}$$

with the integration only up until small $m^2 \ll 1$.

The $m^2$ - derivative of $\gamma_{\text{s},\,-}(m^2)$ cannot be performed straight - forwardly. This can be seen by employing the Schwinger proper time - representation (3.1.2) for the Pauli Villars - regularized log - caloron density and neglecting the $\lambda$ - dependent regulator terms $\gamma_{\text{s},\,-} = -\int_0^\infty \frac{\mathrm{d}s}{s}\, e^{-m^2 s} \int^1 \mathrm{d}^4x\, \mathrm{tr}\, \langle x| \big(e^{-(-D_-^2)s} - e^{-(-\partial_-^2)s}\big)|x\rangle +$ “reg. terms”. Treating $\gamma_{\text{s},\,-}$ as a function $\gamma_{\text{s},\,-}(m^2)$ and noting that divergences appear at the lower integral boundary, i.e., as $s \searrow 0$ where the heat kernel expansion (3.1.10) applies, one has two sources of divergence: the $j = 0$ modes at $k = 0$ and $k = 2$ (cf. (3.1.18.b)). The first has its divergent contribution canceled by the free terms before the $m^2$ - derivative is performed, but the later divergence remains, as it is only canceled by the regulator terms (cf. the order - by - order discussion of the heat kernel expansion in section 3.1.3). This remaining divergence results in the divergence of the integrand $e^{-m^2 s}\, s^{-1}\mathrm{tr}(\langle xs|x\rangle^- - \langle xs|x\rangle_0^-)$ diverging as $s \searrow 0$ and, according to Leibniz’ integral rule, differentiation and integration do not commute for a discontinuous integrand. Thus, an integration cut - off $\varepsilon_s \ll 1$ has to be introduced as in (3.1.18.b) so that the $m^2$ - derivative can be performed inside the $s$ - integral [154]:[16]

$$\left(\frac{\mathrm{d}\gamma_{\text{s},\,-}(m^2)}{\mathrm{d}m^2}\right)_{\varepsilon_s\,\text{- reg.}} = \lim_{\varepsilon_s \searrow 0} \int_{\varepsilon_s}^{\infty} \mathrm{d}s\, e^{-m^2 s} \int^1 \mathrm{d}^4x\, \mathrm{tr}\big(\, \langle xs\,|\,x\rangle^- - \langle(xs\,|\,x\rangle_0^-\,\big)\,. \tag{C.2}$$

The cut - off can be understood as subtracting the divergent terms at $s \searrow 0$ to yield an overall finite result. This is an alternative regularization compared to the point splitting procedure employed for the Taylor expansion.

For practical reasons, one however aims to replace this cut - off regularization and use point splitting again. This is because one is then allowed to perform the limit $\varepsilon_s \searrow 0$ and rewrite the above expression in terms of Euclidean time propagators as discussed below (3.1.2). There we discussed how the anti-periodic proper time - Green’s functions (or heat kernels) $\langle xs\,|\,y\rangle^-_{(0)}$ produce the ordinary anti-periodic Euclidean time - propagators via $s$ - integration: $\Delta^-(x,y,m^2) = \langle x|\frac{1}{-D_-^2+m^2}|y\rangle = \int_0^\infty \mathrm{d}s\ \langle xs\,|\,y\rangle^-\, e^{-m^2 s}$ (analogously for $\Delta_0^-(x,y,m^2)$). The $m^2$ - differentiated log - caloron density can thus be understood as given in terms of $\varepsilon_s$ - regularized propagators. Exchanging the cut - off regularization with the point splitting requires one to subtract additional terms (not just the diverging terms required for overall finiteness) which appear due to this exchange of limits. These terms vanish initially (i.e., before the exchange of the two regularizations) as the point splitting is sent to vanish inside the $\varepsilon_s$ - regularized $s$ - integral (C.2), but become finite after the exchange.

---

[16] The limit $\varepsilon_s \searrow 0$ must not be performed, even though, using the heat kernel expansion for small $s$, it turns out the result would be finite, as this would correspond to having taken the $m^2$ - derivative without the regulator.

Now we determine these additional terms due to introducing a temporal point splitting $x' = x + \varepsilon_\mathcal{T}\,\hat{e}_4,\ \varepsilon_\mathcal{T} \searrow 0$ in (C.2), exchanging it with the $\varepsilon_s$ - regularization and eventually taking the limit $\varepsilon_s \searrow 0$ in the $s$ - integral. We start by introducing the point splitting:

$$\left(\frac{\mathrm{d}\gamma_{\mathrm{s},\,-}(m^2)}{\mathrm{d}m^2}\right)_{\text{reg.}} = \lim_{\varepsilon_s\searrow 0}\ \lim_{\varepsilon_\mathcal{T}\searrow 0} \int_{\varepsilon_s}^{\infty} \mathrm{d}s\, e^{-m^2 s} \int^{1} \mathrm{d}^4x\, \mathrm{tr}\big(\,\langle x's\,|\,x\rangle^- - \langle(x's\,|\,x\rangle_0^-\,\big)\,. \quad \text{(C.3)}$$

Now we exchange the limits and identify the diverging $s$ - integrals for taking $\varepsilon_\mathcal{T} \searrow 0$ after $\varepsilon_s \searrow 0$. Since these divergences appear at $s = 0$, we can analyze them using a heat kernel expansion (cf. (3.1.7)) with non - coincident, finite temperature Seeley - DeWitt coefficients coefficients $\langle x's\,|\,x\rangle^\pm \overset{s\searrow 0}{\cong} e^{-\frac{\varepsilon_\mathcal{T}^2}{4s}} \sum_{k\,\in\,\mathbb{Z}\,\cup\,\mathbb{Z}+\frac{1}{2}} \frac{s^{k-2}}{(4\pi)^2}\, a_{2k}(x',x)$.[17] Performing the $s$ - integrals $\int_0^\infty \mathrm{d}s\, e^{-m^2 s - \frac{\varepsilon_\mathcal{T}^2}{4s}}\, s^{k-2}$ using (3.1.18) with $k \to k+1$ (due to the $m^2$ - derivative in (C.2) and (C.3) adding a factor of $s$ compared to (3.1.2)), one finds divergences as $\varepsilon_\mathcal{T} \searrow 0$ for $k \in \{0, \frac{1}{2}, 1\}$. However, the $a_{2k}(x',x) = a_{2k}(\varepsilon_\mathcal{T}, x)$ reproduce the $a_{2k}(x)$ as $\varepsilon_\mathcal{T} \searrow 0$, i.e., they contain terms which vanish in this limit and thus potentially cancel the $s$ - integral divergences. This is the source of the additional terms one has to subtract. For a more detailed analysis, the general $a_{2k}(\varepsilon_\mathcal{T}, x)$ would be required, which are unavailable, unfortunately. Nevertheless, we can analyze the general structure of the non - coincident heat kernel coefficients and simplify them in case of temporal point splitting. In fact, it turns out that the available parts of the non - coincident heat kernel coefficients are exactly those which we find to be required.

In general, the $a_{2k}(x,y)$ are can be expanded in $(x-y)$, such that the are given by the known $a_{2k}(y)$ and additional terms of order $\mathcal{O}(|x-y|)$ and higher. This means that coefficients $a_{2k}$ which vanish in the coincident limit can be non - zero in general. At $T = 0$, the first three of these expansions are given in [154]:

---

[17] Actually, for the differentiated log - caloron density the traced integral - heat kernel coefficients $b_{2k}$ are required, which is discussed in the following.

$$\begin{aligned}\bar{a}_0(x,y) &= \mathbb{1} + i(x-y)^\mu A^\mu_{\text{BPST}}(y) + \\ &\quad + \frac{i}{4}(x-y)^\mu (x-y)^\nu \big(\partial^{(\mu} A^{\nu)}_{\text{BPST}} + i A^{(\mu}_{\text{BPST}} A^{\nu)}_{\text{BPST}}\big)|_y + \mathcal{O}(|x-y|^3)\,,\end{aligned} \tag{C.4}$$

$$\bar{a}_1(x,y) = 0\,, \qquad \bar{a}_2(x,y) = -\frac{i}{6}(x-y)^\mu [D^\nu, G^{\mu\nu}]|_y + \mathcal{O}(|x-y|^2)\,, \tag{C.5}$$

where (anti-)symmetrization over $N$ indices is defined without the factor $1/N!$. Notice that $\bar{a}_0(x,y) = \mathrm{P}\exp\left(i\int_y^x \mathrm{d}z^\mu A^\mu_{\text{HS}}(z)\right)$ is given by a Wilson line from $y$ to $x$ (cf. (2.1.28) and above (3.2.1)) and that $\bar{a}_2(x,y) = \mathcal{O}(|x-y|^2)$ with the commutator vanishing for an instanton satisfying the classical YM equation. We thus use the following ansatz for the structure of the general, non-coincident heat kernel coefficients:

$$a_{2k}(x,y) = \varphi_0(x,y)\bar{a}_{2k}(x,y) + \sum_{J\,\in\,\mathbb{N}} \mathcal{A}^{\mu_1\ldots\mu_J}_{2k,J}(\varphi_l, \partial^{(a)}A, D^{(b)}E, D^{(c)}G)|_y\,(x-y)^{\mu_1}\cdots(x-y)^{\mu_J} \tag{C.6}$$

so that in the limit $x \to y$ we have $\bar{a}_{2k}(x,y) \to \bar{a}_{2k}(y)$ and $\sum_J(\ldots) \to \mathcal{A}_{2k,0}(y) = \mathcal{A}_{2k}(y)$ given by the known finite-$T$ terms (cf. below (3.1.9) and (3.1.11) for the traced-integral ones). By also demanding $\varphi_l(x,y) \to \varphi_l(y)$ we then reproduce the known $a_{2k}(y)$ in the limit. The known finite-$T$ terms $\mathcal{A}_{2k}(y)$ only contain $j \neq 0$-modes (cf. (3.1.14)) and the same has to hold for the unknown additional terms $\sum_{J\,\in\,\mathbb{N}^+}(\ldots)$. This is because only these modes converge to 0 as $\beta \to \infty$ and all finite $T$ terms have to vanish in this limit. Furthermore, $\mathcal{A}_{0,0} = 0$ [185, 186] and the finite temperature generalization of the Wilson line $\bar{a}_0(x,y)$ is already obtained by plugging $A_{\text{HS}}$ into $\bar{a}_0(x,y)$ instead of $A_{\text{BPST}}$. In case of a temporal point splitting, we can use the fact that the coincident coefficient functions $\varphi_l(\vec{x}, \varrho, s)$ do not depend on time, so that $\varphi_l(x', x) = \varphi_l(\vec{x}\,)$. This simplifies the non-coincident coefficients in the caloron background:

$$\begin{aligned}a_0(\varepsilon_\tau, x) &= \varphi_0(\vec{x}\,)\bar{a}_0(\varepsilon_\tau, x) + \sum_{J\,\in\,\mathbb{N}^+} \mathcal{A}^{0\,\cdots\,0}_{0,J}(\varphi_l, D^{(a)}E^i, D^{(b)}G^{ij})|_x\,\varepsilon_\tau^J \quad \text{with} \\ \bar{a}_0(\varepsilon_\tau, x) &= \mathbb{1} + iA^4_{\text{HS}}(x)\,\varepsilon_\tau + \frac{1}{2}\Big(i\,\partial_\tau A^4_{\text{HS}}\big|_x - \big(A^4_{\text{HS}}(x)\big)^2\Big)\varepsilon_\tau^2 + \mathcal{O}\big(\varepsilon_\tau^3\big)\,,\end{aligned} \tag{C.7}$$

$$a_{2k\,>\,0}(\varepsilon_\tau, x) = \varphi_0(\vec{x}\,)\bar{a}_{2k}(\varepsilon_\tau, x) + \sum_{J\,\in\,\mathbb{N}} \mathcal{A}^{0\,\cdots\,0}_{2k,J}|_x\,\varepsilon_\tau^J\,, \tag{C.8}$$

where $\bar{a}_1 = 0$ in general and $\bar{a}_2 = \mathcal{O}(\varepsilon_\tau^2)$ in a classical background. As we stated above, $\bar{a}_0$ equals the purely temporal Wilson line (3.2.37) in section 3.2.3. We thus also find the non-coincident vacuum heat kernel coefficient $a_{\text{free}}(\varepsilon_\tau, x) = a_{\text{free}}(x) = \varphi_0(\vec{x})|_{A\,=\,0}$.

Additionally, we now have leading $j = 0$ - modes at odd $2k$ which get multiplied by $\varepsilon_\tau^{J>1}$ due to the $\varepsilon_\tau$ - expansion of the $\bar{a}_{2k\,\mathrm{odd}}$.

The log - caloron density and its (regularized) $m^2$ - derivative contain the traced integral - heat kernel coefficients $b_{2k}(x) = \varphi_0(\vec{x}\,)\bar{a}_{2k}(x) + \mathcal{B}_{2k}(\varphi_l, D^{(b)}E, D^{(c)}G)|_x$, however, not the $a_{2k}(x)$. But introducing non - coincident versions of the $b_{2k}(x)$ is not reasonable, as that disagrees with their traced nature[18] and with how they are obtained from the $a_{2k}(x)$. Nevertheless, just as the $a_{2k}(x, y)$ produce $a_{2k}(y)$ in the limit $x \to y$, their trace appearing in the spacetime integral has to yield (after the appropriate transformations using trace cyclicity, IBP, etc.) the $b_{2k}(y)$ and $\sum_J \mathcal{A}_{2k,J}$ has to produce $\mathcal{B}_{2k}$ in the limit and after taking the trace.

Now we plug the coefficients (C.7) and (C.8) into the (C.3) - caloron background - term $\lim_{\varepsilon_\tau \searrow 0} \int_0^\infty \mathrm{d}s\, e^{-m^2 s - \frac{\varepsilon_\tau^2}{4s}} \int^1 \mathrm{d}^4x \sum_k \frac{s^{k-2}}{(4\pi)^2} \operatorname{tr}(a_{2k}(\varepsilon_\tau, x))$ and perform the $s$ - integrals using (3.1.18) with, as stated above, $k \to k+1$. The $s$ - integral divergences are now due to the $j = 0$ - modes for $k = 0$ and $k = 1$. The leading $j = 0$ - mode for $k = \frac{1}{2}$ vanishes due to $\bar{a}_1 = 0$ and the $j = 0$ - modes for $k = \frac{3}{2}$ and $k = 2$ are rendered finite by the $m^2$ - derivative (they would diverge without it). The $j = 0$ - mode of $\varphi_0(\vec{x}\,)\bar{a}_0(\varepsilon_\tau, x)$ gives $I(m^2, 1, \varepsilon_\tau^2; 0) = \frac{4m}{\varepsilon_\tau} K_1(m\varepsilon_\tau) \overset{\varepsilon_\tau \searrow 0}{\sim} \frac{4}{\varepsilon_\tau^2}$ (3.1.18.c), which diverges quadratically, and for $k = 1$ we find the integral $I(m^2, 2, \varepsilon_\tau^2; 0)$ to diverge logarithmically as $-2\ln\big(\frac{1}{2}m\varepsilon_\tau\big)$. The $k = 0$ - contribution is thus given by an infinite, traceful term $\frac{\mathbb{1}}{4\pi^2\varepsilon_\tau^2}$ and a finite, traceful contribution $-\frac{1}{32\pi^2} I(m^2, 1, \varepsilon_\tau^2; 0)(A^4(x))^2 \varepsilon_\tau^2 = -\frac{1}{8\pi^2}(A^4(x))^2$. For $k = 1$ the logarithmic divergence gets multiplied by terms $\mathcal{O}(\varepsilon_\tau^2)$, so that the overall contribution vanishes as $\lim_{\varepsilon_\tau \searrow 0} \varepsilon_\tau^2 \ln(m\varepsilon_\tau) = 0$. The finite temperature $j \neq 0$ - modes of $\varphi_0(\vec{x}\,)a_{2k}(\varepsilon_\tau, x)$ and $\sum_J \mathcal{A}_{2k,J}^{0\cdots0}|_x\, \varepsilon_\tau^J$ are no longer exponentially suppressed (since $m \ngg 1$), but remain finite as long as $m > 0$. In general, we find them to be determined by $s$ - integrals $I\big(m^2, k+1, j^2 + \varepsilon_\tau^2; \frac{c}{2}\big) = I\big(m^2, k+1, j^2; \frac{c}{2}\big) = 2^{-(k-2-\frac{c}{2})}\big(\frac{|j|}{m}\big)^{k-1-\frac{c}{2}} K_{|k-1-\frac{c}{2}|}(|j|m)$; here we safely took the limit $\varepsilon_\tau \searrow 0$. This is finite for $j \neq 0$. Plugging these integrals into the $j$ - mode summation and recalling the general $\varphi_l$ - structure obtained in (3.1.14) in section 3.1.2, we find traceful contributions

$$
\begin{aligned}
&\sum_{j \in \mathbb{Z}\setminus\{0\}} (-1)^j \Omega^j j^c\, I\big(m^2, k+1, j^2; \frac{c}{2}\big) =_{\mathrm{tr}} \\
&=_{\mathrm{tr}} \sum_{j=1}^{\infty} (-1)^j 2^{-(k-3-\frac{c}{2})} \cos(j\pi\omega) \frac{j^{k-1+\frac{c}{2}}}{m^{k-1-\frac{c}{2}}} K_{|k-1-\frac{c}{2}|}(jm)\,.
\end{aligned}
\tag{C.9}
$$

---

[18] Tr includes the spacetime integral over the closed loop proper time - Green's functions, i.e., point splitting makes no sense.

We can analyze the (potentially) interesting regions of small and asymptotically large $j$:

- $\underline{j \ll m^{-1}\sqrt{|k-1-\frac{c}{2}|+1}}$: For $k=0$ we have only $j \neq 0$ - modes with $c=0$ in $\varphi_0$ and thus $K_1(jm) \sim (jm)^{-1}$, while for $k \in \{\frac{1}{2}, 1\}$ we have in general $c \geq 0$ with $K_{|k-1-\frac{c}{2}|}(jm) \sim (jm)^{-|k-1-\frac{c}{2}|}$ for $k-1-\frac{c}{2} \neq 0$ and $K_{|k-1-\frac{c}{2}|}(jm) \sim -\ln\left(\frac{jm}{2}\right)$ for $k-1-\frac{c}{2}=0$. For $k=0$ the summands are therefore $\propto \frac{1}{j^2}$ and for $k \geq 1$ they are $\propto \left(\frac{j}{m}\right)^c \frac{1}{m^{2k-2}}$, $\propto j^{2k-2}\ln\left(\frac{jm}{2}\right)$ and $\propto j^{2k-2}$ for $k-1-\frac{c}{2}>0$, $k-1-\frac{c}{2}=0$ and $k-1-\frac{c}{2}<0$, respectively. As expected, we can see non - analytic behavior at $m=0$ and finite contributions as $m>0$. Only finitely many of these small $j$ - terms get added up and yield an overall finite contribution.

- $\underline{j \gg m^{-1}|((k-1-\frac{c}{2})^2-1/4|}$: At first order of the asymptotic expansion of the modified Bessel function of the second kind (sufficient for asymptotically large $j$) the summands fall off exponentially as $\frac{j^{k-\frac{3}{2}+\frac{c}{2}}}{m^{k-\frac{1}{2}+\frac{c}{2}}}\, e^{-jm}$. By Cauchy's criterion (root test or radical test) the overall infinite $j$ - sum converges to a finite value: $\limsup_{j\to\infty}\left|2^{-(k-3)}\frac{j^{k-\frac{3}{2}+\frac{c}{2}}}{m^{k-\frac{1}{2}+\frac{c}{2}}}\cos(j\pi\omega)e^{-jm}\right|^{\frac{1}{j}} \leq \lim_{j\to\infty} j^{\frac{k-3/2+c/2}{j}}\, e^{-m} = e^{-m} < 1$ for $m>0$, where we used $\lim_{j\to\infty} a^{\frac{1}{j}} = \lim_{j\to\infty} j^{\frac{1}{j}} = 1\ \forall$ finite $a$. This is independent of $k$.

These contributions are either finite ($\forall \bar{a}_{2k}(x) \neq 0$ and $\mathcal{A}_{2k,0} \neq 0$) and thus require no regularization or vanish (for $\mathcal{A}_{2k,J\geq 1}$, as they get multiplied by terms $\mathcal{O}(\varepsilon_\tau^{J\geq 1})$).

All in all, we find two terms produced by the $\varepsilon_\tau$ - regularized $s$ - integrals at heat kernel orders $k \in \{0, \frac{1}{2}, 1\}$: $\frac{\mathbb{1}}{4\pi^2\varepsilon_\tau^2}$, which equals the free term that is already subtracted, and $-\frac{1}{8\pi^2}(A^4(x))^2$, which is an additional term resulting from exchanging the limits. In order to keep the structure of the (differentiated) log - caloron density, we thus have to subtract the second term, arriving at:

$$\frac{\mathrm{d}\gamma_{\mathrm{s},-}}{\mathrm{d}m^2} = \lim_{\varepsilon_\tau \searrow 0} \int^1 \mathrm{d}^4x\, \mathrm{tr}\Big(\Delta^-(x',x,m^2) - \Delta_0^-(x',x,m^2) + \frac{1}{8}\big(A^4_{\mathrm{HS}}(x)\big)^2\Big)\,. \tag{C.10}$$

This is the finite temperature analogue to the $T=0$ - result obtained in [154, eq. (2.26)] and used in [60]. From this one can proceed as discussed in [60].

# D. Numerical Methods

## D.1 Heat Kernel Coefficients - Obtaining the functional Form

We obtain the general functional form of the finite temperature heat kernel coefficients given in (3.1.11) employing *Mathematica* and making extensive use of the *OGRe* package [187] to handle tensor calculus computations.

As the functional forms of the caloron field strength and especially the heat kernel coefficients (3.1.11) with (3.1.6) are quite complicated, *Mathematica* is limited to calculating their structures for a general, unspecified caloron field described not by $\ln\big(\phi(x)\big)$ as in (2.4.37) ($\phi(x)$ in (2.4.36) or (3.2.4)), but by the general function “funct$(x)$”, i.e. $A^{\mu}_{\text{HS}}(x) = -\overline{\eta}^{\,a\mu\nu}\partial^{\nu}\text{funct}(x)$. We then calculate the caloron field and field strength as well as the heat kernel coefficients with respect to funct and then plug funct $= \ln(\phi)$ in the final expressions for (3.1.11). Furthermore, *OGRe* is designed to perform Ricci index calculations in a general relativity setup and can only handle tensors with an explicit coordinate - dependence - and since funct needs to be an *OGRe* - tensor object and $\varrho$ is not a coordinate, using funct $=$ funct$(\varrho, x)$ is not possible. Instead, we introduce $\varrho$ and its specific values when plugging in funct $= \ln(\phi)$.

Moreover, despite $\phi(x) = \phi(r,\tau)$ being spatially rotationally symmetric, the caloron is defined explicitly in Cartesian coordinates. This is because the ’t Hooft symbols (2.4.26) are defined in this coordinate system. A coordinate transformation to spatial spherical coordinates yields no simplification, neither in advance of calculations - as the ’t Hooft symbols possess no spatial rotational symmetry -, nor subsequent to obtaining the heat kernel coefficients - since there is no way in *OGRe* to define symmetric properties for the general (transformed) function funct$(r,\theta,\varphi,\tau)$.

Lastly, general relativity deals only with spacetime - indices, not with index sets of different types, as in the case of the caloron carrying a spacetime- and a Lie algebra - index. Regarding 4 - dimensional Cartesian coordinates with a Euclidean metric as well as an $SU(2)$ - gauge group and thus $\mathfrak{su}(2)$ - instanton, i.e., a 3 - dimensional Lie algebra with again a $\delta$ - “metric”, we overcome this limitation of *OGRe* by adding an extra spacetime dimension to all Lie algebra - valued objects. This extra dimension then stores the three Lie algebra - components and we set the fourth component (the “time” component in the artificial spacetime dimension) to always be 0. For example, in our code the caloron field $A^{a\,\mu}$ is described by the $4\times4$ - matrix

$$A = \begin{pmatrix} A^{1\,1} & A^{1\,2} & A^{1\,3} & A^{1\,4} \\ A^{2\,1} & A^{2\,2} & A^{2\,3} & A^{2\,4} \\ A^{3\,1} & A^{3\,2} & A^{3\,3} & A^{3\,4} \\ 0 & 0 & 0 & 0 \end{pmatrix}, \tag{D.1}$$

where the upper three rows contains the four components of the three spacetime vectors $A^{1\,\mu}$, $A^{2\,\mu}$ and $A^{3\,\mu}$, respectively, and the fourth row contains 0's (as there is no vector $A^{4\,\mu}$). The columns contain the components of the four Lie algebra 3 - vectors $A^{a\,1}$, $A^{a\,2}$, $A^{a\,3}$ and $A^{a\,4}$. With this description of $\mathfrak{su}(2)$ - valued tensors, we can employ general relativity style index calculus as facilitated by *OGRe*. This is another reason why it is necessary for us to obtain the heat kernel coefficients in Cartesian coordinates. General relativity (and therefore also *OGRe*) does not allow for certain indices of a tensor to be contracted by a different metric than the rest (e.g., radial spherical metric for the spacetime indices and Euclidean metric for the Lie algebra ones).

We remark that our method of including Lie algebra indices into *OGRe* - tensor calculus can be straightforwardly extended to higher dimensional gauge groups $SU(N > 2)$. In this case, one has to include indices corresponding to the $N^2 - 1$ - dimensional Lie algebra $\mathfrak{su}(n)$. This is done by again adding artificial spacetime dimension to Lie algebra - valued tensors and extending the spacetime to be $N^2 - 1$ - dimensional with coordinates $(x, y, z, \tau, x^1_{\text{art}}, ..., x^{N^2-5}_{\text{art}})$. One has to make sure that the $N^2 - 5$ extra spacetime - components of any tensor are always set to 0. As an example, the gauge field is then given by the $(N^2 - 1) \times (N^2 - 1)$ - matrix

$$A_{\mathfrak{su}(N)} = \begin{pmatrix} A^{1\,1} & A^{1\,2} & A^{1\,3} & A^{1\,4} & 0 & \dots & 0 \\ A^{2\,1} & A^{2\,2} & A^{2\,3} & A^{2\,4} & 0 & \dots & 0 \\ A^{3\,1} & A^{3\,2} & A^{3\,3} & A^{3\,4} & 0 & \dots & 0 \\ \vdots & \vdots & \vdots & \vdots & \vdots & \vdots & \vdots \\ A^{(N^2-1)\,1} & A^{(N^2-1)\,2} & A^{(N^2-1)\,3} & A^{(N^2-1)\,4} & 0 & \dots & 0 \end{pmatrix} . \qquad \text{(D.2)}$$

## D.2 Spacetime Integration

As we discussed in section 2.4.2, specifically below (2.4.26) and (2.4.37), and showed in figure 2.12, the HS caloron is not invariant, but only covariant, under spatial rotations, with the same being true for the caloron field strength. The $(\varrho, r, \tau)$ - dependent integrands for the coefficient functions of (3.3.1), i.e., $b_{0,\,4,\,6,\,8,\,10}$ (3.1.11) and int$^-$ (3.2.38), however, are rotationally invariant; even though they are explicitly given in Cartesian coordinates. We show this for multiple of these integrands in figures provided in the ancillary files.

Making use of this implicit spatial rotational symmetry, we enhance the performance of our numerical integrations by choosing (without loss of generality) the radial axis to be the $x$ - axis. This then means we can set $y = z = 0$ in the integrands, but have to multiply the integrands by $4\pi\, x^2$, the volume element of our makeshift spatial spherical coordinates. The integral $\int_0^1 \mathrm{d}\tau$ is left unchanged. This reduces the 4 - dimensional numerical integrations down to 2 - dimensional ones.

## D.3 Ancillary Files

Our code and the resulting data are distributed to the following files and can be found at `https://git.rwth-aachen.de/qcd/ancillary_files_finite_t_top_suscep_heavy_quarks`:

- `heat_kernel_coeffs.nb` contains the analytical (tensor) calculations of all heat kernel coefficients (3.1.11), excluding $\bar{b}_{10}$; `heat_kernel_coeff_b10.nb` contains the calculation of $\bar{b}_{10}$
- `heat_kernel_coeffs.m` contains the saved heat kernel coefficients (except $\bar{b}_{10}$) and the auxiliary tensors required for their calculation; `heat_kernel_coeff_b10.m` contains the saved structure for $\bar{b}_{10}$
- `b4_coeff.nb` contains the numerical integration for (3.1.28) to verify our analytical and numerical methods
- `b4_data.dat` contains the data for (3.1.28); `b4_error.dat` and `b4_log_error.dat` contain the (logarithmic) error of the numerical results compared to the theoretical value
- `b6_coeff.nb` contains the numerical integration for (3.1.31)
- `b6_data.dat` contains the data for (3.1.31); `b6_fitting_error.dat` and `b6_log_fitting_error.dat` contain the (logarithmic) error of the of the fitting function (3.1.31) compared to the data
- `b8_coeff.nb` contains the numerical integration for (3.1.36)
- `b8_data.dat` contains the data for (3.1.36); `b8_fitting_error.dat` and `b8_log_fitting_error.dat` contain the (logarithmic) error of the of the fitting function (3.1.36) compared to the data
- `b10_coefficient.zip` contains the numerical integration for (3.1.37); the integrand as a C - function is contained in `b10_coeff_c.txt`
- `b10_data.dat` contains the data for (3.1.37); `b10_fitting_error.dat` and `b10_log_fitting_error.dat` contain the (logarithmic) error of the of the fitting function (3.1.37) compared to the data
- `B0_coeff_finite_T_integration.ipynb` contains the numerical integration for (3.1.23); `B0_coeff_finite_T_fitting.nb` contains the fitting process yielding (3.1.27)

- `B0_data_corrected.txt` and `B0_mrho_corrected.txt` contain the data and $m$ - $\varrho$ - grid for (3.1.23), respectively; `B0_finite_T_fitting_error.dat` contains the error of the fitting function compared to the data

- `B4_coeff_finite_T_fitting.nb` contains the calculation and simplification of the explicit form (3.1.29) and the fitting process to the data; `B4_coeff_finite_T_integration.ipynb` contains the numerical integration

- `B4_data_corrected.txt` and `B4_mrho_corrected.txt` contain the data and $m$ - $\varrho$ - grid for (3.1.29), respectively; `B4_finite_T_fitting_error.dat` contains the error of the fitting function compared to the data

- `B6_coeff_finite_T.nb` contains the calculation and simplification of the explicit form of (3.1.32) and (3.1.33), the numerical integration for (3.1.34) and the fitting process for (3.1.35)

- `B6B_coeff_finite_T_integration.ipynb` contains the numerical integration for (3.1.35); `B6_coeff_D4E_D4E.txt`, `B6_coeff_D4G_D4G.txt`, `B6_coeff_DiE_DiE.txt` and `B6_coeff_EGE.txt` contain the simplified explicit terms of (3.1.33)

- `B6_phi0_data.dat` contains the data for (3.1.34) produced in `B6_coeff_finite_T.nb`, `B6B_results.txt` contains the integration results of `B6B_coeff_finite_T_integration.ipynb` and `B6B_data.dat` contains the full data

- `B6B_fitting_error.dat` contains the error of the fitting function (3.1.35) compared to the data

- `propagator_sum_periodic.nb` contains the summations (3.2.5), (3.2.10), (3.2.16), (3.2.17) and (3.2.18) and the resulting simplification for (3.2.19); `propagator_sum_antiperiodic.nb` contains the summations (3.2.5), (3.2.23), (3.2.24) and (3.2.25) and the resulting simplification for (3.2.22)

- `R4_propagator_limits.nb` contains the $\beta \to \infty$ limits (in $\mathbb{R}^4$) (3.2.13) and of (3.2.19)

- `propagator_sum_coincident.nb` contains the summations (3.2.29), (3.2.31), (3.2.33) and (3.2.34), the Taylor expansion in (3.2.35) as well as discussions concerning the asymptotic behavior of (3.2.35)

- `Taylor_exp_small_m_coeff.nb` contains the numerical integration producing the data for (3.2.40) and the fitting process
- `m2_coeff_data.dat` contains the data for (3.2.40); `m2_coeff_fitting_error.dat` and `m2_coeff_log_fitting_error.dat` contain the (logarithmic) error of the fitting function (3.2.40) compared to the data
- `pade_interpolation.nb` contains the derivation of the large - mass expansion's validity (3.1.40) and the small - mass expansions validity (3.2.42) range of validity as well as the Padé interpolation (3.3.4) - (3.3.15) & figure 3.12. It also produces the figures 3.13 and 3.14.
- `pade_interpol.m` contains the explicit result for the Padé approximant (3.3.4); `caldens_pade.m` contains the full mass dependency of the caloron density with the Padé interpolation plugged in (i.e., including the factor $m_b\varrho$ from (2.4.75))
- `ratio_topological_susceptibilities.nb` contains a discussion of the $b$ - quark's effects on the caloron density and the numerical calculation of (3.3.17), producing also figure 3.16 and the main result shown in figure 3.17; `ratio_topological_susceptibilities_data.dat` contains the data for (3.3.17) and figure 3.17

# List of Figures

1.1 Running of the QCD coupling at 1 - loop order . . . . . . . . . . . . . . . . 3

2.1 Path integral in non - relativistic quantum mechanics . . . . . . . . . . . . 27
2.2 Instanton toy model: double well and periodic potential and tunneling . . 41
2.3 Flipped potential in Euclidean time . . . . . . . . . . . . . . . . . . . . . . . 43
2.4 Instanton toy model: (anti-)instanton solutions and real - time energy . . . 45
2.5 Winding number for toy model maps $S^1 \to S^1$ . . . . . . . . . . . . . . . . 49
2.6 Stereographic projection . . . . . . . . . . . . . . . . . . . . . . . . . . . . 50
2.7 Gluon vacuum maps . . . . . . . . . . . . . . . . . . . . . . . . . . . . . . . 50
2.8 Potential landscape for gluon vacua . . . . . . . . . . . . . . . . . . . . . . . 52
2.9 Instanton tunneling in gluon potential . . . . . . . . . . . . . . . . . . . . . 53
2.10 Boundary $\partial\mathbb{R}^4$ deformed into a hypercylinder . . . . . . . . . . . . . . . . 54
2.11 Caloron as infinite sum of instantons . . . . . . . . . . . . . . . . . . . . . 62
2.12 HS caloron field strength . . . . . . . . . . . . . . . . . . . . . . . . . . . . 65
2.13 Feynman diagrams axial/chiral anomaly . . . . . . . . . . . . . . . . . . . . 86
2.14 Kaon oscillations . . . . . . . . . . . . . . . . . . . . . . . . . . . . . . . . 88
2.15 Mexican hat potential and (massive) axions . . . . . . . . . . . . . . . . . . 94

3.1 Coincident propagators in caloron background . . . . . . . . . . . . . . . . . 100
3.2 $\omega$ - function defining the Polyakov loop . . . . . . . . . . . . . . . . . . . . 106
3.3 Large - mass damping of finite - $T$ terms . . . . . . . . . . . . . . . . . . . . 107
3.4 $m$ - $\varrho$ - plane . . . . . . . . . . . . . . . . . . . . . . . . . . . . . . . . . . 111
3.5 Heat kernel order $k = 0$, finite - $T$ ambiguities: relative fitting error . . . . 112
3.6 $\ln(m)$ - coefficient: relative numerical error . . . . . . . . . . . . . . . . . . 114
3.7 $m^{-2}$ - coefficient: data, interpolation, relative fitting error . . . . . . . . . . 116
3.8 $m^{-4}$ - coefficient: data, interpolation, relative fitting error . . . . . . . . . . 119
3.9 $m^{-6}$ - coefficient: data, interpolation, relative fitting error . . . . . . . . . . 121
3.10 Finite - $T$ large - mass condition . . . . . . . . . . . . . . . . . . . . . . . . 123
3.11 $m^2$ - coefficient: data, interpolation, relative fitting error, non - analyticity . 138
3.12 Parameters $\xi(\varrho)$ and $\mathcal{P}_{0,1}(\rho)$ of the Padé interpolation . . . . . . . . . . . 143

3.13 Interpolation between mass regimes using Padé approximation . . . . . . 144
3.14 Interpolation between mass regimes for several $\varrho$-values . . . . . . . . . . 147
3.15 Modified coupling for asymptotically heavy $b$ quark . . . . . . . . . . . . . 148
3.16 Caloron density for different $b$ masses . . . . . . . . . . . . . . . . . . . . . 149
3.17 Topological susceptibility with dynamical $b$ quark compared to lattice QCD 150
A.1 Spacetime regions for fermionic eigenvalue problem . . . . . . . . . . . . . 153

# Bibliography

[1] BIPM. *Le Système international d'unités / The International System of Units ('The SI Brochure')*. 9th Edition. Bureau international des poids et mesures, 2019/2022. ISBN: 978-92-822-2272-0. URL: `https://www.bipm.org/en/publications/si-brochure/`.

[2] R. L. Workman et al. "Review of Particle Physics". In: *PTEP* 2022 (2022), p. 083C01. DOI: `10.1093/ptep/ptac097`.

[3] Michael E. Peskin and Daniel V. Schroeder. *An Introduction to quantum field theory*. Reading, USA: Addison-Wesley, 1995. ISBN: 978-0-201-50397-5.

[4] Matthew D. Schwartz. *Quantum Field Theory and the Standard Model*. Cambridge University Press, Mar. 2014. ISBN: 978-1-107-03473-0, 978-1-107-03473-0.

[5] Anthony Zee. *Quantum Field Theory in a Nutshell*. 2nd Edition. Princeton University Press, 2010. ISBN: 978-0-691-14034-6.

[6] Michio Kaku. *Quantum Field Theory: A modern Introduction*. Oxford University Press, Mar. 1993, p. 808. ISBN: 978-0195076523.

[7] R Alkofer and J Greensite. "Quark confinement: the hard problem of hadron physics". In: *Journal of Physics G: Nuclear and Particle Physics* 34.7 (May 2007), S3. DOI: `10.1088/0954-3899/34/7/S02`.

[8] Curtis G. Callan, Roger Dashen, and David J. Gross. "Toward a theory of the strong interactions". In: *Phys. Rev. D* 17 (10 May 1978), pp. 2717–2763. DOI: `10.1103/PhysRevD.17.2717`.

[9] Kenneth G. Wilson. "Confinement of quarks". In: *Phys. Rev. D* 10 (8 Oct. 1974), pp. 2445–2459. DOI: `10.1103/PhysRevD.10.2445`.

[10] Mattia Bruno et al. "QCD Coupling from a Nonperturbative Determination of the Three-Flavor $\Lambda$ Parameter". In: *Phys. Rev. Lett.* 119 (10 Sept. 2017), p. 102001. DOI: `10.1103/PhysRevLett.119.102001`.

[11] David J. Gross and Frank Wilczek. “Ultraviolet Behavior of Non-Abelian Gauge Theories”. In: *Phys. Rev. Lett.* 30 (26 June 1973), pp. 1343–1346. DOI: `10.1103/PhysRevLett.30.1343`.

[12] H. David Politzer. “Reliable Perturbative Results for Strong Interactions?” In: *Phys. Rev. Lett.* 30 (26 June 1973), pp. 1346–1349. DOI: `10.1103/PhysRevLett.30.1346`.

[13] Michela D’Onofrio and Kari Rummukainen. “Standard model cross-over on the lattice”. In: *Phys. Rev. D* 93 (2 Jan. 2016), p. 025003. DOI: `10.1103/PhysRevD.93.025003`.

[14] Brian C. Odom et al. “New Measurement of the Electron Magnetic Moment Using a One-Electron Quantum Cyclotron”. In: *Phys. Rev. Lett.* 97 (3 July 2006), p. 030801. DOI: `10.1103/PhysRevLett.97.030801`. Erratum: Gerald Gabrielse et al. “Erratum: New Determination of the Fine Structure Constant from the Electron $g$ Value and QED]”. In: *Phys. Rev. Lett.* 99 (3 July 2007), p. 039902. DOI: `10.1103/PhysRevLett.99.039902`.

[15] R. Brandelik et al. “Evidence for planar events in e+e− annihilation at high energies”. In: *Physics Letters B* 86.2 (1979), pp. 243–249. ISSN: 0370-2693. DOI: `10.1016/0370-2693(79)90830-X`.

[16] TASSO Collaboration et al. “Evidence for a spin-1 gluon in three-jet events”. In: *Physics Letters B* 97.3 (1980), pp. 453–458. ISSN: 0370-2693. DOI: `10.1016/0370-2693(80)90639-5`.

[17] H. Hamber and G. Parisi. “Numerical Estimates of Hadronic Masses in a Pure SU(3) Gauge Theory”. In: *Phys. Rev. Lett.* 47 (25 Dec. 1981), pp. 1792–1795. DOI: `10.1103/PhysRevLett.47.1792`.

[18] Don Weingarten. “Monte Carlo evaluation of hadron masses in lattice gauge theories with fermions”. In: *Physics Letters B* 109.1 (1982), pp. 57–62. ISSN: 0370-2693. DOI: `10.1016/0370-2693(82)90463-4`.

[19] G. Aad et al. “Observation of a new particle in the search for the Standard Model Higgs boson with the ATLAS detector at the LHC”. In: *Physics Letters B* 716.1 (2012), pp. 1–29. ISSN: 0370-2693. DOI: `10.1016/j.physletb.2012.08.020`.

[20] S. Chatrchyan et al. “Observation of a new boson at a mass of 125 GeV with the CMS experiment at the LHC”. In: *Physics Letters B* 716.1 (2012), pp. 30–61. ISSN: 0370-2693. DOI: `10.1016/j.physletb.2012.08.021`.

[21] Vera C. Rubin. “The Rotation of Spiral Galaxies”. In: *Science* 220.4604 (1983), pp. 1339–1344. DOI: `10.1126/science.220.4604.1339`.

[22] Douglas Clowe et al. “A Direct Empirical Proof of the Existence of Dark Matter”. In: *The Astrophysical Journal* 648.2 (Aug. 2006), p. L109. DOI: `10.1086/508162`.

[23] Anton Bergmann, Vahe Petrosian, and Roger Lynds. “Gravitational lens models of arcs in clusters”. In: *The Astrophysical Journal* 350 (Mar. 1990), p. 23. DOI: `10.1086/168359`.

[24] G. F. Smoot et al. “Structure in the COBE Differential Microwave Radiometer First-Year Maps”. In: *The Astrophysical Journal* 396 (Sept. 1992), p. L1. DOI: `10.1086/186504`.

[25] Planck Collaboration et al. “Planck 2018 results - I. Overview and the cosmological legacy of Planck”. In: *Astronomy and Astrophysics* 641 (2020), A1. DOI: `10.1051/0004-6361/201833880`. And: Planck Collaboration et al. “Planck 2018 results - VI. Cosmological parameters”. In: *Astronomy and Astrophysics* 641 (2020), A6. DOI: `10.1051/0004-6361/201833910`. with Erratum: Planck Collaboration et al. “Planck 2018 results - VI. Cosmological parameters (Corrigendum)”. In: *Astronomy and Astrophysics* 652 (2021), p. C4. DOI: `10.1051/0004-6361/201833910e`.

[26] George R. Blumenthal et al. “Formation of galaxies and large-scale structure with cold dark matter”. In: *Nature* 311.5986 (Oct. 1984), pp. 517–525. ISSN: 1476-4687. DOI: `10.1038/311517a0`.

[27] Alexander A. Belavin et al. “Pseudoparticle solutions of the Yang-Mills equations”. In: *Physics Letters B* 59.1 (1975), pp. 85–87. ISSN: 0370-2693. DOI: `10.1016/0370-2693(75)90163-X`.

[28] Barry J. Harrington and Harvey K. Shepard. “Euclidean solutions and finite temperature gauge theory”. In: *Nuclear Physics B* 124.4 (1977), pp. 409–412. ISSN: 0550-3213. DOI: `10.1016/0550-3213(77)90413-8`.

[29] Stephen L. Adler. “Axial-Vector Vertex in Spinor Electrodynamics”. In: *Phys. Rev.* 177 (5 Jan. 1969), pp. 2426–2438. DOI: `10.1103/PhysRev.177.2426`.

[30] John S. Bell and Roman Jackiw. “A PCAC puzzle: $\pi^0 \to \gamma\gamma$ in the $\sigma$ model”. In: *Nuovo Cim. A* 60 (1969), pp. 47–61. DOI: `10.1007/BF02823296`.

[31] William A. Bardeen. “Anomalous Ward Identities in Spinor Field Theories”. In: *Phys. Rev.* 184 (5 Aug. 1969), pp. 1848–1859. DOI: `10.1103/PhysRev.184.1848`.

[32] Y. Nambu and G. Jona-Lasinio. “Dynamical Model of Elementary Particles Based on an Analogy with Superconductivity. I”. In: *Phys. Rev.* 122 (1 Apr. 1961), pp. 345–358. DOI: `10.1103/PhysRev.122.345`.

[33] Sidney R. Coleman. “The Uses of Instantons”. In: *Subnucl. Ser.* 15 (1979). Ed. by Mikhail A. Shifman, pp. 805–941. DOI: `10.1007/978-1-4684-0991-8_16`. URL: `https://www.physics.mcgill.ca/~jcline/742/Coleman-Instantons.pdf`.

[34] Edward Witten. “Current algebra theorems for the U(1) “Goldstone boson””. In: *Nuclear Physics B* 156.2 (1979), pp. 269–283. ISSN: 0550-3213. DOI: `10.1016/0550-3213(79)90031-2`.

[35] Gabriele Veneziano. “U(1) without instantons”. In: *Nuclear Physics B* 159.1 (1979), pp. 213–224. ISSN: 0550-3213. DOI: `10.1016/0550-3213(79)90332-8`.

[36] Jack Dragos et al. “Confirming the existence of the strong CP problem in lattice QCD with the gradient flow”. In: *Phys. Rev. C* 103 (1 Jan. 2021), p. 015202. DOI: `10.1103/PhysRevC.103.015202`.

[37] C. Abel et al. “Measurement of the Permanent Electric Dipole Moment of the Neutron”. In: *Phys. Rev. Lett.* 124 (8 Feb. 2020), p. 081803. DOI: `10.1103/PhysRevLett.124.081803`.

[38] Erick J. Weinberg. *Classical solutions in quantum field theory: Solitons and Instantons in High Energy Physics*. Cambridge Monographs on Mathematical Physics. Cambridge University Press, Sept. 2012. ISBN: 978-0-521-11463-9, 978-1-139-57461-7, 978-0-521-11463-9, 978-1-107-43805-7.

[39] Steven Weinberg. “A New Light Boson?” In: *Phys. Rev. Lett.* 40 (4 Jan. 1978), pp. 223–226. DOI: `10.1103/PhysRevLett.40.223`.

[40] Frank A. Wilczek. “Problem of Strong $P$ and $T$ Invariance in the Presence of Instantons”. In: *Phys. Rev. Lett.* 40 (5 Jan. 1978), pp. 279–282. DOI: `10.1103/PhysRevLett.40.279`.

[41] Roberto D. Peccei and Helen R. A. Quinn. “CP Conservation in the Presence of Instantons”. In: *Phys. Rev. Lett.* 38 (1977), pp. 1440–1443. DOI: `10.1103/PhysRevLett.38.1440`.

[42] Roberto D. Peccei and Helen R. A. Quinn. “Constraints Imposed by CP Conservation in the Presence of Instantons”. In: *Phys. Rev. D* 16 (1977), pp. 1791–1797. DOI: `10.1103/PhysRevD.16.1791`.

[43] Francesca Chadha-Day, John Ellis, and David J. E. Marsh. “Axion dark matter: What is it and why now?” In: *Science Advances* 8.8 (Feb. 2022), eabj3618. DOI: `10.1126/sciadv.abj3618`.

[44] Giovanni Grilli di Cortona et al. “The QCD axion, precisely”. In: *Journal of High Energy Physics* 2016.1 (Jan. 2016), p. 34. DOI: `10.1007/JHEP01(2016)034`.

[45] David J. E. Marsh. “Axion cosmology”. In: *Physics Reports* 643 (July 2016), pp. 1–79. ISSN: 0370-1573. DOI: `10.1016/j.physrep.2016.06.005`.

[46] Markus Kuster, Georg Raffelt, and Berta Beltrán, eds. *Axions. Theory, Cosmology and Experimental Searches*. Vol. 741. 2008, pp. XI, 245. ISBN: 978-3-540-73517-5.

[47] Luca Di Luzio et al. “The landscape of QCD axion models”. In: *Physics Reports* 870 (2020). The landscape of QCD axion models, pp. 1–117. ISSN: 0370-1573. DOI: `10.1016/j.physrep.2020.06.002`.

[48] Olivier Wantz and Edward P. S. Shellard. “Axion cosmology revisited”. In: *Phys. Rev. D* 82 (12 Dec. 2010), p. 123508. DOI: `10.1103/PhysRevD.82.123508`.

[49] Szabolcs Borsányi et al. “Axion cosmology, lattice QCD and the dilute instanton gas”. In: *Physics Letters B* 752 (2016), pp. 175–181. ISSN: 0370-2693. DOI: `10.1016/j.physletb.2015.11.020`.

[50] Igor García Irastorza. “An introduction to axions and their detection”. In: *SciPost Phys. Lect. Notes* (2022), p. 45. DOI: `10.21468/SciPostPhysLectNotes.45`.

[51] Marco Gorghetto and Giovanni Villadoro. “Topological susceptibility and QCD axion mass: QED and NNLO corrections”. In: *Journal of High Energy Physics* 2019.3 (Mar. 2019), p. 33. ISSN: 1029-8479. DOI: `10.1007/JHEP03(2019)033`.

[52] Zhen-Yan Lu et al. “QCD $\theta$-vacuum energy and axion properties”. In: *Journal of High Energy Physics* 2020.5 (May 2020), p. 1. ISSN: 1029-8479. DOI: `10.1007/JHEP05(2020)001`.

[53] Szabolcs Borsányi et al. “Calculation of the axion mass based on high-temperature lattice quantum chromodynamics”. In: *Nature* 539.7627 (2016), pp. 69–71. DOI: `10.1038/nature20115`.

[54] David J. Gross, Robert D. Pisarski, and Laurence G. Yaffe. “QCD and instantons at finite temperature”. In: *Rev. Mod. Phys.* 53 (1 Jan. 1981), pp. 43–80. DOI: `10.1103/RevModPhys.53.43`.

[55] Vincent B. Klaer and Guy D. Moore. “The dark-matter axion mass”. In: *Journal of Cosmology and Astroparticle Physics* 2017.11 (Nov. 2017), p. 049. DOI: `10.1088/1475-7516/2017/11/049`.

[56] Szabocls Borsányi et al. “Full result for the QCD equation of state with 2+1 flavors”. In: *Phys. Lett. B* 730 (2014), pp. 99–104. DOI: `10.1016/j.physletb.2014.01.007`. arXiv: `1309.5258 [hep-lat]`.

[57] A. Bazavov et al. “Equation of state in ( 2+1 )-flavor QCD”. In: *Phys. Rev. D* 90 (2014), p. 094503. DOI: `10.1103/PhysRevD.90.094503`. arXiv: `1407.6387 [hep-lat]`.

[58] Peter Thomas Jahn, Guy D. Moore, and Daniel Robaina. “$\chi_{\text{top}}(T \gg T_{\text{c}})$ in pure-glue QCD through reweighting”. In: *Phys. Rev. D* 98.5 (2018), p. 054512. DOI: `10.1103/PhysRevD.98.054512`. arXiv: `1806.01162 [hep-lat]`.

[59] P. Thomas Jahn, Guy D. Moore, and Daniel Robaina. “Improved Reweighting for QCD Topology at High Temperature”. In: (Feb. 2020). arXiv: `2002.01153 [hep-lat]`.

[60] O-Kab Kwon, Choonkyu Lee, and Hyunsoo Min. “Massive field contributions to the QCD vacuum tunneling amplitude”. In: *Phys. Rev. D* 62 (11 Nov. 2000), p. 114022. DOI: `10.1103/PhysRevD.62.114022`.

[61] Gerald V. Dunne et al. “Calculation of QCD instanton determinant with arbitrary mass”. In: *Phys. Rev. D* 71 (8 Apr. 2005), p. 085019. DOI: `10.1103/PhysRevD.71.085019`.

[62] George Zweig. “An SU(3) model for strong interaction symmetry and its breaking. Version 2”. In: *DEVELOPMENTS IN THE QUARK THEORY OF HADRONS. VOL. 1. 1964 - 1978*. Ed. by D. B. Lichtenberg and Simon Peter Rosen. Feb. 1964, pp. 22–101. URL: `https://cds.cern.ch/record/570209/files/CERN_Report_TH-412_corrected.pdf?version=1`.

[63] Murray Gell-Mann. “A schematic model of baryons and mesons”. In: *Physics Letters* 8.3 (1964), pp. 214–215. ISSN: 0031-9163. DOI: `10.1016/S0031-9163(64)92001-3`.

[64] Harald Fritzsch, Murray Gell-Mann, and Heinrich Leutwyler. “Advantages of the color octet gluon picture”. In: *Physics Letters B* 47.4 (1973), pp. 365–368. ISSN: 0370-2693. DOI: `10.1016/0370-2693(73)90625-4`.

[65] Emmy Noether. “Invariante Variationsprobleme. Invariant Variation Problems”. In: *Nachrichten von der Gesellschaft der Wissenschaften zu Göttingen, Mathematisch-Physikalische Klasse* (1918), pp. 235–257. DOI: `10.1080/00411457108231446`. arXiv: `physics/0503066`. URL: `https://gdz.sub.uni-goettingen.de/id/PPN252457811_1918`.

[66] Jürgen Fuchs and Christoph Schweigert. *Symmetries, Lie algebras and representations: A graduate course for physicists*. Cambridge University Press, Oct. 2003. ISBN: 978-0-521-54119-0.

[67] Martin Schottenloher. *Geometrie und Symmetrie in der Physik: Leitmotive der Mathematischen Physik. Geometry and Symmetry in Physics: Guiding Principles of Mathematical Physics*. Vieweg+Teubner Verlag Wiesbaden, Jan. 1995. ISBN: 978-3-528-06565-2, 978-3-322-89928-6. DOI: `10.1007/978-3-322-89928-6`. URL: `https://www.mathematik.uni-muenchen.de/~schotten/bas/Geometrie%5C%20und%5C%20Symmetrie.pdf`.

[68] Jun J. Sakurai and Jim Napolitano. *Modern Quantum Mechanics*. 3rd Edition. Cambridge University Press, 2020. ISBN: 9781108587280.

[69] Henri Poincaré. “Sur la dynamique de l’électron. On the dynamics of the electron”. In: *Rendiconti del Circolo Matematico di Palermo (1884-1940)* 21.1 (Dec. 1906), pp. 129–175.

[70] Albert Einstein. “Zur Elektrodynamik bewegter Körper. On the electrodynamics of moving bodies”. In: *Annalen der Physik* 322.10 (1905), pp. 891–921. DOI: `10.1002/andp.19053221004`.

[71] Eugene P. Wigner. “On Unitary Representations of the Inhomogeneous Lorentz Group”. In: *Annals Math.* 40 (1939). Ed. by Y. S. Kim and W. W. Zachary, pp. 149–204. DOI: `10.2307/1968551`.

[72] Sidney Coleman and Jeffrey Mandula. “All Possible Symmetries of the $S$ Matrix”. In: *Phys. Rev.* 159 (5 July 1967), pp. 1251–1256. DOI: `10.1103/PhysRev.159.1251`.

[73] Lewis H. Ryder. *Quantum Field Theory*. Cambridge University Press, June 1996. ISBN: 978-0-521-47814-4, 978-1-139-63239-3, 978-0-521-23764-2.

[74] Tommy Ohlsson. *Relativistic Quantum Physics: From Advanced Quantum Mechanics to Introductory Quantum Field Theory*. Cambridge University Press, 2011. ISBN: 9781139032681.

[75] Brian C. Hall. *Lie Groups, Lie Algebras, and Representations: An Elementary Introduction*. Graduate Texts in Mathematics. Springer International, May 2015. ISBN: 978-3-319-13466-6, 978-3-319-37433-8, 978-3-319-13467-3.

[76] Chen-Ning Yang and Robert L. Mills. “Conservation of Isotopic Spin and Isotopic Gauge Invariance”. In: *Phys. Rev.* 96 (1 Oct. 1954), pp. 191–195. DOI: `10.1103/PhysRev.96.191`.

[77] David Hilbert. “Die Grundlagen der Physik . (Erste Mitteilung.)” In: *Nachrichten von der Gesellschaft der Wissenschaften zu Göttingen, Mathematisch-Physikalische Klasse* (1915), pp. 395–408.

[78] Vladimir A. Fock. “Proper time in classical and quantum mechanics”. In: *Sov. Phys.* 12 (1937), p. 404.

[79] Julian Schwinger. “On Gauge Invariance and Vacuum Polarization”. In: *Phys. Rev.* 82 (5 June 1951), pp. 664–679. DOI: `10.1103/PhysRev.82.664`.

[80] Wolfgang Kummer and Johann Weiser. “Quantization of Gauge-Fields in the Fock-Schwinger Gauge”. In: *Zeitschrift für Physik C, Particles and Fields* 31.1 (Mar. 1986), pp. 105–110. ISSN: 1431-5858. DOI: `10.1007/BF01559599`.

[81] Paul A. M. Dirac. “A new classical theory of electrons”. In: *Proc. R. Soc. Lond. A* 209 (1951), pp. 291–296. DOI: `10.1098/rspa.1951.0204`. Reprinted in: *Nature* 168 (1951).

[82] Suraj N. Gupta. “Theory of Longitudinal Photons in Quantum Electrodynamics”. In: *Proceedings of the Physical Society. Section A* 63.7 (July 1950), p. 681. DOI: `10.1088/0370-1298/63/7/301`.

[83] Konrad Bleuler. “Eine neue Methode zur Behandlung der longitudinalen und skalaren Photonen. A new method of treating longitudinal and scalar photons”. In: *Helvetica Physica Acta* 23.V (1950), p. 567. ISSN: 0018-0238. DOI: `10.5169/seals-112124`.

[84] Michel Le Bellac. *Thermal Field Theory*. Cambridge Monographs on Mathematical Physics. Cambridge University Press, Mar. 2011. ISBN: 978-0-511-88506-8, 978-0-521-65477-7.

[85] Joseph I. Kapusta and Charles Gale. *Finite-temperature field theory: Principles and Applications*. Cambridge Monographs on Mathematical Physics. Cambridge University Press, 2011. ISBN: 978-0-521-17322-3, 978-0-521-82082-0, 978-0-511-22280-1.

[86] Ashok Das. *Finite Temperature Field Theory*. WORLD SCIENTIFIC, 1997.

[87] Jacopo Ghiglieri et al. “Perturbative thermal QCD: Formalism and applications”. In: *Physics Reports* 880 (2020). Perturbative Thermal QCD: Formalism and Applications, pp. 1–73. ISSN: 0370-1573. DOI: `10.1016/j.physrep.2020.07.004`.

[88] Hale F. Trotter. “On the Product of Semi-Groups of Operators”. In: *Proceedings of the American Mathematical Society* 10.4 (1959), pp. 545–551. DOI: `10.1090/S0002-9939-1959-0108732-6`.

[89] Hermann Graßmann. *Die lineare Ausdehnungslehre. The Theory of linear Extension*. Wigang Leipzig, 1878. URL: `https://gdz.sub.uni-goettingen.de/id/PPN534901565`.

[90] Felix A. Berezin. *The Method of Second Quantization*. 1st Edition. Translated by Nobumichi Mugibayashi and Alan Jeffrey. Academic Press, 1966. ISBN: 978-0120894505.

[91] Jeffrey Goldstone, Abdus Salam, and Steven Weinberg. "Broken Symmetries". In: *Phys. Rev.* 127 (3 Aug. 1962), pp. 965–970. DOI: `10.1103/PhysRev.127.965`.

[92] Giovanni Jona-Lasinio. "Relativistic field theories with symmetry-breaking solutions". In: *Il Nuovo Cimento (1955-1965)* 34.6 (Dec. 1964), pp. 1790–1795. ISSN: 1827-6121. DOI: `10.1007/BF02750573`.

[93] Ludvig D. Faddeev and Victor N. Popov. "Feynman diagrams for the Yang-Mills field". In: *Physics Letters B* 25.1 (1967), pp. 29–30. ISSN: 0370-2693. DOI: `10.1016/0370-2693(67)90067-6`.

[94] Victor N. Popov and Ludvig D. Faddeev. "Perturbation Theory for gauge-invariant Fields". In: *50 Years of Yang-Mills Theory*. 2005, pp. 40–60. DOI: `10.1142/9789812567147_0003`. Originally in: *Kiev Inst. Theor. Phys. Acad. Sci. preprint* ITP 67-36 (1967).

[95] Donald R. Yennie, Steven C. Frautschi, and Hiroshi Suura. "The infrared divergence phenomena and high-energy processes". In: *Annals of Physics* 13.3 (1961), pp. 379–452. ISSN: 0003-4916. DOI: `10.1016/0003-4916(61)90151-8`.

[96] Takeo Matsubara. "A New approach to quantum statistical mechanics". In: *Prog. Theor. Phys.* 14 (1955), pp. 351–378. DOI: `10.1143/PTP.14.351`.

[97] Hajime Ezawa, Yukio Tomozawa, and Hiroomi Umezawa. "Quantum statistics of fields and multiple production of mesons". In: *Nuovo Cim.* 5 (1957). Ed. by A. Arimitsu et al., pp. 810–841. DOI: `10.1007/BF02903206`.

[98] Munshi G. Mustafa. "An introduction to thermal field theory and some of its application". In: *The European Physical Journal Special Topics* 232.9 (Aug. 2023), pp. 1369–1457. ISSN: 1951-6401. DOI: `10.1140/epjs/s11734-023-00868-8`.

[99] Julian Schwinger. "Brownian Motion of a Quantum Oscillator". In: *Journal of Mathematical Physics* 2.3 (Dec. 2004), pp. 407–432. ISSN: 0022-2488. DOI: `10.1063/1.1703727`.

[100] Pradip M. Bakshi and Kalyana T. Mahanthappa. “Expectation Value Formalism in Quantum Field Theory. I”. In: *Journal of Mathematical Physics* 4.1 (Dec. 2004), pp. 1–11. ISSN: 0022-2488. DOI: `10.1063/1.1703883`.

[101] Pradip M. Bakshi and Kalyana T. Mahanthappa. “Expectation Value Formalism in Quantum Field Theory. II”. In: *Journal of Mathematical Physics* 4.1 (Dec. 2004), pp. 12–16. ISSN: 0022-2488. DOI: `10.1063/1.1703879`.

[102] Kalyana T. Mahanthappa. “Multiple Production of Photons in Quantum Electrodynamics”. In: *Phys. Rev.* 126 (1 Apr. 1962), pp. 329–340. DOI: `10.1103/PhysRev.126.329`.

[103] Leonid V. Keldysh. “Diagram technique for nonequilibrium processes”. In: *Zh. Eksp. Teor. Fiz.* 47 (1964), pp. 1515–1527. Also in: *Sov. Physics JTEP* 20 (1965), p. 1018.

[104] Jørgen Rammer. *Quantum Field Theory of Non-Equilibrium States*. Cambridge University Press, Jan. 2007, p. 550. ISBN: 9780521874991. eprint: `https://www-thphys.physics.ox.ac.uk/talks/CMTjournalclub/sources/Rammer.pdf`.

[105] Yasushi Takahashi and Hiroomi Umezawa. “Thermofield Dynamics”. In: *Collective Phhenomena* 2 (1975), pp. 55–80. Reprinted in: *International Journal of Modern Physics B* 10.13n14 (1996), pp. 1755–1805. DOI: `10.1142/S0217979296000817`.

[106] Hiroomi Umezawa, Hideaki Matsumoto, and M. Tachiki. *Thermofield Dynamics and Condensed States*. Amsterdam, New York: North-Holland Pub. Co. ; Sole distributors for the U.S.A. and Canada, Elsevier Science Pub. Co. Amsterdam, New York, 1982. ISBN: 9780444863614.

[107] Faqir C. Khanna et al. *Thermal Quantum Field Theory: Algebraic Aspects and Applications*. WORLD SCIENTIFIC, 2009. ISBN: 13 978-981-281-887-4, 10 981-281-887-1.

[108] Gian Carlo Wick. “Properties of Bethe-Salpeter Wave Functions”. In: *Phys. Rev.* 96 (4 Nov. 1954), pp. 1124–1134. DOI: `10.1103/PhysRev.96.1124`.

[109] Alexander M. Polyakov. “Compact gauge fields and the infrared catastrophe”. In: *Physics Letters B* 59.1 (1975), pp. 82–84. ISSN: 0370-2693. DOI: `10.1016/0370-2693(75)90162-8`.

[110] Izumi Ojima. “Lorentz Invariance Versus Temperature in QFT”. In: *Lett. Math. Phys.* 11 (1986), p. 73. DOI: `10.1007/BF00417467`.

[111] Hagop Sazdjian. “Introduction to chiral symmetry in QCD”. In: *EPJ Web Conf.* 137 (2017). Ed. by Y. Foka, N. Brambilla, and V. Kovalenko, p. 02001. DOI: `10.1051/epjconf/201713702001`.

[112] Stefan Scherer. “Introduction to Chiral Perturbation Theory”. In: *Advances in Nuclear Physics, Volume 27*. Ed. by J. W. Negele and E. W. Vogt. Boston, MA: Springer US, 2003, pp. 277–538. ISBN: 978-0-306-47916-8. DOI: `10.1007/0-306-47916-8_2`.

[113] Jeffrey Goldstone. “Field theories with « Superconductor » solutions”. In: *Il Nuovo Cimento (1955-1965)* 19.1 (Jan. 1961), pp. 154–164. ISSN: 1827-6121. DOI: `10.1007/BF02812722`.

[114] Jeffrey Goldstone, Abdus Salam, and Steven Weinberg. “Broken Symmetries”. In: *Phys. Rev.* 127 (3 Aug. 1962), pp. 965–970. DOI: `10.1103/PhysRev.127.965`.

[115] Yoichiro Nambu. “Quasi-Particles and Gauge Invariance in the Theory of Superconductivity”. In: *Phys. Rev.* 117 (3 Feb. 1960), pp. 648–663. DOI: `10.1103/PhysRev.117.648`.

[116] Thomas Schäfer and Edward V. Shuryak. “Instantons in QCD”. In: *Rev. Mod. Phys.* 70 (2 Apr. 1998), pp. 323–425. DOI: `10.1103/RevModPhys.70.323`.

[117] Murray Gell-Mann. “The Eightfold Way: A Theory of Strong Interaction Symmetry”. In: *Technical Report at the California Institute of Technology, Synchrotron Laboratory* (Mar. 1961). DOI: `10.2172/4008239`.

[118] Yuval Ne’eman. “Derivation of Strong Interactions from a Gauge Invariance”. In: *Nuclear Physics* 26.2 (1961), pp. 222–229. ISSN: 0029-5582. DOI: `10.1016/0029-5582(61)90134-1`.

[119] Fayyazuddin and Riazuddin. *A Modern Introduction to Particle Physics*. 3rd Edition. World Scientific, 2012. ISBN: 978-981-4338-83-7, 978-981-4338-85-1. eprint: `https://library.oapen.org/handle/20.500.12657/53580`.

[120] Bastian Kubis. *An introduction to chiral perturbation theory*. 2007. arXiv: `hep-ph/0703274 [hep-ph]`.

[121] Steven Weinberg. “Pion Scattering Lengths”. In: *Phys. Rev. Lett.* 17 (11 Sept. 1966), pp. 616–621. DOI: `10.1103/PhysRevLett.17.616`.

[122] Juerg Gasser and Heinrich Leutwyler. “Chiral perturbation theory to one loop”. In: *Annals of Physics* 158.1 (1984), pp. 142–210. ISSN: 0003-4916. DOI: `10.1016/0003-4916(84)90242-2`.

[123] Juerg Gasser and Heinrich Leutwyler. “Chiral perturbation theory: Expansions in the mass of the strange quark”. In: *Nuclear Physics B* 250.1 (1985), pp. 465–516. ISSN: 0550-3213. DOI: `10.1016/0550-3213(85)90492-4`.

[124] Steven Weinberg. “Phenomenological Lagrangians”. In: *Physica A: Statistical Mechanics and its Applications* 96.1 (1979), pp. 327–340. ISSN: 0378-4371. DOI: `10.1016/0378-4371(79)90223-1`.

[125] Steven Weinberg. “Effective field theories - past and future”. In: *Proceedings of 6th International Workshop on Chiral Dynamics — PoS(CD09)*. Vol. 086. 2010, p. 001. DOI: `10.22323/1.086.0001`.

[126] Heinrich Leutwyler. “On the Foundations of Chiral Perturbation Theory”. In: *Annals of Physics* 235.1 (1994), pp. 165–203. ISSN: 0003-4916. DOI: `10.1006/aphy.1994.1094`.

[127] Cesareo A. Dominguez, Mirela S. Fetea, and Marcelo Loewe. “The GMOR relation at finite temperature”. In: *Nuclear Physics B - Proceedings Supplements* 54.1 (1997). Proceedings of QCD 96, pp. 333–337. ISSN: 0920-5632. DOI: `10.1016/S0920-5632(97)00063-7`.

[128] Jishnu Goswami et al. “Searching for the QCD Critical Point Along the Pseudo-critical/Freeze-out Line Using Padé-resummed Taylor Expansions of Cumulants of Conserved Charge Fluctuations”. In: *Acta Phys. Polon. Supp.* 16.1 (2023), 1–A76. DOI: `10.5506/APhysPolBSupp.16.1-A76`.

[129] S. Benić et al. “$\eta'$ multiplicity and the Witten-Veneziano relation at finite temperature”. In: *Phys. Rev. D* 84 (1 July 2011), p. 016006. DOI: `10.1103/PhysRevD.84.016006`.

[130] Hilmar Forkel. *A Primer on Instantons in QCD*. 2002. arXiv: `hep-ph/0009136`.

[131] David Olive, Stefano Sciuto, and Rodney J. Crewther. “Instantons in Field Theory”. In: *La Rivista del Nuovo Cimento* 2 (Aug. 1979), pp. 1–117. DOI: `10.1007/BF02724349`.

[132] Arkady I. Vainshtein et al. “ABC of instantons”. In: *Soviet Physics Uspekhi* 25.4 (Apr. 1982), p. 195. DOI: `10.1070/PU1982v025n04ABEH004533`.

[133] Pierre-Simon Laplace. “Mémoire sur la Probabilité des Causes par les évènemens. Memoir on the probability of the causes of events”. In: *Savants Estranges* 6 (1774), pp. 621–656. DOI: `10.1214/ss/1177013621`.

[134] Ole E. Barndorff-Nielsen. “Laplace’s method. Edgeworth and saddle-point approximations”. In: *Parametric Statistical Models and Likelihood*. New York, NY: Springer New York, 1988, pp. 188–212.

[135] Mikio Nakahara. *Geometry, Topology and Phyiscs*. 2nd Edition. Institute of Phyiscs Publishing Bristol and Philadelphia, June 2003. ISBN: 978-0750306065. eprint: `http://www.stat.ucla.edu/~ywu/GTP.pdf`.

[136] Bert Mendelson. *Introduction to Topology*. 3rd Edition. Dover Publications, July 1990. ISBN: 978-0486663524.

[137] Allen Hatcher. *Algebraic Topology*. Cambridge University Press, 2002. ISBN: 978-0-521-79540-1. eprint: `https://pi.math.cornell.edu/~hatcher/AT/AT.pdf`.

[138] Curtis G. Callan, Roger F. Dashen, and David J. Gross. “The structure of the gauge theory vacuum”. In: *Physics Letters B* 63.3 (1976), pp. 334–340. ISSN: 0370-2693. DOI: `10.1016/0370-2693(76)90277-X`.

[139] Raoul Bott. “An Application of Morse theory to the topology of Lie groups”. In: *Bull. Soc. Math. Fr.* 84 (1956), pp. 251–281.

[140] Stefan Vandoren and Peter van Nieuwenhuizen. *Lectures on instantons*. 2008. arXiv: `0802.1862 [hep-th]`.

[141] Gerard ’t Hooft. “Computation of the quantum effects due to a four-dimensional pseudoparticle”. In: *Phys. Rev. D* 14 (12 Dec. 1976), pp. 3432–3450. DOI: `10.1103/PhysRevD.14.3432`. Erratum: “Erratum: Computation of the quantum effects due to a four-dimensional pseudoparticle”. In: *Phys. Rev. D* 18 (6 Sept. 1978), pp. 2199–2200. DOI: `10.1103/PhysRevD.18.2199.3`.

[142] Gerard ’t Hooft. “Symmetry Breaking through Bell-Jackiw Anomalies”. In: *Phys. Rev. Lett.* 37 (1 July 1976), pp. 8–11. DOI: `10.1103/PhysRevLett.37.8`. Announced susequent publication: “Computation of the quantum effects due to a four-dimensional pseudoparticle”. In: *Phys. Rev. D* 14 (12 Dec. 1976), pp. 3432–3450. DOI: `10.1103/PhysRevD.14.3432`. Erratum: “Erratum: Computation of the quantum effects due to a four-dimensional pseudoparticle”. In: *Phys. Rev. D* 18 (6 Sept. 1978), pp. 2199–2200. DOI: `10.1103/PhysRevD.18.2199.3`.

[143] E. B. Bogomolny. “Stability of Classical Solutions”. In: *Sov. J. Nucl. Phys.* 24 (1976), p. 449.

[144] Michael F. Atiyah et al. “Construction of instantons”. In: *Physics Letters A* 65.3 (1978), pp. 185–187. ISSN: 0375-9601. DOI: `10.1016/0375-9601(78)90141-X`.

[145] Olivier Wantz. “The topological susceptibility from grand canonical simulations in the interacting instanton liquid model: Zero temperature calibrations and numerical framework”. In: *Nuclear Physics B* 829.1 (2010), pp. 48–90. ISSN: 0550-3213. DOI: `10.1016/j.nuclphysb.2009.12.007`.

[146] Roman W. Jackiw and Claudio Rebbi. “Vacuum Periodicity in a Yang-Mills Quantum Theory”. In: *Phys. Rev. Lett.* 37 (3 July 1976), pp. 172–175. DOI: `10.1103/PhysRevLett.37.172`.

[147] Barry J. Harrington and Harvey K. Shepard. “Periodic Euclidean solutions and the finite-temperature Yang-Mills gas”. In: *Phys. Rev. D* 17 (8 Apr. 1978), pp. 2122–2125. DOI: `10.1103/PhysRevD.17.2122`.

[148] Mikko Laine and Aleksi Vuorinen. *Basics of Thermal Field Theory: A Tutorial on Perturbative Computations*. Vol. 925. Lecture Notes in Physics. Springer, 2016. ISBN: 978-3-319-31932-2, 978-3-319-31933-9. DOI: `10.1007/978-3-319-31933-9`. arXiv: `1701.01554 [hep-ph]`.

[149] Guy D. Moore and Marcus Tassler. “The sphaleron rate in $SU(N)$ gauge theory”. In: *Journal of High Energy Physics* 2011.2 (Feb. 2011), p. 105. DOI: `10.1007/JHEP02(2011)105`.

[150] Claude Bernard. “Gauge zero modes, instanton determinants, and quantum-chromodynamic calculations”. In: *Phys. Rev. D* 19 (10 May 1979), pp. 3013–3019. DOI: `10.1103/PhysRevD.19.3013`.

[151] Lowell S. Brown, Robert D. Carlitz, and Choonkyu Lee. “Massless excitations in pseudoparticle fields”. In: *Phys. Rev. D* 16 (2 July 1977), pp. 417–422. DOI: `10.1103/PhysRevD.16.417`.

[152] Lowell S. Brown et al. “Propagation functions in pseudoparticle fields”. In: *Phys. Rev. D* 17 (6 Mar. 1978), pp. 1583–1597. DOI: `10.1103/PhysRevD.17.1583`.

[153] Lowell S. Brown and Choonkyu Lee. “Massive propagators in instanton fields”. In: *Phys. Rev. D* 18 (6 Sept. 1978), pp. 2180–2183. DOI: `10.1103/PhysRevD.18.2180`.

[154] Choonkyu Lee, Hae Won Lee, and P.Y. Pac. “Calculation of one-loop instanton determinants using propagators with space-time dependent mass”. In: *Nuclear Physics B* 201.3 (1982), pp. 429–460. ISSN: 0550-3213. DOI: `10.1016/0550-3213(82)90442-4`.

[155] Albert S. Schwarz. “On regular solutions of Euclidean Yang-Mills equations”. In: *Physics Letters B* 67.2 (1977), pp. 172–174. ISSN: 0370-2693. DOI: `10.1016/0370-2693(77)90095-8`.

[156] Michael F. Atiyah and Isadore M. Singer. “The Index of elliptic operators. I”. In: *Annals Math.* 87 (1968), pp. 484–530. DOI: `10.2307/1970715`.

[157] Michael F. Atiyah and Isadore M. Singer. “The index of elliptic operators on compact manifolds”. In: *Bull. Am. Math. Soc.* 69 (1969), pp. 422–433. DOI: `10.1090/S0002-9904-1963-10957-X`.

[158] Barry J. Harrington and Harvey K. Shepard. “Thermodynamics of the Yang-Mills gas”. In: *Phys. Rev. D* 18 (8 Oct. 1978), pp. 2990–2994. DOI: `10.1103/PhysRevD.18.2990`.

[159] Wolfgang E. Pauli and Felix M. H. Villars. “On the Invariant Regularization in Relativistic Quantum Theory”. In: *Rev. Mod. Phys.* 21 (3 July 1949), pp. 434–444. DOI: `10.1103/RevModPhys.21.434`.

[160] Yu A. Bashilov and Sergey V. Pokrovsky. “Quantum fluctuations in the vicinity of an instanton in the SU(N) group”. In: *Nuclear Physics B* 143.3 (1978), pp. 431–444. ISSN: 0550-3213. DOI: `10.1016/0550-3213(78)90063-9`.

[161] Andreas Ringwald and Fridger Schrempp. “Confronting instanton perturbation theory with QCD lattice results”. In: *Physics Letters B* 459.1 (1999), pp. 249–258. ISSN: 0370-2693. DOI: `10.1016/S0370-2693(99)00682-6`.

[162] Claude Bernard. “Instanton interactions at the one-loop level”. In: *Phys. Rev. D* 18 (6 Sept. 1978), pp. 2026–2041. DOI: `10.1103/PhysRevD.18.2026`.

[163] Fabian Rennecke. “Higher topological charge and the QCD vacuum”. In: *Phys. Rev. Res.* 2 (3 Sept. 2020), p. 033359. DOI: `10.1103/PhysRevResearch.2.033359`.

[164] Tamas G. Kovacs. *The fate of chiral symmetries in the quark-gluon plasma*. Nov. 2023. arXiv: `2311.04208 [hep-lat]`. And: *High temperature* $U(1)_A$ *breaking in the chiral limit*. Dec. 2023. arXiv: `2312.08775 [hep-lat]`.

[165] Guy D. Moore. “Axion dark matter and the Lattice”. In: *EPJ Web Conf.* 175 (2018), p. 01009. DOI: `10.1051/epjconf/201817501009`.

[166] Peter Thomas Jahn, Guy D. Moore, and Daniel Robaina. *Improved Reweighting for QCD Topology at High Temperature*. 2020. arXiv: `2002.01153 [hep-lat]`. Extension to: “$\chi_{\text{top}}(T \gg T_{\text{c}})$ in pure-glue QCD through reweighting”. In: *Phys. Rev. D* 98 (5 Sept. 2018), p. 054512. DOI: `10.1103/PhysRevD.98.054512`.

[167] Kazuo Fujikawa. “Path integral for gauge theories with fermions”. In: *Phys. Rev. D* 21 (10 May 1980), pp. 2848–2858. DOI: `10.1103/PhysRevD.21.2848`. Erratum: “Erratum: Path integral for gauge theories with fermions”. In: *Phys. Rev. D* 22 (6 Sept. 1980), pp. 1499–1499. DOI: `10.1103/PhysRevD.22.1499`.

[168] Kazuo Fujikawa. “Path-Integral Measure for Gauge-Invariant Fermion Theories”. In: *Phys. Rev. Lett.* 42 (18 Apr. 1979), pp. 1195–1198. DOI: `10.1103/PhysRevLett.42.1195`.

[169] Támas F. Csörgő, Róbert Vértesi, and Janos I. Sziklai. “Indirect Observation of an In-Medium $\eta^{'}$ Mass Reduction in $\sqrt{s_{NN}} = 200\ \ \mathrm{GeV}\ \mathrm{Au} + \mathrm{Au}$ Collisions”. In: *Phys. Rev. Lett.* 105 (18 Oct. 2010), p. 182301. DOI: `10.1103/PhysRevLett.105.182301`.

[170] Róbert Vértesi, Támas F. Csörgő, and Janos I. Sziklai. “Significant in-medium $\eta^{'}$ mass reduction in $\sqrt{s_{NN}} = 200$ GeV Au+Au collisions at the BNL Relativistic Heavy Ion Collider”. In: *Phys. Rev. C* 83 (5 May 2011), p. 054903. DOI: `10.1103/PhysRevC.83.054903`.

[171] Joseph I. Kapusta, Dmitri E. Kharzeev, and Larry D. McLerran. “Return of the prodigal Goldstone boson”. In: *Phys. Rev. D* 53 (9 May 1996), pp. 5028–5033. DOI: `10.1103/PhysRevD.53.5028`.

[172] Jihn-eui Kim. “Weak-Interaction Singlet and Strong CP Invariance”. In: *Phys. Rev. Lett.* 43 (2 July 1979), pp. 103–107. DOI: `10.1103/PhysRevLett.43.103`.

[173] Mikhail A. Shifman, Arkady I. Vainshtein, and Valentin I. Zakharov. “Can confinement ensure natural CP invariance of strong interactions?” In: *Nuclear Physics B* 166.3 (1980), pp. 493–506. ISSN: 0550-3213. DOI: `10.1016/0550-3213(80)90209-6`.

[174] Michael Dine, Willy Fischler, and Mark Srednicki. “A simple solution to the strong CP problem with a harmless axion”. In: *Physics Letters B* 104.3 (1981), pp. 199–202. ISSN: 0370-2693. DOI: `10.1016/0370-2693(81)90590-6`.

[175] Ariel R. Zhitnitsky. “On Possible Suppression of the Axion Hadron Interactions. (In Russian)”. In: *Sov. J. Nucl. Phys.* 31 (1980), p. 260.

[176] Gonzalo Alonso-Álvarez, Maria B. Gavela Legazpi, and Pablo Quílez Lasanta. “Axion couplings to electroweak gauge bosons”. In: *The European Physical Journal C* 79.3 (Mar. 2019), p. 223. ISSN: 1434-6052. DOI: `10.1140/epjc/s10052-019-6732-5`.

[177] Masahiro Kawasaki and Kazunori Nakayama. “Axions: Theory and Cosmological Role”. In: *Ann. Rev. Nucl. Part. Sci.* 63 (2013), pp. 69–95. DOI: `10.1146/annurev-nucl-102212-170536`.

[178] Larry McLerran, Robert D. Pisarski, and Vladimir Skokov. “Electroweak instantons, axions, and the cosmological constant”. In: *Physics Letters B* 713.3 (2012), pp. 301–303. ISSN: 0370-2693. DOI: `10.1016/j.physletb.2012.05.057`.

[179] Howard Georgi, David B. Kaplan, and Lisa Randall. “Manifesting the invisible axion at low energies”. In: *Physics Letters B* 169.1 (1986), pp. 73–78. ISSN: 0370-2693. DOI: `10.1016/0370-2693(86)90688-X`.

[180] Justin I. Read. “The local dark matter density”. In: *Journal of Physics G: Nuclear and Particle Physics* 41.6 (May 2014), p. 063101. DOI: `10.1088/0954-3899/41/6/063101`.

[181] Salucci, Paolo et al. “The dark matter density at the Sun’s location”. In: *Astron. Astrophys.* 523 (June 2010), A83. DOI: `10.1051/0004-6361/201014385`.

[182] Dmitri V. Vassilevich. “Heat kernel expansion: user’s manual”. In: *Physics Reports* 388.5 (2003), pp. 279–360. ISSN: 0370-1573. DOI: `10.1016/j.physrep.2003.09.002`.

[183] Denny Fliegner et al. “The Higher Derivative Expansion of the Effective Action by the String Inspired Method, II”. In: *Annals of Physics* 264.1 (1998), pp. 51–74. ISSN: 0003-4916. DOI: `10.1006/aphy.1997.5778`. $a_{12}$ coefficient in: *The Higher derivative expansion of the effective action by the string inspired method. Part 2*. 1998. arXiv: `hep-th/9707189`.

[184] Bryce S. DeWitt. “Quantum field theory in curved spacetime”. In: *Physics Reports* 19.6 (1975), pp. 295–357. ISSN: 0370-1573. DOI: `10.1016/0370-1573(75)90051-4`.

[185] Eugenio Megías, Enrique Ruiz Arriola, and Lorenzo L. Salcedo. “Thermal heat kernel expansion and the one-loop effective action of QCD at finite temperature”. In: *Phys. Rev. D* 69 (11 June 2004), p. 116003. DOI: `10.1103/PhysRevD.69.116003`.

[186] Eugenio Megías, Enrique Ruiz Arriola, and Lorenzo L. Salcedo. “The Polyakov loop and the heat kernel expansion at finite temperature”. In: *Physics Letters B* 563.3 (2003), pp. 173–178. ISSN: 0370-2693. DOI: `10.1016/S0370-2693(03)00699-3`.

[187] Barak Shoshany. “OGRe: An Object-Oriented General Relativity Package for Mathematica”. In: *Journal of Open Source Software* 6.65 (2021), p. 3416. DOI: `10.21105/joss.03416`.

[188] Kenji Fukushima and Vladimir Skokov. “Polyakov loop modeling for hot QCD”. In: *Progress in Particle and Nuclear Physics* 96 (2017), pp. 154–199. ISSN: 0146-6410. DOI: `10.1016/j.ppnp.2017.05.002`.

[189] Milton Abramowitz and Irene Stegun. *Handbook of Mathematical Functions with Formulas, Graphs, and Mathematical Tables*. 10th print, with corr. Selected government publications. New York, 1972. ISBN: 0471800074.

[190] R. B. Dingle. "The Fermi-Dirac integrals $\mathcal{F}_p(\eta) = (p!)^{-1}\int_0^\infty \varepsilon^p(e^{\varepsilon-\eta}+1)^{-1}\mathrm{d}\varepsilon$ ". In: *Applied Scientific Research, Section B* 6.1 (Dec. 1957), pp. 225–239. ISSN: 0365-7140. DOI: `10.1007/BF02920379`.

[191] Aaron Meurer et al. "SymPy: symbolic computing in Python". In: *PeerJ Computer Science* 3 (Jan. 2017), e103. ISSN: 2376-5992. DOI: `10.7717/peerj-cs.103`.

[192] The mpmath development team. *mpmath: a Python library for arbitrary-precision floating-point arithmetic (version 1.3.0)*. `https://mpmath.org`. 2023.

[193] Steven G. Johnson. *Multi-dimensional adaptive integration in C: The Cubature package*. `https://github.com/stevengj/cubature`. 2005.

[194] A. C. Genz and A. A. Malik. "Remarks on algorithm 006: An adaptive algorithm for numerical integration over an $N$-dimensional rectangular region". In: *Journal of Computational and Applied Mathematics* 6 (1980), pp. 295–302. DOI: `10.1016/0771-050x(80)90039-x`.

[195] Jarle Berntsen, Terje O. Espelid, and Alan Genz. "An adaptive algorithm for the approximate calculation of multiple integrals". In: *ACM Transactions on Mathematical Software* 17 (1991), pp. 437–451. DOI: `10.1145/210232.210233`.

[196] J. M. Bull and T. L. Freeman. "Parallel globally adaptive algorithms for multidimensional integration". In: *Applied Numerical Mathematics* 19 (1995), pp. 3–16. DOI: `10.1016/0168-9274(95)00076-7`.

[197] D. A. Kirzhnits and Andrei D. Linde. "Symmetry Behavior in Gauge Theories". In: *Annals Phys.* 101 (1976), pp. 195–238. DOI: `10.1016/0003-4916(76)90279-7`.

# Curriculum Vitae

## Personal Information

| | |
|---|---|
| Name: | Bruno Maria Högl |
| Date of Birth: | 6th December 1993 |
| Place of Birth: | Munich |

## Education and Employment

| | |
|---|---|
| 11/2020 - 11/2024 | **PhD Researcher (Physics)**<br>TU Darmstadt, Group Prof. Moore |
| 04/2019 - 10/2020 | **Research Assistant (Physics)**<br>LMU Munich, Group Prof. Hofmann<br>“Physics in precision-dependent normal neighborhoods”, *Phys. Rev. D 102 (2020) 8, 084065* |
| 04/2016 - 03/2019 | **Master of Science (Physics)**, Grade: 1.56 (“good”)<br>LMU Munich, Master’s Thesis (Group Prof. Hofmann):<br>“Riemann Normal Coordinates - Determination of the Domain of Validity and Application in Quantum Field Theory in Curved Spacetime” |
| 10/2012 - 03/2016 | **Bachelor of Science (Physics)**, Grade: 1.75 (“good”)<br>LMU Munich, Bachelor’s Thesis (Group Prof. Hofmann):<br>“Lie-Groups and Lie-Algebras as a Combination of Group Theory and Differential Geometry” |
| 06/2012 | **Abitur**, Gymnasium Miesbach, Grade: 1.0 (“very good”) |

## Miscellaneous

- Member of the Collaborative Research Center "CRC-TR 211 - strong interaction matter under extreme conditions" during PhD Studies
- 08/2021 - 11/2024: server administrator (supervision of the TU Darmstadt's nuclear physics theory center's web and e-mail server)
- 2021: Teaching Assistant for “Quantum Field Theory” lecture at TU Darmstadt
- 2019/2020: Teaching Assistant for several courses in theoretical and experimental physics at LMU Munich
- Scholarship of the “Max-Weber Programm Bayern” for Bachelor and Master Studies
- 2012 - 2024: Member of the “Deutsche Physikalische Gesellschaft”